TECHNISCHE UNIVERSITÄT WIEN

DISSERTATION

Numerische Simulation und mathematische Analysis von diffusiven Mehrspezies-Systemen in der Biologie und Physik

ausgeführt zum Zwecke der Erlangung des akademischen Grades
eines Doktors der technischen Wissenschaften unter der Leitung von

Univ.-Prof. Dr. rer. nat. Ansgar Jüngel
E101 – Institut für Analysis und Scientific Computing, TU Wien

eingereicht an der Technischen Universität Wien
Fakultät für Mathematik und Geoinformation

von

Dipl.-Ing. Markus Fellner
[redacted]

Diese Dissertation haben begutachtet:

1. **Prof. Dr. Ansgar Jüngel**
   Institut für Analysis und Scientific Computing, Technische Universität Wien
2. **Prof. Dr. Jan-Frederik Pietschmann**
   Institut für Mathematik, Universität Augsburg
3. **Prof. Dr. Marie-Therese Wolfram**
   Institut für Mathematik, Universität Warwick

Wien, am 17. Juli 2023

Kurzfassung

Simulationen von Modellen in der Physik und Biologie können hinsichtlich Rechenzeit und Rechenressourcen sehr kostspielig sein. Darüber hinaus bleibt die mathematische Sinnhaftigkeit dieser Modelle, bezogen auf die Existenz von Lösungen oft ein offenes Problem. Diese ist jedoch in vielen Fällen ein wichtiger Faktor zum Nachweis der Konvergenz der für die Simulation verwendeten numerischen Algorithmen.
Ziel dieser Arbeit ist es nunmehr einen effizienten Algorithmus zur Simulation stochastischer Vielteilchensysteme einschließlich numerischer Analyse für den Fall mehrerer Spezies bereitzustellen und zweitens zwei spezifische Modelle aus der Biologie mathematisch zu analysieren. Diese drehen sich um den Prozess der Blutgefäßbildung aus einem bereits bestehenden Netzwerk bzw. den Transport von Vesikeln innerhalb eines Neurit.
Der Algorithmus basiert auf der Idee des "random batch", bei dem Agenten bei jedem Zeitschritt zufällig in Mengen ("batches") aufgeteilt werden und ihnen nur erlaubt wird, mit Agenten in der selben Menge zu interagieren. Dies führt zu einer Reduzierung der berücksichtigten Interaktionen zwischen Agenten und damit zu einer Reduzierung der Rechenressourcen. Um den mit dieser Strategie eingeführten Fehler im Fall mehrerer Spezien nachweislich klein zu halten, werden optimale Korrekturfaktoren eingeführt.
Die diskutierten biologischen Modelle bestehen aus Systemen partieller Differentialgleichungen, die entweder mit gewöhnlichen Differentialgleichungen oder einer Kombination aus gewöhnlichen und stochastischen Differentialgleichungen gekoppelt sind. Fixpunktargumente werden verwendet um die Existenz von Lösungen zu zeigen und im Falle des Vesikeltransports wird die bekannte Entropiestruktur des Systems ausgenutzt.

Abstract

Simulations of models in physics and biology can be very costly in terms of computation time and resources. Furthermore, the mathematical soundness of these models, in many cases an important factor to prove convergence of numerical algorithms used for simulation, is often left as an open problem.
The aim of this work is to firstly, give an algorithm for simulating stochastic many particle systems complete with numerical analysis in the case of multiple species. Secondly, it is to mathematically analyse two specific models from biology, revolving around the process of blood vessel formation from a pre-existing network, respectively the transport of vesicles inside neurites.
The algorithm is based on the idea of the random batch, separating agents randomly into batches at each time step and only allowing them to interact with agents in the same batch. This leads to a reduction of considered interactions between agents and hence to a reduction in computational resources. Optimal correction factors are introduced to keep the error introduced with this strategy in the multiple species case verifiable small.
The models discussed on the other hand consist of systems of partial differential equations coupled with either ordinary differential equations or a combination of ordinary- and stochastic- differential equations. Fixed point arguments are used to show existence of solutions and in the case of vesicle transport the well known entropy structure of the system is exploited.

Danksagung

An dieser Stelle möchte ich allen Danken die mich auf dieser Reise begleitet haben. Meinem Betreuer Prof. Dr. Ansgar Jüngel der mir spannende Themen zuwies, mir mit seinem fachlichen Rat beiseite stand und der mir dies alles erst ermöglichte. Meinen Kollegen, Prä- und Post-Docs, die mich bei Laune hielten wenn die Arbeit nicht voranzugehen schien. Prof. Dr. Jan-Frederik Pietschmann und Prof Dr. Marie-Therese Wolfram die sich bereit erklärt haben diese Arbeit zu begutachten.
Bei meinen Freunden und Verwandten die sich durch mich mehr mit Mathematik beschäftigen mussten als sie wollten, bedanke und entschuldige ich mich. Ich kann euch versichern das Schlimmste habt ihr überstanden - höchstwahrscheinlich. Besonders erwähnen möchte ich hier meine beste Freundin Carina und meinen Cousin und Bruder im Geiste Florian. Bei meiner Mutter Monika bedanke ich mich für die Zeit, Energie und Liebe die sie investiert hat um mich wieder aufzupäppeln wenn die Last zu schwer wurde - du warst da wenn ich dich gebraucht habe. Bei meinem Vater Franz bedanke ich mich ebenfalls für seine Unterstützung. Ohne die Beiden würde ich heute nicht hier sein. Hier möchte ich mich auch bei meinen persönlichen Heldinnen bedanken - meinen Schwestern Bernadette und Johanna, sowie ihren Partnern Christoph und Franz. Ihr begleitete mich durch emotionalle Berg und Talfahrten, korregiertet mehr wie einen Beistrichfehler in meinen Arbeiten und standet mir mit Rat und Tat zur Seite. Danke euch allen für die Schöne Zeit die ich mit euch verbringen durfte und noch verbringen werde.

Ich würdige die finanzielle Unterstützung dieser Arbeit durch den Austrian Science Fund (FWF) Grant 'Dissipation and Dispersion in NPDEs' mit der Projektnummer W1245-N25 und durch den European Research Council (ERC) Grant 'Emergente Netzwerkstrukturen und neuromorphische Anwendungen' mit der Projektnummer 1948157.

Eidesstattliche Erklärung

Ich erkläre an Eides statt, dass ich die vorliegende Dissertation selbstständig und ohne fremde Hilfe verfasst, andere als die angegebenen Quellen und Hilfsmittel nicht benutzt bzw. die wörtlich oder sinngemäß entnommenen Stellen als solche kenntlich gemacht habe.

Wien, am 17. Juli 2023

Markus Fellner

Contents

1. Introduction

1.1. Overview

Modelling natural phenomena in physics and biology often give rise to diffusive multiple species systems in the form of partial differential equations ([86], [40]) or processes driven by Brownian motion ([8], [83]). The degree of certainty how well these models approximate reality is obtained by simulations and subsequent comparison with data obtained by real life experiments ([8], [48]). In terms of particle systems, these simulations, depending on the number of agents used, can be very costly in terms of computation time and resources. For a system comprised of N interacting particles, the number of interactions N_{int} would be $N_{int} = N(1-N) = \mathcal{O}(N^2)$. All of which would have to be taken into account if one wishes to run a thorough simulation. A linear increase in the number of particles would henceforth lead to an approximately quadratic increase in necessary resources in the simulation. For systems encompassing a large number of agents interacting with each other, considering the whole number N_{int} of interactions for the simulation might therefore not be feasible. Hence, methods are needed for them to reduce the number of considered interactions, while keeping the error made by adopting this methods small. Furthermore, as these methods and simulations in general lead to solving a (discrete) approximation of the considered continuous model, the question of convergence of the used numerical scheme is a valid one. The numerical analysis employed often either proves the convergence of the discrete scheme to a solution directly, doubling as existence result ([60], [28]), or uses the assumption that existence of a suitable solution is already known ([93], [56]). Either way, the models need to be analysed mathematically and demand suitable strategies for proving the existence of solutions to this problems, answering also the question of mathematical soundness of the model.

The aim of this work is twofold. In **Part I**, it is to address the problem of efficient simulation in the case of a stochastic many particle system comprised of multiple species of particles governed by stochastic differential equations. Here we will give an algorithm which reduces the computational cost by one order ($\mathcal{O}(N)$) and prove a convergence result. Part I is based on a collaboration with E. S. Daus (TU Wien) and A. Jüngel (TU Wien), which was published in *Journal of Computational Physics* under the title *Random-batch methods for multi-species stochastic interacting particle systems* [29].

In **Part II**, we will provide existence analysis for two select models from biology. The first model revolves around the formation of new blood vessels from a pre-existing network, a process also known as angiogenesis, treating cells as discrete entities whose movement is governed by stochastic differential equations. The concentration of involved proteins are given by the solutions of non-linear reaction diffusion equations, whereas the evolution of the different components of the underlying matrix is given by ordinary differential equations. The second model deals with the transport of vesicles inside a neurite, an important factor in the growth and polarization of a neuron. It consists of a cross diffusion system describing the concentration of vesicles along the neurite, coupled via boundary conditions with an ordinary differential equation which governs the vesicle concentration in pools at the end of the neurite. For these models we will prove existence of suitable solutions. Part II is based on two collaborations with A. Jüngel (TU Wien) which are submitted for publication under the title *A coupled stochastic differential reaction-diffusion system for angiogenesis* [35], respectively *A cross-diffusion system for vesicle transport - existence analysis of a cross-diffusion system with nonlinear Robin boundary conditions for vesicle transport in neurites* [36].

In the next sections, we give a short overview of the considered many particle system, the biological models and a summary of the mathematical line of reasoning established in Part I and Part II. We furthermore give a state of the art of the considered problems and present the main results of this thesis, together with an outlook for possible future work. A more detailed description of the models and the detailed proofs are found in Part I, respectively Part II.

1.2. Main Results and State of the Art of Part I - Simulation of Stochastic Many Particle Systems

Interacting particle systems can be used to model a variety of real-life phenomena. The swarming of fish [89], the flocking of birds [83] or the process by which consensus of opinions is formed [33], to name but a few. In Part I, we consider the following stochastic interacting many particle system which takes into account multiple species: For $d, n \in \mathbb{N}$ and $\sigma_i > 0$ for $i = 1, \ldots, n$, let

$$\begin{aligned} \mathrm{d}X_i^k &= -\nabla V_i(X_i^k)\mathrm{d}t + \sum_{j=1}^{n} \alpha_{ij} \sum_{\substack{\ell=1 \\ (i,k)\neq(j,\ell)}}^{N_j} K_{ij}(X_i^k - X_j^\ell)\mathrm{d}t + \sigma_i \mathrm{d}B_i^k(t), \\ X_i^k(0) &= X_i^{0,k} \quad \text{for } i = 1, \ldots, n,\ k = 1, \ldots, N_i. \end{aligned} \tag{1.1}$$

Here $\alpha_{ij} = \frac{1}{N_j - \delta_{ij}}$, $N_i \in \mathbb{N}$, $X_i^{0,k}$ are independent identically distributed square integrable $\mathbb{R}^d-$valued random variables, V_i and K_{ij} are twice differentiable $\mathbb{R}^d$-valued bounded functions with bounded derivatives on $\mathbb{R}^d$ and B_i^k are independent Brownian motions. Under these assumptions, standard results guarantee the existence of a unique solution X to system (1.1), see for instance [63]. Our main goal is to find a way to simulate system (1.1) efficiently in the large population case $N = \sum_{i=1}^n N_i >> 1$. We start by looking at important examples of algorithms for simulation in the literature.

1.2.1. State of the Art

This subsection is based on [29, Section 1]. The binary interaction between all particles makes numerical simulations of (1.1) very demanding when many agents need to be modelled, which explains the need for efficient algorithms. Averaged results can be obtained

from the associated mean-field equations, see subsection 2.4, while the individual dynamics is captured by direct simulations, using fast summation algorithms, like fast multipole methods [44], wavelet transforms [6], or variants of Monte–Carlo methods [19]. Motivated by mini-batch gradient descent in machine learning (see, e.g., [71]), the authors of [52] suggested to use small random batches in interacting particle systems, which results in the reduction of the computational cost per time step from $O(N^2)$ to $O(N)$ (N being the number of particles or agents). Compared to other efficient sampling methods, like the Ewald summation or the fast multipole method, this random-batch method is easier to implement and more flexible to apply in complex systems. The results of [52] are valid in the single-species case and the ergodicity and long-time behaviour of this method has been studied in [55]. A discrete version via the Euler-Maruyama scheme has been introduced and analysed in [95]. Motivated by [52], random batch particle methods for the homogeneous Landau equation were established and studied in [23].
In this thesis, we generalize the approach of [52] to multi-species systems. In particular, we work out the dependence of the L^2 error with respect to the batch sizes of the different species and discuss the case of multiplicative noise. In [53], a similar algorithm was proposed to handle, among others, the multi-species case. Although the rate of convergence of the error cannot be improved in general with our method, compared to the results in [52, 53], the introduction of certain adjustable parameters provides an additional control over the error with respect to the simulation runtime. Moreover, we can still find physical situations for which our method performs better than the one in [52, 53]. For instance, when the total numbers of agents per species have the same order of magnitude, our numerical results indicate that our algorithm performs slightly better than the single-species method (i.e. ignoring species) in [52], in particular for larger time step sizes. This is due to the key idea of our method, namely to conserve the ratio between the different species via so-called super-batches and to use some carefully chosen correction factors, instead of the purely random mixing obtained in the multi-species method of [53].

The novelty of this part of the thesis is the extension of the random-batch method and its error analysis of [52] to the multi-species case by investigating different batch sizes of the species (super-batches) and by allowing for stochastic particle systems with multiplicative noise.
What follows is an explanation of the method and a presentation of the main result of Part I, together with essential steps of its proof.

1.2.2. The Random Batch Method and Main Result

To reduce the number of interactions in (1.1), one can proceed according to the following random batch algorithm (see section 2.2) similar to [52]:

i) Set $m = 0$ and choose $\tau > 0$ and $\beta_{ij} > 0$ for $i, j = 1 \dots n$. For every species i, choose the number of allowed interactions $p_i \in \mathbb{N}$, which satisfies $p_i b_i = N_i$ for some $b_i \in \mathbb{N}$.

ii) For every species i, create a random partition, also known as batches, $\mathcal{C}_{i,r}$, $r = 1, \dots b_i$, of the index-set $\{1, \dots, N_i\}$, where every $\mathcal{C}_{i,r}$ contains exactly p_i elements, i.e. $|\mathcal{C}_{i,r}| = p_i$. To $\mathcal{C}_r := \{(j, l) : l \in \mathcal{C}_{j,r}\}$ we also refer to as superbatch.

iii) Let $r(k)$ be the index satisfying $k \in \mathcal{C}_{i,r}$. Solve (1.1) only using the allowed interactions given by $\mathcal{C}_{j,r(k)}$ for $\tilde{X}_i^k$, which correspond to the elements of the superbatch $\mathcal{C}_{r(k)}$:

$$\begin{aligned}
\mathrm{d}\tilde{X}_i^k &= -\nabla V_i(\widetilde{X}_i^k)\mathrm{d}t + \sum_{j=1}^{n} \beta_{ij} \sum_{\substack{\ell \in \mathcal{C}_{j,r(k)} \\ (i,k)\neq(j,\ell)}} K_{ij}(\widetilde{X}_i^k - \widetilde{X}_j^\ell)\mathrm{d}t + \sigma_i \mathrm{d}B_i^k(t), \quad t \in [0,\tau], \\
X_i^k(0) &= X_i^{0,k} \quad \text{for } i = 1,\dots,n,\ k = 1,\dots,N_i.
\end{aligned} \tag{1.2}$$

iv) Set $m = m+1$. Repeat steps ii)–iii) with $X_i^{0,k} = \widetilde{X}_i^k(m\tau)$ on the interval $[(m-1)\tau, m\tau]$ for all $i = 1,\dots,n$ and $k = 1,\dots,N_i$.

In step ii) the partitions, respectively the batches, are created randomly, giving the method its name: random batch method. Given enough time, every particle will interact with every other particle due to the mixing generated by the random creation of batches at each step. Furthermore, the number of interactions per particle reduces to at least $p = \sum_{i=1}^n p_i - 1$, leading to an computational cost of $\mathcal{O}(pN) = \mathcal{O}(N)$ per iteration step. Compared to the computational cost of taking all the interactions into account, i.e. $\mathcal{O}(N(N-1)) = \mathcal{O}(N^2)$, this leads to a reduction of the cost by one order. The main problem with this approach is how to choose the constants β_{ij} to guarantee the convergence of $\widetilde{X}_i^k \to X_i^k$ for $\tau \to 0$. Here they take the role of the constants α_{ij}, which are the reciprocal values of the number of terms of the sum, i.e. the number of considered interactions per particle in (1.1). A possible choice would therefore be

$$\beta_{ij} = \frac{1}{p_j - \delta_{ij}}, \quad i,j = 1,\dots,n.$$

This turns out to be a good pick if $b_i = b_j$ for all $i,j = 1,\dots,n$, which is, for example, automatically satisfied in the single species case discussed in [52]. On the other hand, consider the case of $b_i \neq b_j$, where we can assume without loss of generality $b_i > b_j$. Due to the nature of the algorithm there exists some $1 \leq k \leq N_i$ such that for $r(k)$, as defined in step iii), there exists no corresponding set $\mathcal{C}_{j,r(k)}$. As $b_i > b_j$, the set $\mathcal{C}_{j,b_i}$ is empty and the particle associated with $\widetilde{X}_i^k$, for which $r(k) = b_i$, is missing all interactions with the particles associated with $\widetilde{X}_j^l$, $l = 1\dots,N_j$. To make up for the less frequent interactions with particles of species j in such a case, one needs to scale up the interactions in a sense such that the mean effect of the interactions stay the same, meaning

$$\sum_{j=1}^{n} \alpha_{ij} \mathbb{E}\left(\sum_{\substack{\ell=1 \\ (i,k)\neq(j,\ell)}}^{N_j} K_{ij}(x_i^k - x_j^\ell) \right) = \sum_{j=1}^{n} \beta_{ij} \mathbb{E}\left(\sum_{\substack{\ell \in \mathcal{C}_{j,r(k)} \\ (i,k)\neq(j,\ell)}} K_{ij}(x_i^k - x_j^\ell) \right),$$

for all $x = (x_1^1, \dots x_n^{N_n}) \in \mathbb{R}^{dN_1 \times \dots \times dN_n}$, $i = 1,\dots,n$ and $k = 1,\dots,N_i$. Here the expectation is in respect to the random process ξ used for the creation of the sets $\mathcal{C}_j^r$. To this result we will later refer as consistency of the algorithm and it leads to the choice

$$\beta_{ij} = \frac{b_i}{(p_j - \delta_{ij}) \min\{b_i, b_j\}}, \quad i, j = 1, \dots, n,$$

(see also Proposition 2). For $i = 1, \dots, n$ we assume the existence of $q_i > 0$, such that

$$|\nabla V_i(x)| + |D^2 V_i(x)| \leq C_V (1 + |x|^{q_i}), \quad i = 1, \dots, n.$$

Under this assumption, one can show for some $C_1, C_2 > 0$ a stability result (i.e. Lemma 4) of the form

$$\left|\mathbb{E}\big(\widetilde{X}_i^k(t) - \widetilde{X}_i^k((m-1)\tau)\big|\mathcal{F}_{m-1}\big)\right| \leq C_2 \tau |\widetilde{X}_i^k((m-1)\tau)|^{q_i} + C_1 \tau, \quad t \in [(m-1)\tau, m\tau],$$

where $\mathcal{F}_{m-1}$ is the smallest $\sigma-$algebra for whom all the involved processes evaluated at any $t \in [0, (m-1)\tau]$, are measurable. The consistency of the algorithm and the stability result will be the key to prove the main result of Part I:

Main Result of Part I: (Chapter 2, Theorem 1) *Under the Assumptions* (A1)–(A4)*, made in section 2.3, there exists a constant* $C > 0$*, which is independent of* $(b_i, p_i, N_i)_{i=1,\dots,n}$*,* m *and* T*, such that*

$$\sup_{0<t<T} \sum_{i=1}^n \mathbb{E}|(X_i^k - \widetilde{X}_i^k)(t)|^2 \leq C\sqrt{\tau} \left(\sum_{i=1}^n \Gamma_i\right)^{1/2} + C\tau(1 + \theta^\gamma), \quad t > 0, \tag{1.3}$$

where

$$\theta = \frac{\max_{j=1,\dots,n} b_j}{\min_{j=1,\dots,n} b_j}, \quad \gamma = 3\big(\max\{1, q_1, \dots, q_n\} + 1\big),$$

$$\Gamma_i = \sum_{\substack{j,j'=1 \\ j,j' \neq i,\, j \neq j'}}^n \left(\frac{\max\{b_i, b_j, b_{j'}\}}{\max\{b_j, b_{j'}\}} - 1\right) + \sum_{\substack{j=1 \\ j \neq i}}^n \left(\frac{b_i - \min\{b_i, b_j\}}{\min\{b_i, b_j\}} - \frac{2 - \max\{b_i, b_j\}}{N_j} + \frac{b_i}{p_j \min\{b_i, b_j\}}\right) + \left(\frac{1}{p_i - 1} - \frac{1}{N_i - 1}\right) \geq 0. \quad i = 1, \dots, n.$$

From the definition of Γ_i and θ one can derive that as long as the ratios $\frac{b_j}{b_i}$ for $i, j = 1, \dots, n$ are fixed, Γ_i and θ are bounded with respect to the overall particle number N. Hence, increasing N, while keeping the ratios, does not lead to a significant change in the error estimate (1.3) and hence the step size τ does not have to be decreased, which would mean more iteration steps and increasing computational cost to achieve a similar error-bound. This fact and the cost reduction of one order by the algorithm makes this method very suitable for simulating systems with a big number of particles.

1.2.3. Outlook

The following considerations could act as starting points for future work regarding the random batch method in conjunction with stochastic interacting many particle models:

i) In section 3.4 system (1.1) together with multiplicative noise is considered, i.e. an additional dependency of σ_i on X_i^k is added, meaning

$$\mathrm{d}X_i^k = -\nabla V_i(X_i^k)\mathrm{d}t + \sum_{j=1}^{n} \alpha_{ij} \sum_{\substack{\ell=1 \\ (i,k)\neq(j,\ell)}}^{N_j} K_{ij}(X_i^k - X_j^\ell)\mathrm{d}t + \sigma_i(X_i^k)\mathrm{d}B_i^k(t).$$

In section 3.4, the strategy and ideas used for proving (1.3) also apply in this setting, giving

$$\sup_{0<t<T} \sum_{i=1}^{n} \|(X_i^k - \widetilde{X}_i^k)(t)\| \leq C\sqrt{\tau}\Big(1 + \sum_{i=1}^{n} \Gamma_i\Big)^{1/2} + C\tau(1+\theta^\gamma), \tag{1.4}$$

see Theorem 7, where $C > 0$ is independent of $(b_i, p_i)_{i=1,\dots,n}$, m, and T. To obtain an estimate of the form (1.4) in the case of multiplicative noise with $\sigma_i = \sigma_i(X)$, i.e. depending on the positions of all particles X_j^l, $1 \leq j \leq n$, $1 \leq l \leq N_j$ is, to the knowledge of the author, still an open problem. Other methods of creating random batches or another strategy altogether might have to be considered here.

ii) In the case of interaction kernels K_{ij} with short range, i.e. supp $K_{ij} \subseteq B_r(0)$, with $r > 0$, a non-negligible number of interactions might not contribute as $K_{ij}(X_i^k - X_j^l) = 0$ for $|X_i^k - X_j^l| > r$. A cost effective method of eliminating or sorting out such interactions at every time step could lead to an significant increase in the performance of random batch methods and simulation methods in general in this case. Examples for such short range kernels can, among others, be found in biology. Cells, for instance, detect chemical messenger molecules according to their extension into space, giving them an interaction radius corresponding to their size.

1.3. Main Results and State of the Art of Part II - Cell Based Models - Angiogenesis

Angiogenesis is the process governing the formation of new blood vessels from a pre-existing network, which is an important factor in wound healing or tumour growth. We start by giving a quick overview of the specific model for angiogenesis, which is based on the model in [8] and undergoes mathematical analysis in Part II.
The innermost layer of blood vessels is made up of endothelial cells. Those endothelial cells involved in the angiogenesis process can be divided into tip cells (cell-species 1) and stalk cells (cell-species 2). Their movement is governed, among others, by the volume fractions f_i, $i \in \{B, E, F\}$ via a process called durotaxis, which is driven by changes in stiffness of the surrounding tissue, and the local change in concentration of certain proteins c_j, $j \in \{V, D, M, U\}$. Here f_B, f_F and f_E give the composition of the underlying matrix, i.e. the different shares of its components - boundary membrane, fibrin matrix and extracellular fluid - at each point of the considered bounded domain $\mathcal{D} \subseteq \mathbb{R}^3$. Tip cells follow the concentration-gradient ∇c_V of the VEGF-protein (vascular endothelial growth factor) and secret proteins (c_M, c_U) to degrade the solid part of the tissue - boundary membrane and

fibrin matrix - into extracellular fluid. They furthermore secret the protein (DLL4) to attract stalk cells which follow its concentration gradient ∇c_D. These cells can adhere together via proteins on their surfaces and make up the inner wall of the new blood vessel. For a more in-depth explanation of f_i and c_j, respectively the angiogenesis process, see section 5.2.
Let $N_i \in \mathbb{N}$ for $i = 1, 2$ and $(\Omega, \mathcal{F}, (\mathcal{F}_t)_{t\geq 0}, \mathbb{P})$ be a stochastic basis. The change in the positions X_i^k, $i = 1, 2$, $k \in \{1, \ldots, N_i\}$ of the endothelial cells midpoints can then be modelled via the following system of stochastic differential equations:

$$\begin{aligned} \mathrm{d}X_i^k(t) =& g_i[c, f](X_i^k, t)\mathrm{d}t + \sigma_i(X_i^k)\mathrm{d}B_i^k(t), \quad X_i^k(0) = X_i^{0,k}, \quad t > 0, \\ i =& 1, 2, \quad k = 1, \ldots, N_i, \end{aligned} \tag{1.5}$$

where $\sigma_i(\omega, x, t) : \Omega \times \mathcal{D} \times [0, \infty) \to \mathbb{R}^{3\times 3}$ is uniform Lipschitz continuous in x. The random variables $X_i^{0,k}$ are independent and for each fixed i identically distributed. Here g_i is of the form

$$g_i[c, f](x, t) := M_i(f_S(x, t), x, t) + \gamma(f_S(x, t))\nabla c_{j(i)}(x, t) + \lambda(f_S(x, t))\nabla f_S(x, t), \tag{1.6}$$

$x \in \mathcal{D}$, $t > 0$, for suitable smooth functions M_i, γ and λ, where $j(1) = V, j(2) = D$, $f_S := f_B + f_F$ and B_i^k are $3-$dimensional independent Brownian motions relative to the filtration $(\mathcal{F}_t)_{t\geq 0}$. The Brownian motions thereby simulate random interactions between cells and their environment. For a possible choice of M_i, γ and λ see [8]. The volume fractions f_i, $i \in \{B, E, F\}$ satisfy the ordinary differential equations

$$\begin{aligned} \frac{\mathrm{d}f_B}{\mathrm{d}t} &= -s_B c_M f_B, \quad t > 0, \quad f_B(0) = f_B^0, \\ \frac{\mathrm{d}f_F}{\mathrm{d}t} &= -s_F c_U f_F, \quad t > 0, \quad f_F(0) = f_F^0, \\ \frac{\mathrm{d}f_E}{\mathrm{d}t} &= s_B c_M f_B + s_F c_U f_F, \quad t > 0, \quad f_E(0) = 1 - f_B^0 - f_F^0, \end{aligned} \tag{1.7}$$

with some constants s_B, $s_F > 0$ and bounded initial condition f_i^0. Notice the concentrations c_U, c_M of the proteins degrading the boundary membrane and the fibrin matrix. For the concentrations c_j of the various proteins we have the following reaction-diffusion equations:

$$\begin{aligned} &\partial_t c_V - \mathrm{div}(D_V(f)\nabla c_V) + \alpha_V(x, t)c_V = 0 \quad \text{in } \mathcal{D}, \ t > 0, \\ &\partial_t c_D - \mathrm{div}(D_D(f)\nabla c_D) + \beta_D(x, t)c_D = \alpha_D(x, t)c_V \quad \text{in } \mathcal{D}, \ t > 0, \\ &\partial_t c_M - \mathrm{div}(D_M(f)\nabla c_M) + s_M f_B c_M = \alpha_M(x, t)c_V \quad \text{in } \mathcal{D}, \ t > 0, \\ &\partial_t c_U - \mathrm{div}(D_U(f)\nabla c_U) + s_U f_F c_U = \alpha_U(x, t)c_V \quad \text{in } \mathcal{D}, \ t > 0. \end{aligned} \tag{1.8}$$

where $s_M, s_U > 0$ and

$$D_j(f) = D_j^B f_B + D_j^E f_E + D_j^F f_F, \quad j = V, D, M, U,$$

for some positive constants D_j^i, $i \in \{B, E, F\}$. Regarding the reaction rates α_j, $j \in \{V, D, M, U\}$ and β_D, there exist smooth non-negative potentials $V_j^k : \mathcal{D} \to \mathbb{R}$ such that

$$\alpha_j(x, t) = \sum_{k=1}^{N_1} V_j^k(X_1^k(t) - x), \quad \beta_D(x, t) = \sum_{k=1}^{N_2} V_D^k(X_2^k(t) - x). \tag{1.9}$$

Lastly, the equations (1.8) are complemented with the homogeneous Neumann- and initial-boundary conditions

$$c_j(0) = c_j^0 \quad \text{in } \mathcal{D}, \quad \nabla c_j \cdot \nu = 0 \quad \text{on } \partial\mathcal{D}, \ j = V, D, M, U. \tag{1.10}$$

We aim to prove the existence of a solution of system (1.5)-(1.10). By (1.5), cells in this model are treated as discrete entities who are allowed to move continuously, meaning not on a grid from grid-point to grid-point, but in a continuum of space. The model above is thereby an example of a cell based off-lattice model. This is not the only way to model angiogenesis, which will be briefly discussed in the next subsection, which is based on [35, Section 1.2].

1.3.1. State of the Art

There are several approaches in the literature to model angiogenesis, mostly in the context of tumour growth. Cellular automata models divide the computational domain into a discrete set of lattice points, and endothelial cells move in a discrete way. Such models are quite flexible, and intra-cellular adherence can be easily implemented, but their numerical solution is computationally expensive when the numbers of cells or molecules are large [43]. In individual-based off-lattice models, the cells are treated as discrete entities, and their movement is not restricted to any lattice points [18]. Continuum-scale models consider cell densities whose dynamics is described by partial differential equations; see, e.g., [13] for wound healing and [37] for angiogenesis. Chemotaxis can be modelled in this approach by Keller–Segel-type equations, which admit global weak solutions in two space dimensions without blow-up [27]. A hybrid approach was investigated in [22], where the blood vessel network is implemented on a lattice, tip cells are moving in a lattice-free way, and other cells are modelled macroscopically as densities. An off-lattice cell-based approach was chosen in [8], from where the model of angiogenesis discussed in this work originates. The novelty of [8] is the distinction of tip and stalk cells and the inclusion of proteins segregated by the tip cells.

In other models, stochastic effects have been included. In [87], the movement of the tip cells is modelled by a SDE, with a deterministic part describing chemotaxis, and a stochastic part modelling random motion. The mean-field limit in a stochastic many-particle system, leading to reaction-diffusion equations, was performed in [20, 85]. We also refer to the reviews [24, 81] on further modelling approaches of angiogenesis.

Numerical simulations of a coupled SDE-PDE model for the movement of the tip cells and the dynamics of the tumour angiogenesis factor, fibronectin (a protein of the extracellular matrix), and matrix degrading enzymes were presented in [21]. Other SDE-PDE models in the literature are concerned with the proton dynamics in a tumour [64], acid-mediated tumour invasion [47], and viscoelastic fluids [57]. However, only the works [47, 64] treat a genuine coupling between SDEs and PDEs. While the model in [47] also includes a cross-diffusion term in the equation for the cancer cells, we have simpler reaction-diffusion equations but with nonlocal diffusivities. The model of [64] also includes nonlocal terms, but they are different from ours. Up to our knowledge, the mathematical analysis of system (1.5)–(1.10) is new.

What follows is a presentation of the mathematical line of reasoning used in Part II to obtain an existence result for the discussed angiogenesis model.

1.3.2. Mathematical Challenges and Main Results

Through (1.9), the concentrations c_j, $j \in \{V, D, M, U\}$ and in turn f_l, $l \in \{B, E, F\}$, depend on the paths $X_i^k(t)$, $i = 1, 2$, $1 \leq k \leq N_i$, making them stochastic processes. Popular existence results found in the literature, see for instance [73], can hence no longer be applied, as this results in an additional non-linear and especially non-local dependency of the coefficients g_i on X_i^k and the necessary measurability cannot be simply given by assumption. Additionally, the coefficients g_i and σ_i need to satisfy a Lipschitz- or weak monotonicity- condition regarding the space-variable x, adding an additional requirement on the regularity of ∇c_V, ∇c_D and ∇f_S. Given such sufficiently measurable, bounded and smooth processes σ, ∇c, f and ∇f who are not depending on $X = \left(X_i^k\right)_{i=1,2}^{1\leq k\leq N_i}$ such that the assumptions of [73, Theorem 3.1.1] are satisfied, a unique solution to (1.5) exists. This allows to set up a fixed point argument. By choosing a stochastic process $\widetilde{X} = \left(\widetilde{X}_i^k\right)_{i=1,2}^{1\leq k\leq N_i}$ in a suitable Banach space Y, one can solve (1.7)-(1.10) for almost every fixed $\omega \in \Omega$ to obtain smooth concentrations c and volume fractions f, which can then be used to solve (1.5). This defines an operator Φ:

$$\widetilde{X} \to (\tilde{c}, \tilde{f}) \to X =: \Phi(\widetilde{X}).$$

Every fixed point of Φ is then a solution to (1.5)-(1.10). In order for this operator to be well defined the Banach space Y has to be chosen in a way to guarantee the needed regularity and measurability of c and f. Given smooth enough Hölder continuous coefficients, linear uniformly parabolic partial differential equations give rise to classical Hölder continuous solutions, [67]. Furthermore, the property of c and f to be measurable depends on the measurability of $\widetilde{X}$ (see Lemma 21). A probable choice for Y would therefore be a subspace of the space of adapted processes with almost surely Hölder continuous paths. More precisely, we will set $Y = Y_R(0, T; \mathcal{D})$ for some $R > 0$, where

$$\begin{aligned} Y_R(0,T;\mathcal{D}) := \big\{ X \in C^{1/2}([0,T]; L^4(\Omega)) : \|X\|_{C^{1/2}([0,T];L^4(\Omega))} \leq R, \\ X(t) \text{ is } \mathcal{F}_t\text{-measurable},\ X(t) \in \overline{\mathcal{D}} \text{ a.s. for all } t \in [0,T] \big\} \end{aligned}$$

and we equip it with the standard norm of $C([0,T], L^4(\Omega))$. Assuming the volume filling condition

$$f_B^0 + f_F^0 + f_E^0 \equiv 1, \tag{1.11}$$

and further technical assumptions (B1)-(B5) (see section 6.1), we can show existence of a unique classical solution to (1.7)-(1.10) for almost all $\omega \in \Omega$ (see Theorem 17). Additionally, by Lemma 15 , we obtain for such solutions c a constant $C > 0$ and the uniform estimate

$$\|c\|_{L^\infty(0,T;W^{2,\infty}(\mathcal{D}))} \leq C.$$

This is a direct result from [72], from where we can conclude the required Lipschitz continuity of ∇c. The measurability of c is then obtained by the adaptivity of $\widetilde{X}$. These properties are inherited by f_B and f_F due to

$$f_B(x,t) = f_B^0(x)\exp\Big(-s_B\int_0^t c_M(x,s)\mathrm{d}s\Big),$$
$$f_F(x,t) = f_F^0(x)\exp\Big(-s_F\int_0^t c_U(x,s)\mathrm{d}s\Big).$$

Similarly they follow for f_E as it satisfies $f_E = 1 - f_B - f_F$, which is a direct consequence of the volume filling condition (1.11) and the last equation of (1.7). Hence, (1.5) has a unique solution under the assumptions (B1)-(B5). By Kolmogorovs continuity criteria, this solution has almost surly Hölder continuous paths and can be shown to be bounded in Y. The operator Φ is thereby well defined. To show the existence of a unique fixed point we firstly prove stability results for solutions $\Phi(\widetilde{X}) = X$, $\Phi(\widetilde{X}') = X'$ of (1.5) and the respective solutions c, c' of (1.8)-(1.10). To be more precise, for some constant $C > 0$, we prove in subsection 6.3.3 the estimates

$$\mathbb{E}|X(t) - X'(t)|^4 \le Ct\int_0^t \mathbb{E}\|c(s) - c'(s)\|^4_{C^1(\overline{\mathcal{D}})}\mathrm{d}s,$$
$$\|c - c'\|_{L^4(0,T;W^{2,4}(\mathcal{D}))} \le C\big(\|\alpha - \alpha'\|_{L^4(\mathcal{D}\times(0,T))} + \|\beta - \beta'\|_{L^4(\mathcal{D}\times(0,T))}\big).$$

Here α and β, respectively α' and β', are defined via (1.9) with respect to the paths of $\widetilde{X}$ and $\widetilde{X}'$. By the Sobolev embedding $W^{2,4}(\mathcal{D}) \hookrightarrow C^1(\overline{\mathcal{D}})$, the two stability results can then be combined to conclude Φ is a contraction. This lets us derive the main result of this section of the thesis:

Main Result of Part II - Angiogenesis: (Chapter 6, Theorem 8) *Let Assumptions (B1)–(B5) made in section 6.1 hold. Then there exist a unique solution (f, c, X) to (1.5)–(1.8), (1.10) and some constant $R > 0$ such that*

- $f = (f_B, f_E, f_F)$ *solves (1.7) pathwise a.s., where* $f_i \in C^0([0,T];\ L^2(\mathcal{D})) \cap L^\infty(\mathcal{D}\times(0,T))$*;*
- $c = (c_V, c_D, c_M, c_U)$ *is a classical solution to (1.8) and (1.10) pathwise a.s.;*
- c*,* ∇c*,* f *and* ∇f *are measurable;*
- $X_i^k \in Y_R(0,T;\mathcal{D})$ *is a strong solution to (1.5) for* $i = 1, 2$*,* $k = 1, \ldots, N_i$*.*

For the exact notion of measurability used and the definition of a strong solution we refer to section 6.1 or Definition 41 and Definition 42 in the Appendix A.2.2.

1.3.3. Outlook

The following considerations could act as starting points for future work on the topic of analysing this or similar models for angiogenesis:

i) Depending on the chemical environment, endothelial cells change from stalk cell to tip cell and vice versa. In [8] the probability for this change at each point in time is modelled by exponential distributions $\mathrm{Exp}(\lambda)$, where λ is a function of the concentrations c_V and c_D evaluated at the position X_i^k of the cells midpoint. The existence analyis for the exact model of [8] has, up to the knowledge of the author, not been done.

ii) As in reality endothelial cells are objects extending into three dimensions and are not zero-dimensional points in space, they interact with chemical messenger molecules (i.e. c_V, c_D) over the range given by their size. Therefore a case can be made to replace ∇c_V with $\nabla c_V * \eta$, respectively ∇c_D with $\nabla c_D * \eta$, where $\eta \in C^\infty(\mathbb{R}^3)$ is a mollifier with supp $\eta \subseteq B_\epsilon(0)$, for some suitable $\epsilon > 0$. This might lead to lower requirements regarding the regularity of the initial data, as stability results and estimates regarding the L^p-norm of c might suffice to proof a result akin to Theorem 8 (see **Main Result of Part II - Angiogenesis**), due to the regularity added by the convolution.

1.4. Main Results and State of the Art for Part II - Cell Based Models - Vesicle Transport

Projections from the cell body of an undifferentiated neuron are called neurites. For such a neurite to grow, the necessary material is transported in the form of vesicles from the cell body, also called the soma, to the tip of the neurite. Vice versa, if the neurite undergoes a period of contraction, it is transported in the other direction. Here, vesicles travelling towards the tip are refereed to as anterograde vesicles, respectively retrograde vesicles when travelling away from it. As the diameter of a neurite is comparably small to its length L, in the literature they are often modelled as one-dimensional [48]. Let a and r be the volume fractions of anterograde- and retrograde- vesicles along the length $(0, L)$ of a neurite and $u_0 = 1 - a - r$ the unoccupied space. Furthermore, let Λ_s and Λ_n be the concentration of vesicles in pools in the soma, situated at $x = 0$ and the growth cone at the tip of the neurite at $x = L$. Due to the finite size of the pools, the maximum number of vesicles inside them is bounded, giving upper limits $\Lambda_s^{\max}$ and $\Lambda_n^{\max} > 0$ for Λ_s and Λ_n.
Starting from a cell based on-lattice model, where vesicles move from grid-point to grid-point according to given transition rates, a 2-species system of ordinary differential equations was derived in [48] to describe the general evolution of Λ_s, Λ_n, a and r at the grid-points of the lattice. The transition rates thereby depend among other factors on given potentials V_a and V_r, which determine the direction of the transport. The use of non-specific potentials makes the model more generalized, allowing to describe 2-species systems, where agents of the different species do not have to travel in opposite directions as it is the case with anterograde and retrograde vesicles. Replacing a and r with u_i, $i = 1, 2$ to indicate this more general setting, from this model the following cross diffusion system can be derived

in the diffusion limit (see section 5.3.2):

$$\begin{aligned}
&\partial_t u_1 + \partial_x J_1 = 0, \quad J_1 := -D_1\big(u_0\partial_x u_1 - u_1\partial_x u_0 - u_0 u_1 \partial_x V_1\big), \quad x \in (0,L), \quad t > 0,\\
&\partial_t u_2 + \partial_x J_2 = 0, \quad J_2 := -D_2\big(u_0\partial_x u_2 - u_2\partial_x u_0 - u_0 u_2 \partial_x V_2\big), \quad x \in (0,L), \quad t > 0.
\end{aligned} \tag{1.12}$$

Corresponding to the in- and outflow fluxes of vesicles, these equations are complemented with boundary conditions,

$$\begin{aligned}
J_1(0,t) &= J_1^0[u](t) := \alpha_1 \frac{\Lambda_s(t)}{\Lambda_s^{\max}} u_0(0,t),\\
J_1(L,t) &= J_1^1[u](t) := \beta_1\left(1 - \frac{\Lambda_n(t)}{\Lambda_n^{\max}}\right) u_0(L,t) u_1(L,t),\\
J_2(0,t) &= J_2^0[u](t) := -\beta_2\left(1 - \frac{\Lambda_s(t)}{\Lambda_s^{\max}}\right) u_0(0,t) u_2(0,t),\\
J_2(L,t) &= J_2^1[u](t) := -\alpha_2 \frac{\Lambda_n(t)}{\Lambda_n^{\max}} u_0(L,t) \quad \text{for } t > 0.
\end{aligned} \tag{1.13}$$

Here the parameters D_i, α_i and β_i, $i = 1, 2$ are positive constants. For the concentrations Λ_s, Λ_n we accordingly have the ordinary differential equations

$$\partial_t \Lambda_n = J_1^1[u] + J_2^1[u], \quad \partial_t \Lambda_s = -(J_1^0[u] + J_2^0[u]) \quad , t > 0. \tag{1.14}$$

For a more detailed description of the model and interpretation of terms see section 5.3. Our main result in this section of the thesis is to find a solution of (1.12)-(1.14), supplemented with an appropriate initial value condition

$$u_1(\cdot, 0) = u_1^0, \quad u_2(\cdot, 0) = u_2^0 \quad \text{in } (0,L), \quad \Lambda_s(0) = \Lambda_s^0, \quad \Lambda_n(0) = \Lambda_n^0. \tag{1.15}$$

As volume fractions are non-negative and bounded (by one), we assume $0 \le u_i^0 \le 1$ almost everywhere for $i = 1, 2$. This holds similarly for the starting vesicle concentrations in the pools, giving $0 \le \Lambda_s \le \Lambda_s^{\max}$ and $0 \le \Lambda_n \le \Lambda_n^{\max}$.
Besides (1.12)-(1.15) and the on-lattice model in [48], additional approaches to model vesicle transport can be found in the literature, which will be discussed in the following subsection taken from [36, Section 1].

1.4.1. State of the Art

For the case of single-species vesicles, a Fokker–Planck equation with in- and outflow boundary conditions was analysed in [16]. The work [11] models a limited transport capacity inside the neurites by taking into account size exclusion effects for a single motor-cargo complex with and without vesicles. Advection-diffusion equations for the bidirectional vesicular transport were derived in [12] and dynamically varying neurite lengths are allowed in [75], leading to drift-diffusion-reaction equations. A lattice model for the probability that a receptor travelling with a vesicle is located at a given cell was analysed in [9]. This model was then generalized in [10] by allowing motor-complexes to carry an arbitrary number of vesicles, which leads to Becker–Döring equations for aggregation-fragmentation processes.

The size of the cargo vesicles, which strongly influences the speed of retrograde transport, was taken into account in [82], and a free-boundary problem for the radius of the vesicle has been formulated. We also mention the paper [4] for a related cross-diffusion system with free boundary and non-vanishing flux boundary conditions.

Equations (1.12) are similar to the ion-transport model in [38]. The analysis of this system was based on the boundedness-by-entropy method [15, 58] and a version of the Aubin–Lions compactness lemma which takes into account the degeneracy at $u_0 = 0$ [96]. Compared to previous works like [58], where no-flux boundary conditions are imposed, the novelties are the non-linear Robin boundary conditions and the coupling to ordinary differential equations. The main difficulty here is the treatment of the boundary conditions. Linear Robin boundary conditions were considered in [17] but for stationary drift-diffusion equation for one species only.
What follows is a presentation of the mathematical line of reasoning used in Part II to obtain a weak-existence result for the discussed model (1.12)–(1.15) regarding vesicle transport inside neurites.

1.4.2. Mathematical Challenges and Main Result

Without loss of generality we set $L = 1$ and $\mathcal{D} = (0,1)$. Let $T > 0$, $u = (u_1, u_2)$, $V = (V_1, V_2)$ and $\phi = (\phi_1, \phi_2) \in (L^2(0,T; H^1(\mathcal{D})))^2$. We consider the following weak formulation of (1.12)-(1.13):

$$\int_0^T \langle \partial_t u, \phi \rangle \mathrm{d}t + \int_0^T \int_{\mathcal{D}} \partial_x \phi (A(u) \partial_x u) \mathrm{d}x \mathrm{d}t - \int_0^T \int_{\mathcal{D}} \sum_{i=1}^{2} u_0 u_i \partial_x V_i \partial \phi_i \mathrm{d}x \mathrm{d}t + \sum_{i=1}^{2} \int_0^T \left[J_i(x,t) \phi(x,t) \right]_{x=0}^{x=1} \mathrm{d}t = 0, \tag{1.16}$$

where $\langle \cdot, \cdot \rangle$ denotes the dual product of $H^1(\mathcal{D})$ and $H^1(\mathcal{D})'$. Here the diffusion matrix A is given by

$$A(u) = \begin{pmatrix} D_1(1-u_2) & D_1 u_1 \\ D_2 u_2 & D_2(1-u_1) \end{pmatrix}. \tag{1.17}$$

Standard methods for systems of parabolic partial differential equations use the ellipticity of the corresponding bilinear form given by the respective diffusion matrix to find uniform L^2-bounds of ∂u. This uniform bound is crucial to ensure weak convergence of a series of solutions of approximative problems whose limit can be shown to be a solution. As A is not guaranteed to be strictly positive definite, much less its corresponding bilinear form elliptic, this strategy is not feasible as is. To find a solution to (1.16), we therefore build on top of the methods used in [58], extending them to incorporate (1.14) and the boundary conditions (1.13). The idea is to transform u into a entropy variable $w = h'(u)$ via a suitable entropy density h and to discretise in time to obtain a new system where standard methods can be applied. The solutions of this time-independent problems are then arranged and interpreted as step functions on $[0, T]$ with values in the space $H^1(\mathcal{D}, \mathbb{R}^2)$. Letting the discretisation parameter go to zero, the original problem is recovered and the step functions converge weakly to a solution. For this purpose, we use

$$h(u) = \sum_{i=1}^{2} u_i(\log u_i - 1) + u_0(\log u_0 - 1)$$

as entropy-density. See section 5.3 for more details on the choice of h. Let $\epsilon, \tau > 0$ be the regularity and time-discretisation parameters, $t_k = \tau k$, $k \in \mathbb{N}$ the time steps, $w^0 = h'(u^0)$, and $u(w) = h'(u)^{-1}$. Setting $B = A(u)h''(u)^{-1}$, discretising (1.16) in time and adding a regularization term, we obtain for the unknowns w^k the equations

$$\begin{aligned}\frac{1}{\tau}\int_{\mathcal{D}}(u(w^k) - u^{k-1}) \cdot \phi \mathrm{d}x + \int_{\mathcal{D}} \partial_x\phi \cdot B(w^k)\partial_x w^k \mathrm{d}x - \int_{\mathcal{D}} \sum_{i=1}^{2} u_0(w^k)u_i(w^k)\partial_x V_i \partial_x \phi_i \mathrm{d}x \\ + \sum_{i=1}^{2} \big(J_i^1[u(w^k)](t_k)\phi_i(1) - J_i^0[u(w^k)](t_k)\phi_i(0)\big) + \varepsilon \int_{\mathcal{D}} (\partial_x w^k \cdot \partial_x \phi + w^k \cdot \phi)\mathrm{d}x = 0,\end{aligned} \tag{1.18}$$

for all $\phi_i \in H^1(\mathcal{D})$, $i = 1, 2$, where we notice $B(u)\partial_x w = A(u)\partial_x u$. We define $u^\tau(x,t) := u^k(x)$ for $t \in (t_{k-1}, t_k]$, $w^\tau = h'(u^\tau)$ and the shift operator σ via its action $(\sigma_\tau u^{(\tau)})(\cdot, t) = u^{k-1}$ for $t \in (t_{k-1}, t_k]$. For (1.18) we solve (1.14) regarding σu^τ, where we set $\Lambda_n = \Lambda_n^{(\tau)}$ meaning

$$\Lambda_n^{(\tau)} = \Lambda_n(0) + \beta_1 \int_0^t (1 - \Lambda_n^{(\tau)}(r))\sigma_\tau(u_0^{(\tau)}u_1^{(\tau)})(1, r)\mathrm{d}r - \alpha_2 \int_0^t \Lambda_n^{(\tau)}(r)\sigma_\tau u_0^{(\tau)}(1, r)\mathrm{d}r, \tag{1.19}$$

with a similar equation for $\Lambda_s^{(\tau)}$. In (1.18) Λ_n and Λ_s are evaluated at t_k, where we point out that $\Lambda_n^{(\tau)}(t_k)$ and $\Lambda_s^{(\tau)}(t_k)$ do not depend on w^k or u^k. By integrating (1.18) over t, we get an approximate system for (1.16) in the parameters $(\epsilon,\ \tau)$.

$$\begin{aligned}\frac{1}{\tau}\int_0^T \int_{\mathcal{D}} (u^{(\tau)} - \sigma_\tau u^{(\tau)})\phi \mathrm{d}x\mathrm{d}t + \varepsilon \int_0^T \int_{\mathcal{D}} (\partial_x w^{(\tau)} \partial_x \phi + w^{(\tau)}\phi)\mathrm{d}x\mathrm{d}t \\ + \sum_{i=1}^{2} D_i \int_0^T \int_{\mathcal{D}} (u_0^{(\tau)}\partial_x u_i^{(\tau)} - u_i^{(\tau)}\partial_x u_0^{(\tau)} - u_0^{(\tau)}u_i^{(\tau)}\partial_x V_i)\partial_x \phi_i \mathrm{d}x\mathrm{d}t \\ + \sum_{i=1}^{2} \int_0^T \big(J_i^1[u^{(\tau)}](t)\phi_i(1,t) - J_i^0[u^{(\tau)}](t)\phi_i(0,t)\big)\mathrm{d}t = 0.\end{aligned} \tag{1.20}$$

A short calculation shows $B(w)$ satisfies the following non-negativity property for some $c > 0$ (see lemma 28):

$$\partial_x w \cdot B\partial_x w = (\partial_x u) \cdot h''(u)A(u)(\partial_x u) \geq c\sum_{i=1}^{2} u_0(\partial_x \sqrt{u_i})^2 + c(\partial_x \sqrt{u_0})^2. \tag{1.21}$$

From this property and the assumption $V_i \in H^1(\mathcal{D})$, a uniform bound can be derived

$$\int_{\mathcal{D}} h(u^k) - h(u^{k-1})\mathrm{d}x + \frac{c\tau}{2}\int_{\mathcal{D}} \partial_x w^k \cdot B(w^k)\partial_x w^k \mathrm{d}x + \varepsilon\tau \int_{\mathcal{D}} (|\partial_x w^k|^2 + |w^k|^2)\mathrm{d}x \le C\tau, \tag{1.22}$$

where the positive constant C does not depend on the parameters ϵ and τ. Linearising by replacing $B(w^k)$ with $B(y)$ and $u_i(w^k)$ with $u_i(y)$, $i = 0, 1, 2$, where $y \in C^0(\mathcal{D}; \mathbb{R}^2)$, the lemma of Lax-Milgram can be applied to find an unique solution $w = w^k$ in $H^1(\mathcal{D})$. It is common to use the space $L^\infty(\mathcal{D}, \mathbb{R}^2)$, see [58], but by using $C^0(\mathcal{D}; \mathbb{R}^2)$ the continuity of y guarantees that there exists a well defined boundary. By the compact (Sobolev) embedding $H^1(\mathcal{D}, \mathbb{R}^2) \hookrightarrow C^0(\mathcal{D}, \mathbb{R}^2)$ and Leray-Schauders fixed point theorem, (1.18) has a solution w^k, given $u^{k-1} \in L^\infty(\mathcal{D}; \mathbb{R}^2)$. This last constraint follows from $u^0 \in L^\infty(\mathcal{D}; \mathbb{R}^2)$ and $h' : \mathbb{R}^2 \to [0, 1]^2$. This is the statement of Lemma 30. From (1.22), we obtain uniform bounds of $u^{(\tau)}$ in subsection 7.2.3 and due to the uniformity there exist weakly converging subsequences of $(u_0^{(\tau)})^{1/2}u^{(\tau)}$, $u_0^{(\tau)}u^{(\tau)}$ and $u_0^{(\tau)}$ in $L^2(0, T; H^1(\mathcal{D}))$. Additionally, of $\partial_t u^{(\tau)}$ in $L^2(0, T; H^1(\mathcal{D})')$. As $0 \le u_i \le 1$, $i = 0, 1, 2$, the integrand in (1.19) is bounded and the family $\Lambda_n^{(\tau)}$ therefore equicontinuous and uniformly bounded. The theorem of Arzelà -Ascoli therefore guarantees a uniformly converging subsequence. The same holds true for $\Lambda_s^{(\tau)}$. Going over to the limits of this sequences, we obtain the main result of this part of the thesis:

Main Result Part II - Vesicle Transport in Neurites: (Chapter 7, Theorem 27) *Under the assumptions made above, there exists a weak solution* $(u_1, u_2, \Lambda_n, \Lambda_s)$ *to* (1.12)–(1.15) *satisfying the weak formulation (1.16) and* $u_1, u_2 \ge 0$, $u_1 + u_2 \le 1$ *in* $\mathcal{D} \times (0, T)$. *Additionally,*

$$\sqrt{u_0}u_i,\ \sqrt{u_0} \in L^2(0, T; H^1(\mathcal{D})), \quad \partial_t u_i \in L^2(0, T; H^1(\mathcal{D})'), \quad i = 1, 2 \tag{1.23}$$

and the initial conditions (1.15) *are fulfilled in the sense of* $H^1(\mathcal{D})'$, *and the equations* (1.14) *hold almost everywhere.*

1.4.3. Outlook

The following considerations could act as starting points for future work on the topic of analysing this or similar models for vesicle transport inside neurites:

i) Following the derivation of the on-lattice model for vesicle transport in [48], which also is the basis for the model (1.12)-(1.15), the boundary terms (1.13) take a slightly different form,

$$\begin{aligned} J_1(L, t) = J_1^1[u](t) &:= \beta_1\left(1 - \frac{\Lambda_n(t)}{\Lambda_n^{\max}}\right)u_1(L, t), \\ J_2(0, t) = J_2^0[u](t) &:= -\beta_2\left(1 - \frac{\Lambda_s(t)}{\Lambda_s^{\max}}\right)u_2(0, t), \end{aligned} \tag{1.24}$$

where the ordinary differential equations (1.14) change accordingly. The dependency on u_0 has been dropped in this cases, which due to $H^1((0, 1)) \hookrightarrow C([0, 1])$ and estimate (1.23) guaranteed the well posedness of the boundary terms (1.13). Up to the knowledge of the author, the existence of a weak solution of (1.12), (1.14)-(1.15) coupled with the boundary conditions (1.24) is an open problem.

ii) Vesicles transport the building blocks of neurites and their creation and elimination goes along with growth or contraction of the neurite. Hence, it seems reasonable to consider the length of the neurite L to change in time according to the change in u, Λ_s and Λ_n, meaning $L = L(t, u, \Lambda_n, \Lambda_s)$. The exact dependency of L on u, Λ_s and Λ_n thereby would need to be established according to the relevant biological processes. This introduces an additional unknown L and a changing domain $(0, L)$ on where (1.12) would have to be considered, which adds another layer of complexity to the model.

1.5. Structure of the Thesis

This thesis is divided into 2 parts.
In **Part I**, including chapter 2-4, a random batch method for the stochastic many particle system (1.1) is studied. It is based on [29]. In chapter 2, a deeper explanation of the method, a link to related problems, additional assumptions to the model (1.1) and the main result are given. The numerical analysis to prove the main result is done in chapter 3 and numerical experiments are presented in chapter 4.
Part II is based on [35] and [36]. It ranges from chapter 5-8 and entails the mathematical analysis of the two biological models: The angiogensis model (1.5)-(1.8),(1.10) and model (1.12)-(1.15) for vesicle transport inside neurites. The models are explained in depth in chapter 5, where a formal derivation of the model for vesicle transport is given as well. In chapter 6 and chapter 7, the main existence results together with necessary assumptions are stated and the main results are proven. Numerical experiments and simulations for the two models can be found in chapter 8.
Auxiliary results known from the literature are gathered in **Appendix A**, which in part consists of the appendixes at the end of [29] and [35].

Part I.

Simulation of Stochastic Many Particle Systems

Part I is constructed from the contents of the following article:

[29] E. S. Daus, M. Fellner and Ansgar Jüngel. Random-batch methods for multi-species stochastic interacting particle systems. *Journal of Computational Physics.* Volume 463 (2022), 111220.

2. Introduction to Random Batch Algorithm for Stochastic Many Particle Systems

The collective behaviour of particles or agents of multiple species can be described by interacting particle systems, which are an important tool for modelling complex real-world phenomena with applications in physics, biology, and social sciences. In this chapter, we discuss the stochastic interacting many particle model (1.1) introduced in section 1.2 and the random batch method in more detail and present the main result of Part I. We furthermore give a quick overview over the strategy of the proof and show a link to related problems.

2.1. Setting

The dynamics of the multi-species system is described by

$$\mathrm{d}X_i^k = -\nabla V_i(X_i^k)\mathrm{d}t + \sum_{j=1}^{n} \alpha_{ij} \sum_{\substack{\ell=1 \\ (i,k)\neq(j,\ell)}}^{N_j} K_{ij}(X_i^k - X_j^\ell)\mathrm{d}t + \sigma_i \mathrm{d}B_i^k(t), \tag{2.1}$$

$$X_i^k(0) = X_i^{0,k} \quad \text{for } i = 1,\dots,n,\ k = 1,\dots,N_i, \tag{2.2}$$

where

$$\alpha_{ij} = \frac{1}{N_j - \delta_{ij}}, \quad i,j = 1,\dots,n, \tag{2.3}$$

and δ_{ij} is the Kronecker delta. The stochastic process $X_i^k(t) \in \mathbb{R}^d$ ($d \geq 1$) represents the position of the kth particle (or the features of the kth agent) of species i in a system of $N = \sum_{i=1}^n N_i$ particles. The function ∇V_i describes some (given) external force, K_{ii} and K_{ij} are the interaction kernels between particles of the same and of different species, respectively, $\sigma_i > 0$ are diffusion coefficients, and B_i^k are N independent standard Brownian motions. The initial data $X_{0,i}^1, \dots, X_{0,i}^{N_i}$ are assumed to be independent and identically distributed. We also consider the case of multiplicative noise, where the diffusion $\sigma_i(X_i^k)$ depends on the position of the particle X_i^k; see section 3.4.

Equations (2.1) can be used to model the information flow through social networks [2], the dynamics of opinions [33], the herding of sheep by dogs [88], or the segregation behaviour of populations [25]. Furthermore, stochastic gradient descent can be interpreted as the evolution of interacting particle systems governed by a potential related to the objective function used to train neural networks [84].

2.2. Random-batch method

The random-batch method is defined as follows. Let the number of particles $N_i \in \mathbb{N}$ of the ith species be an even number, where $i = 1, \dots, n$. We introduce the time steps $t_m = m\tau$ with the time step size $\tau > 0$ and $m = 1, \dots, M := \lceil T/\tau \rceil$, and $T > 0$ is the end time. For a given $m \in \{1, \dots, M\}$, we divide the set $\{1, \dots, N_i\}$ randomly into b_i batches $\mathcal{C}_{i,1}, \dots, \mathcal{C}_{i,b_i}$ of size p_i. This means that we choose $p_i \geq 2$ and $b_i \geq 1$ such that $N_i = b_i p_i$, and we consider not all interactions but only those in the same batch. Furthermore, we introduce the super-batches $\mathcal{C}_r = \{(i,k) : k \in \mathcal{C}_{i,r}\}$ for $1 \leq r \leq \max\{b_1, \dots, b_n\}$ (see Figure 2.1). For any particle X_i^k, there exists exactly one super-batch such that $(i,k) \in \mathcal{C}_r$ for some $r \geq 0$.

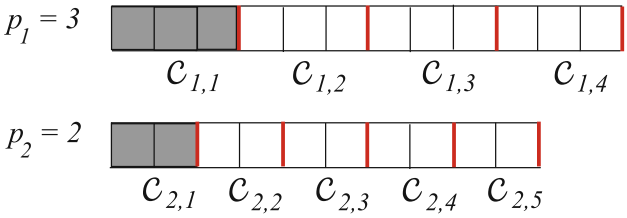

Figure 2.1.: Batches $\mathcal{C}_{i,r}$ for a two-species system with $N = 22$ particles, four batches of size $p_1 = 3$, and five batches of size $p_2 = 2$. The particles in the super-batch $\mathcal{C}_1$ are marked in grey color.

We solve the particle system in the time interval $(t_{m-1}, t_m]$ with initial datum $\widetilde{X}_i^k(t_{m-1})$. The random-batch process $\widetilde{X}_i^k$ is defined for $t_{m-1} < t \leq t_m$ as the solution to

$$\mathrm{d}\widetilde{X}_i^k = -\nabla V_i(\widetilde{X}_i^k)\mathrm{d}t + \sum_{j=1}^n \beta_{ij} \sum_{\substack{\ell \in \mathcal{C}_{j,r} \\ (i,k) \neq (j,\ell)}} K_{ij}(\widetilde{X}_i^k - \widetilde{X}_j^\ell)\mathrm{d}t + \sigma_i \mathrm{d}B_i^k, \tag{2.4}$$

where

$$\beta_{ij} = \frac{b_i}{(p_j - \delta_{ij}) \min\{b_i, b_j\}}, \quad i, j = 1, \dots, n. \tag{2.5}$$

Instead of summing over all interactions, the sum in (2.4) only accounts for the interactions in each small batch. Observe that we use the same Brownian motions as in (2.1). The sum over all $\ell \in \mathcal{C}_{j,r}$ means that we sum over all (j,ℓ) which are in the same super-batch as (i,k). The factor $b_i / \min\{b_i, b_j\}$ in (2.5) does not appear in [52]; it is necessary to achieve consistency and convergence of the scheme. The scaling results from the different number of non-trivial batches $\mathcal{C}_{i,r}$ of the different species. Indeed, let $b_i < b_j$. Only b_i batches of the first b_j super-batches contain a batch of both species i and j, while any super-batch $\mathcal{C}_r$ with $r > b_i$ does not contain neither of them. So, only the share b_i/b_j of particles of the ith species can interact with those of the jth species. In other words, each particle of the ith species interacts with particles of the jth species with probability b_i/b_j. This yields the correction factor b_i/b_j. The random-batch algorithm is summarized in Algorithm 2.2.

When we allow for pairwise interactions between *all* particles, the computational cost at each time step is of order $O(N^2)$. Since we have M time steps, the total cost of this naive

Algorithm 1 (Pseudo-code for the multi-species random-batch algorithm)

for $k = m, \dots, M$ **do**
  for $i = 1, \dots, n$ **do**
    Divide $\{1, \dots, N_i\}$ randomly into b_i batches $\mathcal{C}_{i,1}, \dots, \mathcal{C}_{i,b_i}$ with size p_i each.
    for $r = 1, \dots, b_i$ **do**
      For every $(i,k) \in \mathcal{C}_r$, update $\widetilde{X}_i^k$ by solving (2.4) in the interval $(t_{m-1}, t_m]$ with initial datum $\widetilde{X}_i^k(t_{m-1})$.
    end for
  end for
end for

algorithm is $O(MN^2)$. In the random-batch method, each particle ends up in exactly one super-batch $\mathcal{C}_r$ for some $r \geq 1$ and is chosen only once (i.e. without replacement). Then the total computational cost becomes $O(pMN)$, where $p = \sum_{i=1}^n p_i$. As p is typically a small number (often $p_i = 2$), the total cost has been reduced by approximately one order of magnitude. We show in this part of the thesis that, under suitable conditions on the external potentials and the kernel functions, the L^2 error of the error process $\widetilde{X}_i^k(t) - X_i^k(t)$ converges to zero as $\tau \to 0$ uniformly in time, and the convergence is, as expected, of order $O(\sqrt{\tau})$. The idea of the method is the fact that in time average, the random force is consistent with the full interaction (see Proposition 2), and the convergence is like in the law of large numbers, but in time.

2.3. Assumptions and main result

We start by introducing notation and giving some definitions. Let $(\Omega, \mathcal{F}, \mathbb{F}, \mathbb{P})$ be a filtered probability space, let $\xi_{m-1,i}$ denote the random division of batches of species i at t_{m-1}, and set $\xi_{m-1} = (\xi_{m-1,1}, \dots, \xi_{m-1,n})$. We define the filtrations $(\mathcal{F}_m)_{m\geq 0}$ and $(\mathcal{G}_m)_{m\geq 0}$ by

$$\mathcal{F}_{m-1} = \sigma\big(X_i^{0,k},\, B_i^k(t),\, \xi_{j,i} : t \leq t_{m-1},\, 1 \leq i \leq n,\, 1 \leq j \leq m-1\big),$$
$$\mathcal{G}_{m-1} = \sigma\big(X_i^{0,k},\, B_i^k(t),\, \xi_{j,i} : t \leq t_{m-1},\, 1 \leq i \leq n,\, 1 \leq j \leq m-2\big).$$

The set $\mathcal{F}_{m-1}$ contains the information how the batches are constructed for $t \in [t_{k-1}, t_k)$. Denoting by $\sigma(\xi_{m-1,i})$ the σ-algebra generated by $\xi_{m-1,i}$, it holds that $\mathcal{F}_{m-1} = \sigma(\mathcal{G}_{m-1} \cup \sigma(\xi_{m-1,1}) \cup \dots \cup \sigma(\xi_{m-1,n}))$. We write $\|\cdot\|_p = (\mathbb{E}|\cdot|^p)^{1/p}$ to denote the $L^p(\Omega)$ norm for $1 \leq p < \infty$ and set $\|\cdot\| = \|\cdot\|_2$. In the whole chapter, $C > 0$, $C_i > 0$ denote generic constants whose values change from line to line in the proofs. We set $X = (X_i^k)_{i=1,\dots,n}^{k=1,\dots,N_i}$ and $\widetilde{X} = (\widetilde{X}_i^k)_{i=1,\dots,n}^{k=1,\dots,N_i}$. We impose the following assumptions:

(A1) Kernel functions: $K_{ij} \in C^2(\mathbb{R}^d)$ is bounded, Lipschitz continuous with Lipschitz constant $L_{ij} > 0$, and has a bounded second derivative.

(A2) Potential functions: $V_i \in C^2(\mathbb{R}^d)$, and there exist $C_V > 0$, $q_i > 0$ such that for all $x \in \mathbb{R}^d$,
$$|\nabla V_i(x)| + |D^2 V_i(x)| \leq C_V(1 + |x|^{q_i}), \quad i = 1, \dots, n.$$

(A3) Strong convexity: The function $x \mapsto V_i(x) - r_i|x|^2/2$ is convex, where $r_i > 2\sum_{j=1}^n \max\{L_{ij}, L_{ji}\}$ and $i = 1, \ldots, n$.

(A4) Synchronous coupling: $X_i^k(0) = \widetilde{X}_i^k(0) = X_i^{0,k}$ for $i = 1, \ldots, n$, $k = 1, \ldots, N_i$, where $X_{0,i}^1, \ldots, X_{0,i}^{N_i}$ are independent and identically distributed, and $X_i^{0,k}$ is $\mathbb{F}_0$-measurable with $\mathbb{E}|X_i^{0,k}|^{2\max\{1,q_i\}} < \infty$.

Under these assumptions (in particular, the Lipschitz continuity), standard results for stochastic differential equations [63] guarantee that (2.1) and (2.4) have (up to $\mathbb{P}$-distinguishability) unique strong solutions. The polynomial growth conditions on ∇V_i and D^2V_i are needed to prove the stability; see Lemma 4. The smallness condition on the Lipschitz constants of the kernel functions ensures that the evolution group of the deterministic part of (2.1) is a contraction, thus yielding error bounds uniformly in time.

Our main result reads as follows.

Theorem 1 (Error estimate)**.** *Let Assumptions* (A1)–(A4) *hold. Then there exists a constant $C > 0$, which is independent of $(b_i, p_i, N_i)_{i=1,\ldots,n}$, m, and T, such that*

$$\sup_{0<t<T} \sum_{i=1}^n \|(X_i^k - \widetilde{X}_i^k)(t)\| \le C\sqrt{\tau}\bigg(\sum_{i=1}^n \Gamma_i\bigg)^{1/2} + C\tau(1+\theta^\gamma), \quad t > 0,$$

where

$$\theta = \frac{\max_{j=1,\ldots,n} b_j}{\min_{j=1,\ldots,n} b_j}, \quad \gamma = 3\big(\max\{1, q_1, \ldots, q_n\} + 1\big), \tag{2.6}$$

$$\begin{aligned}\Gamma_i = &\sum_{\substack{j,j'=1\\ j,j'\neq i,\, j\neq j'}}^n \bigg(\frac{\max\{b_i, b_j, b_{j'}\}}{\max\{b_j, b_{j'}\}} - 1\bigg) + \sum_{\substack{j=1\\ j\neq i}}^n \bigg(\frac{b_i - \min\{b_i, b_j\}}{\min\{b_i, b_j\}} - \frac{2 - \max\{b_i, b_j\}}{N_j} \\ &+ \frac{b_i}{p_j \min\{b_i, b_j\}}\bigg) + \bigg(\frac{1}{p_i - 1} - \frac{1}{N_i - 1}\bigg) \ge 0. \quad i = 1, \ldots, n,\end{aligned} \tag{2.7}$$

and q_i is introduced in Assumption (A2)*.*

When the potentials vanish, $V_i \equiv 0$, Assumption (A3) is not satisfied and the error estimate of Theorem 1 on a finite time interval [0,T] changes to

$$\sup_{0<t<T} \sum_{i=1}^n \|X_i^k - \widetilde{X}_i^k\| \le C_T\sqrt{\tau}\bigg(\tau(1+\theta)^6 + \sum_{i=1}^n \Gamma_i\bigg)^{1/2},$$

where $C_T > 0$ is independent of $(b_i, p_i, N_i)_{i=1,\ldots,m}$ but possibly depending on T. It is possible to prove a time-uniform estimate without Assumption (A3) but supposing a bi-Lipschitz property near the origin for K_{ij}; see [65, Theorem 5.1].

Theorem 1 can be generalized to include multiplicative noise. Indeed, if the diffusion σ_i is Lipschitz continuous and the strong convexity condition on V_i is strengthened (see Assumption (B2) at the beginning of section 3.4), then the statement of Theorem 1 still holds. We refer to section 3.4 for details.

The theorem generalizes [52, Theorem 3.1] to the multi-species case. Indeed, if $n = 1$, Γ_1 reduces to $1/(p_1-1) - 1/(N_1-1)$ and $\theta = 1$. Then the error bound becomes $C\sqrt{\tau/(p_1-1)} + C\tau$, which corresponds to (3.9) in [52]. Compared to the result in [52], Theorem 1 shows the influence of the different batch sizes b_i of the species. Indeed, if the batch sizes are very different, θ is much larger than one, which increases the constant in the error estimate. This behaviour is also observed in the numerical simulations; see section 4.1.2.

The proof of Theorem 1 is based on estimates for the error process $Z_i^k := \widetilde{X}_i^k - X_i^k$. Since the noise terms are the same, Z_i^k solves

$$\mathrm{d}Z_i^k(t) = -(\nabla V_i(\widetilde{X}_i^k) - \nabla V_i(X_i^k))\mathrm{d}t + \sum_{j=1}^n \alpha_{ij} \sum_{\substack{\ell=1 \\ (j,k)\neq(j,\ell)}} \Delta K_{ij}^\ell \mathrm{d}t + \chi_i^k(\widetilde{X})\mathrm{d}t$$

for $t_{m-1} < t \le t_m$, where $\Delta K_{ij}^\ell := K_{ij}(\widetilde{X}_i^k - \widetilde{X}_j^\ell) - K_{ij}(X_i^k - X_j^\ell)$ and $\chi_i^k(\widetilde{X})$ is a remainder term (defined in (3.2) below). An important ingredient of the proof is the computation of the variance of χ_i^k, which is more involved than in [52], since the multi-species case requires to distinguish several cases in the choice of indices (i,k) and (j,ℓ).

A straightforward computation, detailed in section 3.3, shows that the error process satisfies

$$\frac{1}{2}\frac{\mathrm{d}}{\mathrm{d}t}\mathbb{E}|Z_i^k(t)|^2 \le -\Big(r_i - 2\sum_{j=1}^n \max\{L_{ij}, L_{ji}\}\Big)\mathbb{E}|Z_j^k(t)|^2 + \mathbb{E}\big(\chi_i^k(\widetilde{X}(t)) \cdot Z_i^k(t)\big).$$

The main difficulty is the estimate of the last term. The idea is to write it in terms of differences $Z_i^k(t) - Z_i^k(t_{m-1})$, $\chi_i^k(\widetilde{X}(t)) - \chi_i^k(\widetilde{X}(t_{m-1}))$, and $\chi_i^k(\widetilde{X}(t)) - \chi_i^k(X(t))$. These differences are estimated from the integral formulations of the differential equations satisfied by the corresponding processes, using Assumptions (A1)–(A4) and the stability results for X_i^k, $\widetilde{X}_i^k$, and Z_i^k. After some computations, we arrive at the differential inequality

$$\frac{\mathrm{d}u}{\mathrm{d}t} \le -\min_{i=1,\dots,n}\Big(r_i - 2\sum_{j=1}^n \max\{L_{ij}, L_{ji}\}\Big)u + C'(\theta)\tau(u^{1/2} + \tau) + C''\tau\sum_{i=1}^n \Gamma_i,$$

where $u = \sum_{i=1}^n \|Z_i^k\|^2$ and the constants $C'(\theta) > 0$ and $C'' > 0$ do not depend on $(b_i, p_i)_{i=1,\dots,n}$, m, or T. In view of Assumption (A2), the first term on the right-hand side is non-positive. The dependence of $C'(\theta)$ on θ arises from the terms involving $b_i/\min\{b_i, b_j\}$; see (2.5). It follows that $u(t)$ is bounded from above by $C(\theta)\tau + C\sqrt{\tau\sum_{i=1}^n \Gamma_i}$ for some other constants $C(\theta) > 0$ and $C > 0$.

2.4. Link to related problems

The random-batch scheme can be interpreted as a Monte–Carlo method to solve the mean-field equations associated to (2.1). In the mean-field limit $N \to \infty$, system (2.1) converges to

$$\mathrm{d}\overline{X}_i = -\nabla V_i(\overline{X}_i)\mathrm{d}t + \sum_{j=1}^n (K_{ij} * u_j)(\overline{X}_i)\mathrm{d}t + \sigma_i \mathrm{d}B_i, \quad i = 1, \dots, n,$$

where u_i is the probability density of $\overline{X}_i$ and solves the mean-field system

$$\partial_t u_i = \operatorname{div}(u_i \nabla V_i(x)) - \operatorname{div}\left(\sum_{j=1}^n u_i(K_{ij} * u_j)\right) + \frac{\sigma_i^2}{2}\Delta u_i \quad \text{in } \mathbb{R}^d,\ i = 1, \ldots, n;$$

see, e.g., the review [49]. If $K_{ij} = \nabla k_{ij}$, it holds that $K_{ij} * u_j = k_{ij} * \nabla u_j$, and the density u_i solves a non-local cross-diffusion system. Moreover, if $k_{ij} = k_{ij}^\eta$ approximates the delta distribution δ according to $k_{ij}^\eta \to a_{ij}\delta$ in $\mathcal{D}'$ as $\eta \to 0$ for some numbers $a_{ij} \geq 0$, it was shown in [25] that the limit $N \to \infty$ and $\eta \to 0$ (in a certain sense) leads to the local cross-diffusion system

$$\partial_t u_i = \operatorname{div}(u_i \nabla V_i(x)) - \operatorname{div}\left(\sum_{j=1}^n a_{ij} u_i \nabla u_j\right) \quad \text{in } \mathbb{R}^d,\ i = 1, \ldots, n.$$

The mean-field limit of the random-batch method was investigated in [50]. The authors showed that the (single-species) N-particle system is reduced to a p-particle system. This mean-field limit does not depend on the law of large numbers, and it is different from the standard mean-field limit, since the chaos is imposed at every time step, while in the standard limit, the chaos is propagated to later times.

The idea of choosing particles in a random way has been exploited in kinetic theory. For instance, subsampling was used in Monte–Carlo simulations [45] and for the symmetric Nabu algorithm, which relates to the random-batch method for $p_i = 2$ [1].

Random-batch methods can also be applied to second-order particle systems [54], many-particle Schrödinger equations [42], and kinetic equations [70]. They have been used to sample complicated or unknown probability distributions [69, 94], and they have been combined with model predictive control strategies to control the guiding problem for a herd of evaders [66]. In molecular dynamics, the interaction kernel is generally singular and given by, e.g., the Coulomb or Lennard–Jones potential. This situation is excluded in this work because of Assumption (A1). However, one may split the kernel function into (singular) short-range and (smooth) long-range parts and apply the random-batch method only to the long-range part. This yields similar convergence results as above but with constants depending on the end time [54]. We refer to the review [51] for further applications and references.

Theorem 1 provides the strong convergence with rate $O(\sqrt{\tau})$ of the error process. In [53], the weak convergence with rate $O(\tau)$ is proved for the single-species case. The proof makes use of the backward Kolmogorov equation and the contraction of the associated semigroup in $L^\infty(\mathbb{R}^d)$. In the multi-species situation, we obtain a system of equations for which contraction properties can be expected under Assumption (A2), but possibly in a weaker topology. A possible way out is to use estimates in the space $H^s(\mathbb{R}^d) \subset L^\infty(\mathbb{R}^d)$ for $s > d/2$, derived for the mean-field limit [25]. We leave the details to future work.

Theorem 1 can be generalized to particle systems with multiplicative noise when the diffusion coefficients are Lipschitz continuous. We can only prove stability for particle systems with *interacting* diffusion coefficients like in [26], which lead in a mean-field-type limit to the Shigesada–Kawasaki–Teramoto population model. For details, we refer to section 3.4.

The part of this thesis concerning the random batch method for stochastic many particle systems is distributed as follows. The consistency of the scheme and stability of the stochastic processes X_i^k and $\widetilde{X}_i^k$ are proved in section 3.1. Section 3.2 is concerned with the control of the error process $Z_i^k = \widetilde{X}_i^k - X_i^k$ and corresponding uniform estimates. Theorem 1 is proved in section 3.3. We comment on the error estimate for particle systems with multiplicative noise in section 3.4. Some numerical simulations, illustrating the convergence behaviour and the influence of the batch sizes, are presented in chapter 4. Finally, we collect some known results about the conditional expectation used in this part of the thesis in Appendix A.1.2.

3. Numerical Analysis

The main goal of this chapter is to provide the numerical analysis of the random batch algorithm given in subsection 2.2, which cumulates to the proof of Theorem 1 - the main result of Part 1. This algorithm provides an approximation of the stochastic many particle system 2.1 we are interested in. We prove consistency and stability results, which will then lead to convergence of the scheme to solutions of the system 2.1. At the end of this chapter, we apply the techniques discussed here to a special particle system with multiplicative noise, broadening the use-case of our algorithm, giving a result akin to Theorem 1 also in this instance.

3.1. Consistency and stability

We assume that Assumptions (A1)–(A4) of chapter 2 hold. Let $i \in \{1, \dots, n\}$, $k \in \{1, \dots, N_i\}$ and let $\widetilde{X}_i^k$ with $k \in \mathcal{C}_{i,r}$ be a solution to (2.4). Then $\widetilde{X}_i^k$ solves

$$\mathrm{d}\widetilde{X}_i^k = -\nabla V_i(\widetilde{X}_i^k)\mathrm{d}t + \sum_{j=1}^{n} \alpha_{ij} \sum_{\substack{\ell=1\\(i,k)\neq(j,\ell)}}^{N_j} K_{ij}(\widetilde{X}_i^k - \widetilde{X}_j^\ell)\mathrm{d}t + \sigma_i \mathrm{d}B_i^k + \chi_i^k(\widetilde{X})\mathrm{d}t, \tag{3.1}$$

where the remainder χ_i^k is defined for $x = (x_1^1, \dots, x_n^{N_n}) \in \mathbb{R}^{dN_1 \times \cdots \times dN_n}$ by

$$\begin{aligned}\chi_i^k(x) &= \sum_{j=1}^{n} \beta_{ij} \sum_{\substack{\ell\in\mathcal{C}_{j,r}\\(i,k)\neq(j,\ell)}} K_{ij}(x_i^k - x_j^\ell) - \sum_{j=1}^{n} \alpha_{ij} \sum_{\substack{\ell=1\\(i,k)\neq(j,\ell)}}^{N_j} K_{ij}(x_i^k - x_j^\ell) \\ &=: f_i^k(x) - g_i^k(x).\end{aligned} \tag{3.2}$$

The following proposition shows that the scheme is consistent.

Proposition 2 (Consistency)**.** *Let $p_i \geq 2$ for $i = 1, \dots, n$ and $x = (x_1^1, \dots, x_n^{N_n}) \in \mathbb{R}^{dN_1 \times \cdots \times dN_n}$. Then the expectation and variance of χ_i^k, defined in (3.2), are $\mathbb{E}(\chi_i^k(x)) = 0$ and*

$$\begin{aligned}\mathrm{Var}(\chi_i^k(x)) = &\sum_{\substack{j,j'=1\\j,j'\neq i,\, j\neq j'}}^{n} \left(\frac{\max\{b_i, b_j, b_{j'}\}}{\max\{b_i, b_{j'}\}} - 1\right) A_i^{jj'}(x) \\ &+ \sum_{\substack{j=1\\j\neq i}}^{n} \left(\frac{b_i - \min\{b_i, b_j\}}{\min\{b_i, b_j\}} - \frac{1}{N_j} + \frac{b_i}{p_j \min\{b_i, b_j\}}\right) A_i^j(x) + \frac{\max\{b_i, b_j\} - 1}{N_j} A_{i,1}^j(x)\end{aligned} \tag{3.3}$$

$$+\left(\frac{1}{p_i-1}-\frac{1}{N_i-1}\right)A_i(x),$$

where $i=1,\dots,n$, $k=1,\dots,N_i$, *and*

$$A_i^{jj'}(x)=\frac{1}{N_jN_{j'}}\sum_{\ell=1}^{N_j}\sum_{\ell'=1}^{N_{j'}}K_{ij}(x_i^k-x_j^\ell)\cdot K_{ij'}(x_i^k-x_{j'}^{\ell'}),$$

$$A_i^j(x)=\frac{1}{N_j(N_j-1)}\sum_{\ell,\ell'=1,\,\ell\neq\ell'}^{N_j}K_{ij}(x_i^k-x_j^\ell)\cdot K_{ij}(x_i^k-x_j^{\ell'}),$$

$$A_{i,1}^j(x)=\frac{1}{N_j}\sum_{\ell=1}^{N_j}\left|K_{ij}(x_i^k-x_j^\ell)\right|^2,$$

$$A_i(x)=\frac{1}{N_i-2}\sum_{\ell=1,\,\ell\neq k}^{N_i}\left|K_{ii}(x_i^k-x_i^\ell)-\frac{1}{N_i-1}\sum_{\ell'=1,\,\ell'\neq k}^{N_i}K_{ii}(x_i^k-x_i^{\ell'})\right|^2.$$

Proof. The proof is similar to [52, Lemma 3.1], but since we have multiple species, the computations are more involved. Let $i\in\{1,\dots,n\}$ and $k\in\{1,\dots,N_i\}$ be arbitrary but fixed. We write $I_i^k(j,\ell)=1$ if (i,k) and (j,ℓ) are in the same super-batch, i.e., if there exists $r\geq 1$ such that $(i,k),(j,\ell)\in\mathcal{C}_r$. Otherwise, we set $I_i^k(j,\ell)=0$. With this notation, we can write $f_i^k=f_i^k(x)$, defined in (3.2), as

$$f_i^k=\sum_{j=1}^n\beta_{ij}\sum_{\ell=1}^{N_j}K_{ij}(x_i^k-x_j^\ell)I_i^k(j,\ell).$$

Step 1: Computation of the expection. We claim that

$$\mathbb{E}I_i^k(j,\ell)=\begin{cases}\frac{p_i-1}{N_i-1} & \text{if } i=j,\\ \frac{\min\{b_i,b_j\}}{b_ib_j} & \text{if } i\neq j.\end{cases}\tag{3.4}$$

The case $i=j$ is proved in [52, Lemma 3.1]. For $i\neq j$, we define $a(i,k)$ as the index of the super-batch $\mathcal{C}_r$ that contains (i,k), i.e. $a(i,k)=r$ if and only if $(i,k)\in\mathcal{C}_r$ or, equivalently, $k\in\mathcal{C}_{i,r}$. We have

$$\begin{aligned}\mathbb{P}(I_i^k(j,\ell)=1)=\mathbb{P}((j,\ell)\in\mathcal{C}_{a(i,k)})&=\sum_{r=1}^{\min\{b_i,b_j\}}\mathbb{P}((j,\ell)\in\mathcal{C}_r|a(i,k)=r)\mathbb{P}(a(i,k)=r)\\ &=\sum_{r=1}^{\min\{b_i,b_j\}}\mathbb{P}((j,\ell)\in\mathcal{C}_r)\mathbb{P}(a(i,k)=r).\end{aligned}$$

The distribution of a particle of a certain species is uniform with respect to the species' batch in which it ends up, i.e. $\mathbb{P}(\ell\in\mathcal{C}_{j,r})=\mathbb{P}(\ell\in\mathcal{C}_{j,s})$ for all $r,s=1,\dots,b_j$. Consequently, we have $\mathbb{P}(\ell\in\mathcal{C}_{j,r})=1/b_j$ for all $r=1,\dots,b_j$ and $\mathbb{P}(\ell\in\mathcal{C}_{j,r})=0$ otherwise, since $\mathcal{C}_{j,r}=\emptyset$ if $r>b_j$. This leads for $i\neq j$ to

$$\mathbb{E}I_i^k(j,\ell)=1\cdot\mathbb{P}(I_i^k(j,\ell)=1)=\min\{b_i,b_j\}\frac{1}{b_j}\frac{1}{b_i}.$$

We infer from the definitions of α_{ij} and β_{ij} in (2.3) and (2.5), respectively, and from (3.4) that

$$\begin{aligned}\mathbb{E}(f_i^k) &= \sum_{j=1}^{n} \beta_{ij} \sum_{\ell=1}^{N_j} K_{ij}(x_i^k - x_j^\ell)\mathbb{E} I_i^k(j,\ell) \\ &= \frac{1}{N_i - 1} \sum_{\ell=1,\,\ell\neq k}^{N_i} K_{ii}(x_i^k - x_i^\ell) + \sum_{j=1,\,j\neq i}^{n} \frac{1}{N_j} \sum_{\ell=1}^{N_j} K_{ij}(x_i^k - x_j^\ell) \\ &= \sum_{j=1}^{n} \alpha_{ij} \sum_{\substack{\ell=1 \\ (i,k)\neq(j,\ell)}} K_{ij}(x_i^k - x_j^\ell) = g_i^k.\end{aligned}$$

This shows that $\mathbb{E}(\chi_i^k(x)) = \mathbb{E}(f_i^k) - g_i^k = 0$.

Step 2: Preparation for the computation of the variance. We introduce the notation $G_j^\ell := K_{ij}(x_i^k - x_j^\ell) I_i^k(j,\ell)$ if $(i,k) \neq (j,\ell)$ and $G_j^\ell = 0$ if $(i,k) = (j,\ell)$. Then

$$\mathbb{E}(f_i^k)^2 = \sum_{j,j'=1}^{n} \beta_{ij}\beta_{ij'} \sum_{\ell=1}^{N_j} \sum_{\ell'=1}^{N_{j'}} \mathbb{E}(G_j^\ell G_{j'}^{\ell'}).$$

The expectation of $G_j^\ell G_{j'}^{\ell'}$ can be written as

$$\begin{aligned}\mathbb{E}(G_j^\ell G_{j'}^{\ell'}) &= K_{ij}(x_i^k - x_j^\ell) K_{ij'}(x_i^k - x_{j'}^{\ell'}) \mathbb{E}(I_i^k(j,\ell) I_i^k(j',\ell')) \\ &= K_{ij}(x_i^k - x_j^\ell) K_{ij'}(x_i^k - x_{j'}^{\ell'}) \mathbb{P}(I_i^k(j,\ell) I_i^k(j',\ell') = 1).\end{aligned}$$

Thus, we need to calculate $\mathbb{P}(I_i^k(j,\ell) I_i^k(j',\ell') = 1)$. For this, we distinguish several cases.

Case 1: $j, j' \neq i$ and $j \neq j'$. We compute, using the definition of the super-batches,

$$\begin{aligned}\{I_i^k(j,\ell) I_i^k(j',\ell') = 1\} &= \big\{(j,\ell) \in \mathcal{C}_{a(i,k)},\ (j',\ell') \in \mathcal{C}_{a(i,k)}\big\} \\ &= \big\{\ell \in \mathcal{C}_{j,a(i,k)},\ \ell' \in \mathcal{C}_{j',a(i,k)}\big\} = \bigcup_{r\in\mathbb{N}} \big\{\ell \in \mathcal{C}_{j,a(i,k)},\ \ell' \in \mathcal{C}_{j',a(i,k)},\ r = a(i,k)\big\}.\end{aligned}$$

The random division $\xi_{m.1}$ of the batch $\mathcal{C}_{i,r}$ at time t_{m-1} is independent of the random division of the batches $\mathcal{C}_{j,r}$ and $\mathcal{C}_{j',r}$. Thus, we can write

$$\begin{aligned}\mathbb{P}(I_i^k(j,\ell) I_i^k(j',\ell') = 1) &= \sum_{r=1}^{\min\{b_i,b_j,b_{j'}\}} \mathbb{P}(k \in \mathcal{C}_{i,r}) \mathbb{P}(\ell \in \mathcal{C}_{j,r}) \mathbb{P}(\ell' \in \mathcal{C}_{j',r}) \\ &= \min\{b_i, b_j, b_{j'}\} \frac{1}{b_i} \frac{1}{b_j} \frac{1}{b_{j'}}.\end{aligned}$$

Case 2: $j, j' \neq i$, $j = j'$ and $\ell \neq \ell'$. In this case, both ℓ and ℓ' are in the same batch such that

$$\{I_i^k(j,\ell) I_i^k(j,\ell') = 1\} = \bigcup_{r\in\mathbb{N}} \big\{\ell, \ell' \in \mathcal{C}_{j,r},\ r = a(i,k)\big\} \tag{3.5}$$

$$= \bigcup_{r\in\mathbb{N}} \{I_j^k(j,\ell') = 1\} \cap \{\ell \in \mathcal{C}_{j,r}\} \cap \{k \in \mathcal{C}_{i,r}\}.$$

Because of the uniformity of the random division (as in Case 1), we have

$$\mathbb{P}(I_j^\ell(j,\ell') = 1,\, \ell \in \mathcal{C}_{j,r}) = \mathbb{P}(I_j^\ell(j,\ell') = 1,\, \ell \in \mathcal{C}_{j,s}) \quad \text{for all } 1 \le r,s \le b_j.$$

Since, by (3.4), $\mathbb{P}(I_j^\ell(j,\ell') = 1) = (p_j - 1)/(N_j - 1)$, we deduce from (3.5) that

$$\begin{aligned}\mathbb{P}(I_i^k(j,\ell)I_i^k(j',\ell') = 1) &= \sum_{r=1}^{\min\{b_i,b_j\}} \mathbb{P}(I_j^\ell(j,\ell') = 1,\, \ell \in \mathcal{C}_{j,r})\mathbb{P}(k \in \mathcal{C}_{i,r}) \\ &= \frac{1}{b_i b_j} \sum_{r=1}^{\min\{b_i,b_j\}} \mathbb{P}(I_j^\ell(j,\ell') = 1) = \frac{\min\{b_i,b_j\}(p_j-1)}{b_i b_j (N_j - 1)}.\end{aligned}$$

Case 3: $j \neq i$, $j' = i$. If $\ell = k$, it follows from the definition of G_j^ℓ that $G_i^{\ell'} = G_i^k = 0$. If $\ell \neq k$, the definition of G_j^ℓ gives

$$\mathbb{E}(G_j^\ell G_{j'}^{\ell'}) = K_{ij}(x_i^k - x_j^\ell)K_{ii}(x_i^k - x_i^{\ell'})\mathbb{E}(I_i^k(j,\ell)I_i^k(i,\ell')),$$

and it remains the compute the expectation on the right-hand side. Proceeding as in the previous cases, we find that

$$\begin{aligned}\mathbb{P}(I_i^k(j,\ell)I_i^k(i,\ell') = 1) &= \sum_{r=1}^{\min\{b_i,b_j\}} \mathbb{P}(I_i^k(i,\ell') = 1,\, k \in \mathcal{C}_{i,r})\mathbb{P}(\ell \in \mathcal{C}_{j,r}) \\ &= \frac{1}{b_i b_j} \sum_{r=1}^{\min\{b_i,b_j\}} \mathbb{P}(I_i^k(i,\ell') = 1) = \frac{\min\{b_i,b_j\}(p_i-1)}{b_i b_j (N_i - 1)}.\end{aligned}$$

Case 4: $j,j' = i$, $\ell \neq \ell' \neq k$. We need to compute the probability of $I_i^k(i,\ell)I_i^k(i,\ell') = 1$. This case happens exactly when the indices ℓ, ℓ', and k are in the same batch $\mathcal{C}_{i,a(i,k)}$. Similar arguments as for $\mathbb{P}(I_i^k(i,\ell) = 1)$ in the proof of Lemma 3.1 in [52] yield

$$\mathbb{P}(I_i^k(i,\ell)I_i^k(i,\ell') = 1) = \frac{(p_i-1)(p_i-2)}{(N_i-1)(N_i-2)}.$$

Case 5: $j,j' = i$, $\ell = \ell'$, $\ell \neq k$. We only need $\mathbb{E}(I_i^k(i,\ell))$, which we already computed:

$$\mathbb{P}(I_i^k(i,\ell) = 1) = \frac{p_i - 1}{N_i - 1}.$$

Summarizing these five cases, we obtain $\mathbb{E}(f_i^k)^2 = J_1 + \cdots + J_5$, where the term J_j corresponds to case j and

$$J_1 = \sum_{\substack{j,j'=1 \\ j,j'\neq i,\, j\neq j'}}^{n} \frac{\min\{b_i,b_j,b_{j'}\}b_i}{N_j N_{j'} \min\{b_i,b_j\}\min\{b_i,b_{j'}\}} \sum_{\ell,\ell'=1}^{N_j,N_{j'}} K_{ij}(x_i^k - x_j^\ell)K_{ij'}(x_i^k - x_{j'}^{\ell'}),$$

$$J_2 = \sum_{\substack{j=1\\j\neq i}}^{n} \frac{(p_j-1)b_i}{(N_j-1)N_j \min\{b_i,b_j\}p_j} \sum_{\ell,\ell'=1,\,\ell\neq\ell'}^{N_j} K_{ij}(x_i^k - x_j^\ell)K_{ij}(x_i^k - x_j^{\ell'}),$$

$$J_2' = \sum_{\substack{j=1\\j\neq i}}^{n} \frac{b_i}{N_j \min\{b_i,b_j\}p_j} \sum_{\ell=1}^{N_j} K_{ij}(x_i^k - x_j^\ell)^2,$$

$$J_3 = 2\sum_{\substack{j=1\\j\neq i}}^{n} \frac{1}{(N_i-1)N_j} \sum_{\substack{\ell,\ell'=1\\ \ell'\neq k}}^{N_j,N_i} K_{ij}(x_i^k - x_j^\ell)K_{ii}(x_i^k - x_i^{\ell'}),$$

$$J_4 = \frac{p_i-2}{(p_i-1)(N_i-1)(N_i-2)} \sum_{\substack{\ell,\ell'=1\\ \ell\neq\ell'}}^{N_i} K_{ii}(x_i^k - x_i^\ell)K_{ii}(x_i^k - x_i^{\ell'}),$$

$$J_5 = \frac{1}{(p_i-1)(N_i-1)} \sum_{\ell=1}^{N_i} K_{ii}(x_i^k - x_i^\ell)^2.$$

For the term $(\mathbb{E}(f_i^k))^2 = (\mathbb{E}(g_i^k))^2$, we expand the square:

$$\begin{aligned}
(\mathbb{E}(f_i^k))^2 &= \Bigg(\sum_{j=1}^{n} \alpha_{ij} \sum_{\substack{\ell=1\\(i,k)\neq(j,\ell)}} K_{ij}(x_i^k - x_j^\ell) \sum_{j'=1}^{n} \alpha_{ij'} \sum_{\substack{\ell'=1\\(i,k)\neq(j',\ell')}} K_{ij'}(x_i^k - x_{j'}^{\ell'})\Bigg)^2 \\
&= \widehat{J}_1 + \cdots + \widehat{J}_5, \quad \text{where} \\
\widehat{J}_1 &= \sum_{\substack{j,j'=1\\ j,j'\neq i,\, j\neq j'}}^{n} \frac{1}{N_j N_{j'}} \sum_{\ell,\ell'=1}^{N_j,N_{j'}} K_{ij}(x_i^k - x_j^\ell)K_{ij'}(x_i^k - x_{j'}^{\ell'}), \\
\widehat{J}_2 &= \sum_{j=1,\,j\neq i}^{n} \frac{1}{N_j^2} \sum_{\ell,\ell'=1}^{N_j} K_{ij}(x_i^k - x_j^\ell)K_{ij}(x_i^k - x_j^{\ell'}), \\
\widehat{J}_3 &= 2\sum_{j=1,\,j\neq i}^{n} \frac{1}{(N_i-1)N_j} \sum_{\ell=1}^{N_j} \sum_{\substack{\ell'=1\\ \ell'\neq k}}^{N_i} K_{ij}(x_i^k - x_j^\ell)K_{ii}(x_i^k - x_i^{\ell'}), \\
\widehat{J}_4 &= \frac{1}{(N_i-1)^2)} \sum_{\substack{\ell,\ell'=1\\ \ell\neq\ell'}}^{N_i} K_{i,i}(x_i^k - x_i^\ell)K_{ii}(x_i^k - x_i^{\ell'}), \\
\widehat{J}_5 &= \frac{1}{(N_i-1)^2} \sum_{\ell=1}^{N_i} K_{ii}(x_i^k - x_i^\ell)^2.
\end{aligned}$$

The variance of f_i^k is the difference $(J_1 + \cdots + J_5) - (\widehat{J}_1 + \cdots + \widehat{J}_5)$. We observe that

$J_3 - \widehat{J}_3 = 0$ and that

$$\frac{\min\{b_i, b_j, b_{j'}\}b_i}{\min\{b_i, b_j\}\min\{b_i, b_{j'}\}} = \frac{\max\{b_i, b_j, b_{j'}\}}{\max\{b_j, b_{j'}\}},$$

A tedious but straightforward computation yields for the other terms:

$$\begin{aligned}
\mathrm{Var}(f_i^k) &= \mathbb{E}(f_i^k)^2 - (\mathbb{E}f_i^k)^2 = (J_1 - \widehat{J}_1) + (J_2 + J_2' - \widehat{J}_2) + (J_4 + J_5 - \widehat{J}_4 - \widehat{J}_5) \\
&= \sum_{\substack{j,j'=1 \\ j,j' \neq i,\, j \neq j'}}^{n} \left(\frac{\max\{b_i, b_j, b_{j'}\}}{\max\{b_j, b_{j'}\}} - 1\right) \frac{1}{N_j N_{j'}} \sum_{\ell=1}^{N_j} \sum_{\ell'=1}^{N_{j'}} K_{ij}(x_i^k - x_j^\ell) K_{ij'}(x_i^k - x_{j'}^{\ell'}) \\
&\quad + \sum_{j=1,\, j\neq i}^{n} \left(\frac{b_i - \min\{b_i, b_j\}}{\min\{b_i, b_j\}} - \frac{1}{N_j} + \frac{b_i}{\min\{b_i, b_j\}p_j}\right) \frac{1}{N_j(N_j - 1)} \\
&\quad \times \sum_{\ell,\ell'=1,\, \ell\neq\ell'}^{N_j} K_{ij}(x_i^k - x_j^\ell) K_{ij}(x_i^k - x_j^{\ell'}) \\
&\quad + \sum_{j=1,\, j\neq i}^{n} \left(\frac{\max\{b_i, b_j\} - 1}{N_j}\right) \frac{1}{N_j} \sum_{\ell=1}^{N_j} K_{ij}(x_i^k - x_j^\ell)^2 \\
&\quad + \left(\frac{1}{p_i - 1} - \frac{1}{N_i - 1}\right) \frac{1}{N_i - 2} \sum_{\substack{\ell=1 \\ k \neq \ell}}^{N_i} \left(K_{ii}(x_i^k - x_j^\ell) - \frac{1}{N_i - 1} \sum_{\substack{\ell'=1 \\ \ell' \neq k}}^{N_i} K_{ii}(x_i^k - x_j^{\ell'})\right)^2.
\end{aligned}$$

The right-hand side equals (3.3), which finishes the proof. □

Using definition (2.7), we can estimate the variance of $\chi_i^k(x)$ from above according to

$$\mathrm{Var}(\chi_i^k(x)) \leq 8 \max_{i,j=1,\ldots,n} \|K_{ij}\|_\infty^2 \sum_{k=1}^{n} \Gamma_k.$$

As expected, for larger batch sizes p_i, the variance is smaller and the noise level is lower. In the single-species case, we recover [52, Lemma 3.1] since

$$\mathrm{Var}(\chi_i^k(x)) = \left(\frac{1}{p_i - 1} - \frac{1}{N_i - 1}\right) A_i(x).$$

If the species numbers and batch sizes are the same, i.e. $N_i = N$ and $b_i = b$ for all $i = 1, \ldots, n$, it follows that

$$\mathrm{Var}(\chi_i^k(x)) = \left(\frac{1}{p} - \frac{1}{N}\right) \sum_{j=1,\, j\neq i}^{n} \left(A_i^j(x) + A_{i,1}^j(x)\right) + \left(\frac{1}{p-1} - \frac{1}{N-1}\right) A_i(x).$$

We observe that the first term on the right-hand side of (3.3) vanishes. This means that, in case of different species numbers or batch sizes, the noise level is larger than in the uniform case, i.e., the case for which p is chosen such that $b_i = b_j$ for all i, j and consequently, $\theta = 1$.

For later use, we prove the following auxiliary result, which generalizes Lemma 3.2 in [52] to the multi-species case.

Lemma 3. *Let $i \in \{1, \ldots, n\}$, $k \in \{1, \ldots, N_i\}$, and $(i,k) \in \mathcal{C}_{i,r}$ for some $r = a(i,k) \le b_i$. Let $S_j^\ell \in \mathbb{R}^d$ with j, $\ell \in \mathbb{N}$ be random variables which are independent of the partitioning random variable ξ_m. Then it holds*

$$\left\| \frac{1}{p_j} \sum_{\ell \in \mathcal{C}_{j,r}} S_j^\ell \right\| = \max_{\ell=1,\ldots,N_j} \|S_j^\ell\| \quad \text{if } i \ne j,$$

$$\left\| \frac{1}{p_j - 1} \sum_{\ell \in \mathcal{C}_{i,r},\, \ell \ne k} S_i^\ell \right\| = \max_{\ell=1,\ldots,N_i} \|S_i^\ell\| \quad \text{if } i = j,$$

recalling that $\| \cdot \| = (\mathbb{E}(\cdot)^2)^{1/2}$.

Proof. The proof is similar to that one of [52, Lemma 3.2]. We present it for completeness. Let $i \ne j$ and set $I_i^k(j,\ell) = 1$ if (i,k) and (j,ℓ) are in same batch and $I_i^k(j,\ell) = 0$ otherwise. Due to the independency of S_j^ℓ and ξ_m, we have

$$\begin{aligned} \left\| \frac{1}{p_j} \sum_{\ell \in \mathcal{C}_{j,r}} S_j^\ell \right\|^2 &= \frac{1}{p_j^2} \mathbb{E}\Big(\sum_{\ell=1}^{N_j} I_i^k(j,\ell) S_j^\ell \Big)^2 = \frac{1}{p_j^2} \sum_{\ell,\ell'=1}^{N_j} \mathbb{E}\big(I_i^k(j,\ell) I_i^k(j,\ell') S_j^\ell S_j^{\ell'}\big) \\ &= \frac{1}{p_j^2} \sum_{\ell,\ell'=1}^{N_j} \mathbb{E}(I_i^k(j,\ell) I_i^k(j,\ell')) \mathbb{E}(S_j^\ell S_j^{\ell'}). \end{aligned}$$

We know from (3.4) that $\mathbb{E}(I_i^k(j,\ell) I_i^k(j,\ell')) \le 1/b_j$ in the case of $\ell = \ell'$ and from Case 2 of Proposition 2 that $\mathbb{E}(I_i^k(j,\ell) I_i^k(j,\ell')) \le (p_j - 1)/(b_j(N_j - 1))$, if $\ell \ne \ell'$. Therefore, using the Cauchy–Schwarz inequality and the fact that $N_j = b_j p_j$,

$$\begin{aligned} \left\| \frac{1}{p_j} \sum_{\ell \in \mathcal{C}_{j,r}} S_j^\ell \right\|^2 &\le \frac{1}{p_j^2} \Bigg(\sum_{\ell,\ell'=1,\, \ell \ne \ell'}^{N_j} \frac{p_j - 1}{b_j(N_j - 1)} \|S_j^\ell\| \, \|S_j^{\ell'}\| + \sum_{\ell=1}^{N_j} \frac{1}{b_j} \|S_j^\ell\|^2 \Bigg) \\ &\le \max_{\ell=1,\ldots,N_j} \|S_j^\ell\|^2 \left(\frac{(p_j - 1)(N_j - 1) N_j}{p_j N_j (N_j - 1)} + \frac{1}{p_j} \right) \le \max_{\ell=1,\ldots,N_j} \|S_j^\ell\|^2. \end{aligned}$$

The case $i = j$ is shown in a similar way. ☐

The next result is concerned with the stability of X_i^k and $\widetilde{X}_i^k$.

Lemma 4 (Stability). *Let $q \ge 2$, and $X_i^{0,k} \in L^q(\Omega)$, where $i \in \{1, \ldots, n\}$ and $k \in \{1, \ldots, N_i\}$. Then there exist constants $C(q)$, $C_1 > 0$, independent of $(p_i, b_i)_{i=1,\ldots,n}$, m, and T, such that*

$$\sup_{t>0} \mathbb{E}|X_i^k(t)|^q \le C(q), \quad \sup_{t>0} \mathbb{E}|\widetilde{X}_i^k(t)|^q \le C(q)(1 + \theta^q), \tag{3.6}$$

$$\sup_{t_{m-1}<t<t_m} \mathbb{E}\big(|\widetilde{X}_i^k(t)|^q \big| \mathcal{F}_{m-1}\big) \le |\widetilde{X}_i^k(t_{m-1})|^q + C(q)(1 + \theta^q), \tag{3.7}$$

where θ is defined in (2.6). Furthermore, it holds that

$$\big|\mathbb{E}\big(\widetilde{X}_i^k(t) - \widetilde{X}_i^k(t_{m-1}) \big| \mathcal{F}_{m-1}\big)\big| \le C_V \tau |\widetilde{X}_i^k(t_{m-1})|^{\widetilde{q}_i} + C_1 \tau (1 + \theta^{\widetilde{q}_i}), \tag{3.8}$$

where $\widetilde{q}_i = \max\{2, q_i\}$ and $C_V > 0$ is introduced in Assumption (A2).

Proof. Let $i \in \{1, \dots, n\}$ and $k \in \{1, \dots, N_i\}$ be arbitrary but fixed. The proof is similar to [52, Lemma 3.3] with the exception that we work out the dependence on the number of batches b_i in terms of the quotient θ.

Step 1: Stability for $X_i^k(t)$. Let $d \geq 2$. We use Itô's calculus for the process $|X_i^k|^q$ and apply the expectation as in [52, Lemma 3.3], which yields

$$\begin{aligned}\frac{\mathrm{d}}{\mathrm{d}t}\mathbb{E}|X_i^k(t)|^q &= -q\mathbb{E}\big(|X_i^k(t)|^{q-2}X_i^k(t)\cdot\nabla V_i(X_i^k(t))\big)\\ &\quad+\frac{q}{N_i-1}\mathbb{E}\bigg(|X_i^k(t)|^{q-2}X_i^k(t)\cdot\sum_{\ell=1,\,\ell\neq k}^{N_i}K_{ii}(X_i^k(s)-X_i^\ell(s))\bigg)\\ &\quad+\sum_{j=1,\,j\neq i}^{n}\frac{q}{N_j}\mathbb{E}\bigg(|X_i^k(t)|^{q-2}X_i^k(t)\cdot\sum_{\ell=1}^{N_j}K_{ij}(X_i^k(s)-X_j^\ell(s))\bigg)\\ &\quad+\frac{\sigma_i^2}{2}q(q+d-2)\mathbb{E}|X_i^k(t)|^{q-2}.\end{aligned}$$

The mean-value theorem with intermediate value $\zeta \in \mathbb{R}^d$ and the convexity of $x \mapsto V_i(x) - r_i|x|^2/2$ (Assumption (A2)) imply that for all $x \in \mathbb{R}^d$,

$$x\cdot\nabla V_i(x) = x^T D^2V_i(\zeta)x + x\cdot\nabla V_i(0) \geq r_i|x|^2 + x\cdot\nabla V_i(0).$$

Together with Fubini's theorem, the boundedness of the kernels K_{ij} (Assumption (A1)), and Young's inequality, it follows that

$$\begin{aligned}\frac{\mathrm{d}}{\mathrm{d}t}\mathbb{E}|X_i^k(t)|^q &\leq -qr_i\mathbb{E}|X_i^k(t)|^q + q\bigg(|\nabla V_i(0)|+\sum_{j=1}^{n}\|K_{ij}\|_\infty\bigg)\mathbb{E}|X_i^k(t)|^{q-1}\\ &\quad+\frac{\sigma_i^2}{2}q(q+d-2)\mathbb{E}|X_i^k(t)|^{q-2} \leq -\frac{qr_i}{2}\mathbb{E}|X_i^k(t)|^q + C_2,\end{aligned}$$

where $C_2 > 0$ depends on ∇V_i, K_{ij}, σ_i, d, and q. Grönwall's lemma implies that $\mathbb{E}|X_i^k(t)|^q$ is bounded by a constant depending on q (and not depending on T).

Step 2: Stability for $\widetilde{X}_i^k$. Let $t \in (t_{m-1}, t_m]$ and let $(i,k) \in \mathcal{C}_r$ for some $r \in \mathbb{N}$. Similarly as in the previous step, we use Itô's calculus and apply the conditional expectation with respect to $\mathcal{F}_{m-1}$, observing that $|\widetilde{X}_i^k(t_{m-1})|^q$ is $\mathcal{F}_{m-1}$-measurable. Then, applying Lemmas 45 and 46 in the appendix,

$$\begin{aligned}\frac{\mathrm{d}}{\mathrm{d}t}\mathbb{E}\big(|\widetilde{X}_i^k(t)|^q\big|\mathcal{F}_{m-1}\big) &= -q\mathbb{E}\big(|\widetilde{X}_i^k(t)|^{q-2}\widetilde{X}_i^k\cdot\nabla V_i(\widetilde{X}_i^k(t))\big|\mathcal{F}_{m-1}\big)\\ &+\frac{q}{p_i-1}\sum_{\ell\in\mathcal{C}_{i,r},\,\ell\neq k}\mathbb{E}\big(|\widetilde{X}_i^k(t)|^{q-2}\widetilde{X}_i^k(t)\cdot K_{ii}(\widetilde{X}_i^k-\widetilde{X}_i^\ell)\big|\mathcal{F}_{m-1}\big)\\ &+\sum_{j=1,\,j\neq i}^{n}\frac{qb_i}{p_j\min\{b_i,b_j\}}\sum_{\ell\in\mathcal{C}_{j,r}}\mathbb{E}\big(|\widetilde{X}_i^k(t)|^{q-2}\widetilde{X}_i^k(t)\cdot K_{ij}(\widetilde{X}_i^k(t)-\widetilde{X}_j^\ell(t))\big|\mathcal{F}_{m-1}\big)\\ &+\frac{\sigma_i^2}{2}q(q+d-2)\mathbb{E}\big(|\widetilde{X}_i^k(t)|^{q-2}\big|\mathcal{F}_{m-1}\big).\end{aligned}$$

Proceeding as in the previous step and using $b_i/\min\{b_i,b_j\} \le \theta$, we infer that

$$\frac{\mathrm{d}}{\mathrm{d}t}\mathbb{E}\big(|\widetilde{X}_i^k(t)|^q\big|\mathcal{F}_{m-1}\big) \le -\frac{qr_i}{2}\mathbb{E}\big(|\widetilde{X}_i^k(t)|^q\big|\mathcal{F}_{m-1}\big) + C_3(1+\theta)^q,$$

and Grönwall's lemma on $(t_{m-1}, t_m]$ implies (3.7). Finally, the second estimate in (3.6) is proved in a similar way, using the Grönwall lemma on $[0,t]$ and taking into account that $\mathbb{E}|X_i^{0,k}|^q$ is bounded by assumption.

Step 3: Proof of estimate (3.8). We apply Itô's lemma, take the conditional expectation of $\widetilde{X}_i^k(t) - \widetilde{X}_i^k(t_{m-1})$, and use the polynomial growth condition for ∇V_i in Assumption (A2) as well as the boundedness of K_{ij}:

$$\begin{aligned}
\mathbb{E}\big(\widetilde{X}_i^k(t) - \widetilde{X}_i^k(t_{m-1})\big|\mathcal{F}_{m-1}\big) &= -\int_{t_{m-1}}^t \mathbb{E}\big(\nabla V_i(\widetilde{X}_i^k(s))\big|\mathcal{F}_{m-1}\big)\mathrm{d}s \\
&\quad + \frac{1}{p_i-1}\int_{t_{m-1}}^t \mathbb{E}\bigg(\sum_{\ell\in\mathcal{C}_{i,r},\,\ell\ne k} K_{ii}(\widetilde{X}_i^k(s) - \widetilde{X}_i^\ell(s))\big|\mathcal{F}_{m-1}\bigg)\mathrm{d}s \\
&\quad + \sum_{j=1,\,j\ne i} \frac{b_i}{p_j\min\{b_i,b_j\}}\int_{t_{m-1}}^t \mathbb{E}\bigg(\sum_{\ell\in\mathcal{C}_{j,r}} K_{ij}(\widetilde{X}_i^k(s) - \widetilde{X}_j^\ell(s))\big|\mathcal{F}_{m-1}\bigg)\mathrm{d}s \\
&\le C_V\tau + C_V\int_{t_{m-1}}^t \mathbb{E}\big(|\widetilde{X}_i^k(s)|^{q_i}\big|\mathcal{F}_{m-1}\big)\mathrm{d}s + \tau\sum_{j=1}^n \frac{\|K_{ij}\|_\infty b_i}{\min\{b_i,b_j\}}.
\end{aligned}$$

It follows from (3.7) with $q = \widetilde{q}_i := \max\{2, q_i\}$ that

$$\begin{aligned}
&\mathbb{E}\big(\widetilde{X}_i^k(t) - \widetilde{X}_i^k(t_{m-1})\big|\mathcal{F}_{m-1}\big) \\
&\quad\le C_V\tau|\widetilde{X}_i^k(t_{m-1})|^{\widetilde{q}_i} + \tau\bigg(C_V + C_V C(\widetilde{q}_i)(1+\theta^{\widetilde{q}_i}) + \sum_{j=1}^n \frac{\|K_{ij}\|_\infty b_i}{\min\{b_i,b_j\}}\bigg) \\
&\quad\le C_V\tau|\widetilde{X}_i^k(t_{m-1})|^{\widetilde{q}_i} + C_4(\widetilde{q}_i)(1+\theta^{\widetilde{q}_i}).
\end{aligned}$$

This completes the proof. □

3.2. Control of the error process

We prove first a bound for the difference $\widetilde{X}_i^k(t) - \widetilde{X}_i^k(t_{m-1})$.

Lemma 5. *Let $t \in (t_{m-1}, t_m]$, let $\widetilde{X}$ be the stochastic process defined in* (2.4)*, and let $i \in \{1,\ldots,n\}$. Set $q_i' = 2\max\{1, q_i\}$, where q_i is defined in Assumption (A2). Then, for any $(i,k) \in \mathcal{C}_r$ for some $r \le b_i$ such that $X_i^{0,k} \in L^{q_i'}(\Omega)$, there exists a constant $C > 0$, independent of $(p_i, b_i)_{i=1,\ldots,n}$, and ξ_m, such that*

$$\mathbb{E}\big(|\widetilde{X}_i^k(t) - \widetilde{X}_i^k(t_{m-1})|^2\big|\mathcal{F}_{m-1}\big) \le C\tau(1+\theta^{q_i'/2+1})\big(1 + |\widetilde{X}_i^k(t_{m-1})|^{q_i'/2+1}\big).$$

Proof. Again, the proof is similar to [52, Lemma 3.3] and based on Itô's calculus. Let $t \in (t_{m-1}, t_m]$ and $(i,k) \in \mathcal{C}_r$ for some $r \le b_i$, satisfying the assumptions of the lemma. Set

$S(t) := \widetilde{X}_i^k(t) - \widetilde{X}_i^k(t_{m-1})$. We apply Itô's lemma to $|S(t)|^2$ and the conditional expectation and use Lemmas 45 and 46:

$$\begin{aligned}\mathbb{E}(|S(t)|^2|\mathcal{F}_{m-1}) &\le 2\int_{t_{m-1}}^t \big|\mathbb{E}\big(S(s)\cdot\nabla V_i(\widetilde{X}_i^k(s))\big|\mathcal{F}_{m-1}\big)\big|\mathrm{d}s + d\int_{t_{m-1}}^t \sigma_i^2\mathrm{d}s \qquad (3.9)\\ &+ \frac{2}{p_i-1}\int_{t_{m-1}}^t \bigg|\mathbb{E}\bigg(\sum_{\ell\in\mathcal{C}_{i,r},\,\ell\ne k} K_{ii}(\widetilde{X}_i^k(s)-\widetilde{X}_i^\ell(t))\cdot S(s)\bigg|\mathcal{F}_{m-1}\bigg)\bigg|\mathrm{d}s\\ &+ \sum_{j=1,\,j\ne i}\frac{2b_i}{p_j\min\{b_i,b_j\}}\int_{t_{m-1}}^t \bigg|\mathbb{E}\bigg(\sum_{\ell\in\mathcal{C}_{i,r},\,\ell\ne k} K_{ij}(\widetilde{X}_i^k(s)-\widetilde{X}_j^\ell(t))\cdot S(s)\bigg|\mathcal{F}_{m-1}\bigg)\bigg|\mathrm{d}s\\ &=: J_6+\cdots+J_9.\end{aligned}$$

By the Cauchy–Schwarz inequality, the polynomial growth condition on ∇V_i (Assumption (A2)), and stability estimate (3.6) with $q = q_i'$, we have

$$\begin{aligned}J_6 &\le 2C_V^{1/2}\int_{t_{m-1}}^t \big(\mathbb{E}(|S(s)|^2|\mathcal{F}_{m-1})\big)^{1/2}\big(\mathbb{E}(1+|\widetilde{X}_i^k(s)|^{2q_i}|\mathcal{F}_{m-1})\big)^{1/2}\mathrm{d}s\\ &\le 2C_V^{1/2}\big(1+C(q)(1+\theta^q)+|\widetilde{X}_i^k(t_{m-1})|^q\big)^{1/2}\int_{t_{m-1}}^t \big(\mathbb{E}(|S(s)|^2|\mathcal{F}_{m-1})\big)^{1/2}\mathrm{d}s.\end{aligned}$$

Next, using the boundedness of K_{ii}, Lemma 44, and Hölder's inequality,

$$\begin{aligned}J_8 &\le C\|K_{ii}\|_\infty\int_{t_{m-1}}^t \big(\mathbb{E}(|S(s)|^2|\mathcal{F}_{m-1})\big)^{1/2}\mathrm{d}s,\\ J_9 &\le C\sum_{j=1,\,j\ne i}^n\frac{b_i}{\min\{b_i,b_j\}}\|K_{ii}\|_\infty\int_{t_{m-1}}^t \big(\mathbb{E}(|S(s)|^2|\mathcal{F}_{m-1})\big)^{1/2}\mathrm{d}s\\ &\le C\theta\int_{t_{m-1}}^t \big(\mathbb{E}(|S(s)|^2|\mathcal{F}_{m-1})\big)^{1/2}\mathrm{d}s.\end{aligned}$$

Hence, we infer from (3.9) that

$$\mathbb{E}(|S(t)|^2|\mathcal{F}_{m-1}) \le C_5\int_{t_{m-1}}^t \big(\mathbb{E}(|S(s)|^2|\mathcal{F}_{m-1})\big)^{1/2}\mathrm{d}s + d\sigma_i^2(t-t_{m-1}), \qquad (3.10)$$

where $C_5 := 2C_V^{1/2}(1+C(q)(1+\theta^q)+|\widetilde{X}_i^k(t_{m-1})|^q)^{1/2}+C\theta$. We deduce from estimate (3.6) that the integrand on the right-hand side can be estimated according to

$$\begin{aligned}\mathbb{E}(|S(s)|^2|\mathcal{F}_{m-1}) &\le \frac12\mathbb{E}\big(|\widetilde{X}_i^k(s)|^2\big|\mathcal{F}_{m-1}\big)+\frac12|\widetilde{X}_i^k(t_{m-1})|^2\\ &\le \frac{C(2)}{2}(1+\theta^2)+\frac12|\widetilde{X}_i^k(t_{m-1})|^2.\end{aligned}$$

Inserting this estimate into (3.10), we conclude that

$$\mathbb{E}(|S(t)|^2|\mathcal{F}_{m-1}) \le C_6\tau(1+\theta^{q/2+1})\big(1+|\widetilde{X}_i^k(t_{m-1})|^{q/2+1}\big),$$

where $C_6 > 0$ does not depend on b_i, p_i, or ξ_m. $\square$

We define the error process $Z_i^k(t) := \widetilde{X}_i^k(t) - X_i^k(t)$ and prove some estimates for $Z_i^k(t)$, generalizing [52, Lemma 3.4].

Lemma 6 (Control of the error process)**.** *Let $i \in \{1, \dots, n\}$, $k \in \{1, \dots, N_i\}$, and $X_i^{0,k} \in L^{q_i'}(\Omega)$, where $q_i' = 2\max\{1, q_i\}$ and q_i is introduced in Assumption (A2). Then there exists a constant $C > 0$, which is independent of $(b_i, p_i)_{i=1,\dots,n}$, and m such that for all $t \in (t_{m-1}, t_m]$,*

$$\|Z_i^k(t) - Z_i^k(t_{m-1})\| \le C\tau(1 + \theta^{q_i'/2}), \quad |Z_i^k(t)| \le C\tau\theta + |Z_i^k(t_{m-1})|, \tag{3.11}$$

$$\begin{aligned} &\big|\mathbb{E}\big((Z_i^k(t) - Z_i^k(t_{m-1}))\chi_i^k(X(t))\big)\big| \qquad (3.12)\\ &\quad \le C\tau\bigg((1 + \theta^{3q_i'/2})\tau + (1 + \theta^{q_i'})\|Z_i^k(t)\| + \sum_{j=1}^n \|Z_j^1(t)\|\bigg) + 8\tau \max_{j=1,\dots,n} \|K_{ij}\|_\infty^2 \Gamma_i, \end{aligned}$$

where Γ_i and χ_i^k are defined in (2.7) and (3.2), respectively.

Proof. Since the Brownian motions are the same for X_i^k and $\widetilde{X}_i^k$, the process $Z_i^k(t)$ solves for $t \in (t_{m-1}, t_m]$ the deterministic equation

$$\begin{aligned} \mathrm{d}Z_i^k(t) &= -\big(\nabla V_i(\widetilde{X}_i^k(t)) - \nabla V_i(X_i^k(t))\big)\mathrm{d}t + \sum_{j=1}^n \beta_{ij} \sum_{\ell \in \mathcal{C}_{j,r},\,(i,k)\neq(j,\ell)} K_{ij}(\widetilde{X}_i^k - \widetilde{X}_j^\ell)\mathrm{d}t \qquad (3.13)\\ &\quad - \sum_{j=1}^n \alpha_{ij} \sum_{\ell=1,\,(i,k)\neq(j,\ell)}^{N_j} K_{ij}(X_i^k - X_j^\ell)\mathrm{d}t. \end{aligned}$$

Step 1: Proof of (3.11). Let $(i,k) \in \mathcal{C}_{i,r}$ for some $r \le b_i$. We take the expectation of the difference of the equations (3.13) solved by $Z_i^k(t)$ and $Z_i^k(t_{m-1})$, respectively, and distinguish the cases $j = i$ and $j \neq i$, leading to

$$\|Z_i^k(t) - Z_i^k(t_{m-1})\| \le J_{10} + \cdots + J_{14}, \quad \text{where} \tag{3.14}$$

$$\begin{aligned} J_{10} &= \bigg\|\int_{t_{m-1}}^t \big(\nabla V_i(\widetilde{X}_i^k(s)) - \nabla V_i(X_i^k(s))\big)\mathrm{d}s\bigg\|,\\ J_{11} &= \frac{1}{p_i - 1}\bigg\|\int_{t_{m-1}}^t \sum_{\ell \in \mathcal{C}_{j,r},\,(i,k)\neq(j,\ell)} K_{ii}(\widetilde{X}_i^k(s) - \widetilde{X}_i^\ell(s))\mathrm{d}s\bigg\|,\\ J_{12} &= \sum_{j=1,\,j\neq i}^n \frac{b_i}{p_j \min\{b_i, b_j\}}\bigg\|\int_{t_{m-1}}^t \sum_{\ell \in \mathcal{C}_{j,r}} K_{ij}(\widetilde{X}_i^k(s) - \widetilde{X}_j^\ell(s))\mathrm{d}s\bigg\|,\\ J_{13} &= \frac{1}{N_i - 1}\sum_{\ell=1,\,\ell\neq k}^{N_j}\bigg\|\int_{t_{m-1}}^t K_{ii}(X_i^k(s) - X_i^\ell(s))\mathrm{d}s\bigg\|,\\ J_{14} &= \sum_{j=1,\,j\neq i}^n \frac{1}{N_j}\sum_{\ell=1}^{N_j}\bigg\|\int_{t_{m-1}}^t K_{ij}(X_i^k(s) - X_j^\ell(s))\mathrm{d}s\bigg\|. \end{aligned}$$

For the first term, we use the Cauchy–Schwarz inequality, the growth condition of ∇V_i, and stability estimate (3.6) with $q = q_i'$:

$$\begin{aligned} J_{10} &\le \sqrt{\tau}\bigg(\mathbb{E}\int_{t_{m-1}}^t \big|\nabla V_i(\widetilde{X}_i^k(s)) - \nabla V_i(X_i^k(s))\big|^2 \mathrm{d}s\bigg)^{1/2} \\ &\le C_V\sqrt{\tau}\bigg(\mathbb{E}\int_{t_{m-1}}^t (1+\mathbb{E}|\widetilde{X}_i^k(s)|^q + \mathbb{E}|X_i^k(s)|^q)\mathrm{d}s\bigg)^{1/2} \le C\tau(1+\theta^{q/2}). \end{aligned}$$

For the remaining terms, we exploit the boundedness of K_{ij}, yielding

$$J_{11} + \cdots + J_{14} \le C\tau\sum_{j=1}^n\bigg(1+\frac{b_i}{\min\{b_i,b_j\}}\bigg)\|K_{ij}\|_\infty \le C\tau(1+\theta).$$

Thus, we deduce from (3.14) that

$$\|Z_i^k(t) - Z_i^k(t_{m-1})\| \le C\tau(1+\theta+\theta^{q/2}),$$

which proves the first inequality in (3.11).

We estimate similarly as in the proof of Lemma 4, using the strong convexity of V_i and the boundedness of K_{ij}:

$$\frac{\mathrm{d}}{\mathrm{d}t}|Z_i^k(t)|^2 \le -r_i|Z_i^k(t)|^2 + \sum_{j=1}^n \frac{b_i\|K_{ij}\|_\infty}{\min\{b_i,b_j\}}|Z_i^k(t)| \le C\theta|Z_i^k(t)|.$$

This implies after integration with respect to time that $|Z_i^k(t)| \le C\theta\tau + |Z_i^k(t_{m-1})|$, showing the second inequality in (3.11).

Step 2: Proof of (3.12). Set $\Delta K_{ij}^\ell := K_{ij}(\widetilde{X}_i^k - \widetilde{X}_j^\ell) - K_{ij}(X_i^k - X_j^\ell)$. Using the formulation (3.1) for $\widetilde{X}_i^k$, we find that

$$\big|\mathbb{E}\big((Z_i^k(t) - Z_i^k(t_{m-1}))\chi_i^k(X(t))\big)\big| \le J_{15} + \cdots + J_{18}, \quad \text{where} \tag{3.15}$$

$$\begin{aligned} J_{15} &= \mathbb{E}\bigg(\int_{t_{m-1}}^t \big|\nabla V_i(\widetilde{X}_i^k(s)) - \nabla V_i(X_i^k(s))\big|\mathrm{d}s|\chi_i^k(X(t))|\bigg), \\ J_{16} &= \mathbb{E}\bigg(\frac{1}{p_i-1}\int_{t_{m-1}}^t \sum_{\ell\in\mathcal{C}_{i,r},\,\ell\ne k}|\Delta K_{ii}^\ell(s)|\mathrm{d}s|\chi_i^k(X(t))|\bigg), \\ J_{17} &= \mathbb{E}\bigg(\sum_{j=1,\,j\ne i}^n \frac{b_i}{p_j\min\{b_i,b_j\}}\int_{t_{m-1}}^t \sum_{\ell\in\mathcal{C}_{j,r}}|\Delta K_{ij}^\ell(s)|\mathrm{d}s|\chi_i^k(X(t))|\bigg), \\ J_{18} &= \mathbb{E}\bigg|\int_{t_{m-1}}^t \chi_i^k(X(s))\mathrm{d}s\cdot\chi_i^k(X(t))\bigg|. \end{aligned}$$

For the term J_{15}, we use the mean-value theorem and the growth condition for D^2V_i (Assumption (A2)):

$$\big|\nabla V_i(\widetilde{X}_i^k - \nabla V_i(X_i^k)\big| \le |\widetilde{X}_i^k - X_i^k|\int_0^1 |D^2V_i(\widetilde{X}_i^k - \eta(\widetilde{X}_i^k - X_i^k))|\mathrm{d}\eta$$

$$\leq C_V|Z_i^k|\int_0^1 \big(1+|\widetilde X_i^k-\eta(\widetilde X_i^k-X_i^k)|^{q_i}\big)d\eta \leq C|Z_i^k|(1+|\widetilde X_i^k|^{q_i}+|X_i^k|^{q_i}).$$

Since $|\chi_i^k|\leq 2\sum_{j=1}^n\|K_{ij}\|_\infty$, the Cauchy–Schwarz inequality and stability estimate (3.6) lead to

$$\begin{aligned}J_{15}&\leq C\sum_{j=1}^n\|K_{ij}\|_\infty\int_{t_{m-1}}^t \mathbb{E}\big(|Z_i^k(s)|(1+|\widetilde X_i^k(s)|^{q_i}+|X_i^k(s)|^{q_i})\big)\mathrm{d}s\\&\leq C\sum_{j=1}^n\|K_{ij}\|_\infty\int_{t_{m-1}}^t \|Z_i^k(s)\|\|1+|\widetilde X_i^k(s)|^{q_i}+|X_i^k(s)|^{q_i}\|\mathrm{d}s\\&\leq C(q)\tau(1+\theta^{q_i})\big(\tau(1+\theta^{q_i/2})+\|Z_i^k(t)\|\big).\end{aligned}$$

The last inequality follows from

$$\begin{aligned}\|Z_i^k(s)\|&\leq \|Z_i^k(s)-Z_i^k(t_{m-1})\|+\|Z_i^k(t_{m-1})-Z_i^k(t)\|+\|Z_i^k(t)\|\\&\leq 2C\tau(1+\theta^{q_i/2})+\|Z_i^k(t)\|,\end{aligned}\tag{3.16}$$

which in turn is a consequence of estimate (3.11). We conclude that

$$J_{15}\leq C\tau^2(1+\theta^{3q_i/2})+C\tau(1+\theta^{q_i})\|Z_i^k(t)\|.$$

We use the Lipschitz continuity of K_{ij} (Assumption (A1)) to obtain

$$\begin{aligned}J_{16}&\leq \frac{2}{p_i-1}\sum_{j=1}^n\|K_{ij}\|_\infty\int_{t_{m-1}}^t\mathbb{E}\sum_{\ell\in\mathcal{C}_{i,r},\,\ell\neq k}|\Delta K_{ij}^\ell(s)|\mathrm{d}s\\&\leq\frac{CL_{ii}}{p_i-1}\int_{t_{m-1}}^t\mathbb{E}\sum_{\ell\in\mathcal{C}_{i,r},\,\ell\neq k}\big(|\widetilde X_i^k(s)-X_i^k(s)|+|X_i^\ell(s)-\widetilde X_i^\ell(s)|\big)\mathrm{d}s\\&\leq\frac{CL_{ii}}{p_i-1}\int_{t_{m-1}}^t\bigg(\bigg\|\sum_{\ell\in\mathcal{C}_{i,r},\,\ell\neq k}Z_i^k(s)\bigg\|+\bigg\|\sum_{\ell\in\mathcal{C}_{i,r},\,\ell\neq k}Z_i^\ell(s)\bigg\|\bigg)\mathrm{d}s.\end{aligned}$$

It follows from the second estimate in (3.11), i.e. $|Z_i^k(t)|\leq C\tau\theta+|Z_i^k(t_{m-1})|$, that

$$J_{16}\leq\frac{CL_{ii}}{p_i-1}\int_{t_{m-1}}^t\bigg((p_i-1)C\tau\theta+(p_i-1)\|Z_i^k(s)\|+\bigg\|\sum_{\ell\in\mathcal{C}_{i,r},\,\ell\neq k}Z_i^\ell(t_{m-1})\bigg\|\bigg)\mathrm{d}s.$$

The variable $Z_i^\ell(s)$ is $\mathcal{G}_{m-1}$-measurable for all $t_{m-1}<s<t$ and hence it is independent of ξ_{m-1}. Therefore, we can apply Lemma 3 to the last term of the integrand to find that

$$J_{16}\leq CL_{ii}\int_{t_{m-1}}^t\big(C\tau\theta+\|Z_i^k(s)\|+\|Z_i^k(t_{m-1})\|\big)\mathrm{d}s.\tag{3.17}$$

Here, we have taken into account the fact that $\|Z_i^k(t)\|=\|Z_i^\ell(t)\|$ for every $k,\ell=1,\ldots,N_i$. The last two terms of the integrand can be estimated, by estimate (3.11), according to (3.16) and

$$\|Z_i^k(t_{m-1})\|\leq\|Z_i^k(t_{m-1})-Z_i^k(t)\|+\|Z_i^k(t)\|\leq C\tau(1+\theta^{q_i/2})+\|Z_i^k(t)\|.$$

Hence, we conclude from (3.17) that

$$J_{16} \le C\tau\big(\tau(1+\theta^{q/2}) + \|Z_i^k(t)\|\big),$$

where $C > 0$ does not depend on b_i, p_i, or m and recalling that we have chosen $q = 2\max\{1, q_i\}$. Similar arguments lead to

$$\begin{aligned} J_{17} &\le 2\tau \sum_{j=1,\, j\neq i}^{n} \|K_{ij}\|_\infty \big(\tau(1+\theta^{q/2}) + \|Z_i^k(t)\| + \|Z_j^1(t)\|\big) \\ &\le C\tau\left(\tau(1+\theta^{q/2}) + \|Z_i^k(t)\| + \sum_{j=1,\, j\neq i}^{n} \|Z_j^1(t)\|\right). \end{aligned}$$

Finally, we estimate the remaining term. By the Cauchy–Schwarz inequality,

$$J_{18} = \int_{t_{m-1}}^{t} \mathbb{E}\big|\chi_i^k(X(s)) \cdot \chi_i^k(X(t))\big| \mathrm{d}s \le \int_{t_{m-1}}^{t} \|\chi_i^k(X(s))\| \, \|\chi_i^k(X(t))\| \mathrm{d}s. \tag{3.18}$$

By Lemma 44 in the appendix,

$$\|\chi_i^k(X(s))\|^2 = \mathbb{E}|\chi_i^k(X(s))|^2 = \mathbb{E}\big[\mathbb{E}\big(|\chi_i^k(X(s))|^2 \big| \sigma(X(s))\big)\big],$$

where $\sigma(X(s))$ is the σ-algebra generated by $X(s)$. Proposition 2 states that $\mathbb{E}\chi_i^k(X(s)) = 0$ and $\mathrm{Var}(\chi_i^k(X(s))) \le 8\max_{j=1,\ldots,n} \|K_{ij}\|_\infty^2 \Gamma_i$. Therefore,

$$\|\chi_i^k(X(s))\|^2 = \mathrm{Var}_{\sigma(X(s))}(\chi_i^k(X(s))) \le 8 \max_{j=1,\ldots,n} \|K_{ij}\|_\infty^2 \Gamma_i.$$

Inserting this estimate into (3.18) leads to

$$J_{18} \le 8\tau \max_{j=1,\ldots,n} \|K_{ij}\|_\infty^2 \Gamma_i.$$

Summarizing, we obtain from (3.15)

$$\begin{aligned} &\big|\mathbb{E}\big((Z_i^k(t) - Z_i^k(t_{m-1}))\chi_i^k(X(t))\big)\big| \\ &\quad \le C(q)\tau\left(\tau(1+\theta^{3q/2}) + (1+\theta^q)\|Z_i^k(t)\| + \sum_{j=1}^{n} \|Z_j^1(t)\|\right) + 8 \max_{j=1,\ldots,n} \|K_{ij}\|_\infty^2 \Gamma_i, \end{aligned}$$

which finishes the proof. □

3.3. Proof of Theorem 1

Let $i \in \{1, \ldots, n\}$ and $k \in \{1, \ldots, N_i\}$ be such that $(i,k) \in \mathcal{C}_{i,r}$ for some $r \le b_i$. As in the last section, we set $\Delta K_{ij}^\ell := K_{ij}(\widetilde{X}_i^k - \widetilde{X}_j^\ell) - K_{ij}(X_i^k - X_j^\ell)$. The process Z_i^k satisfies

$$\mathrm{d}Z_i^k(t) = -(\nabla V_i(\widetilde{X}_i^k(t)) - \nabla V_i(X_i^k(t)))\mathrm{d}t + \frac{1}{N_i - 1} \sum_{\ell=1,\, \ell\neq k}^{N_i} \Delta K_{ii}^\ell(t)\mathrm{d}t$$

$$+\sum_{j=1,\,j\neq i}^{n}\frac{1}{N_j}\sum_{\ell=1}^{N_j}\Delta K_{ij}^{\ell}(t)\mathrm{d}t+\chi_i^k(\widetilde{X}(t))\mathrm{d}t.$$

In particular, Z_i^k is pathwise a.e. differentiable in time.

Step 1: Differential inequality for $|Z_i^k|^2$. Together with the strong convexity of V_i (Assumption (A2)) and the Lipschitz continuity of K_{ij} (Assumption (A1)), we find that

$$\begin{aligned}\frac{1}{2}\frac{\mathrm{d}}{\mathrm{d}t}|Z_i^k|^2 &= -(\nabla V_i(\widetilde{X}_i^k)-\nabla V_i(X_i^k))\cdot Z_i^k+\frac{1}{N_i-1}\sum_{\ell=1,\,\ell\neq k}^{N_i}\Delta K_{ii}^{\ell}\cdot Z_i^k\\ &\quad+\sum_{j=1,\,j\neq i}^{n}\frac{1}{N_j}\sum_{\ell=1}^{N_j}\Delta K_{ij}^{\ell}\cdot Z_i^k+\chi_i^k(\widetilde{X})\cdot Z_i^k\\ &\leq -r_i|Z_i^k|^2+\frac{L_{ii}}{N_i-1}\sum_{\ell=1,\,\ell\neq k}^{N_i}(|Z_i^k|+|Z_i^\ell|)|Z_i^k|\\ &\quad+\sum_{j=1,\,j\neq i}^{n}\frac{L_{ij}}{N_j}\sum_{\ell=1}^{N_j}(|Z_i^k|+|Z_j^\ell|)|Z_i^k|+\chi_i^k(\widetilde{X})\cdot Z_i^k.\end{aligned}$$

By taking the expectation and using Young's inequality, it follows after a standard computation that

$$\frac{1}{2}\frac{\mathrm{d}}{\mathrm{d}t}\mathbb{E}|Z_i^k|^2\leq -r_i\mathbb{E}|Z_i^k|^2+\frac{3}{2}\sum_{j=1}^{n}L_{ij}\mathbb{E}|Z_i^k|^2+\frac{1}{2}\sum_{j=1}^{n}L_{ij}|Z_j^k|^2+\mathbb{E}(\chi_i^k(\widetilde{X})\cdot Z_i^k).$$

Without loss of generality, we may take $k=1$ (since the distributions coincide). A summation over $i=1,\ldots,n$ and exchanging the summation indices in the third term of the right-hand side leads to

$$\begin{aligned}\frac{1}{2}\frac{\mathrm{d}}{\mathrm{d}t}\sum_{i=1}^{n}\mathbb{E}|Z_i^1|^2 &\leq -\sum_{i=1}^{n}r_i\mathbb{E}|Z_i^1|^2+\frac{3}{2}\sum_{i,j=1}^{n}L_{ij}\mathbb{E}|Z_i^1|^2+\frac{1}{2}\sum_{i,j=1}^{n}L_{ji}\mathbb{E}|Z_i^1|^2\\ &\quad+\sum_{i=1}^{n}\mathbb{E}(\chi_i^1(\widetilde{X})\cdot Z_i^1)\\ &\leq -\min_{i=1,\ldots,n}\left(r_i-2\sum_{j=1}^{n}\max\{L_{ij},L_{ji}\}\right)\sum_{i=1}^{n}\|Z_i^1\|^2+\mathbb{E}(\chi_i^1(\widetilde{X})\cdot Z_i^1).\end{aligned}\tag{3.19}$$

It remains to estimate the last term $\mathbb{E}(\chi(\widetilde{X})\cdot Z_i^1)$. To this end, we write

$$\begin{aligned}&\mathbb{E}(\chi(\widetilde{X}(t))\cdot Z_i^1(t))=J_{19}+\cdots+J_{22},\quad\text{where}\\ &J_{19}=\mathbb{E}\big(Z_i^1(t_{m-1})\cdot\chi_i^1(\widetilde{X}(t_{m-1}))\big),\\ &J_{20}=\mathbb{E}\big((Z_i^1(t)-Z_i^1(t_{m-1}))\cdot\chi_i^1(X(t))\big),\\ &J_{21}=\mathbb{E}\big(Z_i^1(t_{m-1})\cdot(\chi_i^1(\widetilde{X}(t))-\chi_i^1(\widetilde{X}(t_{m-1})))\big),\end{aligned}\tag{3.20}$$

$$J_{22} = \mathbb{E}\big((Z_i^1(t) - Z_i^1(t_{m-1})) \cdot (\chi_i^1(\widetilde{X}(t)) - \chi_i^1(X(t)))\big).$$

Step 2: Estimate of J_{19} and J_{20}. Since $\xi_{m,i}$ is independent of $\mathcal{G}_{m-1}$ and $Z_i^1(t_{m-1})$ is $\mathcal{G}_{m-1}$-measurable, we obtain from Lemma 44 in the appendix that

$$\begin{aligned} \mathbb{E}\big(Z_i^1(t_{m-1})\big|\mathcal{G}_{m-1}\big) &= Z_i^1(t_{m-1}), \\ \mathbb{E}\big(Z_i^1(t_{m-1}) \cdot \chi(\widetilde{X}(t_{m-1}))\big|\mathcal{G}_{m-1}\big) &= Z_i^1(t_{m-1}) \cdot \mathbb{E}\big(\chi(\widetilde{X}(t_{m-1}))\big|\mathcal{G}_{m-1}\big). \end{aligned}$$

This shows that, using Proposition 2,

$$J_{19} = \mathbb{E}\big[\mathbb{E}\big(Z_i^1(t_{m-1}) \cdot \chi(\widetilde{X}(t_{m-1}))\big|\mathcal{G}_{m-1}\big)\big] = \mathbb{E}\big[Z_i^1(t_{m-1}) \cdot \mathbb{E}\big(\chi(\widetilde{X}(t_{m-1}))\big|\mathcal{G}_{m-1}\big)\big] = 0.$$

The term J_{20} can be directly estimated from (3.12):

$$J_{20} \le C\tau\bigg((1+\theta^{3q_i'/2})\tau + (1+\theta^{q_i'})\|Z_i^1(t)\| + \sum_{j=1}^n \|Z_j^1(t)\|\bigg) + 8\tau \max_{j=1,\ldots,n} \|K_{ij}\|_\infty^2 \Gamma_i.$$

Step 3: Estimate of J_{21}. We observe that $Z_i^1(t_{m-1})$ is $\mathcal{F}_{m-1}$-measurable. By the law of total expectation (Lemma 44) and the Cauchy–Schwarz inequality,

$$\begin{aligned} J_{21} &= \mathbb{E}\big[Z_i^1(t_{m-1})\mathbb{E}\big(\chi_i^1(\widetilde{X}_i^1(t)) - \chi_i^1(\widetilde{X}(t_{m-1}))\big|\mathcal{F}_{m-1}\big)\big] \\ &\le \|Z_i^1(t_{m-1})\| \, \big\|\mathbb{E}\big(\chi_i^1(\widetilde{X}_i^1(t)) - \chi_i^1(\widetilde{X}(t_{m-1}))\big|\mathcal{F}_{m-1}\big)\big\|. \end{aligned} \tag{3.21}$$

We deduce from (3.16) that the first factor on the right-hand side is bounded from above by

$$\|Z_i^1(t_{m-1})\| \le C\tau(1+\theta^{q_i'/2}) + \|Z_i^k(t)\|. \tag{3.22}$$

For the second factor, we introduce the notation

$$\begin{aligned} \Delta\widetilde{K}_{ij}^\ell &:= K_{ij}(\widetilde{X}_i^1(t) - \widetilde{X}_j^\ell(t)) - K_{ij}(\widetilde{X}_i^1(t_{m-1}) - \widetilde{X}_j^\ell(t_{m-1})), \\ \Delta\widetilde{X}_{ij}^\ell &:= (\widetilde{X}_i^1(t) - \widetilde{X}_j^\ell(t)) - (\widetilde{X}_i^1(t_{m-1}) - \widetilde{X}_j^\ell(t_{m-1})). \end{aligned}$$

Since ξ_m is $\mathcal{F}_{m-1}$-measurable, we can write the second factor on the right-hand side of (3.21) as follows:

$$\begin{aligned} &\mathbb{E}\big(\chi_i^1(\widetilde{X}(t)) - \chi_i^1(\widetilde{X}(t_{m-1}))\big|\mathcal{F}_{m-1}\big) \\ &\quad= \frac{1}{p_i-1}\sum_{\ell\in\mathcal{C}_{i,r},\,\ell\ne 1} \mathbb{E}(\Delta\widetilde{K}_{ii}^\ell|\mathcal{F}_{m-1}) - \frac{1}{N_i-1}\sum_{\ell=1,\,\ell\ne i}^{N_i} \mathbb{E}(\Delta\widetilde{K}_{ii}^\ell|\mathcal{F}_{m-1}) \\ &\qquad+ \sum_{j=1,\,j\ne i}^n \frac{b_i}{p_j\min\{b_i,bj\}}\sum_{\ell\in\mathcal{C}_{j,r}} \mathbb{E}(\Delta\widetilde{K}_{ij}^\ell|\mathcal{F}_{m-1}) - \sum_{j=1,\,j\ne i}\frac{1}{N_j}\sum_{\ell=1}^{N_j}\mathbb{E}(\Delta\widetilde{K}_{ij}^\ell|\mathcal{F}_{m-1}). \end{aligned} \tag{3.23}$$

We perform a Taylor expansion of K_{ij} at $\widetilde{X}_i^1(t_{m-1}) - \widetilde{X}_j^\ell(t_{m-1})$ and use the fact that K_{ij} is Lipschitz continuous with constant L_{ij}, such that DK_{ij} can be bounded from above by L_{ij}:

$$\big|\mathbb{E}(\Delta\widetilde{K}_{ii}^\ell|\mathcal{F}_{m-1})\big| \le L_{ij}\big|\mathbb{E}(\Delta\widetilde{X}_{ij}^\ell|\mathcal{F}_{m-1})\big| + \frac{d}{2}\|D^2K_{ij}\|_\infty\mathbb{E}\big(|\Delta\widetilde{X}_{ij}^\ell|^2\big|\mathcal{F}_{m-1}\big).$$

Inserting
$$\Delta\widetilde{X}_{ij}^{\ell} = \big(\widetilde{X}_i^1(t) - \widetilde{X}_i^1(t_{m-1})\big) + \big(\widetilde{X}_j^{\ell}(t) - \widetilde{X}_j^{\ell}(t_{m-1})\big)$$
into the previous estimate and taking into account the stability estimates of Lemmas 4 and 5, we infer that
$$\begin{aligned}\big\|\mathbb{E}(\Delta\widetilde{K}_{ii}^{\ell}|\mathcal{F}_{m-1})\big\| &\le C\tau L_{ij}\big(1+\theta^{\widetilde{q}_i}+\theta^{\widetilde{q}_j}\big)\\ &\quad + C\tau\|D^2K_{ij}\|_\infty(1+\theta^{q_i'/2+1})\big(1+\||\widetilde{X}_i^1(t_{m-1})|^{q_i'/2+1}\|\big)\\ &\le C\tau\big(1+\theta^{q_i'+2}\big),\end{aligned}$$
where the constant $C>0$ does not depend on b_i, p_i, or m. We use this estimate in (3.23) and observe that $b_i/\min\{b_i,b_j\}\le\theta$, yielding
$$\big\|\mathbb{E}\big(\chi_i^1(\widetilde{X}_i^1(t)) - \chi_i^1(\widetilde{X}(t_{m-1}))\big|\mathcal{F}_{m-1}\big)\big\| \le C\tau\big(1+\theta^{q_i'+3}\big). \tag{3.24}$$
Finally, we combine estimates (3.22) and (3.24) to conclude from (3.21) that
$$J_{21} \le C\tau(1+\theta^{q_i'+3})\|Z_i^1(t)\| + C\tau^2(1+\theta^{3q_i'/2+3}).$$

Step 4: Estimate of J_{22}. Set $\Delta K_{ij}^{\ell} := K_{ij}(\widetilde{X}_i^1(t)-\widetilde{X}_j^{\ell}(t)) - K_{ij}(X_i^1(t)-X_j^{\ell}(t))$. We use the Cauchy–Schwarz inequality and (3.11) to obtain
$$\begin{aligned}J_{22} &\le \|Z_i^1(t)-Z_i^1(t_{m-1})\|\,\|\chi_i^1(\widetilde{X}(t))-\chi_i^1(X(t))\| \\ &\le C\tau(1+\theta^{q_i'/2})\|\chi_i^1(\widetilde{X}(t))-\chi_i^1(X(t))\| \\ &\le C\tau(1+\theta^{q_i'/2})\bigg(\frac{1}{p_i-1}\bigg\|\sum_{\ell\in\mathcal{C}_{i,r},\,\ell\neq k}\Delta K_{ii}^{\ell}\bigg\| + \frac{1}{N_i-1}\sum_{\ell=1,\,\ell\neq k}^{N_i}\|\Delta K_{ii}^{\ell}\| \\ &\quad + \sum_{j=1,\,j\neq i}^{n}\frac{b_i}{p_j\min\{b_i,b_j\}}\bigg\|\sum_{\ell\in\mathcal{C}_{j,r}}\Delta K_{ij}^{\ell}\bigg\| + \sum_{j=1,\,j\neq i}^{n}\frac{1}{N_j}\sum_{\ell=1}^{N_j}\|\Delta K_{ij}^{\ell}\|\bigg).\end{aligned}\tag{3.25}$$
The difference ΔK_{ij}^{ℓ} can be estimated according to (see the second inequality in (3.11))
$$|\Delta K_{ij}^{\ell}| \le L_{ij}\big(|Z_i^1(t)|+|Z_j^{\ell}(t)|\big) \le C\big(\tau\theta + |Z_i^1(t_{m-1})| + |Z_j^{\ell}(t_{m-1})|\big).$$
Then, with the help of the auxiliary Lemma 3,
$$\begin{aligned}\frac{1}{p_i-1}\bigg\|\sum_{\ell\in\mathcal{C}_{i,r},\,\ell\neq k}\Delta K_{ii}^{\ell}\bigg\| &\le \frac{C}{p_i-1}\bigg\|\sum_{\ell\in\mathcal{C}_{i,r},\,\ell\neq k}\big(\tau\theta+|Z_i^1(t_{m-1})|+|Z_i^{\ell}(t_{m-1})|\big)\bigg\| \\ &\le C\tau\theta + C\|Z_i^1(t_{m-1})\| \le C\tau(1+\theta^{q_i'/2}) + C\|Z_i^1(t)\|,\\ \frac{1}{p_j}\bigg\|\sum_{\ell\in\mathcal{C}_{j,r},\,\ell\neq k}\Delta K_{ij}^{\ell}\bigg\| &\le C\tau(1+\theta^{\gamma/2}) + C\|Z_i^1(t)\| + C\|Z_j^1(t)\|,\end{aligned}$$
where $\gamma = \max_{j=1,\dots,n} q_j'$. Therefore, because of $b_i/\min\{b_i,b_j\}\le\theta$, (3.25) becomes
$$J_{22} \le C\tau(1+\theta^{q_i'/2})(1+\theta)\bigg(\tau(1+\theta^{\gamma/2}) + \sum_{j=1}^{n}\|Z_j^1(t)\|\bigg).$$

We deduce from (3.20) and the previous estimates for $J_{19},\ldots,J_{22}$ that

$$\begin{aligned}\sum_{i=1}^n \mathbb{E}\big(\chi_i^1(\widetilde{X}(t))\cdot Z_i^1\big) &\le C\tau^2(1+\theta^{3\gamma/2+3}) + C\tau(1+\theta^{\gamma+3})\sum_{i=1}^n \|Z_i^1(t)\| + C\tau\sum_{i=1}^n \Gamma_i \\ &\le C_7(\theta)\tau^2 + C_8(\theta)\tau\bigg(\sum_{i=1}^n \|Z_i^1(t)\|^2\bigg)^{1/2} + C_9\tau\sum_{i=1}^n\Gamma_i.\end{aligned} \tag{3.26}$$

Step 5: End of the proof. Let

$$u(t) = \sum_{i=1}^n \|Z_i^1(t)\|^2, \quad r = \min_{i=1,\ldots,n}\bigg(r_i - 2\sum_{j=1}^n \max\{L_{ij},L_{ji}\}\bigg) > 0.$$

We infer from (3.19) and (3.26) that

$$\frac{\mathrm{d}u}{\mathrm{d}t} \le -ru + C_7\tau^2 + C_8\tau u^{1/2} + C_9\tau\sum_{i=1}^n \Gamma_i.$$

The positive solution z_+ of the quadratic equation $-rz^2 + C_7\tau^2 + C_8\tau z + C_9\tau\sum_{i=1}^n \Gamma_i = 0$ gives us an upper bound for $u(t)^{1/2}$, since $\mathrm{d}u/\mathrm{d}t \le 0$ otherwise. Consequently,

$$\begin{aligned}u(t)^{1/2} \le z_+ &= \frac{C_9}{2r}\tau + \frac{\sqrt{\tau}}{2r}\bigg(C_8^2\tau + 4C_7r\tau + 4C_9r\sum_{i=1}^n\Gamma_i\bigg)^{1/2} \\ &\le C\tau(1+\theta^{3\gamma/2+3}) + C\sqrt{\tau}\bigg(\sum_{i=1}^n \Gamma_i\bigg)^{1/2}.\end{aligned}$$

This ends the proof of Theorem 1.

3.4. Particle systems with multiplicative noise

The technique of the proof of Theorem 1 can be applied to particle systems with multiplicative noise,

$$\mathrm{d}X_i^k = -\nabla V_i(X_i^k)\mathrm{d}t + \sum_{j=1}^n \alpha_{ij}\sum_{\substack{\ell=1\\(i,k)\neq(j,\ell)}}^{N_j} K_{ij}(X_i^k - X_j^\ell)\mathrm{d}t + \sigma_i(X_i^k)\mathrm{d}B_i^k(t), \tag{3.27}$$

with initial conditions (2.2), and $\alpha_{ij} = 1/(N_j - \delta_{ij})$, $i,j = 1,\ldots,n$, $k = 1,\ldots,N_i$. The random-batch process $\widetilde{X}_i^k$ is defined as in (2.4) but with $\sigma_i(\widetilde{X}_i^k)$ instead of σ_i. In addition to Assumptions (A1)–(A4), we suppose the following conditions:

(A1′) Diffusion: $\sigma_i \in C^0(\mathbb{R}^d)$ is bounded and Lipschitz continuous with Lipschitz constant $L_i > 0$.

(A2′) Strong convexity: The function $x \mapsto V_i(x) - r_i|x|^2/2$ is convex, where $r_i > 2\sum_{j=1}^n \max\{L_{ij},L_{ji}\} + L_i^2 d$ and $r_i > 2L_i^2(2\max\{1,q_i\} + d - 2)$, $i = 1,\ldots,n$.

Theorem 7. *Let Assumptions* (A1)–(A2), (A4), (A1′)–(A2′) *hold. Then there exists a constant* $C > 0$*, which is independent of* $(b_i, p_i)_{i=1,\ldots,n}$*,* m*, and* T*, such that*

$$\sup_{0<t<T} \sum_{i=1}^{n} \|(X_i^k - \widetilde{X}_i^k)(t)\| \le C\sqrt{\tau}\Big(1 + \sum_{i=1}^{n} \Gamma_i\Big)^{1/2} + C\tau(1 + \theta^\gamma),$$

and θ*,* γ*,* Γ_i *are defined in* (2.6)–(2.7).

Sketch of the proof. The proof is similar to that one for Theorem 1 except for some additional estimates for the multiplicative noise term. In particular, Proposition 2 keeps unchanged since it is concerned with the shuffling process only. For the stability (Lemma 4), we need the condition $2 \le q \le q_i' = 2\max\{1, q_i\}$. The proof is essentially the same, except for the estimate of the term $\frac{1}{2}q(q + d - 2)\mathbb{E}(\sigma_i^2|X_i^k|^{q-2})$. Here, we use the Lipschitz continuity of σ_i and the stricter condition on r_i in Assumption (B2). In the estimate for $\widetilde{X}_i^k(t) - \widetilde{X}_i^k(t_{m-1})$ (Lemma 5), the diffusion σ_i is controlled by the Lipschitz continuity, $\sigma_i(\widetilde{X}_i^k)^2 \le 2L_i^2|\widetilde{X}_i^k|^2 + 2\sigma_i(0)^2$, and Lemma 4. Finally, for the control of the error process (Lemma 6), estimates (3.11)–(3.12) need to be changed to

$$\|Z_i^k(t) - Z_i^k(t_{m-1})\| \le C\tau(1 + \theta^{q_i'/2}) + C\sqrt{\theta}, \tag{3.28}$$

$$\begin{aligned}\big|\mathbb{E}\big((Z_i^k(t) - Z_i^k(t_{m-1}))\chi_i^k(\widetilde{X}(t_{m-1}))\big)\big| &\le C\tau^2(1 + \theta^{3q_i'/2}) + 8\tau \max_{j=1,\ldots,n} \|K_{ij}\|_\infty^2 \Gamma_i \\ &+ \sqrt{\tau}\Big((1 + \sqrt{\tau})(1 + \theta^{q_i'})\|Z_i^k(t)\| + \sqrt{\tau}(1 + \sqrt{\tau}) \sum_{j=1}^{n} \|Z_j^1(t)\|\Big).\end{aligned} \tag{3.29}$$

For the proof of estimate (3.28), the right-hand side of (3.14) contains the additional term

$$\widetilde{J}_{14} = \Big\| \int_{t_{m-1}}^{t} (\sigma_i(\widetilde{X}_i^k) - \sigma_i(X_i^k))\mathrm{d}B_i^k \Big\|.$$

The square of $\widetilde{J}_{14}$ is estimated by using the Itô isometry and the Lipschitz continuity of σ_i. Integrating and taking the square root then leads to the additional $C\sqrt{\tau}$ term.

The proof of (3.29) is very similar to (3.12), except that we need the inequality

$$\Big\| \frac{1}{p_i - 1} \sum_{\ell \in \mathcal{C}_{i,r},\, \ell \ne k} |Z_i^k| \Big\| \le C\theta(\tau + \|Z_i^1(t_{m-1})\|).$$

The square of the left-hand side is formulated as

$$\Big\| \frac{1}{p_i - 1} \sum_{\ell \in \mathcal{C}_{i,r},\, \ell \ne k} |Z_i^k| \Big\|^2 = \mathbb{E}\Big\{\mathbb{E}\Big[\Big(\sum_{\ell \in \mathcal{C}_{i,r},\, \ell \ne k} |Z_i^k|\Big)^2 |\mathcal{F}_{m-1}\Big]\Big\}.$$

Since ξ_{m-1} is $\mathcal{F}_{m-1}$ measurable, the inner expectation becomes

$$\mathbb{E}\Big[\Big(\sum_{\ell \in \mathcal{C}_{i,r},\, \ell \ne k} |Z_i^k|\Big)^2 |\mathcal{F}_{m-1}\Big] = \sum_{\ell,\ell' \in \mathcal{C}_{i,r},\, \ell,\ell' \ne k} \mathbb{E}\big(|Z_i^\ell|\,|Z_i^{\ell'}|\,|\mathcal{F}_{m-1}\big)$$

$$\leq \sum_{\ell,\ell' \in \mathcal{C}_{i,r},\, \ell,\ell' \neq k} \sqrt{\mathbb{E}(|Z_i^\ell|^2|\mathcal{F}_{m-1})}\sqrt{\mathbb{E}(|Z_i^{\ell'}|^2|\mathcal{F}_{m-1})},$$

using the Cauchy–Schwarz inequality for the conditional expectation. A straightforward computation leads to

$$\mathbb{E}(|Z_i^\ell|^2|\mathcal{F}_{m-1}) \leq C\theta^2(\tau + |Z_i^k(t_{m-1})|)^2,$$

from which we infer that

$$\mathbb{E}\bigg[\bigg(\sum_{\ell \in \mathcal{C}_{i,r},\, \ell \neq k} |Z_i^k|\bigg)^2 |\mathcal{F}_{m-1}\bigg] \leq C\theta^2\bigg(\sum_{\ell \in \mathcal{C}_{i,r},\, \ell \neq k} (\tau + |Z_i^k(t_{m-1})|)\bigg)^2.$$

As $Z_i^\ell(t_{m-1})$ is independent of ξ_{m-1}, the proof finishes after applying Lemma 3. □

A more complicated particle system with multiplicative noise was considered in [26], which leads in a mean-field-type limit to the Shigesada–Kawasaki–Teramoto population model:

$$\mathrm{d}X_i^k = -\nabla V_i(X_i^k)\mathrm{d}t + \bigg(\sigma_i^2 + \sum_{j=1}^n f\bigg(\alpha_{ij} \sum_{\substack{\ell=1 \\ (i,k)\neq(j,\ell)}}^{N_j} K_{ij}(X_i^k - X_j^\ell)\bigg)\bigg)^{1/2} \mathrm{d}B_i^k(t),$$

with initial conditions (2.2), $i = 1, \ldots, n$, $k = 1, \ldots, N_i$, and the function f is globally Lipschitz continuous. Again, the random-batch process $\widetilde{X}_i^k$ is similar to (2.4). For this system, we have been not able to prove an error estimate of order $\sqrt{\tau}$, but only a stability estimate of the form

$$\sum_{i=1}^n \|(X_i^k - \widetilde{X}_i^k)(t)\| \leq C(t)\sqrt{t}\bigg(\sqrt{\tau}h(t,\tau,\theta) + \sum_{i=1}^n \Gamma_i\bigg), \quad t > 0,$$

where $h(t,\tau,\theta)$ is a smooth function. Compared to the error estimates of Theorems 1 and 7, the bound $\sum_{i=1}^n \Gamma_i$ for the variance of the remainder (3.2) is not multiplied by $\sqrt{\tau}$. Numerical simulations (not shown) reveal a saturation effect when τ becomes very small, indicating that the previous estimate cannot be improved.

4. Simulations

In this chapter, we present numerical results for a test example, a population system, and a opinion-formation model. We end with a conclusion based on this experiments.

4.1. Numerical simulations

In the subsequent numerical simulations, the algorithm is implemented in Matlab. The random shuffling is realized using the command `randperm`, and the stochastic differential equations are discretised by the standard Euler–Maruyama scheme. We often choose the number p_i of particles per batch b_i in such a way that the ratio of the total numbers of agents per species is conserved,

$$\frac{p_i}{p_j} = \frac{N_i}{N_j} = \frac{p_i}{p_j}\frac{b_i}{b_j} \quad \text{for } 1 \leq i, j \leq n.$$

This choice automatically leads to $b_i = b_j$ and hence to $\theta = 1$, which is the best case scenario in terms of the error estimate.

4.1.1. Discrete L^2 error for a test example

We generalize the test example of [52, Section 4.1]. For this, we consider system (2.1) with $n = 3$ species in $d = 2$ dimensions and specify the functions

$$\nabla V_i(x) = r_i(x - m^{(i)}), \quad K_{ij}(x) = \frac{Q_i Q_j x}{1 + |x|^2}, \quad x \in \mathbb{R}^2,\ i, j = 1, 2, 3,$$

where the model parameters are $(Q_1, Q_2, Q_3) = (-1, 2, -2)$, $(r_1, r_2, r_3) = (1, 4, 2)$, and $m^{(1)} = (1, 0)^T$, $m^{(2)} = -(1, 1)^T$, $m^{(3)} = (1, 1)^T$. This choice incorporates different repulsive and attracting effects. The initial data are centered Gaussian distributions with the variances $(v_1, v_2, v_3) = (2, 2, 1)$, where the index signifies the number of the species.

For the first experiment, we choose the diffusion coefficients $\sigma_i = 0.5$ for $i = 1, 2, 3$ and the time step sizes $\tau = 2^{-2}, \ldots, 2^{-6}$. The end time is $T = 1$, the batch sizes are $p_i = 2$ for $i = 1, 2, 3$, and the numbers N_i of particles of the ith species are $(N_1, N_2, N_3) = (100, 100, 200)$, $(1000, 1000, 2000)$, or $(2500, 2500, 5000)$. Thus the total number of particles is $N = 400$, 4000, or 10000. We compare the random-batch solution with a reference solution, obtained by solving the fully coupled system using the time step size $2^{-4}, \ldots, 2^{-8}$. Figure 4.1 (left) shows the discrete $L^2(\Omega)$ error for the different time step sizes, defined by

$$E = \left(\sum_{i=1}^{n} \frac{1}{N_i} \sum_{k=1}^{N_i} |\widetilde{X}_i^k(T) - X_i^k(T)|^2 \right)^{1/2}.$$

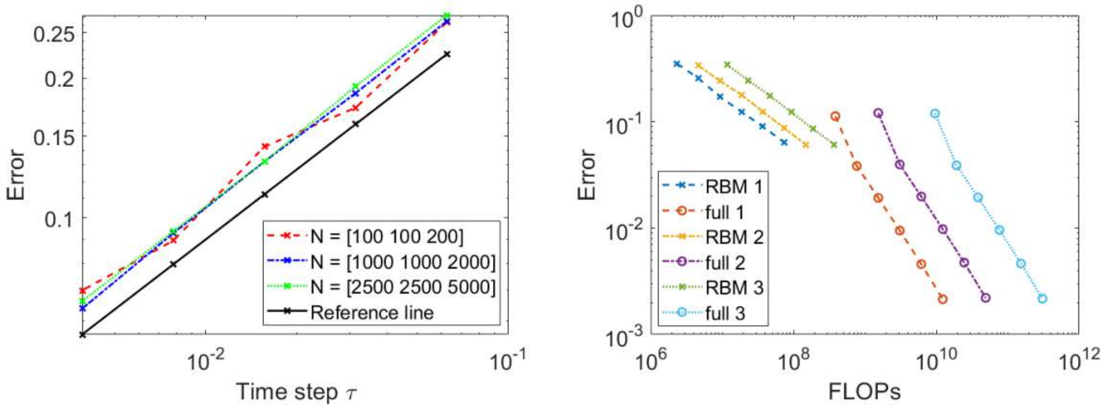

Figure 4.1.: Left: Discrete $L^2(\Omega)$ error E versus time step size τ for various total particle numbers N. Right: Discrete $L^2(\Omega)$ error versus number of FLOPs for various random-batch simulations (RBM) and the corresponding reference solutions (ref).

The reference line has the slope 1/2. The results clearly show that the convergence rate is of order $O(\sqrt{\tau})$ as predicted by Theorem 1.

Figure 4.1 (right) illustrates the $L^2(\Omega)$ error as a function of the computational time, represented by the number of FLOPs (floating-point operations). We choose $\sigma_i = 0$ for all $i = 1, \dots, n$ to allow for the comparison of the random-batch solution with a reference solution that is calculated beforehand. The parameters for the random-batch algorithm are $T = 1$, $n = 2$, $d = 2$, $(p_1, p_2) = (2, 2)$, $\tau = 2^{-3}, \dots, 2^{-7}$, and $(N_1, N_2) = (1250, 1250)$ (RBM1, full 1), $(2500, 2500)$ (RBM2, full 2), or $(5000, 5000)$ (RBM3, full 3). The reference solution is calculated from an explicit Euler scheme with the time step size $\tau = 2^{-1}, \dots, 2^{-5}$. The number of FLOPs needed for the Matlab-internal functions are determined by the lightspeed toolbox of Tom Minka (https://github.com/tminka/lightspeed). The total numbers of FLOPs are then calculated by adding all needed operations manually.

Figure 4.1 (right) shows that the random-batch algorithm needs almost three orders of magnitude less FLOPs than the reference algorithm. As expected, the discrete $L^2(\Omega)$ error of the random-batch scheme is larger than that one of the reference scheme for a given time step. However, for a given error, the number of FLOPs of the random-batch algorithm is still much smaller compared to the reference algorithm, namely by about two orders of magnitude.

4.1.2. L^2 error comparison for a test example

We compare the output of our algorithm with the results obtained from the single-batch method of [53], applied to the example from section 4.1.1. The model parameters Q_i are chosen randomly according to a uniform distribution on the interval $[-1, 1]$. To ensure that our assumptions on V_i are met, we use $r_i = 1$ for every species. The initial distribution is given by a centred Gaussian distribution with the variance $\mathrm{Var} = 2$.

We choose $N = [100, 200, 400]$ for our particle numbers per species. Our analytical and numerical results show (see section 4.1.1) that an increase of the number of particles does not lead to significant changes in the error (estimate), which justifies our choice of using a relatively low total particle number. We simulate the above system with final time $T = 1$ and step sizes $\tau = 2^{-k}$, $k = 3, \dots, 7$, using our RBM algorithm and the RBM algorithm from [53]. Regarding the batches of our RBM algorithm, three different choices are tested: $p^{(1)} = [2,2,2]$, $p^{(2)} = [2,4,4]$, $p^{(3)} = [2,4,8]$, giving $\theta^{(1)} = 4$, $\theta^{(2)} = 2$, $\theta^{(3)} = 1$, respectively. For the batches of the algorithm in [53], we take $q^{(1)} = 4$, $q^{(2)} = 10$, and $q^{(3)} = 14$, which guarantees a comparable computational cost for the simulations. The reference solution is calculated from an Euler–Maruyama scheme with time step size 2^{-k-2}. For each step size τ and choice of p, we repeat the simulation 10^3 times and collect the error in the (error-) vectors $\mathrm{err}_\theta^{k,j}$ and $\mathrm{err}_q^{k,j}$, where j is the index representing the choice of θ or q.

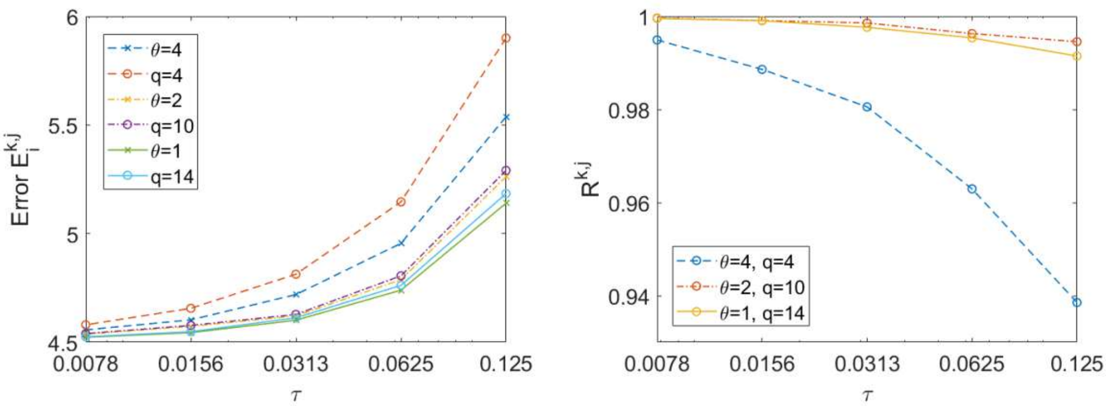

Figure 4.2.: Left: Mean error $E_i^{k,j}$ for different choices of θ (our method) and q (method of [53]) versus the time step size τ. Right: Error quotient $R^{k,j} = E_\theta^{k,j}/E_q^{k,j}$ for different choices of θ and q versus τ.

The reference error $E_i^{k,j} = \|\mathrm{err}_i^{k,j}\|$ in the ℓ^2 norm and the error quotient $R^{k,j} = E_\theta^{k,j}/E_q^{k,j}$ for $i = \theta, q$, $j = 1,2,3$ are plotted in Figure 4.2. We see that our RBM algorithm leads to slightly smaller errors compared to the single-species RBM scheme of [53]. Interestingly, even suboptimal super-batches (in terms of the error estimate) can still lead to better results; see the outcomes for $\theta = 4$, $q = 4$. This may be possibly explained by the fact that the step size is not sufficiently small to guarantee a good mixing in terms of the composition of the batches for the algorithm of [53], while our method, based on super-batches and (multiplicative) correction terms, leads to (slightly) smaller errors.

4.1.3. The Poisson–Boltzmann problem

We apply our algorithm to the stochastic particle model for the Poisson–Nernst–Planck system introduced in [70] and compare it with the numerical results obtained by the algorithm from [53]. We consider the following (dimensionless) Poisson–Boltzmann problem:

$$\begin{aligned} -\frac{\partial^2\phi}{\partial x^2} &= \rho_\infty(e^{-\phi} - e^{\phi}) + f(x) \quad \text{in } \mathbb{R}, \\ \phi(x) &\to 0 \quad \text{as} \quad |x| \to \infty, \end{aligned} \tag{4.1}$$

where ϕ is an electrostatic potential, $\rho_\infty > 0$ is the far-field density, and $f(x)$ is some given background charge. This problem is the thermal equilibrium of the Poisson–Nernst–Planck system

$$\begin{aligned} &\frac{\partial\rho_\pm}{\partial t} = \frac{\partial}{\partial x}\left(\frac{\partial\rho_\pm}{\partial x} + z_\pm\rho_\pm\frac{\partial\phi}{\partial x}\right), \quad -\frac{\partial^2\phi}{\partial x^2} = \rho_+ - \rho_- \quad \text{in } \mathbb{R}, \\ &\rho_\pm(x,t) \to \rho_\infty, \quad \phi(x,t) \to 0 \quad \text{as } |x| \to \infty, \end{aligned} \tag{4.2}$$

assuming electro-neutrality in the far field, where $\rho_\pm$ are the densities and $z_\pm$ the associated charges. In thermal equilibrium, the fluxes vanish and we find that $\rho_\pm = \rho_\infty \exp(\mp\phi)$. The solution to the first equation in (4.2) can be interpreted as the probability density associated to the stochastic differential equation

$$\mathrm{d}X_\pm = -\frac{\partial}{\partial x}(z_\pm\phi)\mathrm{d}t + \sqrt{2}\mathrm{d}B_\pm(t),$$

which in turns is the mean-field limit of the particle system

$$\mathrm{d}X_i^k = f * F(X_i^k)\mathrm{d}t + \sum_{j=\pm}\sum_{\ell=1,\,(j,\ell)\neq(i,k)}^{N_j} z_i z_j q F(X_i^k - X_j^\ell)\mathrm{d}t + \sqrt{2}\mathrm{d}B_i^k(t) \tag{4.3}$$

for $i \in \{+,-\}$, $k = 1,\dots,N_i$, where $q = Q/N$, Q is the charge for both positively and negatively particles, N is the number of particles, and $F(x) = \operatorname{sgn}(x)/2$ is the repulsive Coulomb force in one space dimension. It is shown in [52] that (4.1) can be approximated by the equation on the interval $(-L, L)$ for sufficiently large $L > 0$:

$$-\frac{\partial^2\phi}{\partial x^2} = \rho_\infty(e^{-\phi} - e^{\phi}) + f(x) \quad \text{in } (-L,L), \qquad \frac{\partial\phi}{\partial x} = 0 \quad \text{for } x = \pm L. \tag{4.4}$$

We compute approximations of solutions to (4.4), respectively (4.1), by simulating the particle system (4.3) for large times. The authors of [70] already showed that random-batch algorithms can be meaningfully applied to such problems.

As the simulation domain in (4.4) is bounded, we need a strategy for the particles close to domain boundary. The idea is to implement, as in [52], reflecting boundary conditions, i.e., particles arriving at $x = \pm L$ are reflected back into the interval $(-L, L)$.

For the simulations, we choose the parameters $L = 10$, $N = [10^5, 10^5]$, $Q = 1$, $\tau = 10^{-2}$, $T = 40$, and the background charge

$$f(x) = \begin{cases} 3x^2 - R^2 & \text{for } |x| \le R, \\ 0 & \text{else,} \end{cases}$$

where $R = 3/2$. Equation (4.4) is solved for reference by a finite-difference (FD) scheme, together with a Newton method, where $\rho_\infty = 0.048$ was obtained from a previous simulation of (4.3) and the identities $\rho_\pm = \rho_\infty \exp(\mp\phi)$. They are also used to compute the charge densities from the potential ϕ as the solution to the finite-difference scheme. Figure 4.3 (left) illustrates the densities $\rho_\pm$ obtained from the RBM and the FD schemes, which both agree very well. As expected, the background density is repulsive with respect to ρ_- and attractive with respect to ρ_+.

Figure 4.3 shows a comparison of our method with that one of [53]. With the same notation and setup as in section 4.1.2, we choose $N = [500, 500]$, $p = [2, 2]$ for the super-batches and $q = 4$ as the batch size for the algorithm of [52]. The figure shows that our method performs slightly better than that one of [52], but the difference becomes arbitrarily small when $\tau \to 0$.

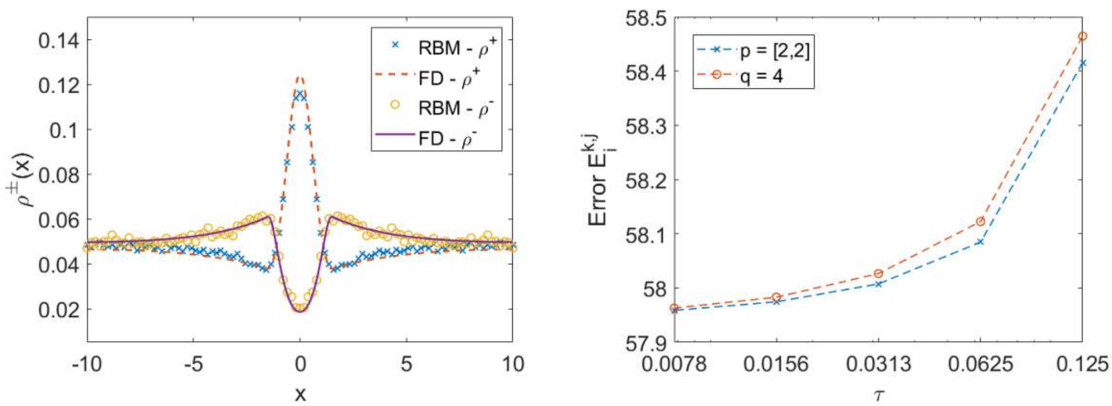

Figure 4.3.: Left: Different approximations of the charge densities $\rho^\pm$ obtained from the RBM algorithm and the finite-difference (FD) scheme. Right: Mean error $E_i^{k,j}$ versus time step size τ for Example 4.1.3.

4.1.4. A population system

We consider the population system derived in [25] without external potentials using the following parameters: $n = 3$, $d = 1$, $T = 2$, $N_i = 5000$ for $i = 1, 2, 3$, and $(\sigma_1, \sigma_2, \sigma_3) = (1, 2, 3)$. The interaction kernels are given by $K_{ij} = \nabla B^\eta_{ij}$, where $B^\eta_{ij}(x) = \eta^{-1} B_{ij}(x/\eta)$, $B_{ij}(x) = D_{ij} \exp(1 - 1/(1 - |x|^2))1_{\{|x|<1\}}(x)$ for $x \in \mathbb{R}$, $\eta = 2$, and

$$(D_{ij}) = \begin{pmatrix} 0 & 355 & 355 \\ 25 & 0 & 25 \\ 355 & 0 & 0 \end{pmatrix}.$$

The initial data are Gaussian normal distributions with means $(m_1, m_2, m_3) = (-1, 2, 3)$ and variances $(v_1, v_2, v_3) = (2, 2, 2)$.

Figure 4.4 (left) illustrates the approximate probability densities at time $T = 2$ obtained by simulating the particle system 1000 times with the batch sizes $p_i = 20$ for $i = 1, 2, 3$ and the time step size $\tau = 10^{-2}$. We observe that the species segregate and avoid each other. Each of the simulation requires about $2 \cdot 10^{10}$ FLOPs, which needs to be compared to about $5 \cdot 10^{12}$ FLOPs required when using full interactions. This is a reduction of the numerical effort of more than two orders of magnitude.

Clearly, the reduction of computational cost comes at the price of an increased error. Figure 4.4 (right) presents the discrete $L^2(\Omega)$ error versus the number of FLOPs for various configurations of the batch sizes and various time step sizes. The end time is $T = 1$, and we used batch sizes $p_i = 2, 10, 100, 1000$ and time step sizes $\tau = 2^{-1}, \ldots, 2^{-7}$. The different points per line correspond to different values of τ. The reference solution is computed from the Euler–Maruyama scheme with the step size $\tau = 2^{-9}$; this simulation needed about 10^{13} FLOPs. We see that the error decreases with the time step size and larger batch sizes. The red dot in the figure indicates the number of FLOPs needed to compute a numerical solution with full interactions and step size $\tau = 10^{-2}$, to give a more practical point of reference. This simulation required about $2.5 \cdot 10^{12}$ FLOPs, while the random-batch algorithm with $\tau = 2^{-7}$ was about four times faster.

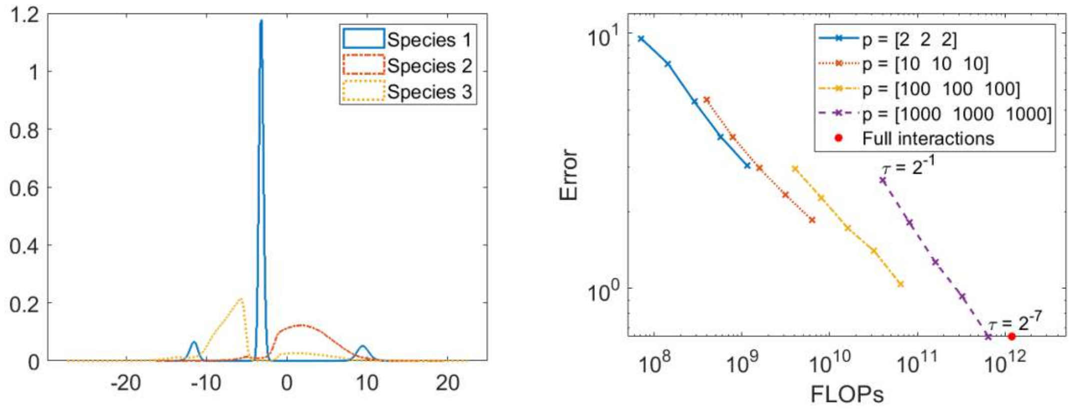

Figure 4.4.: Left: Histogram of the population model derived in [25] for three species at time $T = 2$. Right: Discrete $L^2(\Omega)$ error versus number of FLOPs for various batch sizes p and time step sizes τ.

4.1.5. Opinion dynamics model

We model a company whose internal hierarchy regulates the communication between three different types of agents: workers (species 1), managers (species 2), and CEOs (species 3). The agents obey the following rules:

- CEOs can be only influenced by other CEOs. They influence managers (but not vice versa) and they do not interact with workers.
- Managers can influence workers but not other managers or CEOs.
- Workers can only influence each other.

The dynamics of opinions is described by the system

$$\mathrm{d}X_i^k(t) = \sum_{j=1}^{3} \frac{1}{N_i - \delta_{ij}} \sum_{\ell=1,\,(i,k)\neq(j,\ell)}^{N_j} K_{ij}(X_i^k(t) - X_j^\ell(t))\mathrm{d}t + \sigma \mathrm{d}t,$$
$$X_i^k(0) = X_i^{0,k}, \quad i,j = 1,2,3,\ k = 1,\dots,N_i,\ 0 < t \le T,$$

which is a generalization of a model discussed in [77]. Although this model does not feature any external potentials, our algorithm can be applied meaningfully to this situation. The interaction is modelled by $K_{ij}(x) = -D_{ij}\phi(x/R_j)x$ for $x \in \mathbb{R}$, where $\phi(x) = \exp(1-1/(1-|x|^{10}))1_{(-1,1)}$ is a smooth approximation of the characteristic function $1_{(-1,1)}$. The value D_{ij} is a measure of the influence that an agent of species j has over an agent of species i. According to the above-mentioned interaction rules, the matrix $D = (D_{ij})$ has the structure

$$D = \begin{pmatrix} D_{11} & D_{12} & 0 \\ 0 & 0 & D_{23} \\ 0 & 0 & D_{33} \end{pmatrix}.$$

As the only way for CEOs to communicate with the workers happens indirectly via the managers, we wish to explore the influence of the managers to achieve a consensus. In particular, we consider managers that are very submissive to authority ($D_{23} \gg 1$) or that are less obedient ($D_{23} \le 1$). For the simulations, we use 5000 workers, 10 managers and 2 CEOs. The parameters are $\sigma = 0.1$, $T = 5$, $\tau = 10^{-5}$, and $(p_1, p_2, p_3) = (20, 2, 2)$. The initial conditions are drawn from a uniform distribution on the interval $[0, 10]$. The interaction radii are $(R_1, R_2, R_3) = (1, 2.5, 5)$. In the first case (submissive managers), we choose the influence values

$$D_{11} = 5, \quad D_{12} = 10, \quad D_{23} = 25, \quad D_{33} = 0.1.$$

Figure 4.5 (left) shows one simulation of the particle system. We observe that the managers are very eager to find a compromise between the opinions of the two CEOs. This change of the opinion occurs too fast for the workers with more extreme opinions, as they are not as susceptible as the managers (since $D_{12} < D_{23}$). Therefore, they leave quickly the range of interaction of the managers and form their own clusters. Only those workers who have an opinion already close to that one of the CEOs, agree with the company policy and change their opinion accordingly.

In the second case (less obedient managers), we choose the same values of D_{ij} as before except $D_{23} = 1$. This means that the influence of the CEOs over the managers is rather small. Figure 4.5 (right) shows that the managers change their opinion slowly enough for the workers to adapt their opinion, as they stay within their range of interaction. Eventually, this leads to a consensus of opinion.

The simulations suggest that small changes over time are more likely to lead in an adjustment of the opinion and eventually to a consensus. In this picture, managers should not impose their opinion too quickly, but they should introduce the changes sufficiently slowly such that the workers can adjust in time.

Finally, we explore the influence of the batch size on the running time and the error. We consider 10000 workers, 100 managers, and 10 CEOs and choose the parameters $\tau =$

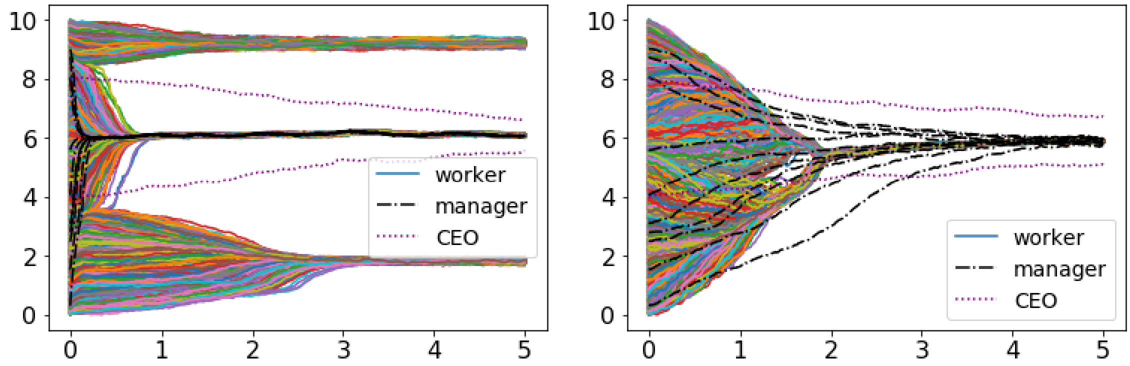

Figure 4.5.: Opinion versus time of the CEOs and managers in the case of very submissive (left) or less obedient (right) managers.

$2^{-3}, \ldots, 2^{-7}$, $T = 4$, and $\sigma = 0.1$. The batch sizes are $(p_1, p_2, p_3) = (2, 2, 2)$, $(20, 5, 2)$, $(200, 20, 2)$, and $(2000, 20, 2)$. Figure 4.6 shows that the discrete $L^2(\Omega)$ error decreases with larger batch sizes (since this involves more interactions), smaller time step sizes, or θ closer to one, which is consistent with our error estimate. Clearly, the number of FLOPs increases with larger batch sizes.

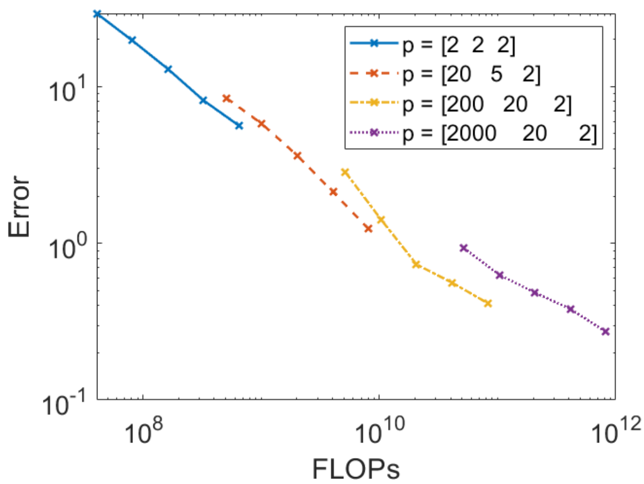

Figure 4.6.: $L^2(\Omega)$ error versus number of FLOPs for different batch sizes and time step sizes $\tau = 2^{-3}, \ldots, 2^{-7}$.

4.2. Conclusion

In this section we give our conclusion based on the numerical experiments presented in this chapter.

Our random-batch algorithm extends the scheme developed in [52] to the multi-species case, allowing for multiplicative noise. Although it does not improve the convergence rate compared to the algorithm in [53], numerical experiments suggest that our algorithm has a slightly better error performance for particle systems for which the particle numbers of each species are of the same order of magnitude. This is useful, for instance, when one is interested in the mean-field limit of a system, since this limit is formally obtained by performing the many-particle limit, and consequently small differences between the numbers of particles of different species become negligible in the limit.

Our numerical examples suggest that our algorithm can be used for an even larger class of systems than (2.1) and (3.27). However, the algorithm – and to our best knowledge, random batch methods in general – fail to approximate the population system presented in [26]. Furthermore, we are not aware of any method that allows for a priori estimates for the error level and the computational efficiency of random-batch methods before running the simulation. A possible way is to perform a simulation with small particle numbers to estimate roughly the error level and the computational efficiency, since the constants C and Γ_i in Theorem 1 are independent of N_i. Our numerical results in section 4.1.1 support this idea, since they show some stability of the error level with respect to changes of the particle numbers.

Part II.

Mathematical Analysis of Biological Models

Part II is constructed from the contents of the following works which are submitted for publication:

[35] M. Fellner and Ansgar Jüngel. A coupled stochastic differential reaction-diffusion system for angiogenesis, 2022. arXiv:2206.11510.

[36] M. Fellner and Ansgar Jüngel. A cross-diffusion system for vesicle transport - existence analysis of a cross-diffusion system with nonlinear Robin boundary conditions for vesicle transport in neurites. 2023. arXiv:2305.15281.

5. Introduction to the Biological Models

In this chapter we give a short overview of two important types of models used in computational biology: Cell-based and continuum-based models. We introduce models for angiogenesis and for vesicle transport in neurites in this context and furthermore give a formal derivation of the latter.

5.1. Cell-Based and Continuum-Based Models

In computational biology a variety of mathematical models are used for the simulation of single cells and populations of cells [76], [5]. The choice of model thereby depends, among other factors, on the quantities of interest together with the size of the population and available computational resources [74]. They can be separated into cell-based and continuum-based models. Whereas in cell-based models, or more general agent-based models, cells are treated as discrete entities and individual statistics of the single cells are tracked, in continuum-based models averaged quantities are used. In both cases this models can be coupled with further systems. This includes, among others, systems of ordinary differential equations for intra cellular dynamics, see for instance (5.17)-(5.18), or partial differential equations in the form of reaction-diffusion equations describing the transport of involved chemical signalling molecules, (5.5). Instead of cells also the behaviour of other biological structures, like vesicles [48], can be described using this type of models. See [76] for more information and examples from cancer biology and [5] for modelling approaches regarding cell mechanics.

5.1.1. Cell-Based Models: On- and Off- Lattice

Due to the individual treatment of cells, effects on the population level can be tracked back to the collective behaviour of individuals in cell based models, for instance collective motion [78]. The two main representatives of cell based models are off- and on- lattice models.

In off-lattice models, cells are allowed to move freely in space and the positions of cells are tracked via the center of mass or volume of the cell or via vertexes along its boundary. In center-based methods, cells are often assumed to be spherical [8] or ellipsoid [46] and the update of the position follows according to the forces acting on the cell centers. Often the underlying dynamics are therefore given by equations of motion which take the form of Langevin equations [8], [78]. We give an example for an off-lattice model for angiogenesis in section 5.2. For vertex based methods, cells are modelled as polygons and for the update of the positions the forces acting on the vertices are considered. They are for instance applicable to describe tissue deformation [3].

In on-lattice models, cells move between averaged discrete units of space aligned on a grid. At every time step the positions of the cells are updated, where they jump from a lattice site or unit of space to a neighbouring lattice site or unit according to given jump-rates or probabilities, see subsection 5.3.2, or [48] for an example regarding vesicle transport. These models are simpler and fast to implement, but cannot incorporate the mechanical interactions between cells in such detail then their off-lattice counterpart. In both cases, off- and on- lattice, the computational cost for simulations increases with the number of individual cells, which can be prohibitive to simulate larger populations depending on the exact model. In large population settings, to reduce this costs, continuous models which do not scale with the number of cells can often be derived from these discrete models [74].

5.1.2. Continuum-Based Models

Continuum-based models are based on continuum mechanics, for instance to describe cell mechanics [5], and consider quantities averaged over the single units of the considered cell-like organisms or structures. They often often adhere to physical principles like conservation of mass and consist of partial differential equations describing the evolution of the concentration or density of the respective biological objects, for instance vesicles in neurites, see section 5.3, or biofilms [41]. As they are not dependent on the number of individuals, they tend to be less computational expensive to simulate then cell based models. But in contrast to the latter, only average behaviour on the population-level can be studied using such models, as the exact behaviour of individual agents can not be captured. They sometimes can be seen as the limit of a series of on-lattice models with mesh sizes and time steps becoming exceedingly smaller. See section 5.3 for an example. Another approach to obtain continuum-based models is to interpret a corresponding lattice model as a finite -volume or finite-difference approximation of a suitable partial differential equation [74].

5.2. Off-Lattice Cell Based Model - A Coupled Stochastic Differential System for Angiogenesis

Angiogenesis is the process of expanding existing blood vessel networks by sprouting and branching. Its mathematical modelling is important to understand, for instance, wound healing, inflammation, and tumour growth. In this part of the thesis, we introduce a variant of the off-lattice cell-based model suggested in [8] that is used to simulate the early stages of angiogenesis. The model takes into account the dynamics of the tip (leading) endothelial cells by solving stochastic differential equations, the influence of various proteins triggering the cell dynamics by solving reaction-diffusion equations, and the change of some components of the extracellular matrix into extracellular fluid by solving ordinary differential equations. Up to our knowledge, this is the first analysis of the model of [8].

Angiogenesis is mainly triggered by local tissue hypoxia (low oxygen level in the tissue), which activates the production of the signal protein vascular endothelial growth factor (VEGF). Endothelial cells, which form a barrier between vessels and tissues, reached by the VEGF signal initiate the angiogenic program. These cells break out of the vessel wall, degrade the basement membrane (a thin sheet-like structure separating the endothelial cells from the underlying tissue), proliferate, and invade the surrounding tissue while still connected with the vessel network. The angiogenic program specifies the activated endothelial cells into tip cells (cells at the front of the vascular sprouts) and stalk cells (highly proliferating cells). The tip cells lead the sprout towards the source of VEGF, while the stalk cells proliferate to follow the tip cells supporting sprout elongation; see Figure 5.1.

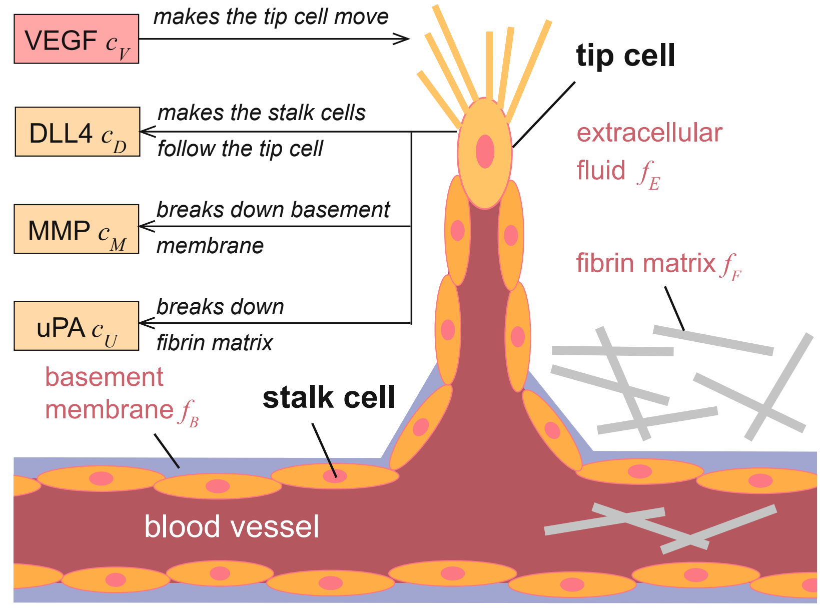

Figure 5.1.: Schematic model of sprout formation in a blood vessel corresponding to an in-vitro experiment described in [8]. Tip cells are activated by VEGF and they secrete the proteins DLL4, MMP, and uPA. The vessels are embedded in the fibrin matrix, which acts as a substrate and is surrounded by extracellular fluid. The basement membrane is the top layer of the matrix and separates it from the extracellular fluid.

Following [8], the tip cells secrete the proteins delta-like ligand 4 (DLL4), matrix metalloproteinase (MMP), and urokinase plasminogen activator (uPA). The chemokine DLL4 makes the stalk cells follow the tip cells, MMP breaks down the basement membrane, and uPA degrades the fibrin matrix such that cells can move into the matrix. There are many other molecular mechanisms and mediators in the angiogenesis process; see, e.g., [7, 91] for details.

5.2.1. Model equations

The unknowns are

- the positions $X_1^k(t)$ of the kth tip cell and $X_2^k(t)$ of the kth stalk cell;
- the volume fractions of the basement membrane $f_B(x,t)$, the extracellular fluid $f_E(x,t)$, and the fibrin matrix $f_F(x,t)$;
- the concentrations of the proteins VEGF $c_V(x,t)$, DLL4 $c_D(x,t)$, MMP $c_M(x,t)$, and uPA $c_U(x,t)$,

where $t \geq 0$ is the time and $x \in \mathcal{D} \subset \mathbb{R}^3$ the spatial variable. All unknowns depend additionally on the stochastic variable $\omega \in \Omega$, where Ω is the set of events. We assume that the mixture of basement membrane, extracellular fluid, and fibrine matrix is saturated, i.e., the volume fractions f_B, f_E, and f_F sum up to one. We introduce the vectors $X_i = (X_i^k)_{k=1,\ldots,N_i}$ for $i = 1,2$, $f = (f_B, f_E, f_F)$, and $c = (c_V, c_D, c_M, c_U)$.

Stochastic differential equations

The tip cells move according to chemotaxis force, driven by the gradient of the VEGF concentration, the durotaxis force, driven by the gradient of the solid fraction $f_S := f_B + f_F$, and random motion modelling uncertainties. The dynamics of $X_i^k(t)$ is assumed to be governed by the stochastic differential equations (SDEs), understood in the Itô sense,

$$\mathrm{d}X_i^k(t) = g_i[c,f](X_i^k,t)\mathrm{d}t + \sigma_i(X_i^k)\mathrm{d}B_i^k(t), \quad t > 0, \quad X_i^k(0) = X_i^{0,k}, \tag{5.1}$$

where $i = 1,2$, $k = 1,\ldots,N_i$ for $N_i \in \mathbb{N}$, $B_i^k(t)$ are Brownian motions, and the drift terms

$$\begin{aligned} g_1[c,f](X_1,t) &:= \alpha_0 M_1(f_S(X_1),X_1)z_1 + \gamma(f_S(X_1))\nabla c_V(X_1) + \lambda(f_S(X_1))\nabla f_S(X_1), \\ g_2[c,f](X_2,t) &:= \alpha_0 M_2(f_S(X_2),X_2)z_2 + \gamma(f_S(X_2))\nabla c_D(X_2) + \lambda(f_S(X_2))\nabla f_S(X_2), \end{aligned} \tag{5.2}$$

(we omitted the argument t for f_S and X_i on the right-hand side) include a constant $\alpha_0 > 0$, the strain energy M_i, the direction of movement determined by the strain energy density z_i, the chemotaxis force ∇c_V in the direction of VEGF (tip cells) and ∇c_D in the direction of DLL4 (stalk cells), and the migration as a result of the durotaxis force ∇f_S. We refer to [8] for a motivation of the specific choice (5.2). Here, we allow for general drift terms by imposing suitable Lipschitz continuity conditions; see Assumption (A4) below. In the numerical experiments, we choose the functions M_i, γ, and λ as in Appendix 8.1.1.

Ordinary differential equations

The proteins MMP and uPA degrade the basement membrane and fibrin matrix, respectively, while enhancing the extracellular fluid component. Therefore, the volume fractions f_B, f_E, and f_F are determined by the ordinary differential equations (ODEs)

$$\begin{aligned} \frac{\mathrm{d}f_B}{\mathrm{d}t} &= -s_B c_M f_B, \quad t > 0, \quad f_B(0) = f_B^0, \\ \frac{\mathrm{d}f_F}{\mathrm{d}t} &= -s_F c_U f_F, \quad t > 0, \quad f_F(0) = f_F^0, \\ \frac{\mathrm{d}f_E}{\mathrm{d}t} &= s_B c_M f_B + s_F c_U f_F, \quad t > 0, \quad f_E(0) = 1 - f_B^0 - f_F^0, \end{aligned} \tag{5.3}$$

where s_B, $s_F > 0$ are some rate constants. Note that the last differential equation is redundant because of the volume-filling condition $f_B + f_E + f_F = 1$. Clearly, equations (5.3) can be solved explicitly, giving for $(x,t) \in \mathcal{D} \times (0,T)$ and pathwise in Ω (we omit the argument ω),

$$\begin{aligned} f_B(x,t) &= f_B^0(x)\exp\left(-s_B\int_0^t c_M(x,s)\mathrm{d}s\right), \\ f_F(x,t) &= f_F^0(x)\exp\left(-s_F\int_0^t c_U(x,s)\mathrm{d}s\right). \end{aligned} \tag{5.4}$$

Reaction-diffusion equations

The mass concentrations are modelled by reaction-diffusion equations, describing the consumption and production of the proteins:

$$\begin{aligned}
&\partial_t c_V - \operatorname{div}(D_V(f)\nabla c_V) + \alpha_V(x,t)c_V = 0 \quad \text{in } \mathcal{D},\ t>0,\\
&\partial_t c_D - \operatorname{div}(D_D(f)\nabla c_D) + \beta_D(x,t)c_D = \alpha_D(x,t)c_V \quad \text{in } \mathcal{D},\ t>0,\\
&\partial_t c_M - \operatorname{div}(D_M(f)\nabla c_M) + s_M f_B c_M = \alpha_M(x,t)c_V \quad \text{in } \mathcal{D},\ t>0,\\
&\partial_t c_U - \operatorname{div}(D_U(f)\nabla c_U) + s_U f_F c_U = \alpha_U(x,t)c_V \quad \text{in } \mathcal{D},\ t>0,
\end{aligned} \tag{5.5}$$

with initial and no-flux boundary conditions

$$c_j(0) = c_j^0 \quad \text{in } \mathcal{D}, \quad \nabla c_j \cdot \nu = 0 \quad \text{on } \partial\mathcal{D},\ j = V, D, M, U, \tag{5.6}$$

where the rate terms are given by $\alpha_V = s_V\widetilde{\alpha}_V$, $\alpha_j = r_j\widetilde{\alpha}_j$ for $j = D, M, U$, $\beta_D = s_D\widetilde{\beta}_D$, and

$$\widetilde{\alpha}_j(x,t) = \sum_{k=1}^{N_1} V_j^k(X_1^k(t)-x), \quad \widetilde{\beta}_D(x,t) = \sum_{k=1}^{N_2} V_D^k(X_2^k(t)-x), \tag{5.7}$$

for $j = V, D, M, U$ and $V_j^k : \mathbb{R}^3 \to \mathbb{R}$ are non-negative smooth potentials approximating the delta distribution. The parameters r_j and s_j are positive. In [8], the rate terms are given by delta distributions instead of smooth potentials. We assume smooth potentials because of regularity issues, but they can be given by delta-like functions as long as they are smooth. Indeed, we need $C^{1+\delta}(\overline{\mathcal{D}})$ solutions c_j to solve the SDEs (5.1), and this regularity is not possible when the source terms of (5.5) include delta distributions. As the number of the proteins is typically much larger than the number of tip cells, the stochastic fluctuations in the concentrations are expected to be much smaller than those associated with the tip cells, which justifies the macroscopic approach using reaction-diffusion equations for the concentrations.

In equation (5.5) for c_V, the term $\alpha_V c_V$ models the consumption of VEGF along the trajectory of the tip cells. The protein DLL4 is regenerated from conversion of VEGF, modelled by $\alpha_D c_V$ along the trajectories of the tip cells, and consumed by the stalk cells, modelled by $\beta_D c_D$ along the trajectories of the stalk cells. In equation (5.5) for c_M, the term $s_M f_B c_M$ describes the decay of the MMP concentration with rate $s_B > 0$ as a result of the breakdown of the basement membrane, and $\alpha_M c_V$ models the production of MMP due to conversion from VEGF. Similarly, $s_U f_F c_U$ describes the decay of the uPA concentration, which breaks down the fibrin matrix, and the protein uPA is regenerated, leading to the term $\alpha_U c_V$.

The diffusivities are given by the mixing rule

$$D_j(f) = D_j^B f_B + D_j^E f_E + D_j^F f_F, \quad j = V, D, M, U,$$

where $D_j^i > 0$ for $i = B, E, F$. Then

$$0 < \min\{D_j^B, D_j^E, D_j^F\} \le D_j(f) \le \max\{D_j^B, D_j^E, D_j^F\}, \tag{5.8}$$

and equations (5.5) are uniformly parabolic. Note, however, that equations (5.5) are non-local and quasilinear, since the diffusivities are determined by the time integrals of c_M or c_U; see (5.4).

Various biological phenomena are not modelled by our equations. For instance, we do not include the initiation of sprouting from pre-existing parental vessels, the branching from a tip cell, and anastomosis (interconnection between blood vessels). Moreover, in contrast to [8], we do not allow for the transition between the phenotypes "tip cell" and "stalk cell" to simplify the presentation. On the other hand, we may include further angiogenesis-related proteins, if the associated reaction-diffusion equations are of the structure (5.5).
The mathematical analysis of our model for angiogenesis, cumulating to the existence result Theorem 8, is done in chapter 6. A numerical experiment based on this model can be found in chapter 8.

5.3. Continuum Based Model - A Cross Diffusion System for Vesicle Transport in Neurites derived from an On-Lattice Approach

Neurite growth is a fundamental process to generate axons and dendritic trees that connect to other neurons. During their development, neurites show periods of extension and retraction until neuron polarity is established. Then one of the neurites becomes the axon, while the other neurites do not grow further. The process of elongation and retraction depends, besides many other mechanisms [80], on the motor-driven transport of vesicles inside the neurites. Vesicles are biological structures consisting of liquid or cytoplasm and are enclosed by a lipid membrane. They are produced in the cell body (soma) and transport material to the tip of a neurite (the so-called growth cone). Vesicles that fuse with the plasma membrane of the growth cone deliver their membrane lipids to the tip, causing the neurite shaft to grow. Vesicles moving to the growth cone are called anterograde vesicles. Retrograde vesicles are generated via endocytosis at the growth cone plasma membrane and move back in the direction of the soma.

5.3.1. Model equations

We model anterograde and retrograde vesicles as two different particle species as in [48]. Because of the finite size of the vesicles, we take into account size exclusion effects. In the diffusion limit of a deterministic lattice model, the authors of [48] derived formally mass balance equations with fluxes that depend on the gradients of both the concentrations of the anterograde and retrograde vesicles, leading to cross-diffusion equations. The dynamics of the vesicle concentrations in the neurite pools at the soma and growth cone are governed by ordinary differential equations, which are linked to the cross-diffusion equations through non-linear Robin boundary conditions.

The dynamics of the concentrations (or volume fractions) of the anterograde vesicles $u_1(x,t)$ and the retrograde vesicles $u_2(x,t)$ along the one-dimensional neurite is governed by

$$\partial_t u_1 + \partial_x J_1 = 0, \quad J_1 = -D_1\big(u_0\partial_x u_1 - u_1\partial_x u_0 - u_0 u_1 \partial_x V_1\big), \tag{5.9}$$

$$\partial_t u_2 + \partial_x J_2 = 0, \quad J_2 = -D_2\big(u_0 \partial_x u_2 - u_2 \partial_x u_0 - u_0 u_2 \partial_x V_2\big), \tag{5.10}$$

solved in the bounded interval $\mathcal{D} = (0,1)$ with the soma at $x = 0$ and the growth cone at $x = 1$ for times $t > 0$, supplemented with the initial conditions

$$u_1(\cdot, 0) = u_1^0, \quad u_2(\cdot, 0) = u_2^0 \quad \text{in } \mathcal{D}. \tag{5.11}$$

Here, $u_0 = 1 - u_1 - u_2$ describes the void volume fraction, J_i are the corresponding fluxes, D_i the diffusion coefficients, and V_i given potentials. Equations (5.9)–(5.10) form a cross-diffusion system with a non-symmetric and generally not positive definite diffusion matrix, given by

$$A(u) = \begin{pmatrix} D_1(1-u_2) & D_1 u_1 \\ D_2 u_2 & D_2(1-u_1) \end{pmatrix}. \tag{5.12}$$

Moreover, if $u_0 = 0$, the equations are of degenerate type; see (7.13).

Let $\Lambda_n(t)/\Lambda_n^{\max}$ and $\Lambda_s(t)/\Lambda_s^{\max}$ be the percentage of currently occupied space in the soma and the growth cone, respectively. Anterograde vesicles leave the soma and enter the neurite at $x = 0$ if there is enough space with rate $\alpha_1(\Lambda_s/\Lambda_s^{\max})u_0(0,\cdot)$, and they enter the growth cone with rate $\beta_1(1 - \Lambda_n/\Lambda_n^{\max})u_0(1,\cdot)u_1(\cdot,1)$. Retrograde vesicles enter the soma with rate $\beta_1(1 - \Lambda_s/\Lambda_s^{\max})u_0(1,\cdot)u_2(\cdot,0)$ and leave the growth cone with rate $\alpha_2(\Lambda_n/\Lambda_n^{\max})u_0(1,\cdot)$, where $\alpha_i, \beta_i > 0$ for $i = 1, 2$ are some constants. Thus, the fluxes at $x = 0$ and $x = 1$ are given by the non-linear Robin boundary conditions

$$J_1(0,t) = J_1^0[u](t) := \alpha_1 \frac{\Lambda_s(t)}{\Lambda_s^{\max}} u_0(0,t), \tag{5.13}$$

$$J_1(1,t) = J_1^1[u](t) := \beta_1 \left(1 - \frac{\Lambda_n(t)}{\Lambda_n^{\max}}\right) u_0(1,t) u_1(1,t), \tag{5.14}$$

$$J_2(0,t) = J_2^0[u](t) := -\beta_2 \left(1 - \frac{\Lambda_s(t)}{\Lambda_s^{\max}}\right) u_0(0,t) u_2(0,t), \tag{5.15}$$

$$J_2(1,t) = J_2^1[u](t) := -\alpha_2 \frac{\Lambda_n(t)}{\Lambda_n^{\max}} u_0(1,t) \quad \text{for } t > 0, \tag{5.16}$$

where $u = (u_1, u_2)$. Compared to [48], the boundary conditions (5.14) and (5.15) depend on u_0 to account for the resistance of entering the growth cone and soma, respectively, for instance due to viscosity. There is also a mathematical reason for this choice, which is explained in section 7.1.

Finally, the change of vesicle numbers in the soma and growth cone is determined by the corresponding in- and outflow fluxes,

$$\partial_t \Lambda_n = J_1^1[u] + J_2^1[u], \quad t > 0, \quad \Lambda_n(0) = \Lambda_n^0, \tag{5.17}$$

$$\partial_t \Lambda_s = -(J_1^0[u] + J_2^0[u]) \quad t > 0, \quad \Lambda_s(0) = \Lambda_2^0. \tag{5.18}$$

Inserting (5.13)–(5.16) into these equations, they become linear ordinary differential equations in Λ_n and Λ_n, coupled to equations (5.9)–(5.10).

Next, we give a formal derivation of this model for vesicle transport. The mathematical analysis together with the proof of the corresponding existence result, Theorem 27, is done in chapter 7. Numerical experiments can be found in chapter 8.

5.3.2. Formal derivation of the model

Equations (5.9)-(5.16) can be formally derived from discrete dynamics on a lattice, which takes into account the in- and outflow of vesicles into the respective lattice cell. The derivation is similar to the presentation in [48]; we repeat it for the convenience of the reader and to highlight the main difference to [48]. We divide the domain $\mathcal{D} = (0, 1)$ into m cells K_j of length $h > 0$ and midpoint $x_j = hj$, where $j = 0, \ldots, m-1$. The cell K_j is occupied by anterograde vesicles with volume fraction $u_{1,j}(t) = u_1(x_j, t)$ and retrograde vesicles with volume fraction $u_{2,j}(t) = u_2(x_j, t)$.

The transition rate of a vesicle to jump from cell j to a neighbouring cell $j \pm 1$ equals

$$u_{i,j} u_{0,j\pm1} \exp[-\eta_i(V_i(x_{j\pm1}) + V_i(x_j))], \quad i = 1, 2,$$

where $\eta_i > 0$ is some constant and $V_{i,j} = V_i(x_j, \cdot)$, taking into account that a jump is possible only if the cell j is not empty ($u_{i,j} > 0$) and the cell $j \pm 1$ is not fully occupied ($u_{0,j\pm1} > 0$). The dynamics of $u_{i,j}$ is then given by

$$\begin{aligned} \gamma_i h^2 \partial_t u_{i,j} = &-u_{i,j} u_{0,j-1} e^{-\eta_i(V_{i,j} - V_{i,j-1})} + u_{i,j-1} u_{0,j} e^{-\eta_i(V_{i,j-1} - V_{i,j})} \\ &- u_{i,j} u_{0,j+1} e^{-\eta_i(V_{i,j} - V_{i,j+1})} + u_{i,j+1} u_{0,j} e^{-\eta_i(V_{i,j+1} - V_{i,j})}, \end{aligned} \tag{5.19}$$

where $\gamma_i > 0$. The factor h^2 on the left-hand side corresponds to a diffusion scaling. By Taylor expansion, we have $e^{-\eta_i z} = 1 - \eta_i z + \eta_i^2 z^2/2 + O(z^3)$ and $V_{i,j} - V_{i,j-1} = h\partial_x V_{i,j-1/2} + O(h^3)$, where $V_{i,j\pm1/2} = V_i((j \pm 1/2)h, \cdot)$. Then

$$\begin{aligned} e^{-\eta_i(V_{i,j} - V_{i,j-1})} &= 1 - \eta_i h \partial_x V_{i,j-1/2} + \eta_i^2 h^2 (\partial_x V_{i,j-1/2})^2 + O(h^3), \\ e^{-\eta_i(V_{i,j-1} - V_{i,j})} &= 1 + \eta_i h \partial_x V_{i,j-1/2} + \eta_i^2 h^2 (\partial_x V_{i,j-1/2})^2 + O(h^3). \end{aligned}$$

In a similar way, we expand $u_{i,j\pm1} = u_{i,j} \pm h\partial_x u_{i,j} + (h^2/2)\partial_x^2 u_{i,j} + O(h^3)$. Inserting these expansions into (5.19), we find after a computation that

$$\begin{aligned} \gamma_i h^2 \partial_t u_{i,j} &= (u_{0,j} \partial_x^2 u_{i,j} - u_{i,j} \partial_x^2 u_{0,j}) h^2 - 2\eta_i u_{i,j} u_{0,j} (\partial_x V_{i,j+1/2} - \partial_x V_{i,j-1/2}) h \\ &\quad - \eta_i (u_{0,j} \partial_x u_{i,j} + u_{i,j} \partial_x u_{0,j})(\partial_x V_{i,j+1/2} + \partial_x V_{i,j-1/2}) h^2 + O(h^3) \\ &= (u_{0,j} \partial_x^2 u_{i,j} - u_{i,j} \partial_x^2 u_{0,j}) h^2 - 2\eta_i u_{i,j} u_{0,j} \partial_x^2 V_{i,j} h^2 \\ &\quad - 2\eta_i (u_{0,j} \partial_x u_{i,j} + u_{i,j} \partial_x u_{0,j}) \partial_x V_{i,j} h^2 + O(h^3), \end{aligned}$$

where we expanded $h\partial_x V_{i,j\pm1/2} = h\partial_x V_{i,j} \pm (h^2/2)\partial_x^2 V_{i,j} + O(h^3)$. We divide this equation by h^2, and pass to the formal limit $h \to 0$:

$$\begin{aligned} \gamma_i \partial_t u_i &= (u_0 \partial_x^2 u_i - u_i \partial_x^2 u_0) - 2\eta_i u_i u_0 \partial_x^2 V_i - 2\eta_i (u_0 \partial_x u_i + u_i \partial_x u_0) \partial_x V \\ &= \partial_x \big(u_0 \partial_x u_i - u_i \partial_x u_0 - 2\eta_i u_0 u_i \partial_x V \big). \end{aligned}$$

Setting $\eta_i = 1/2$ and $D_i = 1/\gamma_i$, we obtain (5.9)–(5.10).

At the points $x = 0$ and $x = 1$, there are reservoirs with concentrations Λ_s at $x = 0$ and Λ_n at $x = 1$. The in- and outflow rates are given by

$$A_i(\Lambda_\ell) = a_i u_{0,0} \frac{\Lambda_\ell}{\Lambda_\ell^{\max}}, \quad B_i(\Lambda_\ell) = b_i u_{0,m} \left(1 - \frac{\Lambda_\ell}{\Lambda_\ell^{\max}}\right), \quad \ell = n, s,$$

where $a_i, b_i > 0$. We have multiplied these rates by the factor $u_{0,j}$ with $j = 0$ and $j = m$, respectively, which models the resistance of entering the first and last cell. This is the main difference to the derivation in [48]. Taken into account the inflow and outflow of vesicles at $x = 0$, the change of the fraction of the anterograde vesicles is given by

$$\begin{aligned} h^2 \partial_t u_{1,0} &= -u_{1,0}(t) u_{0,1}(t) e^{-\eta_1 (V_1(x_1) - V_1(x_0))} \\ &\qquad + u_{1,1}(t) u_{0,0}(t) e^{-\eta_1 (V_1(x_0) - V_1(x_1))} + a_1 \frac{\Lambda_s(t)}{\Lambda_s^{\max}} u_{0,0}(t) h, \end{aligned}$$

An expansion similarly as before, up to $O(h^2)$ instead of $O(h^3)$, leads to

$$\begin{aligned} h^2 \partial_t u_{1,0} &= -u_{1,0}(u_{0,0} + h\partial_x u_{0,0})(1 + \eta_1 h \partial_x V_{1,0}) \\ &\qquad + (u_{1,0} + h\partial_x u_{1,0}) u_{0,0}(1 - \eta_1 h \partial_x V_{1,0}) + O(h^2) \\ &= h(u_{0,0}\partial_x u_{1,0} + u_{1,0}\partial_x u_{0,0}) - 2\eta_i h u_{0,0} u_{1,0} \partial_x V_{1,0} + a_i h \frac{\Lambda_s}{\Lambda_s^{\max}} u_{0,0} + O(h^2). \end{aligned}$$

We divide the previous equation by h and perform the limit $h \to 0$:

$$0 = (u_{0,0}\partial_x u_{1,0} + u_{1,0}\partial_x u_{0,0}) - 2\eta_i u_{0,0} u_{1,0} \partial_x V_{1,0} + a_i \frac{\Lambda_s}{\Lambda_s^{\max}} u_{0,0}.$$

We set $\eta_i = 1/2$ and $\alpha_i = a_i D_i$ and multiply the equation by D_i:

$$J_1(0, \cdot) = -D_i\big((u_{0,0}\partial_x u_{1,0} + u_{1,0}\partial_x u_{0,0} - u_{0,0} u_{1,0} \partial_x V_{1,0}\big) = \alpha_i \frac{\Lambda_s}{\Lambda_s^{\max}} u_0(0, \cdot),$$

which equals (5.13). The boundary conditions (5.14)–(5.16) are shown in a similar way.

6. Analysis of a Model for Angiogenesis

The goal of this chapter is the analysis of the model (5.4)–(5.7), (5.1) and to proof Theorem 8. We start by clarifying notation and present the main existence result, Theorem 8, together with necessary assumptions.

6.1. Assumptions and Main Result

Let $(\Omega, \mathcal{F}, \mathbb{P})$ be a complete probability space and $(\Omega, \mathcal{F}, (\mathcal{F}_t)_{t\geq 0}, \mathbb{P})$ be a stochastic basis with a complete and right-continuous filtration. Furthermore, let $(B_i^k(t))_{t\geq 0}$ for $i = 1, 2$, $k = 1, \dots, N_i$ be independent standard Brownian motions on $\mathbb{R}^3$ relative to $(\mathcal{F}_t)_{t\geq 0}$. We write $L^p(\Omega, \mathcal{F}; B)$ for the set of all $\mathcal{F}$-measurable random variables with values in a Banach space B, for which the L^p norm is finite. Furthermore, let $\mathcal{D} \subset \mathbb{R}^3$ be a bounded domain with boundary $\partial\mathcal{D} \in C^3$ (needed to obtain parabolic regularity; see Theorem 51). We set $Q_T = \mathcal{D} \times (0, T)$.

We write $C^{k+\delta}(\overline{\mathcal{D}})$ with $k \in \mathbb{N}_0$, $\delta \in (0, 1)$ for the space of C^k functions u such that the kth derivative $\mathrm{D}^k u$ is Hölder continuous of index δ. The space of Lipschitz continuous functions on $\overline{\mathcal{D}}$ is denoted by $C^{0,1}(\overline{\mathcal{D}})$. For notational convenience, we do not distinguish between the spaces $C^{k+\delta}(\overline{\mathcal{D}}; \mathbb{R}^n)$ and $C^{k+\delta}(\overline{\mathcal{D}})$. Furthermore, we usually drop the dependence on the variable $\omega \in \Omega$ in the ODEs and PDEs, which hold pathwise $\mathbb{P}$-a.s. Accordingly, we write c instead of $c(\omega, \cdot, \cdot)$ and $c(t)$ instead of $c(\omega, \cdot, t)$. Finally, we write "a.s." instead of "$\mathbb{P}$-a.s.".

As we deal with stochastic processes depending also on the space variable x, we use the following definition of a progressively measurable process: We call a stochastic process $X : \Omega \times \mathcal{D} \times [0, T] \to \mathbb{R}$ *progressively measurable* with respect to a filtration $(\mathcal{F}_t)_{t\geq 0}$, if X is an $\mathcal{F}_t \times \mathcal{B}(\mathcal{D}) \times \mathcal{B}([0, t])$-measurable random variable for all $t \in [0, T]$. Here, $\mathcal{B}(G)$ denotes the Borel-σ algebra of the corresponding topological space G.

We impose the following assumptions:

(B1) Initial data: $X_i^{0,k} \in L^4(\Omega, \mathcal{F}_0)$ are identically distributed and independent for fixed i, satisfy $X_i^{0,k} \in \mathcal{D}$ a.s. ($i = 1, 2$, $1 \leq k \leq N_i$), $c^0 \in L^\infty(\Omega, \mathcal{F}_0; C^{2+\delta_0}(\overline{\mathcal{D}}))$, $f^0 \in L^\infty(\Omega, \mathcal{F}_0; C^{1+\delta_0}(\overline{\mathcal{D}}))$ for some $0 < \delta_0 < 1$; $c_j^0 \geq 0$ ($j = V, D, M, U$), $f_i^0 \geq 0$ ($i = B, E, F$), and $f_B^0 + f_E^0 + f_F^0 = 1$ in $\mathcal{D}$ a.s.; $\nabla c_j^0 \cdot \nu = 0$ on $\partial\mathcal{D}$ a.s.

(B2) Diffusion: $\sigma_i : \Omega \times \mathcal{D} \times [0, T] \to \mathbb{R}$ ($i = 1, 2$) is progressively measurable, satisfies $\sigma_i = 0$ on $\partial\mathcal{D}$ a.s., and there exists a constant $L > 0$ such that for all x, $y \in \mathcal{D}$, $t \in [0, T]$, and $\omega \in \Omega$,

$$\big|\sigma_i(\omega, x, t) - \sigma_i(\omega, y, t)\big| \leq L\big|x - y\big|, \quad \big|\sigma_i(\omega, x, t)\big| \leq L\big(1 + |x|\big).$$

(B3) Drift: $g_i(x, y, p, q) : \mathbb{R} \times \mathbb{R} \times \mathbb{R}^3 \times \mathbb{R}^3 \to \mathbb{R}^3$ is measurable and $g_i(c, f, \nabla c, \nabla f)=0$ for $x \in \partial\mathcal{D}$, $t \in [0, T]$ if (c, f) is a solution to (5.4)-(5.6). We write $g_i[c, f]$ instead of $g_i(c, f, \nabla c, \nabla f)$ to shorten the notation.

(B4) Lipschitz continuity for g_i: For $c, c', f, f' \in C^1(\overline{\mathcal{D}} \times [0, T])$, there exists $L_1 > 0$ such that for $(x, t) \in \overline{\mathcal{D}} \times [0, T]$ and $i = 1, 2$,

$$\begin{aligned}\big|g_i[c, f](x, t) - g_i[c', f'](x, t)\big| \le L_1\big(1 + \|c\|_{L^\infty(0,t;C^1(\overline{\mathcal{D}}))} + \|f\|_{L^\infty(0,t;C^1(\overline{\mathcal{D}}))}\big) \\ \times \big(\|c(t) - c'(t)\|_{C^1(\overline{\mathcal{D}})} + \|f(t) - f'(t)\|_{C^1(\overline{\mathcal{D}})}\big).\end{aligned}$$

Furthermore, for $c, f \in L^\infty(0, T; W^{2,\infty}(\mathcal{D}))$, there exists $L_2 > 0$ such that for (x, t), $(x', t) \in \overline{\mathcal{D}} \times [0, T]$ and $i = 1, 2$,

$$\begin{aligned}\big|g_i[c, f](x, t) - g_i[c, f](x', t)\big| \le L_2\big(1 + \|c\|_{L^\infty(0,T;W^{2,\infty}(\mathcal{D}))} + \|f\|_{L^\infty(0,T;W^{2,\infty}(\mathcal{D}))}\big) \\ \times |x - x'|.\end{aligned}$$

(B5) Potentials: $V_j^k \in C^{0,1}(\mathbb{R}^3)$ for $j = V, D, M, U$, $k = 1, \ldots, N_i$ are non-negative functions.

Let us discuss these assumptions. Since we need $C^{1+\delta}$ solutions (c, f) to obtain Hölder continuous coefficients of the SDEs (which ensures their solvability), we need some regularity conditions on the initial data in Assumption (B1). Accordingly, $\nabla c_j^0 \cdot \nu = 0$ on $\partial\mathcal{D}$ is a compatibility condition needed for such a regularity result. In Assumption (B1), we impose the volume-filling condition initially, $f_B^0 + f_E^0 + f_F^0 = 1$ in $\mathcal{D}$. Equations (5.3) then show that this condition is satisfied for all time. The conditions $\sigma_i = 0$ and $g_i[c, f] = 0$ on $\partial\mathcal{D}$ in Assumptions (B2) and (B3), respectively, guarantee that the tip and stalk cells do not leave the domain $\mathcal{D}$. The conditions on σ_i in Assumption (B2) and the Lipschitz continuity of $g_i[c, f]$ in Assumption (B4) are standard hypotheses to apply existence results for (5.1). Note that $g_i[c, f]$ in example (5.2) satisfies Assumption (B4). As g_i is assumed to be measurable by Assumption (B3), $g_i[c, f]$ is progressively measurable if c and f are. Assumption (B5) is a simplification to ensure the parabolic regularity results needed, in turn, for the solvability of (5.1).

Under these assumptions, the solution to (5.1) will turn out to be an element of the following metric space for some $R > 0$:

$$\begin{aligned}Y_R(0, T; \mathcal{D}) := \big\{X \in C^{1/2}([0, T]; L^4(\Omega)) : \|X\|_{C^{1/2}([0,T];L^4(\Omega))} \le R, \\ X(t) \text{ is } \mathcal{F}_t\text{-measurable},\ X(t) \in \overline{\mathcal{D}} \text{ a.s. for all } t \in [0, T]\big\},\end{aligned} \tag{6.1}$$

equipped with the standard norm of $C^0([0, T]; L^4(\Omega))$.

Theorem 8 (Global existence and uniqueness)**.** *Let Assumptions (B1)–(B5) hold. Then there exist a unique solution (f, c, X) to* (5.4)–(5.7), (5.1) *and some constant $R > 0$ such that*

- $f = (f_B, f_E, f_F)$ *solves* (5.3) *pathwise a.s. in the sense of* (5.4), *where $f_i \in C^0([0, T]; L^2(\mathcal{D})) \cap L^\infty(Q_T)$;*

- *$c = (c_V, c_D, c_M, c_U)$ is a classical solution to (5.5)–(5.6) pathwise a.s.;*
- *c, ∇c, f and ∇f are progressive measurably;*
- *$X_i^k \in Y_R(0,T;\mathcal{D})$ is a strong solution to (5.1) for $i = 1, 2$, $k = 1, \ldots, N_i$.*

A strong solution (X_1, X_2) to (5.1) means that $(X_i^k(t))_{t\geq 0}$ is an a.s. continuous $(\mathcal{F}_t)$-adapted process such that for all $t \in [0,T]$,

$$X_i^k(t) = X_i^{0,k} + \int_0^t g_i[c,f](X_i^k(s), s)\mathrm{d}s + \int_0^t \sigma_i(X_i^k(s))\mathrm{d}B_i^k(s) \quad a.s. \tag{6.2}$$

6.1.1. Strategy of the proof

The proof of Theorem 8 is based on a variant of Banach's fixed-point theorem [68, Theorem 2.4] yielding global solutions. Let $\widetilde{X}$ be a stochastic process with a.s. Hölder continuous paths and values in $\mathcal{D}$ a.s. More precisely, $\widetilde{X}_i^k \in Y_R(0,T;\mathcal{D})$, defined in (6.1). Then α_j and β_j are Hölder continuous in $\overline{\mathcal{D}} \times [0,T]$ a.s. as a function of $\widetilde{X}$. As a first step, we prove some uniform regularity results and a priori estimates for solutions to the linearised problem of (5.5), which are independent of the path $t \mapsto X(\omega,t)$. Moser's iteration method shows that the weak solution is in fact bounded, and a general regularity result for evolution equations yields $\partial_t c \in L^2(Q_T)$. Then, interpreting (the linearised) equations of the form (5.5) as elliptic equations with right-hand side $\partial_t c \in L^2(Q_T)$, we conclude the Hölder continuity of $c(t)$ for any fixed $t \in (0,T)$. Thus, the diffusivities are Hölder continuous, and we infer $C^{1+\delta}(\overline{\mathcal{D}})$ and $W^{2,\infty}(\mathcal{D})$ solutions c via a bootstrap-type argument for solutions to the original non-linear problem (5.5). Second, we show the existence of a classical solution to (5.5) by an application of the fixed-point theorem of Schauder and the existence and regularity results of Ladyženskaya et al. [67].

In the third step, we solve the SDEs (5.1). The functions (c,f) have Hölder continuous gradients, and we show that (c,f) and $(\nabla c, \nabla f)$ are progressively measurable. Therefore, together with Assumption (A4), the conditions of the existence theorem of [73, Theorem 3.1.1] are satisfied, and we obtain a solution X to (5.1) in the sense (6.2).

Fourth, we define fixed-point operator $\Phi : \widetilde{X} \mapsto X$ on $Y_R(0,T;\mathcal{D})$, which can be written as the concatenation

$$\Phi : \widetilde{X} \mapsto (\alpha, \beta_D) \mapsto (c,f) \mapsto X,$$

where $\alpha = (\alpha_V, \alpha_D, \alpha_M, \alpha_U)$. It remains to show that Φ is a self-mapping and a contraction, which is possible for a sufficiently large $R > 0$. In fact, we show that for any $n \in \mathbb{N}$,

$$\sup_{0<s<t} \left(\mathbb{E}|\Phi^n(X(t)) - \Phi^n(X'(t))|^4\right)^{1/4} \leq c_n \sup_{0<s<t} \left(\mathbb{E}|X(t) - X'(t)|^4\right)^{1/4}$$

for all X, $X' \in Y_R(0,T;\mathcal{D})$, where $c_n \to 0$ as $n \to \infty$. It follows from the variant of Banach's fixed-point theorem in [68, Theorem 2.4] that Φ has a unique fixed point, which gives a unique solution (X,c,f) to (5.1), (5.3)–(5.7).

This part of the thesis is organized as follows. In section 6.2 a special case of ordinary differential equation in a Bochner space is studied and in section 6.3, the existence of a unique classical solution to the reaction-diffusion equations (5.5)–(5.6) and some stability results are proved. The progressive measurability of the solutions to (5.3) and (5.5) as well as the solvability of the SDEs (5.1) is verified in section 6.4. Based on these results, Theorem 8 is proved in section 6.5. Some numerical experiments are illustrated in section 8.1, showing stalk cells following the tip cells and forming a premature sprout. Appendix A.2.2 summarizes some regularity results for elliptic and parabolic equations used in this work.

6.2. Solution of ODEs in Bochner spaces

We prove a result for ODEs in some Bochner space, which is needed for the solution of (5.3) when the concentrations c_j are only $L^2(\mathcal{D})$ functions.

Lemma 9. *Let $u \in L^\infty(0,T;L^2(\mathcal{D}))$ and $g^0 \in L^\infty(\mathcal{D})$ be non-negative functions. Then*

$$\frac{\mathrm{d}g}{\mathrm{d}t} = -ug, \quad t > 0, \quad g(0) = g^0 \quad \text{a.e. in } \mathcal{D}, \tag{6.3}$$

has a unique solution $g \in C^0([0,T];L^2(\mathcal{D})) \cap L^\infty(Q_T)$ satisfying $0 \le g \le \|g^0\|_{L^\infty(\mathcal{D})}$ a.e. in Q_T.

Proof. Set $[u]_k := \max\{k,u\} = u(t) - (u(t)-k)^+$ for $k \ge 0$, where $z^+ = \max\{0,z\}$. We claim that $[u]_k \in L^\infty(Q_T)$ has the properties $[u(t)]_k \to u(t)$ strongly in $L^2(\mathcal{D})$ as $k \to \infty$ for a.e. $t \in [0,T]$ and

$$\|[u(t)]_k - [u(t)]_j\|_{L^2(\mathcal{D})} \le \|[u(t)]_j - u(t)\|_{L^2(\mathcal{D})} \le C \quad \text{a.e. in } [0,T] \tag{6.4}$$

for $0 \le j \le k$, where $C > 0$ does not depend on k or j. Indeed, the first inequality follows from

$$\begin{aligned}
\|[u(t)]_k - [u(t)]_j\|^2_{L^2(\mathcal{D})} &= \int_{\mathcal{D}} \big((u(t)-k)^+ - (u(t)-j)^+\big)^2 \mathrm{d}x \\
&= \int_{\{u(t)\ge k\}} \big((u(t)-k)^+ - (u(t)-j)^+\big)^2 \mathrm{d}x + \int_{\{j \le u(t) \le k\}} [(u(t)-j)^+]^2 \mathrm{d}x \\
&= \int_{\{u(t)\ge k\}} (k-j)^2 \mathrm{d}x + \int_{\{j \le u(t) \le k\}} (u(t)-j)^2 \mathrm{d}x \\
&\le \int_{\{u(t)\ge k\}} (u(t)-j)^2 \mathrm{d}x + \int_{\{j \le u(t) \le k\}} (u(t)-j)^2 \mathrm{d}x \\
&= \int_{\mathcal{D}} [(u(t)-j)^+]^2 \mathrm{d}x = \|[u(t)]_j - u(t)\|^2_{L^2(\mathcal{D})}.
\end{aligned}$$

Furthermore, we have

$$\|[u(t)]_j - u(t)\|^2_{L^2(\mathcal{D})} = \int_{\mathcal{D}} [(u(t)-j)^+]^2 \mathrm{d}x \le \|u\|^2_{L^\infty(0,T;L^2(\mathcal{D}))} \le C.$$

The function $u(t)^2$ is an integrable upper bound for $(u(t)-k)^+$. Furthermore, $[u(t)]_k - u(t) = -(u(t)-k)^+$ converges to zero a.e. in $\mathcal{D}$ as $k \to \infty$. Therefore, we conclude from dominated convergence that $[u(t)]_k - u(t) \to 0$ strongly in $L^2(\mathcal{D})$. This proves the claim.

Next, we consider the differential equation

$$\frac{\mathrm{d}g_k}{\mathrm{d}t} = -[u]_k g_k, \quad t > 0, \quad g_k(0) = g^0 \quad \text{a.e. in } \mathcal{D}. \tag{6.5}$$

Since $[u]_k$ is bounded, there exists a unique solution $g_k \in C^0([0,T]; L^\infty(\mathcal{D}))$, given by

$$g_k(t) = g^0 \exp\left(- \int_0^t [u(s)]_k \mathrm{d}s \right), \quad 0 < t < T.$$

Clearly, we have $0 < g_k(t) \leq K := \|g^0\|_{L^\infty(\mathcal{D})}$. We want to prove that (g_k) converges as $k \to \infty$ to a solution of the original equation. It follows that

$$\begin{aligned}
\frac{1}{2}\frac{\mathrm{d}}{\mathrm{d}t}\|g_k - g_j\|^2_{L^2(\mathcal{D})} &= -\int_{\mathcal{D}} ([u]_k g_k - [u]_j g_j)(g_k - g_j)\mathrm{d}x \\
&= -\int_{\mathcal{D}} [u]_k (g_k - g_j)^2 \mathrm{d}x - \int_{\mathcal{D}} ([u]_k - [u]_j) g_j (g_k - g_j)\mathrm{d}x \\
&\leq \frac{K}{2}\|[u]_k - [u]_j\|^2_{L^2(\mathcal{D})} + \frac{K}{2}\|g_k - g_j\|^2_{L^2(\mathcal{D})}.
\end{aligned}$$

We conclude from Gronwall's lemma and (6.4) that

$$\begin{aligned}
\|g_k(t) - g_j(t)\|^2_{L^2(\mathcal{D})} &\leq \int_0^t e^{K(t-s)} \|[u(s)]_k - [u(s)]_j\|^2_{L^2(\mathcal{D})} \mathrm{d}s \\
&\leq e^{Kt} \int_0^t \|[u(s)]_j - u(s)\|^2_{L^2(\mathcal{D})} \mathrm{d}s.
\end{aligned}$$

Because of $\|[u(s)]_j - u(s)\|^2_{L^2(\mathcal{D})} \to 0$ as $j \to \infty$ and the uniform upper bound for $[u(s)]_j - u(s)$, the dominated convergence theorem implies that, for any $t \in [0,T]$,

$$\|g_k(t) - g_j(t)\|^2_{L^2(\mathcal{D})} \leq e^{KT} \int_0^T \|[u(s)]_j - u(s)\|^2_{L^2(\mathcal{D})} \mathrm{d}s \to 0 \quad \text{as } j,k \to \infty.$$

Thus, $(g_k(t))$ is a Cauchy sequence for every $t \in [0,T]$ and we infer that $g_k(t) \to g(t)$ in $L^2(\mathcal{D})$. Because of the $L^\infty(0,T; L^2(\mathcal{D}))$ bound for (g_k) and dominated convergence again, $g_k \to g$ in $L^2(Q_T)$, where $g \in L^\infty(0,T; L^2(\mathcal{D}))$. There exists a subsequence, which is not relabelled, such that $g_k(t) \to g(t)$ a.e. in $\mathcal{D}$, for any $t \in [0,T]$. We deduce from $g_k(t) \leq K$ that $g(t) \leq K$ for all $t \in [0,T]$. This shows that $g \in L^\infty(Q_T)$. Writing (6.5) as an integral equation and performing the limit $k \to \infty$, the previous convergence results show that g solves (6.3). □

We also need the following stability result, which relates the difference $f_1 - f_2$ of solutions to (5.3) with the difference $c_1 - c_2$ of solutions to (5.5).

Lemma 10. *Let u_1, $u_2 \in L^\infty(0,T; W^{k,\infty}(\mathcal{D}))$ with $k \in \mathbb{N}_0$, g_1^0, $g_2^0 \in W^{k,\infty}(\mathcal{D})$, and let g_1, $g_2 \in C^0([0,T]; W^{k,\infty}(\mathcal{D}))$ be the unique solutions to*

$$\frac{\mathrm{d}g_i}{\mathrm{d}t} = -u_i g_i, \quad 0 < t < T, \quad g_i(0) = g_i^0 \quad \textit{a.e. in } \mathcal{D}, \ i = 1, 2.$$

Then there exists $C > 0$, only depending on T, the $L^\infty(0,T;W^{k,\infty}(\mathcal{D}))$ norm of u_i, and the $W^{k,\infty}(\mathcal{D})$ norm of g_i^0, such that for $p > 1$,

$$\|g_1 - g_2\|_{W^{k,p}(\mathcal{D})} \leq C\big(\|g_1^0 - g_2^0\|_{W^{k,p}(\mathcal{D})} + \|u_1 - u_2\|_{L^1(0,T;W^{k,p}(\mathcal{D}))}\big).$$

Proof. The regularity of g_i follows from the explicit formula and the regularity for g_i^0 and u_i. Furthermore, taking the $W^{k,p}(\mathcal{D})$ norm of

$$g_1(t) - g_2(t) = g_1^0 - g_2^0 - \int_0^t \big(u_1(g_1 - g_2) + (u_1 - u_2)g_2\big)\mathrm{d}x,$$

the result follows from the regularity $u_1 \in L^\infty(0,T;W^{k,\infty}(\mathcal{D}))$ and $g_2 \in W^{k,\infty}(\mathcal{D})$. $\square$

6.3. Solution of the reaction-diffusion equations

We show first some a priori estimates, prove then the existence of classical solutions to (5.5)–(5.6) and finally the uniqueness of solutions.

6.3.1. A priori estimates

The existence theory for SDEs requires some regularity for the solution c to (5.5), and in particular uniform estimates are needed. We consider first the linear system

$$\begin{aligned}
&\partial_t c_V - \operatorname{div}(D_V(\widehat{f})\nabla c_V) + \alpha_V(x,t)c_V = 0,\\
&\partial_t c_D - \operatorname{div}(D_D(\widehat{f})\nabla c_D) + \beta_D(x,t)c_D = \alpha_D(x,t)c_V,\\
&\partial_t c_M - \operatorname{div}(D_M(\widehat{f})\nabla c_M) + s_M\widehat{f}_B c_M = \alpha_M(x,t)c_V,\\
&\partial_t c_U - \operatorname{div}(D_U(\widehat{f})\nabla c_U) + s_U\widehat{f}_F c_U = \alpha_U(x,t)c_V,
\end{aligned} \tag{6.6}$$

where $\widehat{f}$ is calculated from (5.4), given some a.e. non-negative function $\widehat{c} \in L^2(0,T;C^\delta(\overline{\mathcal{D}}))$, and it fulfils the volume-filling condition $\widehat{f}_B + \widehat{f}_F + \widehat{f}_E = 1$. Note that the bounds in (5.8) still hold and that $0 \leq \widehat{f} \leq 1$ a.e. Therefore, the following Lemmas 11 and 12 do not depend on the choice of $\widehat{c}$ and δ. We will hence omit the dependency of the diffusion coefficients D_j on $\widehat{f}$ in this case.

We prove L^∞ bounds for the solution c to (6.6). We suppose that Assumptions (A1)–(A5) hold throughout this section.

Lemma 11. *Let c be a weak solution to (5.6), (6.6). Then $c \in L^\infty(Q_T)$, it holds for all $0 < t < T$ that $\|c_V(t)\|_{L^\infty(\mathcal{D})} \leq \|c_V^0\|_{L^\infty(\mathcal{D})}$,*

$$\|c_j(t)\|_{L^\infty(\mathcal{D})} \leq e^t\big(\|c_j^0\|_{L^\infty(\mathcal{D})} + \|\alpha_j\|_{L^\infty(0,T;L^\infty(\mathcal{D}))}\|c_V^0\|_{L^\infty(\mathcal{D})}\big), \quad j = D, M, U,$$

and $c_j(t) \geq 0$ a.e. for $t > 0$ and $j \in \{V, D, M, U\}$.

Proof. First, we use $(c_V - K)^+ := \max\{0, c_V - K\}$ with $K := \|c_V^0\|_{L^\infty(\mathcal{D})}$ as a test function in the weak formulation of equation (5.5) for c_V:

$$\frac{1}{2}\frac{\mathrm{d}}{\mathrm{d}t}\int_{\mathcal{D}}[(c_V - K)^+]^2\mathrm{d}x + \int_{\mathcal{D}} D_V|\nabla(c_V - K)^+|^2\mathrm{d}x = -\int_{\mathcal{D}}\alpha_V c_V(c_V - K)^+\mathrm{d}x \leq 0.$$

We conclude that $c_V(t) \le K$ in $\mathcal{D}$ for $t > 0$.

Second, we show that c_D is bounded. For this, set $M(t) = M_0 e^t$, where $M_0 = \|c_D^0\|_{L^\infty(\mathcal{D})} + \|\alpha_D\|_{L^\infty(0,T;L^\infty(\mathcal{D}))}\|c_V^0\|_{L^\infty(\mathcal{D})}$. Then $(c_D(0) - M)^+ = 0$ and, choosing $(c_D - M)^+$ as a test function in the weak formulation of equation (5.5) for c_D,

$$\begin{aligned}
&\frac{1}{2}\frac{\mathrm{d}}{\mathrm{d}t}\int_{\mathcal{D}}[(c_D - M)^+]^2 \mathrm{d}x + \int_{\mathcal{D}} D_D|\nabla(c_D - M)^+|^2 \mathrm{d}x \\
&\quad = -\int_{\mathcal{D}} \partial_t M (c_D - M)^+ \mathrm{d}x + \int_{\mathcal{D}} (\alpha_D c_V - \beta_D c_D)(c_D - M)^+ \mathrm{d}x \\
&\quad \le \int_{\mathcal{D}} \big(- M_0 + \|\alpha_D\|_{L^\infty(0,T;L^\infty(\mathcal{D}))}\|c_V^0\|_{L^\infty(\mathcal{D})}\big)(c_D - M)^+ \mathrm{d}x \le 0,
\end{aligned}$$

where we used $\beta_D \ge 0$, and the last inequality follows from the choice of M_0. This shows that $c_D(t) \le M_0 e^t$ in $\mathcal{D}$, $t > 0$. The bounds for c_M and c_U are shown in an analogous way.

The non-negativity of c_D and then of c_j, $j \in \{D, M, U\}$ follows by using $c_j^- := \min\{0, c_j\}$ as a test function in the weak formulation of (6.6) and using the non-negativity of the coefficients α_j and β_D. $\square$

Next, we prove that the solution $c(t)$ is Hölder continuous.

Lemma 12. *Let c be a weak solution to (5.6), (6.6). We suppose that there exists $\Lambda > 0$ such that for a.e. $0 < t < T$,*

$$\|\alpha_j(t)\|_{L^\infty(\mathcal{D})} + \|\beta_D(t)\|_{L^\infty(\mathcal{D})} \le \Lambda, \quad j = V, D, M, U. \tag{6.7}$$

Then there exists $\delta > 0$ such that for $0 < t < T$,

$$\|\partial_t c\|_{L^2(Q_T)} \le C_2, \quad \|c(t)\|_{C^{0+\delta}(\overline{\mathcal{D}})} \le C_\delta\big(\|c(t)\|_{L^2(\mathcal{D})} + \|\partial_t c(t)\|_{L^2(\mathcal{D})}\big), \tag{6.8}$$

where $C_2 > 0$ depends on the $L^2(\mathcal{D})$ norm of c^0, the $L^\infty(\mathcal{D})$ norm of f^0, and Λ, and δ, C_δ depend on the lower and upper bounds (5.8) for D_j and Λ.

Proof. The $L^2(Q_T)$ bound for $\partial_t c$ follows immediately from Theorem 48 and the Hölder estimate follows from Proposition 47 in Appendix A.2.2. Indeed, we interpret equation (5.5) for c_V,

$$\operatorname{div}(D_V \nabla c_V) + \alpha_V c_V = -\partial_t c_V \in L^2(\mathcal{D}) \quad \text{for } t \in (0, T)$$

as an elliptic equation with bounded diffusion coefficient D_V and right-hand side in $L^p(\mathcal{D})$ with $p > d/2$. By Proposition 47, there exists $\delta > 0$ such that $c_V(t) \in C^{0+\delta}(\mathcal{D})$ and

$$\|c_V(t)\|_{C^{0+\delta}(\overline{\mathcal{D}})} \le C\big(\|c_V\|_{L^2(\mathcal{D})} + \|\partial_t c_V\|_{L^p(\mathcal{D})}\big).$$

The result follows by observing that $d \le 3$ implies that $p < 2$. The dependency of δ and C_δ on the data follows from [39, Theorem 8.24], which is the essential result needed in the proof of Proposition 47. The regularity for the other concentrations is proved in a similar way. $\square$

Lemma 13. *Let $\widehat{c}(t) \in L^2(0,T;C^\delta(\overline{\mathcal{D}}))$ with $\delta > 0$ as in Lemma 12, satisfying estimate (6.8), and let c be a weak solution to (5.6), (6.6). Furthermore, let $c_j^0 \in C^{1+\delta}(\overline{\mathcal{D}})$ be such that $\nabla c_j^0 \cdot \nu = 0$ on $\partial\mathcal{D}$, α_j, $\beta_j \in C^0(\overline{\mathcal{D}} \times [0,T])$ satisfying (6.7), and $f_j^0 \in C^{0+\delta}(\overline{\mathcal{D}})$ for $j = V, D, M, U$, where $\delta > 0$ is as in Lemma 12 or smaller. Then $c \in C^{1+\delta,(1+\delta)/2}(\overline{\mathcal{D}}\times[0,T])$ and there exists $C_{1+\delta} > 0$ such that*

$$\|c\|_{C^{1+\delta,(1+\delta)/2}(\overline{\mathcal{D}}\times[0,T])} \leq C_{1+\delta},$$

where $C_{1+\delta} > 0$ depends only on T, Λ, C_δ, $\|f_0\|_{C^\delta(\mathcal{D})}$, $\|c_0\|_{C^{1+\delta}(\mathcal{D})}$, the L^∞ bound proven in Lemma 11, and the lower and upper bounds (5.8) for D_j.

The space $C^{1+\delta,(1+\delta)/2}(\overline{\mathcal{D}} \times [0,T])$ consists of all functions being $C^{1+\delta}$ in space and $C^{(1+\delta)/2}$ in time; see Appendix A.2.2 for a precise definition.

Proof. We know from Lemma 12 that $c(t)$ is Hölder continuous in $\overline{\mathcal{D}}$ for a.e. $t \in (0,T)$. We claim that $\widehat{f}$ is Hölder continuous in $\overline{\mathcal{D}} \times [0,T]$. Let $x, y \in \overline{\mathcal{D}}$ and $\tau, t \in [0,T]$. We assume without loss of generality that $\tau < t$. The Lipschitz continuity of $z \mapsto \exp(-z)$ implies, using the explicit formula for f_B, that

$$\begin{aligned}
|\widehat{f}_B(x,t) - \widehat{f}_B(y,t)| &\leq |f_B^0(x) - f_B^0(y)| + s_B \int_0^t |\widehat{c}_M(x,s) - \widehat{c}_M(y,s)| \mathrm{d}s, \\
&\leq \|f_B^0\|_{C^{0+\delta}(\overline{\mathcal{D}})} |x-y|^\delta + s_B C_\delta \big(\|\widehat{c}_M\|_{L^1(0,t;L^2(\mathcal{D}))} + \|\partial_t \widehat{c}_M\|_{L^1(0,t;L^2(\mathcal{D}))}\big)|x-y|^\delta, \\
|\widehat{f}_B(x,t) - \widehat{f}_B(x,\tau)| &\leq |f_B^0(x)| s_B \int_\tau^t |\widehat{c}_M(x,s)| \mathrm{d}s \\
&\leq \|f_B^0\|_{C^{0+\delta}(\overline{\mathcal{D}})} s_B \|\widehat{c}_M\|_{L^\infty(Q_T)} T^{1-\delta/2} |t-\tau|^{\delta/2},
\end{aligned}$$

where we also used Lemma 12. Similar estimates hold for $\widehat{f}_E$ and $\widehat{f}_F$. Thus, the assumptions of Theorem 49 in Appendix A.2.2 are fulfilled, yielding the statement. □

The next lemma will be needed to show ∇c is Lipschitz for solutions c to (5.5).

Lemma 14. *Let $d \in \mathbb{N}$, $\mathcal{D}' \subset \mathbb{R}^d$ be an open set and let $f \in C^\delta(\overline{\mathcal{D}'})$ for every $0 < \delta < 1$. If the Hölder norm of f can be bounded uniformly, i.e., there exists a $C^* > 0$ such that $\|f\|_{C^\delta(\overline{\mathcal{D}'})} \leq C^*$ for all $0 < \delta < 1$, then f is a Lipschitz continuous function on $\mathcal{D}'$.*

Proof. Let $x, y \in \mathcal{D}'$ with $x \neq y$. Then there exists $0 < \delta < 1$ such that $|x-y|^{1-\delta} \geq 1/2$. With this choice of δ, we compute

$$\frac{|f(x) - f(y)|}{|x-y|} = \frac{|f(x) - f(y)|}{|x-y|^\delta} \frac{1}{|x-y|^{1-\delta}} \leq 2C^*.$$

As C^* does not depend on δ and $x, y \in \mathcal{D}'$ are arbitrary, we infer that f is Lipschitz continuous with Lipschitz constant $L \leq 2C^*$. □

As solutions to (5.5)–(5.6) are also solutions to (5.6), (6.6) with the choice $\widehat{c} = c$, we can use the previous lemmas to prove the following unform bound in $L^\infty(0,T;W^{2,\infty}(\mathcal{D}))$ for solutions c to (5.5).

Lemma 15. *Let the assumptions of Lemma 13 hold and let additionally $c_0 \in W^{2,\infty}(\mathcal{D})$ and $\alpha_j, \beta_D \geq 0$, $j \in \{V, D, M, U\}$. Then every weak solution c to (5.5)–(5.6), with f given by (5.4), is an element of $L^\infty(0,T; W^{2,\infty}(\mathcal{D}))$, and there exists a constant $C > 0$ such that*

$$\|c\|_{L^\infty(0,T;W^{2,\infty}(\mathcal{D}))} \leq C,$$

where C depends on $\|f_0\|_{W^{1,\infty}(\mathcal{D})}$, $\|c_0\|_{W^{2,\infty}(\mathcal{D})}$, and has otherwise the same dependencies as $C_{1+\delta}$ in Lemma 13.

Proof. We deduce from Lemma 12 that $c \in L^2(0,T; C^\delta(\overline{\mathcal{D}}))$ and c satisfies (6.8). Then Lemma 13 implies that $c \in C^{1+\delta,(1+\delta)/2}(\overline{\mathcal{D}} \times [0,T])$ with $\|c\|_{C^{1+\delta,(1+\delta)/2}(\overline{\mathcal{D}}\times[0,T])} \leq C_{1+\delta}$. Taking into account the explicit representation (5.4) of f, the regularity of c carries over to f. Let now $V \subset \mathbb{R}^3$ be a fixed bounded and open set satisfying $\mathcal{D} \Subset V$. We can extend c to a function $\widetilde{c} \in W^{1,\infty}(\mathbb{R}^3)$ with compact support in V such that [32, Section 5.4, Theorem 1]

$$\|\widetilde{c}\|_{W^{1,\infty}(\mathbb{R}^3)} \leq C(V)\|c\|_{W^{1,\infty}(\mathcal{D})} \leq C(V)C_{1+\delta}, \tag{6.9}$$

where $C(V)$ only depends on the choice of V. By [32, Section 5.8, Theorem 4], c is Lipschitz continuous, and due to (6.9), the Lipschitz coefficient is bounded by $C(V)C_{1+\delta}$ (see the first part of the proof of [32, Section 5.8, Theorem 4]). We conclude that, for $x, y \in \mathcal{D}$ and $0 < \zeta < 1$,

$$\frac{|c(x) - c(y)|}{|x-y|^\zeta} = |x-y|^{1-\zeta}\frac{|c(x)-c(y)|}{|x-y|} \leq \max\Big\{1, \sup_{x',y'\in\mathcal{D}} |x'-y'|\Big\}C(V)C_{1+\delta}.$$

The map c is hence Hölder continuous of index ζ and its Hölder norm can be bounded independently of ζ. Repeating the proof of Lemma 13, we can show the existence of a constant $K(C_{1+\delta}, \Lambda, V)$ such that

$$\|c\|_{C^{1+\zeta,(1+\zeta)/2}(\overline{\mathcal{D}}\times[0,T])} \leq K(C_{1+\delta}, \Lambda, V),$$

where $K(C_{1+\delta}, \Lambda, V)$ is again independent of ζ, see [72, Theorem 1.2]. Applying Lemma 14 for $f = \partial c/\partial x_i$ together with Rademacher's theorem completes the proof. □

Remark 16. *All the results proven in Lemmas 11–15 may depend on the L^∞ bound of the processes α, β, but they do not depend on the Hölder norm of index δ and therefore not on the process (X_1, X_2) itself as long as $X_i(\omega, t) \in \overline{\mathcal{D}}$ for $i = 1, 2$ a.s.*

6.3.2. Existence

We show the existence of solutions to the reaction-diffusion and ordinary differential equations.

Theorem 17 (Existence)**.** *Let $c_j^0 \in C^{2+\delta}(\overline{\mathcal{D}})$ be such that $\nabla c_j^0 \cdot \nu = 0$ on $\partial\mathcal{D}$, let α_j, $\beta_j \in C^{\delta,\delta/2}(\overline{\mathcal{D}} \times [0,T])$ be non-negative and satisfy (6.7), and let $f_j^0 \in C^{1+\delta}(\overline{\mathcal{D}})$ for $j = V, D, M, U$, where $\delta > 0$ is as in Lemma 13 or smaller. Then there exists a pair (c, f) such that $c \in C^{2+\delta,1+\delta/2}(\overline{\mathcal{D}} \times [0,T])$ is a classical solution to (5.5)–(5.6) and f is given by (5.4).*

Proof. Let $\widehat{c} \in C^{1+\delta',(1+\delta')/2}(\overline{\mathcal{D}} \times [0,T]) \cap H^1(0,T;L^2(\mathcal{D}))$ for some $0 < \delta' < \delta$ and let $\widehat{c}$ satisfy (6.8). Furthermore, let $(\widehat{f}_B, \widehat{f}_F)$ be given by (5.4) with c_j replaced by $\widehat{c}$, and $\widehat{f}_E$ is defined by the volume-filling condition $\widehat{f}_B + \widehat{f}_E + \widehat{f}_F = 1$. By Theorem 51 in Appendix A.2.2, the linear system (6.6), together with (5.6), has a classical solution c which satisfies the estimate

$$\begin{aligned}\|c\|_{C^{2+\delta',(2+\delta')/2}(\overline{\mathcal{D}}\times[0,T])} &\leq K_0(\widehat{f},\alpha,\beta)\big(\|c_0\|_{C^{2+\delta',(2+\delta')/2}(\overline{\mathcal{D}}\times[0,T])} \\ &\qquad + \|c_V\|_{C^{2+\delta',(2+\delta')/2}(\overline{\mathcal{D}}\times[0,T])}\big) \\ &\leq K(\widehat{f},\alpha,\beta)\|c_0\|_{C^{2+\delta',(2+\delta')/2}(\overline{\mathcal{D}}\times[0,T])}.\end{aligned} \tag{6.10}$$

We deduce from Lemma 13 that $\|c\|_{C^{1+\delta,(1+\delta)/2}(\overline{\mathcal{D}}\times[0,T])} \leq C_{1+\delta}$, where $C_{1+\delta}$ is independent of $\widehat{f}$ and the choice of $\widehat{c}$.

We define now the fixed-point operator. Let

$$\begin{aligned}\widehat{c} \in W := \big\{&u \in C^{1+\delta,(1+\delta)/2}(\overline{\mathcal{D}} \times [0,T]) \cap H^1(0,T;L^2(\mathcal{D})) : \\ &\|u\|_{C^{1+\delta,(1+\delta)/2}(\overline{\mathcal{D}}\times[0,T])} \leq C_{1+\delta}, \quad u \text{satisfies } (6.8)\big\}.\end{aligned}$$

Then the operator $\Gamma : W \to W$, mapping $\widehat{c}$ to the solution c to (5.5)–5.6 is well-defined. Furthermore, by estimate (6.10), it holds that

$$\|\Gamma(\widehat{c})\|_{C^{2+\delta',(2+\delta')/2}(\bar{\mathcal{D}}\times[0,T])} \leq K_1(\alpha,\beta)\|c_0\|_{C^{2+\delta',(2+\delta')/2}(\bar{\mathcal{D}}\times[0,T])}, \tag{6.11}$$

where the constant K_1 does not depend on $\widehat{f}$ thanks to the uniform bound $C_{1+\delta}$ in W. Given two elements $\widehat{c}_1$, $\widehat{c}_2 \in W$, we set $\Gamma(\widehat{c}_i) = c_i$ and define $u := c_{1,V} - c_{2,V}$. Then u satisfies

$$\begin{aligned}&\partial_t u - \operatorname{div}(D_V(\widehat{f}_1)\nabla u) + \alpha_V u = \operatorname{div}\big((D(\widehat{f}_1) - D(\widehat{f}_2))\nabla c_2\big), \quad \text{in } \mathcal{D} \times (0,T], \\ &u(0) = 0 \quad \text{in } \mathcal{D}, \quad \nabla u \cdot \nu = 0 \quad \text{in } \partial\mathcal{D} \times [0,T],\end{aligned}$$

where $\widehat{f}_i$ is the corresponding solution to (5.3) associated with $\widehat{c}_i$. By Theorem 51 and estimate (6.11), $u = c_{1,V} - c_{2,V}$ satisfies the inequality

$$\begin{aligned}&\|c_{1,V} - c_{2,V}\|_{C^{2+\delta',(2+\delta')/2}(\overline{\mathcal{D}}\times[0,T])} \\ &\quad \leq K_2(\widehat{f}_1,\alpha)\|c_2\|_{C^{2+\delta',(2+\delta')/2}(\overline{\mathcal{D}}\times[0,T])}\|\widehat{f}_1 - \widehat{f}_2\|_{C^{1+\delta',(1+\delta')/2}(\overline{\mathcal{D}}\times[0,T])} \\ &\quad \leq K_2(\widehat{f}_1,\alpha)K_3(\alpha,\beta,c^0)\|\widehat{c}_1 - \widehat{c}_2\|_{C^{1+\delta',(1+\delta')/2}(\overline{\mathcal{D}}\times[0,T])},\end{aligned}$$

where we also used (5.4). We obtain similar estimates for the other components $c_{1,i} - c_{2,i}$, $i = D, M, U$. From these inequalities, we directly infer the continuity of Γ in the norm $\|\cdot\|_{C^{1+\delta',(1+\delta')/2}(\overline{\mathcal{D}}\times[0,T])}$. Since W is compactly embedded in $C^{1+\delta',(1+\delta')/2}(\overline{\mathcal{D}} \times [0,T])$, using $\delta' < \delta$, we conclude from Schauder's fixed-point theorem that there exists a fixed point c for Γ and hence a solution to (5.5)–(5.6). ☐

6.3.3. Stability and uniqueness

The stability results are used for the solution of the SDEs; they also imply the uniqueness of solutions. We start with a stability estimate in the norms of $L^\infty(0,T;L^2(\mathcal{D}))$ and $L^2(0,T;H^1(\mathcal{D}))$. Let Assumptions (A1)–(A5) hold.

Lemma 18. *Let c_i for $i=1,2$ be weak solutions to* (5.5)–(5.6) *with the same initial data (c^0,f^0) but possibly different coefficients α_i and β_i. Then there exists $C>0$, which is independent of c_i, such that for all $t\in[0,T]$,*

$$\begin{aligned}&\|(c_1-c_2)(t)\|_{L^2(\mathcal{D})}+\|c_1-c_2\|_{L^2(0,t;H^1(\mathcal{D}))}\le h(t), \quad \textit{where}\\ &h(t):=C\big(\|\alpha_1-\alpha_2\|_{L^2(Q_T)}+\|\beta_1-\beta_2\|_{L^2(Q_T)}\big).\end{aligned}$$

Proof. We first consider c_V. We take the difference of the equations satisfied by $c_{1,V}-c_{2,V}$ and take the test function $c_{1,V}-c_{2,V}$ in its weak formulation. This leads to

$$\begin{aligned}\frac{1}{2}\frac{\mathrm{d}}{\mathrm{d}t}\int_{\mathcal{D}}(c_{1,V}-c_{2,V})^2\mathrm{d}x+\int_{\mathcal{D}}D_V(f_1)|\nabla(c_{1,V}-c_{2,V})|^2\mathrm{d}x+\int_{\mathcal{D}}\alpha_{1,V}(c_{1,V}-c_{2,V})^2\mathrm{d}x\\ =\int_{\mathcal{D}}(D_V(f_1)-D_V(f_2))\nabla c_{2,V}\cdot\nabla(c_{1,V}-c_{2,V})\mathrm{d}x\\ +\int_{\mathcal{D}}(\alpha_{1,V}-\alpha_{2,V})c_{2,V}(c_{1,V}-c_{2,V})\mathrm{d}x.\end{aligned}$$

Let $\varepsilon:=\min\{D^i_j: j=V,D,M,U,\ i=B,E,F\}>0$. Using Young's inequality and the estimate $\|(f_1-f_2)(t)\|_{L^2(\mathcal{D})}\le C\|c_1-c_2\|_{L^1(0,T;L^2(\mathcal{D}))}$ from Lemma 10, we find that

$$\begin{aligned}&\frac{\mathrm{d}}{\mathrm{d}t}\|c_{1,V}-c_{2,V}\|^2_{L^2(\mathcal{D})}+\frac{\varepsilon}{2}\|\nabla(c_{1,V}-c_{2,V})\|^2_{L^2(\mathcal{D})}\\ &\quad\le C(\varepsilon)\|\nabla c_{2,V}\|^2_{L^\infty(Q_T)}\|D_V(f_1)-D_V(f_2)\|^2_{L^2(\mathcal{D})}\\ &\qquad+\|c_{2,V}\|^2_{L^\infty(Q_T)}\|\alpha_{1,V}-\alpha_{2,V}\|^2_{L^2(\mathcal{D})}+\|c_{1,V}-c_{2,V}\|^2_{L^2(\mathcal{D})}\\ &\quad\le C\|c_1-c_2\|^2_{L^2(\mathcal{D})}+C\|\alpha_{1,V}-\alpha_{2,V}\|^2_{L^2(\mathcal{D})}.\end{aligned}$$

The estimates for $c_{1,j}-c_{2,j}$ with $j=D,M,V$ are similar. This gives

$$\frac{\mathrm{d}}{\mathrm{d}t}\|c_1-c_2\|^2_{L^2(\mathcal{D})}+\frac{\varepsilon}{2}\|\nabla(c_1-c_2)\|^2_{L^2(\mathcal{D})}\le Ch(t)^2+C\|c_1-c_2\|^2_{L^2(\mathcal{D})}.$$

An application of Gronwall's lemma finishes the proof. ☐

A stability estimate can also be proved with respect to the $H^2(\mathcal{D})$ norm.

Lemma 19. *Let c_i for $i=1,2$ be weak solutions to* (5.5)–(5.6) *with the same initial data (c^0,f^0) but possibly different coefficients α_i and β_i. Then there exists $C>0$ such that for all $t\in[0,T]$,*

$$\begin{aligned}&\|\partial_t(c_1-c_2)\|_{L^2(Q_T)}+\|c_1-c_2\|_{L^\infty(0,T;H^1(\mathcal{D}))}+\|c_1-c_2\|_{L^2(0,T;H^2(\mathcal{D}))}\\ &\quad\le C\big(\|\alpha_1-\alpha_2\|_{L^2(Q_T)}+\|\beta_1-\beta_2\|_{L^2(Q_T)}\big),\end{aligned}$$

where $C>0$ depends on $\|c_1\|_{L^\infty(0,T;W^{2,\infty}(\mathcal{D}))}$.

Proof. The difference $u := c_{1,V} - c_{2,V}$ is the solution to the linear problem

$$\begin{aligned} &\partial_t u - \operatorname{div}(D_V(f_1)\nabla u) = g(x,t) \quad \text{in } \mathcal{D},\ t > 0, \\ &\nabla u \cdot \nu = 0 \quad \text{on } \partial\mathcal{D}, \quad u(0) = 0 \quad \text{in } \mathcal{D}, \end{aligned} \tag{6.12}$$

where, by Lemma 15, the right-hand side

$$g := -\operatorname{div}\big((D_V(f_1) - D_V(f_2))\nabla c_{2,V}\big) + \alpha_{1,V}(c_{1,V} - c_{2,V}) + (\alpha_{1,V} - \alpha_{2,V})c_{2,V} \tag{6.13}$$

is an element of $L^2(Q_T)$. Since the diffusion coefficient is bounded, we can apply Theorem 48 in Appendix A.2.2 to conclude that

$$\|u\|_{L^\infty(0,T;H^1(\mathcal{D}))} + \|\partial_t u\|_{L^2(Q_T)} \le C\|g\|_{L^2(Q_T)}.$$

For the estimate of the right-hand side, we recall from Lemma 10 that

$$\|\nabla(f_1 - f_2)\|_{L^2(Q_T)} \le C\|c_1 - c_2\|_{L^1(0,T;H^1(\mathcal{D}))}.$$

Then, using the linearity of D_V and the estimate for $c_{2,V}$ from Lemma 15, we infer that

$$\begin{aligned} \|g\|_{L^2(Q_T)} &\le C\|\nabla(f_1 - f_2)\|_{L^2(Q_T)}\|\nabla c_{2,V}\|_{L^\infty(Q_T)} + C\|f_1 - f_2\|_{L^2(Q_T)}\|\Delta c_{2,V}\|_{L^\infty(Q_T)} \\ &\quad + \|\alpha_{1,V}\|_{L^\infty(Q_T)}\|u\|_{L^2(Q_T)} + \|\alpha_{1,V} - \alpha_{2,V}\|_{L^2(Q_T)}\|c_{2,V}\|_{L^\infty(Q_T)} \\ &\le C\big(\|c_1 - c_2\|_{L^2(0,T;H^1(\mathcal{D}))} + \|\alpha_{1,V} - \alpha_{2,V}\|_{L^2(Q_T)}\big). \end{aligned}$$

The difference $c_1 - c_2$ in the $L^2(0,T;H^1(\mathcal{D}))$ norm can be estimated according to Lemma 18. Therefore,

$$\|u\|_{L^\infty(0,T;H^1(\mathcal{D}))} + \|\partial_t u\|_{L^2(Q_T)} \le C\big(\|\alpha_1 - \alpha_2\|_{L^2(Q_T)} + \|\beta_1 - \beta_2\|_{L^2(Q_T)}\big). \tag{6.14}$$

Similar estimates can be derived for the differences $c_{1,j} - c_{2,j}$ $(j = D, M, U)$.

To estimate u in the $L^2(0,T;H^2(\mathcal{D}))$ norm, we use the inequality

$$\|u\|_{H^2(\mathcal{D})} \le C\big(\|\Delta u\|_{L^2(\mathcal{D})} + \|u\|_{L^2(\mathcal{D})}\big).$$

Thus, it remains to consider Δu. We deduce from

$$\begin{aligned} D_V(f_1)\Delta u &= \operatorname{div}\big(D_V(f_1)\nabla c_{1,V} - D_V(f_2)\nabla c_{2,V}\big) - \nabla(D_V(f_1) - D_V(f_2)) \cdot \nabla c_{2,V} \\ &\quad - (D_V(f_1) - D_V(f_2))\Delta c_{2,V} - \nabla D_V(f_1) \cdot \nabla(c_{1,V} - c_{2,V}) \\ &= \partial_t u - \alpha_{1,V} u - (\alpha_{1,V} - \alpha_{2,V})c_{2,V} - \nabla(D_V(f_1) - D_V(f_2)) \cdot \nabla c_{2,V} \\ &\quad - (D_V(f_1) - D_V(f_2))\Delta c_{2,V} - \nabla D_V(f_1) \cdot \nabla u \end{aligned}$$

and $\|\nabla(D_V(f_1) - D_V(f_2))\|_{L^2(Q_T)} \le C\|c_1 - c_2\|_{L^2(0,T;H^1(\mathcal{D}))}$ (see Lemma 10) that

$$\|\Delta u\|_{L^2(Q_T)} \le C\big(\|\alpha_1 - \alpha_2\|_{L^2(Q_T)} + \|\beta_1 - \beta_2\|_{L^2(Q_T)} + \|u\|_{L^2(0,T;H^1(\mathcal{D}))}\big).$$

We infer from (6.14) and related inequalities for $c_{1,j} - c_{2,j}$ that

$$\|\Delta(c_1 - c_2)\|_{L^2(Q_T)} \le C\big(\|\alpha_1 - \alpha_2\|_{L^2(Q_T)} + \|\beta_1 - \beta_2\|_{L^2(Q_T)}\big),$$

which concludes the proof. □

Lemma 20. *Let c_i for $i = 1, 2$ be weak solutions to (5.5)–(5.6) with the same initial data (f^0, c^0) but possibly different coefficients α_i and β_i. Then there exists $C > 0$ such that for all $t \in [0, T]$,*

$$\|c_1 - c_2\|_{L^4(0,T;W^{2,4}(\mathcal{D}))} \leq C\big(\|\alpha_1 - \alpha_2\|_{L^4(Q_T)} + \|\beta_1 - \beta_2\|_{L^4(Q_T)}\big).$$

Proof. Let $u = c_{1,V} - c_{2,V}$ be the solution to (6.12). Since $g \in L^4(Q_T)$ by Lemma 15 (recall definition (6.13) of g), Theorem 50 in Appendix A.2.2 shows that $u \in L^4(0, T; W^{2,4}(\mathcal{D})) \cap H^1(0, T; L^4(\mathcal{D}))$ and, because of $\nabla c_{2,V} \in L^\infty(0, T; W^{1,\infty}(\mathcal{D}))$,

$$\begin{aligned}\|c_{1,V} - c_{2,V}\|_{L^4(0,T;W^{2,4}(\mathcal{D}))} &\leq C\|g\|_{L^4(Q_T)} \\ &\leq C\big(\|c_1 - c_2\|_{L^1(0,T;W^{1,4}(\mathcal{D}))} + \|c_{1,V} - c_{2,V}\|_{L^4(Q_T)} + \|\alpha_{1,V} - \alpha_{2,V}\|_{L^4(Q_T)}\big).\end{aligned}$$

The first and second terms on the right-hand side can be estimated by using the embedding $H^2(\mathcal{D}) \hookrightarrow W^{1,4}(\mathcal{D})$ and Lemma 19:

$$\begin{aligned}\|c_1 - c_2\|_{L^1(0,T;W^{1,4}(\mathcal{D}))} &\leq C\|c_1 - c_2\|_{L^2(0,T;H^2(\mathcal{D}))} \\ &\leq C\big(\|\alpha_1 - \alpha_2\|_{L^2(Q_T)} + \|\beta_1 - \beta_2\|_{L^2(Q_T)}\big), \\ \|c_{1,V} - c_{2,V}\|_{L^4(Q_T)} &\leq C\|c_{1,V} - c_{2,V}\|_{L^4(0,T;H^1(\mathcal{D}))} \\ &\leq C\big(\|\alpha_1 - \alpha_2\|_{L^2(Q_T)} + \|\beta_1 - \beta_2\|_{L^2(Q_T)}\big).\end{aligned}$$

This gives

$$\|c_{1,V} - c_{2,V}\|_{L^4(0,T;W^{2,4}(\mathcal{D}))} \leq C\big(\|\alpha_1 - \alpha_2\|_{L^4(Q_T)} + \|\beta_1 - \beta_2\|_{L^2(Q_T)}\big).$$

The estimates for $c_{1,j} - c_{2,j}$ $(j = D, M, U)$ are similar. □

6.4. Solution of the stochastic differential equations

Let α, β be given by (5.7). We first study the measurability of (c, f).

Lemma 21. *Let $f^0 \in L^\infty(\Omega; C^{1+\delta}(\overline{\mathcal{D}}))$ and $c^0 \in L^\infty(\Omega; W^{2,\infty}(\mathcal{D}))$ be such that $\nabla c_j^0 \cdot \nu = 0$ on $\partial\mathcal{D}$, $j = V, D, M, U$. Furthermore, let (c, f) be a pathwise solution to (5.3), (5.5)–(5.6) and let (X_1, X_2) in (5.7) be adapted stochastic processes with Hölder continuous paths (with Hölder index δ) almost surely. Then f, ∇f are measurable as maps from $(\Omega \times \mathcal{D} \times [0, t], \mathcal{F}_t \times \mathcal{B}(\mathcal{D}) \times \mathcal{B}([0, t]))$ to $\mathcal{B}(\mathbb{R}^3)/\mathcal{B}(\mathbb{R}^{3\times3})$, and c, ∇c are measurable as maps from $(\Omega \times \mathcal{D} \times [0, t], \mathcal{F}_t \times \mathcal{B}(\mathcal{D}) \times \mathcal{B}([0, t]))$ to $\mathcal{B}(\mathbb{R}^4)/\mathcal{B}(\mathbb{R}^{4\times3})$ for all $t \in [0, T]$. In particular, these functions are progressively measurable.*

Proof. Since f_j can be represented as a function depending on the time integral of c, it is sufficient to show the measurability of c_j. The continuity of the potentials defining α_j and β_j in (5.7) shows that α_j and β_j are processes with càdlàg paths almost surely. By approximating the initial data c^0, f^0 and the processes α_j, β_j by suitable simple processes, which are adapted to the filtration by construction, we can obtain the $\mathcal{F}_t$-measurability of $c_j(t) : \Omega \to C^1(\overline{\mathcal{D}})$ for $t \in [0, T]$. We conclude from Lemma 18 and the compactness of

$W^{2,\infty}(\mathcal{D}) \subset C^{1+\delta}(\overline{\mathcal{D}})$ in $C^1(\overline{\mathcal{D}})$ the measurability of c_j as the limit of measurable functions. For details of this construction, we refer to [47, Section 3.3].

It is known that càdlàg processes $Y_t : \Omega \times [0,T] \to H$ with $H = \mathbb{R}^n$, which are adapted to the filtration, are progressively measurable [62, Prop. 1.13]. A straightforward modification of the proof of [62, Prop. 1.13], utilizing [31, Theorem 4.2.2], shows that this holds for arbitrary Banach spaces H. The estimate $\|c_j(t) - c_j(s)\|_{C^1(\overline{\mathcal{D}})} \leq C|t-s|^\delta$, which follows from Lemma 13, implies that $c_j(t)$ has almost surely continuous paths and consequently, $c_j(t)$ is progressively measurable. To be precise, this yields the measurability of c_j as a function from $(\Omega \times [0,t], \mathcal{F}_t \times \mathcal{B}([0,t]))$ to $(C^1(\overline{\mathcal{D}}), \mathcal{B}(C^1(\overline{\mathcal{D}})))$ for every $t \in [0,T]$.

The function $(c,x) \mapsto c(x)$, $C^1(\overline{\mathcal{D}}) \times \overline{\mathcal{D}} \to \mathbb{R}^4$, is continuous and hence, it is measurable as a mapping from $(C^1(\overline{\mathcal{D}}) \times \overline{\mathcal{D}}, \mathcal{B}(C^1(\overline{\mathcal{D}})) \times \mathcal{B}(\overline{\mathcal{D}}))$ to $(\mathbb{R}^4, \mathcal{B}(\mathbb{R}^4))$. Now, we can write $c(\omega,x,t)$ as the concatenation

$$(\omega,x,t) \mapsto (c(\omega,\cdot,t),x) \mapsto c(\omega,x,t), \quad \Omega \times \overline{\mathcal{D}} \times [0,T] \to C^1(\overline{\mathcal{D}}) \times \overline{\mathcal{D}} \to \mathbb{R}^4,$$

of measurable functions, which yields the measurability of c. In a similar way, we can prove the measurability of $\partial c_j/\partial x_i$ for $i = 1,2,3$ by considering the continuous mapping $(c,x) \mapsto (\partial c/\partial x_i)(x)$. □

Remark 22. *As (X_1, X_2) only almost surely have Hölder continuous paths, c and f are also defined only almost surely. So to be more precise Lemma 21 shows the existence of progressive measurable processes $\tilde{c}$ and $\tilde{f}$ (by defining c and f on the null set where they are not defined, for example by setting them zero) whose paths coincide almost surely with those of c and f. All such suitable progressive measurable processes $\tilde{c}$ (and $\tilde{f}$) are indistinguishable from each other and are equivalent in this manner. We hence identify all these processes with c and f, dropping the use of a specific progressively measurable representative.*

Lemma 23. *Let Assumptions (B1)–(B5) and the assumptions of Lemma 21 hold. Then there exists a unique, progressively measurable solution (X_i^k) to (5.1) such that $X_i^k(t) \in \overline{\mathcal{D}}$ a.s. for every $t \in [0,T]$, $i = 1,2$.*

Proof. We extend the coefficients g_i and σ_i by setting them to zero outside of $\mathcal{D}$. The extended coefficients are still uniformly Lipschitz continuous. We infer from Lemma 21 that g_i is progressively measurable. Thus, by [73, Theorem 3.1.1], also see Theorem 43, there exists a strong solution to (5.1).

It remains to show that $X_i^k(t) \in \overline{\mathcal{D}}$ a.s. Let ϕ be a smooth test function satisfying $\operatorname{supp}\phi \subset \mathcal{D}^c$. We obtain from Itô's lemma that

$$\mathrm{d}\phi(X_i^k) = \nabla\phi(X_i^k) \cdot g_i[c,f](X_i^k,t)\mathrm{d}t + \frac{1}{2}\sigma_i(X_i^k)^2\Delta\phi(X_i^k)\mathrm{d}t + \nabla\phi(X_i^k)\cdot\sigma_i(X_i^k)\mathrm{d}B_i^k. \quad (6.15)$$

If $X_i^k(t) \in \mathcal{D}$, we have $\phi(X_i^k) = 0$. If $X_i^k(t) \in \mathcal{D}^c$ then $g_i[c,f](X_i^k(t),t) = 0$ by Assumption (B3) and $\sigma_i(X_i^k(t)) = 0$ by Assumption (B2). Equation (6.15) then shows that $\phi(X_i^k(t)) = \phi(X_i^{0,k}) = 0$ and $X_i^k(t) \in \overline{(\operatorname{supp}\phi)^c}$ a.s. Since ϕ with $\operatorname{supp}\phi \subset \mathcal{D}^c$ was arbitrary, we conclude that $X_i^k(t) \in \overline{\mathcal{D}}$ a.s. for $t \in (0,T)$. □

6.5. Proof of Theorem 8

The fixed-point operator is defined as a function that maps $\widetilde{X} \mapsto (\alpha, \beta_D) \mapsto (c, f) \mapsto X$, where (α, β_D) is defined in (5.7) with X replaced by $\widetilde{X}$. To define its domain, we need some preparations.

Lemma 24. *The space $Y_R(0,T;\mathcal{D})$, defined in (6.1), is complete. Furthermore, any $X \in Y_R(0,T;\mathcal{D})$ has a progressively measurable modification with almost surely Hölder continuous paths.*

Proof. Let (X_n) be a Cauchy sequence in $Y_R(0,T;\mathcal{D})$ and let $\varepsilon > 0$. Then there exists $N \in \mathbb{N}$ such that for all $n, m \geq N$,

$$\|X_n(t) - X_m(t)\|_{L^4(\Omega)} \leq \|X_n - X_m\|_{C^0([0,T];L^4(\Omega))} < \varepsilon.$$

For any $t \in [0,T]$, $(X_n(t))$ is a Cauchy sequence in $L^4(\Omega)$. Consequently, $X_n(t) \to X(t)$ in $L^4(\Omega)$, where $X(t) \in L^4(\Omega)$ is $\mathcal{F}_t$-measurable. Furthermore, there exists a subsequence of $(X_n(t))$ (not relabelled) that converges pointwise to $X(t)$ a.s., proving that $X(t) \in \overline{\mathcal{D}}$ a.s. The definition of the Hölder norm implies that $\|X_n(t) - X_n(s)\|_{L^4(\Omega)} \leq R|t-s|^{1/2}$ for all $s,t \in [0,T]$. This gives in the limit $n \to \infty$ that $\|X(t) - X(s)\|_{L^4(\Omega)} \leq R|t-s|^{1/2}$ and consequently $X \in C^{1/2}(0,T;L^4(\mathcal{D}))$. We conclude that $X \in Y_R(0,T;\mathcal{D})$. By the Kolmogorov continuity criterion, (a modification of) X has almost surely Hölder continuous paths. As $X(t)$ is an adapted process with respect to the filtration $\mathcal{F}_t$, X is progressively measurable. $\square$

Lemma 25. *Let $(\widetilde{X}_1, \widetilde{X}_2) \in Y_R(0,T;\mathcal{D})$ for some $R > 0$, and let (c, f) be a solution to (5.3), (5.5)–(5.6), where α, β are given by (5.7) with X replaced by $\widetilde{X}$. Then, for fixed initial datum (X_1^0, X_2^0), there exists $R_0 > 0$ not depending on R such that the solution (X_1, X_2) to (5.1) satisfies $(X_1, X_2) \in Y_{R_0}(0,T;\mathcal{D})$.*

Proof. According to Lemma 15, c is bounded in the $L^\infty(0,T;W^{2,\infty}(\mathcal{D}))$ norm by a constant that is independent of R. Then, by Lemma 23, there exists a unique solution (X_1, X_2) to (5.1). Since $X_i^k(t) \in \overline{\mathcal{D}}$ a.s., c, ∇c, f, ∇f are bounded uniformly in R, i.e., there exists $K = K(c^0, f^0) > 0$, which is independent of R, such that $|g_i[c,f](X_i^k(t), t)| \leq K$ a.s. Thus, for $s, t \in [0,T]$, using the Burkholder–Davis–Gundy inequality,

$$\begin{aligned}
\mathbb{E}|X_i^k(t) - X_i^k(s)|^4 &\leq C(K)|t-s|^4 + C\mathbb{E}\bigg(\int_s^t \sigma(X_i^k(s))\mathrm{d}B_i^k(s)\bigg)^4 \\
&\leq C(K)|t-s|^4 + C\mathbb{E}\bigg(\int_s^t \sigma(X_i^k(s))^2\mathrm{d}s\bigg)^2 \\
&\leq C(K)\big(|t-s|^2 + \|\sigma\|^4_{L^\infty(\mathcal{D})}\big)|t-s|^2 \leq C(K,T,\sigma,\mathcal{D})|t-s|^2.
\end{aligned}$$

The lemma follows after choosing $R_0 := \max\{C(K,T,\sigma,\mathcal{D})^{1/4}, (K\sqrt{T} + C\|\sigma\|_{L^\infty(\mathcal{D})})\sqrt{T} + \|X_0\|_{L^4(\Omega)}\}$. $\square$

The previous lemma shows that the fixed-point operator $\Phi : Y_{R_0}(0,T;\mathcal{D}) \to Y_{R_0}(0,T;\mathcal{D})$, $\widetilde{X} \mapsto X$, is well defined. We need to verify that Φ is a contraction. We first prove an auxiliary result.

Lemma 26. *Let (c, f) and (c', f') be progressively measurable solutions to (5.3)–(5.6), where α, β are given by (5.7) with X replaced by $\widetilde{X}$, $\widetilde{X}' \in Y_R(0,T;\mathcal{D})$ for some $R > 0$, respectively. Then the associated solutions X and X' to (5.1) satisfy*

$$\mathbb{E}|X(t) - X'(t)|^4 \leq Ct \int_0^t \mathbb{E}\|c(s) - c'(s)\|^4_{C^1(\overline{\mathcal{D}})} \mathrm{d}s,$$

where the constant $C > 0$ does not depend on R, (c, f), or (c', f').

Proof. The Itô integral representation of $X(t) - X'(t)$ gives

$$\begin{aligned}\mathbb{E}|X_i^k(t) - (X')_i^k(t)|^4 &\leq C\mathbb{E}\Big(\int_0^t \big(g_i[c,f](X_i^k(s),s) - g_i[c',f']((X')_i^k(s),s)\big)\mathrm{d}s\Big)^4 \\ &\quad + C\mathbb{E}\Big(\int_0^t \big(\sigma(X_i^k(s)) - \sigma((X')_i^k(s))\big)\mathrm{d}B_i^k(s)\Big)^4 =: I_1 + I_2.\end{aligned} \tag{6.16}$$

It follows from Assumption (A4) and the explicit representation (5.4) that

$$\begin{aligned} I_1 &\leq C\mathbb{E}\Big| \int_0^t \big(g_i[c,f](X_i^k(s),s) - g_i[c',f'](X_i^k(s),s)\big)\mathrm{d}s\Big|^4 \\ &\quad + \mathbb{E}\Big| \int_0^t \big(g_i[c',f'](X_i^k(s),s) - g_i[c',f']((X')_i^k(s),s)\big)\mathrm{d}s\Big|^4 \\ &\leq L_1^4 \mathbb{E}\big(1 + \|c\|_{L^\infty(0,T;C^1(\overline{\mathcal{D}}))}\big)^4 \Big(\int_0^t \|c(s) - c'(s)\|_{C^1(\overline{\mathcal{D}})}\mathrm{d}s\Big)^4 \\ &\quad + L_2^4 \mathbb{E}\big(1 + \|c'\|_{L^\infty(0,T;W^{2,\infty}(\mathcal{D}))}\big)^4 \Big(\int_0^t |X(s) - X'(s)|\mathrm{d}s\Big)^4. \end{aligned}$$

Furthermore, by the Burkholder–Davis–Gundy inequality and the Lipschitz continuity of σ,

$$I_2 \leq C\mathbb{E}\Big(\int_0^t \big((\sigma(X_i^k(s)) - \sigma((X')_i^k(s))\big)^2 \mathrm{d}s\Big)^2 \leq C\mathbb{E}\Big(\int_0^t |X(s) - X'(s)|^2 \mathrm{d}s\Big)^2.$$

We insert these estimates into (6.16) and use Hölder's inequality:

$$\begin{aligned}\mathbb{E}|X(t) - X'(t)|^4 &\leq Ct^3 \mathbb{E} \int_0^t \|c(s) - c'(s)\|^4_{C^1(\overline{\mathcal{D}})}\mathrm{d}s \\ &\quad + Ct^3 \mathbb{E}\int_0^t |X(s) - X'(s)|^4 \mathrm{d}s + Ct\mathbb{E}\int_0^t |X(s) - X'(s)|^4 \mathrm{d}s.\end{aligned}$$

Then Gronwall's lemma concludes the proof. □

We prove now that $\Phi : Y_{R_0}(0,T;\mathcal{D}) \to Y_{R_0}(0,T;\mathcal{D})$, $\widetilde{X} \mapsto X$, is a contraction. By Lemmas 26 and 20, we have

$$\mathbb{E}|\Phi(X(t)) - \Phi(X'(t))|^4 \leq Ct \int_0^t \mathbb{E}\|c(s) - c'(s)\|^4_{C^1(\overline{\mathcal{D}})}\mathrm{d}s$$

$$\begin{aligned}&\leq Ct\mathbb{E}\big(\|\alpha-\alpha'\|^4_{L^4(Q_T)}+\|\beta-\beta'\|^4_{L^4(Q_T)}\big)\\&\leq Ct\mathbb{E}\|X-X'\|^4_{L^4(0,t,L^4(\mathcal{D}))}=Ct\int_0^t\mathbb{E}|X(s)-X'(s)|^4\mathrm{d}s.\end{aligned}$$

We iterate this inequality to find after n times that

$$\begin{aligned}\mathbb{E}|\Phi^n(X(t))-\Phi^n(X'(t))|^4&\leq (Ct)^n\int_0^t\int_0^{s_1}\cdots\int_0^{s_{n-1}}\mathbb{E}|X(s_n)-X'(s_n)|^4\mathrm{d}s_n\cdots\mathrm{d}s_1\\&\leq (Ct)^n\frac{t^n}{n!}\sup_{0<s<t}\mathbb{E}|X(s)-X'(s)|^4.\end{aligned}$$

We conclude that

$$\sup_{0<s<T}\big(\mathbb{E}|\Phi^n(X(t))-\Phi^n(X'(t))|^4\big)^{1/4}\leq\frac{(CT^2)^{n/4}}{(n!)^{1/4}}\sup_{0<s<T}\big(\mathbb{E}|X(s)-X'(s)|^4\big)^{1/4}.$$

The sequence $(CT^2)^{n/4}/(n!)^{1/4}$ converges to zero as $n\to\infty$. Hence, there exists $n\in\mathbb{N}$ such that Φ^n is a contraction. By the variant [68, Theorem 2.4] of Banach's fixed-point theorem, Φ has a fixed point, proving Theorem 8.

7. Analysis of a Model for Vesicle Transport in Neurites

The aim of this chapter is the analysis of the cross-diffusion systems (5.9)–(5.18), modeling the intracellular transport of vesicles in neurites. We start by giving some key ideas and the main existence result, Theorem 27, together with necessary assumptions.

7.1. Assumptions and Main Result

The key idea of our analysis is to work with the entropy (or, more precisely, free energy)

$$\begin{aligned} E(u) &= \int_{\mathcal{D}} (h(u) - u_1 V_1 - u_2 V_2)\mathrm{d}x, \quad \text{where} \\ h(u) &= \sum_{i=1}^{2} u_i(\log u_i - 1) + u_0(\log u_0 - 1) \quad \text{and} \quad u_0 = 1 - u_1 - u_2. \end{aligned} \tag{7.1}$$

Introducing the electrochemical potentials $\mu_i = \delta E/\delta u_i = \log(u_i/u_0) - V_i$ for $i = 1, 2$, system (5.9)-(5.10) can be written as a formal gradient flow in the sense

$$\partial_t u_i = \operatorname{div} \sum_{j=1}^{2} B_{ij} \nabla \mu_j, \quad \text{where } B_{ij} = D_i u_0 u_i \delta_{ij},\ i = 1, 2,$$

and δ_{ij} is the Kronecker symbol. The advantage of this formulation is that the drift terms are eliminated and that the new diffusion matrix (B_{ij}) is (diagonal and) positive definite. This formulation is the basis of the boundedness-by-entropy method [59, Chap. 4]. The use of the electrochemical potentials has another benefit. Inverting the relation $(u_1, u_2) \mapsto (\mu_1, \mu_2)$, we infer from

$$u_i = \frac{\exp(\mu_i + V_i)}{1 + \exp(\mu_1 + V_1) + \exp(\mu_2 + V_2)}, \quad i = 1, 2,$$

that

$$u = (u_1, u_2) \in \mathcal{D} := \{u \in \mathbb{R}^2 : u_1 > 0,\ u_2 > 0,\ u_1 + u_2 < 1\}, \tag{7.2}$$

guaranteeing the physical bounds without the use of a maximum principle.

Furthermore, a formal computation (see the proof of (7.10)) shows that

$$\frac{\mathrm{d}E}{\mathrm{d}t}(u) + \int_{\mathcal{D}} \sum_{i=1}^{2} D_i u_0 u_i \left| \nabla \left(\log \frac{u_i}{u_0} - V_i \right) \right|^2 \mathrm{d}x = -\sum_{i=1}^{2} \left[J_i \cdot \nu \left(\log \frac{u_i}{u_0} - V_i \right) \right]_{x=0}^{x=1}, \tag{7.3}$$

where $\nu(0) = -1$ and $\nu(1) = 1$. The most delicate terms are $J_1 \cdot \nu(\log(u_1/u_0) - V_1)|_{x=0}$ and $J_2 \cdot \nu(\log(u_2/u_0) - V_2)|_{x=1}$. To estimate these expressions, we exploit the fact that both terms factorize u_0. For instance,

$$-J_1 \cdot \nu\bigg(\log\frac{u_i}{u_0} - V_i\bigg)\bigg|_{x=0} = \alpha_1 \frac{\Lambda_s}{\Lambda_s^{\max}} u_0(\log u_1 - \log u_0 - V_1)|_{x=0}$$

is bounded from above since $\Lambda_s \geq 0$, $-u_0 \log u_0$ is bounded, and $u_0 \log u_1$ is non-positive due to $0 < u_1 < 1$. Similarly, the other boundary terms are bounded, and we conclude that the right-hand side of (7.3) is bounded from above. An estimation of the entropy production term (the second term on the left-hand side of (7.3)) shows that (see, e.g., the proof of Lemma 6 in [38])

$$\begin{aligned}\int_{\mathcal{D}} \sum_{i=1}^2 D_i u_0 u_i \bigg|\nabla\bigg(\log\frac{u_i}{u_0} - V_i\bigg)\bigg|^2 \mathrm{d}x \\ \geq c\int_{\mathcal{D}}\bigg(\sum_{i=1}^2 u_0|\nabla\sqrt{u_i}|^2 + |\nabla\sqrt{u_0}|^2\bigg)\mathrm{d}x - C\int_{\mathcal{D}}\sum_{i=1}^2|\nabla V_i|^2\mathrm{d}x.\end{aligned} \tag{7.4}$$

Together with the $L^\infty(\mathcal{D})$ bounds for u_i, this provides $H^1(\mathcal{D})$ bounds for u_0 and u_0u_i for $i = 1, 2$, which are needed to apply the "degenerate" Aubin–Lions lemma [58]. Moreover, the bounds show that we can define the traces of u_0u_i and u_0, which is needed to give a meaning to the boundary conditions (5.13)–(5.16). At this point, we need the factor u_0u_i in (5.14) and (5.15). Indeed, without the factor u_0, we are not able to define u_1 and u_2 at $x = 0, 1$. This is the mathematical reason to introduce this factor.

We note that our method also works for more than two species and in several space dimensions. Thanks to the $L^\infty(\mathcal{D})$ bounds, no restriction on the space dimension due to Sobolev embeddings is needed. For more than two species, one may apply the techniques elaborated in [38].

For our main result, we impose the following assumptions:

(C1) Domain: $\mathcal{D} = (0, 1)$, $T > 0$, $\mathcal{D}_T := \mathcal{D} \times (0, T)$.

(C2) Parameter: α_i, β_i, $D_i > 0$, $V_i \in H^1(\mathcal{D})$ for $i = 1, 2$ and $\Lambda_n^{\max}$, $\Lambda_s^{\max} > 0$.

(C3) Initial data: $u_1^0, u_2^0 \in L^1(\mathcal{D})$ satisfies $(u_1^0, u_2^0)(x) \in \mathcal{D}$ for a.e. $x \in \mathcal{D}$ (see Definition 7.2 of $\mathcal{D}$) and $\Lambda_n^0/\Lambda_n^{\max}$, $\Lambda_s^0/\Lambda_s^{\max} \in [0, 1]$.

Theorem 27 (Global existence)**.** *Let Assumptions (C1)–(C3) hold. Then there exists a weak solution* $(u_1, u_2, \Lambda_n, \Lambda_s)$ *to* (5.9)–(5.18) *satisfying* $u_1, u_2 \geq 0$ *and* $u_1 + u_2 \leq 1$ *in* $\mathcal{D}_T$,

$$\sqrt{u_0}u_i,\ \sqrt{u_0} \in L^2(0, T; H^1(\mathcal{D})), \quad \partial_t u_i \in L^2(0, T; H^1(\mathcal{D})'), \quad i = 1, 2,$$

the weak formulation

$$\int_0^T \langle\partial_t u_i, \phi_i\rangle \mathrm{d}t - \int_0^T\int_{\mathcal{D}} J_i\partial_x\phi_i \mathrm{d}x\mathrm{d}t + \int_0^T \left[J_i(x,t)\phi_i(x,t)\right]_{x=0}^{x=1}\mathrm{d}t = 0$$

where $\langle\cdot,\cdot\rangle$ is the dual product between $H^1(\mathcal{D})'$ and $H^1(\mathcal{D})$, the fluxes are defined as

$$J_i = \sqrt{u_0}\partial_x(\sqrt{u_0}u_i) - 3\sqrt{u_0}u_i\partial_x\sqrt{u_0} - u_0u_i\partial_x V_i \in L^2(\mathcal{D}_T), \quad i=1,2,$$

the initial conditions (5.11) *are satisfied in the sense of $H^1(\mathcal{D})'$, and equations* (5.17)–(5.18) *are fulfilled in the sense of $L^2(\partial\mathcal{D})$.*

As mentioned above, the regularity of u_0 and u_i for $i=1,2$ allows us to define the trace of u_0 and u_0u_i such that the boundary conditions and the differential equations for Λ_n and Λ_s are well defined. The proof of Theorem 27 is based on the entropy identity (7.3), a regularization of equations (5.9)–(5.10), the Leray–Schauder fixed-point theorem, and a compactness argument using uniform gradient estimates coming from (7.4).

7.2. Proof of Theorem 27

After proving some auxiliary lemmas, we regularize system (5.9)–(5.10) in time and space and prove the existence of a solution to this approximate problem by using the Leray–Schauder fixed-point theorem. The compactness of the fixed-point operator follows from the discrete entropy inequality analogous to (7.3). This inequality also provides a priori estimates uniform in the approximation parameters. The relative compactness of the sequence of approximate solutions then follows from a "degenerate" Aubin–Lions-type result. Finally, we verify that the limit function is a solution to (5.10)–(5.16). To simplify the notation, we set $\Lambda_n^{\max}=1$ and $\Lambda_s^{\max}=1$ in the analysis.

7.2.1. Auxiliary lemmas

The following lemma follows from a straightforward computation (also see [59, (4.61)]).

Lemma 28. *Let $h(u)$ be given by* (7.1) *and let $A=(A_{ij}(u))\in\mathbb{R}^{2\times 2}$ be defined by* (5.12)*. Then, for any $u\in\mathcal{D}$ and $z\in\mathbb{R}^2$,*

$$\begin{aligned} z\cdot h''(u)A(u)z &= \min\{D_1,D_2\}u_0\left(\frac{z_1^2}{u_1}+\frac{z_2^2}{u_2}\right)+\min\{D_1,D_2\}\left(\frac{1}{u_0}+1\right)(z_1+z_2)^2 \\ &\quad + |D_2-D_1|\frac{u_2}{u_0}\left|z_1-\frac{1-u_2}{u_2}z_2\right|^2. \end{aligned}$$

Let $w=h'(u)$, i.e. $w_i=\partial h/\partial u_i=\log(u_i/u_0)$ for $i=1,2$, and recall that $B=A(u)h''(u)^{-1}$. Then, by Lemma 28, for some $c>0$,

$$\partial_x w\cdot B\partial_x w = (\partial_x u)\cdot h''(u)A(u)(\partial_x u) \ge c\sum_{i=1}^2 u_0(\partial_x\sqrt{u_i})^2 + c(\partial_x\sqrt{u_0})^2,$$

which provides gradient bounds; also see (7.12) below.

Lemma 29. *Let $f_i,g_i\in L^2(0,T)$ be such that $f_i,g_i\ge 0$ for $i=1,2$. Then there exists a unique solution to*

$$\partial_t\Lambda_n = \beta_1(1-\Lambda_n)f_1(t) - \alpha_2\Lambda_n g_1(t), \tag{7.5}$$

$$\partial_t \Lambda_s = \beta_2(1-\Lambda_s)f_2(t) - \alpha_1\Lambda_s g_2(t), \quad t>0, \tag{7.6}$$

with the initial conditions $\Lambda_n(0) = \Lambda_n^0 \in [0,1]$ *and* $\Lambda_s(0) = \Lambda_s^0 \in [0,1]$ *satisfying* $0 \le \Lambda_n(t), \Lambda_s(t) \le 1$ *for* $t \ge 0$.

Proof. The existence of a unique absolutely continuous solution to the differential system (7.5)–(7.6) follows from a standard application of Banach's fixed-point theorem. We sketch the argument for the convenience of the reader.

Let $T' < T$ and

$$\Gamma[\widetilde{\Lambda}](t) := \Lambda_n^0 + \int_0^t \big[\beta_1(1-\widetilde{\Lambda}(s))f_1(s) - \alpha_2\widetilde{\Lambda}(s)g_1(s)\big]\mathrm{d}s, \quad t\in[0,T'].$$

Exploiting the linearity with respect to $\widetilde{\Lambda}$, standard estimates show the Lipschitz continuity of $\Gamma : C^0([0,T']) \to C^0([0,T'])$:

$$\|\Gamma[\widetilde{\Lambda}_1] - \Gamma[\widetilde{\Lambda}_2]\|_{L^\infty(0,T')} \le (\alpha_2\|g_1\|_{L^1(0,T')} + \beta_1\|f_1\|_{L^1(0,T')})\|\widetilde{\Lambda}_1 - \widetilde{\Lambda}_2\|_{L^\infty(0,T')}.$$

Due to

$$\|f_1\|_{L^1(0,T')} + \|g_1\|_{L^1(0,T')} \le \sqrt{T'}(\|f_1\|_{L^2(0,T)} + \|g_1\|_{L^2(0,T)}) \to 0$$

as $T' \to 0$, there exists some $T_0 < T$ such that

$$\alpha_2\|g_1\|_{L^1(0,T_0)} + \beta_1\|f_1\|_{L^1(0,T_0)} < \sqrt{T_0}(\alpha_2\|g_1\|_{L^2(0,T)} + \beta_1\|f_1\|_{L^2(0,T)}) < 1, \tag{7.7}$$

i.e., Γ is a contraction on $C^0([0,T_0])$. Banach's fixed-point theorem yields a unique solution to (7.5) on $[0,T_0]$. In view of (7.7), this procedure can be repeated on intervals $[a,b]$, satisfying $0 \le a < b \le T$ and $b-a < T_0$. Hence, the solution can be progressively extended to the whole interval $[0,T]$. Similarly, one proceeds for (7.6).

Multiplying (7.5) by $\Lambda_n^- := \max\{0,\Lambda_n\}$ yields

$$\frac{1}{2}\frac{d}{dt}(\Lambda_n^-)^2 = \beta_1 f_1(t)(1-\Lambda_n)\Lambda_n^- - \alpha_2 g_1(t)(\Lambda_n^-)^2 \le 0,$$

using $f_1 \ge 0$ and $g_1 \ge 0$. We conclude from $\Lambda_n^-(0) = 0$ that $\Lambda_n(t) \ge 0$ for $t \ge 0$. In a similar way, we infer after multiplication of (7.6) by $(\Lambda_n - 1)^+ := \max\{0, \Lambda_n - 1\}$ that

$$\frac{1}{2}\frac{d}{dt}[(\Lambda_n-1)^+]^2 = -\beta_1 f_1(t)(\Lambda_n-1)(\Lambda_n-1)^+ - \alpha_2 g_1(t)\Lambda_n(\Lambda_n-1)^+ \le 0,$$

which implies that $\Lambda_n(t) \le 1$ since $\Lambda_n(0) \le 1$. The proof of $0 \le \Lambda_s \le 1$ is similar. $\square$

7.2.2. Solution of an approximate system

The approximate system is defined by an implicit Euler discretization and a regularization in the entropy variable. Let $T > 0$, $N \in \mathbb{N}$, $\tau = T/N$, $t_k = k\tau$ for $k = 0,\ldots,N$, and $\varepsilon > 0$. Let $k \ge 1$ and $u^{k-1} \in L^\infty(\mathcal{D};\mathbb{R}^2)$ be given. We wish to find a solution $w^k = (w_1^k, w_2^k) \in H^1(\mathcal{D};\mathbb{R}^2)$ to

$$\frac{1}{\tau}\int_{\mathcal{D}}(u(w^k) - u^{k-1})\cdot\phi\mathrm{d}x + \int_{\mathcal{D}}\partial_x\phi\cdot B(w^k)\partial_x w^k\mathrm{d}x - \int_{\mathcal{D}}\sum_{i=1}^2 u_0(w^k)u_i(w^k)\partial_x V_i\partial_x\phi_i\mathrm{d}x$$

$$+ \sum_{i=1}^{2} \big(J_i^1[u(w^k)](t_k)\phi_i(1) - J_i^0[u(w^k)](t_k)\phi_i(0) \big) + \varepsilon \int_{\mathcal{D}} (\partial_x w^k \cdot \partial_x \phi + w^k \cdot \phi) \mathrm{d}x = 0 \tag{7.8}$$

for all $\phi \in H^1(\mathcal{D};\mathbb{R}^2)$. The function $u_i(w^k)$ equals $u_i(w^k) = \exp B_i^k/(1+\exp w_1^k + \exp w_2^k)$, and the entries of the matrix $B(w^k)$ are $B_{ij}(w^k) = D_i u_0(w^k) u_i(w^k)\delta_{ij}$ for $i,j = 1,2$. We set $u^k := u(w^k)$ to simplify the notation.

The pool concentrations Λ_n^k and Λ_s^k at iteration step k are defined by $\Lambda_j^k = \Lambda_j(t)$ for $(k-1)\tau < t \leq k\tau$, where Λ_j for $j = n,s$ are the solutions of the following fixed-point problem

$$\begin{aligned} \Lambda_n(t) = \Lambda_n^0 + \sum_{j=0}^{k-2} \bigg(\beta_1 \int_{j\tau}^{(j+1)\tau} (1-\Lambda_n(r)) u_0^j(1,r) u_1^j(1,r) \mathrm{d}r - \alpha_2 \int_{j\tau}^{(1+j)\tau} \Lambda_n(r) u_0^j(1,r) \mathrm{d}r \bigg) \\ + \beta_1 \int_{(k-1)\tau}^{t} (1-\Lambda_n(r)) u_0^{k-1}(1,r) u_1^{k-1}(1,r) \mathrm{d}r - \alpha_2 \int_{(k-1)\tau}^{t} \Lambda_n(r) u_0^{k-1}(1,r) \mathrm{d}r, \end{aligned} \tag{7.9}$$

$$\begin{aligned} \Lambda_s(s) = \Lambda_s^0 + \sum_{j=0}^{k-2} \bigg(\beta_2 \int_{j\tau}^{(j+1)\tau} (1-\Lambda_s(r)) u_0^j(0,r) u_2^j(0,r) \mathrm{d}r - \alpha_1 \int_{j\tau}^{(1+j)\tau} \Lambda_s(r) u_0^j(0,r) \mathrm{d}r \bigg) \\ + \beta_2 \int_{(k-1)\tau}^{t} (1-\Lambda_n(r)) u_0^{k-1}(0,r) u_2^{k-1}(0,r) \mathrm{d}r - \alpha_2 \int_{(k-1)\tau}^{t} \Lambda_n(r) u_0^{k-1}(0,r) \mathrm{d}r. \end{aligned}$$

These equations can be interpreted as differential equations of the form

$$\begin{aligned} \partial_t \Lambda_n &= \beta_1 (1-\Lambda_n) f_1(t) - \alpha_2 \Lambda_n g_1(t), \\ \partial_t \Lambda_s &= \beta_2 (1-\Lambda_s) f_2(t) - \alpha_1 \Lambda_s g_2(t), \quad t > 0, \end{aligned}$$

with suitable step functions f_i, g_i, $i = 1,2$. It follows from $|u_0^k|, |u_i^k| \leq 1$ that $f_i, g_i \in L^2(0,T)$, and Lemma 29 guarantees a unique solution to (7.9).

The variable $B_i^k = \log(u_i(w^k)/u_0(w^k))$ can be interpreted as the chemical potential, different from the electrochemical potential μ_i used in the introduction, which also includes the electric potential V_i. The following analysis could also be carried out using μ_i instead of w_i.

Lemma 30. *There exists a solution $w^k \in H^1(\mathcal{D})$ to (7.8) satisfying the discrete entropy inequality*

$$H(u^k) - H(u^{k-1}) + \frac{c\tau}{2} \int_{\mathcal{D}} \partial_x w^k \cdot B(w^k) \nabla_x w^k \mathrm{d}x + \varepsilon\tau \int_{\mathcal{D}} (|\partial_x w^k|^2 + |w^k|^2) \mathrm{d}x \leq C\tau, \tag{7.10}$$

where $c = \min\{D_1, D_2\}$ and $C > 0$ only depends on α_i, η_i, D_i, and the $L^2(\mathcal{D})$ norm of $|\partial_x V_i|^2$ for $i = 1,2$.

Proof. The proof is similar to that one of Lemma 5 in [38], and we highlight the differences only. By the Lax–Milgram lemma, for any given $y \in H^1(\mathcal{D};\mathbb{R}^2)$ and $\sigma \in [0,1]$, there exists a unique solution to the linear problem $a(v,\phi) = \sigma F(\phi)$ for all $\phi \in H^1(\mathcal{D};\mathbb{R}^2)$, where

$$\begin{aligned} a(v,\phi) &= \int_{\mathcal{D}} \partial_x \phi \cdot B(y)\partial_x v \mathrm{d}x + \varepsilon \int_{\mathcal{D}} (\partial_x w \cdot \partial_x \phi + w \cdot \phi)\mathrm{d}x, \\ F(\phi) &= -\frac{1}{\tau}\int_{\mathcal{D}} (u(y) - u^{k-1}) \cdot \phi \mathrm{d}x + \int_{\mathcal{D}} \sum_{i=1}^{2} u_0(y)u_i(y)\partial_x V_i \partial_x \phi_i \mathrm{d}x \\ &\quad - \sum_{i=1}^{2} \big(J_i^1[u(y)](t_k)\phi_i(1) - J_i^0[u(y)](t_k)\phi_i(0) \big) \quad \text{for } v,\phi \in H^1(\mathcal{D};\mathbb{R}^2). \end{aligned}$$

This defines the fixed-point operator $S : C^0([0,T];\mathbb{R}^2) \times [0,1] \to C^0([0,T];\mathbb{R}^2)$, $S(y,\sigma) = v$, where v lies in fact in the space $H^1(\mathcal{D};\mathbb{R}^2)$. Compared to [58], we work with the space $C^0([0,T];\mathbb{R}^2)$ instead of $L^\infty(\mathcal{D};\mathbb{R}^2)$ to ensure that the evaluation on the boundary points is well defined. By standard arguments (see, e.g., [58, Lemma 5]), $S(y,0) = 0$, S is continuous and compact, since the embedding $H^1(\mathcal{D}) \hookrightarrow C^0([0,T])$ is compact. It remains to prove a uniform bound for all fixed points of $S(\cdot,\sigma)$.

We choose $\phi = v$ in $a(v,\phi) = \sigma F(\phi)$ to find that

$$\begin{aligned} &\frac{\sigma}{\tau}\int_{\mathcal{D}} (u(v) - u^{k-1}) \cdot v \mathrm{d}x + \int_{\mathcal{D}} \partial_x v \cdot B(v)\partial_x v \mathrm{d}x + \varepsilon \int_{\mathcal{D}} (|\partial_x v|^2 + |v|^2)\mathrm{d}x \\ &= \sigma \int_{\mathcal{D}} \sum_{i=1}^{2} u_0(v)u_i(v)\partial_x V_i \partial_x v_i \mathrm{d}x - \sigma \sum_{i=1}^{2} \big(J_i^1[u(v)](t_k)v_i(1) - J_i^0[u(v)](t_k)v_i(0) \big) \\ &=: I_1 + I_2. \end{aligned} \tag{7.11}$$

The convexity of the entropy density h implies that

$$(u(v) - u^{k-1}) \cdot v = (u(v) - u^{k-1}) \cdot h'(u(v)) \geq h(u(v)) - h(u^{k-1}).$$

We conclude from Lemma 28 that

$$\begin{aligned} \partial_x v \cdot B(v)\partial_x v &= \partial_x u(v) \cdot h''(u(v))A(u(v))\partial_x u(v) \\ &\geq c\bigg(\sum_{i=1}^{2} u_0(v)\frac{|\partial_x u_i(v)|^2}{u_i(v)} + \frac{|\partial_x u_0(v)|^2}{u_0(v)} \bigg), \end{aligned} \tag{7.12}$$

where $c = \min\{D_1, D_2\} > 0$. For the first term on the right-hand side of (7.11), we observe that the derivative of $v_i = \log(u_i/u_0)$ equals $\partial_x v_i = \partial_x u_i(v)/u_i(v) - \partial_x u_0(v)/u_0(v)$. Therefore, for any $\delta > 0$,

$$\begin{aligned} I_1 &\leq \int_{\mathcal{D}} \sum_{i=1}^{2} \big(u_0(v)|\partial_x u_i(v)| + u_i(v)|\partial_x u_0(v)| \big) |\partial_x V_i| \mathrm{d}x \\ &\leq \delta \int_{\mathcal{D}} \sum_{i=1}^{2} \big(u_0(v)^2|\partial_x u_i(v)|^2 + u_i(v)^2|\partial_x u_0(v)|^2 \big)\mathrm{d}x + C(\delta) \int_{\mathcal{D}} \sum_{i=1}^{2} |\partial_x V_i|^2 \mathrm{d}x \end{aligned}$$

$$\leq \delta \int_{\mathcal{D}} \bigg(\sum_{i=1}^{2} u_0(v) \frac{|\partial_x u_i(v)|^2}{u_i(v)} + \frac{|\partial_x u_0(v)|^2}{u_0(v)} \bigg) \mathrm{d}x + C(\delta),$$

where we used $u_i(v) \leq 1$, $u_0(v) \leq 1$, and the assumption $V_i \in H^1(\mathcal{D})$ in the last step. Choosing $\delta = c/2$, the first term on the right-hand side can be absorbed by the second term on the left-hand side of (7.11), thanks to (7.12). Finally, using definitions (5.13)–(5.16) and $v_i = \log(u_i(v)/u_0(v))$,

$$\begin{aligned} I_2 = &-\sigma\beta_1(1-\Lambda_n)u_0(v(1))u_1(v(1)) \log \frac{u_1(v(1))}{u_0(v(1))} + \sigma\alpha_1\Lambda_s u_0(v(0)) \log \frac{u_1(v(0))}{u_0(v(0))} \\ &+ \sigma\alpha_2\Lambda_n u_0(v(1)) \log \frac{u_2(v(1))}{u_0(v(1))} - \sigma\beta_2(1-\Lambda_s)u_0(v(0))u_2(v(0)) \log \frac{u_2(v(0))}{u_0(v(0))}. \end{aligned}$$

Since $z \mapsto z \log z$ is bounded for $z \in [0,1]$ and $\Lambda_n \leq 1$, $\Lambda_s \leq 1$ by Lemma 29, the first and fourth terms on the right-hand side are bounded from above. Furthermore, we deduce from the fact that $\log u_i(v(x))$ is non-positive for $i = 1,2$ and $x = 0,1$ that the second and third terms are non-positive. This shows that $I_2 \leq C$ for some constant $C > 0$ which depends only on α_i and β_i.

Summarizing, (7.11) becomes

$$H(u(v)) - H(u^{k-1}) + \frac{\tau}{2} \int_{\mathcal{D}} \partial_x v \cdot B(v) \partial_x v \mathrm{d}x + \varepsilon \int_{\mathcal{D}} (|\partial_x v|^2 + |v|^2) \mathrm{d}x \leq C\tau,$$

and $C > 0$ only depends on α_i, β_i, D_i, and the $L^2(\mathcal{D})$ norm of $|\partial_x V_i|^2$ for $i = 1,2$. In view of the positive semidefiniteness of $B(v)$, this inequality provides a uniform bound for v in $H^1(\mathcal{D};\mathbb{R}^2)$ (also being uniform in $\sigma \in [0,1]$, but not uniform in ε). Hence, we can apply the fixed-point theorem of Leray and Schauder to conclude the existence of a fixed point of $S(\cdot,1)$, which is a solution to (7.8). Defining $w^k := v$, this fixed point satisfies (7.10). □

Summing the discrete entropy inequality (7.10) over k leads to the following result.

Lemma 31. *There exists $C > 0$ independent of (ε, τ) (but depending on T) such that*

$$\begin{aligned} H(u^j) + c \sum_{k=1}^{j} \tau \int_{\mathcal{D}} \bigg(\sum_{i=1}^{2} u_0^k |\partial_x (u_i^k)^{1/2}|^2 + |\partial_x u_0^k|^2 + |\partial_x (u_0^k)^{1/2}|^2 \bigg) \mathrm{d}x \\ + \varepsilon C \sum_{k=1}^{j} \tau \sum_{i=1}^{2} \|B_i^k\|_{H^1(\mathcal{D})}^2 \leq H(u^0) + C. \end{aligned} \tag{7.13}$$

Proof. We infer from (7.10) and Lemma 28 that

$$\begin{aligned} H(u^k) - H(u^{k-1}) + c\tau \int_{\mathcal{D}} \bigg(\sum_{i=1}^{2} u_0^k |\partial_x (u_i^k)^{1/2}|^2 + |\partial_x u_0^k|^2 + |\partial_x (u_0^k)^{1/2}|^2 \bigg) \mathrm{d}x \\ + \varepsilon\tau \sum_{i=1}^{2} \|B_i^k\|_{H^1(\mathcal{D})}^2 \leq C\tau, \end{aligned}$$

where $c > 0$ depends only on D_1, D_2 and $C > 0$ is independent of ε, τ and k. We sum this inequality over $k = 1, \ldots, j$ and observe that $\tau j \leq T$ to conclude the proof. □

7.2.3. Uniform estimates

We introduce the piecewise constant in time functions $u_i^{(\tau)}(x,t) = u_i^k$ and $w_i^{(\tau)} = B_i^k$ for $x \in \mathcal{D}$, $t \in ((k-1)\tau, k\tau]$, $i = 1, 2,$. We set $u^{(\tau)}(\cdot, 0) = u^0$ and $w^{(\tau)}(\cdot, 0) = h'(u^0)$ at time $t = 0$. Furthermore, we introduce the shift operator $(\sigma_\tau u^{(\tau)})(\cdot, t) = u^{k-1}$ for $t \in ((k-1)\tau, k\tau]$. Summing (7.8) over $k = 1, \ldots, N$ and using the definitions of $B(w^{(\tau)})$ and $w^{(\tau)}$, we infer that the pair $(u^{(\tau)}, w^{(\tau)})$ solves

$$\begin{aligned}\frac{1}{\tau}\int_0^T\int_{\mathcal{D}}(u_i^{(\tau)} - \sigma_\tau u_i^{(\tau)})\phi_i \mathrm{d}x\mathrm{d}t + \varepsilon\int_0^T\int_{\mathcal{D}}(\partial_x w_i^{(\tau)}\partial_x\phi_i + w_i^{(\tau)}\phi_i)\mathrm{d}x\mathrm{d}t \\ + D_i\int_0^T\int_{\mathcal{D}}(u_0^{(\tau)}\partial_x u_i^{(\tau)} - u_i^{(\tau)}\partial_x u_0^{(\tau)} - u_0^{(\tau)}u_i^{(\tau)}\partial_x V_i)\partial_x\phi_i \mathrm{d}x\mathrm{d}t \\ + \int_0^T \big(J_i^1[u^{(\tau)}](t)\phi_i(1,t) - J_i^0[u^{(\tau)}](t)\phi_i(0,t)\big)\mathrm{d}t = 0,\end{aligned} \tag{7.14}$$

where $\phi_i : (0,T) \to H^1(\mathcal{D})$ is piecewise constant, $i = 1, 2$, and $J_i^j[u^{(\tau)}](t)$ is evaluated at the time points $\lceil t/\tau \rceil \tau$, which means, for instance,

$$J_1^0[u^{(\tau)}](t) = \alpha_1 \Lambda_s(k\tau) u_0^{(\tau)}(1,t) \quad \text{for } t \in ((k-1)\tau, k\tau].$$

The discrete entropy inequality gives the following uniform bounds.

Lemma 32 (Gradient bounds)**.** *There exists $C > 0$ independent of (ε, τ) such that*

$$\sum_{i=1}^2 \|(u_0^{(\tau)})^{1/2} u_i^{(\tau)}\|_{L^2(0,T;H^1(\mathcal{D}))} + \|(u_0^{(\tau)})^{1/2}\|_{L^2(0,T;H^1(\mathcal{D}))} \le C,$$
$$\sum_{i=1}^2 \|u_0^{(\tau)} u_i^{(\tau)}\|_{L^2(0,T;H^1(\mathcal{D}))} + \|u_0^{(\tau)}\|_{L^2(0,T;H^1(\mathcal{D}))} \le C.$$

Proof. The first estimate follows from the bound $0 \le u_i^{(\tau)} \le 1$ and (7.10) since

$$\big|\partial_x\big((u_0^{(\tau)})^{1/2} u_i^{(\tau)}\big)\big| \le \big|(u_0^{(\tau)})^{1/2}\partial_x u_i^{(\tau)}\big| + \big|u_i^{(\tau)}\big|\big|\partial_x (u_0^{(\tau)})^{1/2}\big|.$$

We deduce from the first estimate and

$$\begin{aligned}|\partial_x(u_0^{(\tau)} u_i^{(\tau)})| &\le \big|(u_0^{(\tau)})^{1/2}\partial_x((u_0^{(\tau)})^{1/2} u_i^{(\tau)})\big| + \big|(u_0^{(\tau)})^{1/2} u_i^{(\tau)}\partial_x (u_0^{(\tau)})^{1/2}\big| \\ &\le \big|\partial_x((u_0^{(\tau)})^{1/2} u_i^{(\tau)}\big| + \big|\partial_x (u_0^{(\tau)})^{1/2}\big|,\end{aligned}$$

the second estimate. □

Lemma 33 (Discrete time bounds)**.** *There exists $C > 0$ independent of (ε, τ) such that*

$$\|u_i^{(\tau)} - \sigma_\tau u_i^{(\tau)}\|_{L^2(0,T;H^1(\mathcal{D})')} \le C\tau, \quad i = 1, 2.$$

Proof. Let $\phi_i : (0,T) \to H^1(\mathcal{D})$ be piecewise constant. Then, by (7.14) and the $L^\infty(\mathcal{D}_T)$ bound of $u_i^{(\tau)}$,

$$\begin{aligned} &\frac{1}{\tau}\Big|\int_0^T\int_{\mathcal{D}}(u_i^{(\tau)}-\sigma_\tau u_i^{(\tau)})\phi_i \mathrm{d}x\mathrm{d}t\Big| \qquad (7.15)\\ &\le D_i\big(\|(u_0^{(\tau)})^{1/2}\partial_x u_i^{(\tau)}\|_{L^2(\mathcal{D}_T)}+\|\partial_x u_0^{(\tau)}\|_{L^2(\mathcal{D}_T)}+\|\partial_x V_i\|_{L^2(\mathcal{D}_T)}\big)\|\partial_x\phi_i\|_{L^2(\mathcal{D}_T)}\\ &\quad+\sum_{j=0}^{1}\|J_i^j[u^{(\tau)}]\|_{L^2(0,T)}\|\phi_i\|_{L^2(0,T;H^1(\mathcal{D}))}+\varepsilon\|w_i^{(\tau)}\|_{L^2(0,T;H^1(\mathcal{D}))}\|\phi_i\|_{L^2(0,T;H^1(\mathcal{D}))}\\ &\le C\|\phi_i\|_{L^2(0,T;H^1(\mathcal{D}))}. \end{aligned}$$

The last step follows from the boundedness of $J_i^j[u^{(\tau)}]$, since $0 \le u_i^{(\tau)}(x,t) \le 1$ for $x \in [0,1]$ and $0 \le \Lambda_{n/s}(t) \le 1$. Inequality (7.15) holds for all piecewise constant functions $\phi_i : (0,T) \to H^1(\mathcal{D})$. By a density argument, we obtain

$$\tau^{-1}\|u_i^{(\tau)}-\sigma_\tau u_i^{(\tau)}\|_{L^2(0,T;H^1(\mathcal{D})')} \le C,$$

concluding the proof. □

7.2.4. Limit $(\varepsilon,\tau)\to 0$

Lemmas 32 and 33 allow us to apply the Aubin–Lions lemma in the version of [30], giving the existence of a subsequence, which is not relabelled, such that as $(\varepsilon,\tau)\to 0$,

$$u_0^{(\tau)} \to u_0 \quad \text{in } L^2(\mathcal{D}_T),$$

and because of the uniform $L^\infty(\mathcal{D}_T)$ bound, this convergence holds in any $L^p(\mathcal{D}_T)$ for $p<\infty$. Moreover, we conclude the following weak convergences (up to subsequences):

$$\begin{aligned} u_i^{(\tau)} &\rightharpoonup u_i && \text{weakly* in } L^\infty(\mathcal{D}_T),\\ \tau^{-1}(u_i^{(\tau)}-\sigma_\tau u_i^{(\tau)}) &\rightharpoonup \partial_t u_i && \text{weakly in } L^2(0,T;H^1(\mathcal{D})),\\ \varepsilon w_i^{(\tau)} &\to 0 && \text{strongly in } L^2(0,T;H^1(\mathcal{D})). \end{aligned}$$

Since both $(u_i^{(\tau)})$ and $(\partial_x u_0^{(\tau)})$ are only weakly converging, we cannot obtain the convergence of the product. However, the uniform bounds for $((u_0^{(\tau)})^{1/2}u_i^{(\tau)})$ and $((u_0^{(\tau)})^{1/2})$ in $L^2(0,T;H^1(\mathcal{D}))$ allow us to apply the "degenerate" version of the Aubin–Lions lemma [15, 58] so that (for a subsequence)

$$(u_0^{(\tau)})^{1/2}u_i^{(\tau)} \to \sqrt{u_0}u_i \quad \text{strongly in } L^p(\mathcal{D}_T),\ p<\infty \text{ as } (\varepsilon,\tau)\to 0.$$

This shows that

$$\begin{aligned} u_0^{(\tau)}\partial_x u_i^{(\tau)}-u_i^{(\tau)}\partial_x u_0^{(\tau)} &= (u_0^{(\tau)})^{1/2}\partial_x\big((u_0^{(\tau)})^{1/2}u_i^{(\tau)}\big)-3(u_0^{(\tau)})^{1/2}u_i^{(\tau)}\partial_x(u_0^{(\tau)})^{1/2}\\ &\rightharpoonup \sqrt{u_0}\partial_x(\sqrt{u_0}u_i)-3\sqrt{u_0}u_i\partial_x\sqrt{u_0} \end{aligned}$$

weakly in $L^1(\mathcal{D}_T)$, and since this sequence is bounded in $L^2(\mathcal{D}_T)$, the convergence holds true in that space.

It follows from the linearity and continuity of the trace operator $H^1(\mathcal{D}) \to L^2(\partial\mathcal{D})$ that this operator is weakly continuous and therefore,

$$u_0^{(\tau)}(x,\cdot) \to u_0(x,\cdot), \quad (u_0^{(\tau)}u_i^{(\tau)})(x,\cdot) \rightharpoonup (u_0u_i)(x,\cdot) \quad \text{weakly in } L^2(0,T),\ x=0,1.$$

In fact, these sequences are even bounded in $L^\infty(0,T)$ because of the embedding $H^1(\mathcal{D}) \hookrightarrow C^0(\overline{\mathcal{D}}) \hookrightarrow L^\infty(\partial\mathcal{D})$. Let $\Lambda_j^{(\tau)}$ be the solution to (5.17) if $j=n$ or (5.18) if $j=s$ with u replaced by $u^{(\tau)}$. Then $\Lambda_n^{(\tau)}$ solves the integral equation

$$\Lambda_n^{(\tau)} = \Lambda_n(0) + \beta_1\int_0^t (1-\Lambda_n^{(\tau)}(r))\sigma_\tau(u_0^{(\tau)}u_1^{(\tau)})(1,r)\mathrm{d}r - \alpha_2\int_0^t \Lambda_n^{(\tau)}(r)\sigma_\tau u_0^{(\tau)}(1,r)\mathrm{d}r.$$

Since the integrand is uniformly bounded, this gives $|\Lambda_n^{(\tau)}(t)-\Lambda_n^{(\tau)}(s)| \le C|t-s|$ for $s,t\in[0,T]$. Thus, $(\Lambda_n^{(\tau)})$ is uniformly bounded and uniformly equicontinuous. By the Arzelà–Ascoli theorem, there exists a subsequence (not relabeled) such that $\Lambda_n^{(\tau)} \to \Lambda_n$ uniformly in $[0,T]$. In a similar way, we prove that $\Lambda_s^{(\tau)} \to \Lambda_s$ uniformly in $[0,T]$. We need to identify the limits Λ_n and Λ_s as the solutions to (5.17) and (5.18), respectively.

Set $G^{(\tau)}(t) := \Lambda_n^{(\tau)}(k\tau)$ for $t\in((k-1)\tau,k\tau]$. Then, for instance,

$$J_1^1[u^{(\tau)}](t) = \beta_1(1-G^{(\tau)}(t))u_0^{(\tau)}(1,t)u_1^{(\tau)}(1,t) \quad \text{for } t\in((k-1)\tau,k\tau].$$

It holds for $s\in((m-1)\tau,m\tau]$ and $t\in((k-1)\tau,k\tau]$ that

$$|G^{(\tau)}(t)-G^{(\tau)}(s)| \le C|m\tau-k\tau| \le C(|t-s|+\tau).$$

Therefore, since $G^{(\tau)}(\lceil t/\tau\rceil\tau) = \Lambda_n^{(\tau)}(\lceil t/\tau\rceil\tau)$,

$$\begin{aligned} |G^{(\tau)}(t)-\Lambda_n(t)| &\le |G^{(\tau)}(t)-G^{(\tau)}(\lceil t/\tau\rceil\tau)| + |\Lambda_n^{(\tau)}(\lceil t/\tau\rceil\tau)-\Lambda_n^{(\tau)}(t)| + |\Lambda_n^{(\tau)}(t)-\Lambda_n(t)| \\ &\le C|t-\lceil t/\tau\rceil\tau| + C\tau + \|\Lambda_n^{(\tau)}(t)-\Lambda_n(t)\|_{L^\infty(0,T)} \to 0 \end{aligned}$$

as $(\varepsilon,\tau)\to 0$, and this convergence is uniform in $[0,T]$. Hence, for instance,

$$J_1^1[u^{(\tau)}] \to \beta_1(1-\Lambda_n)u_0(1,\cdot)u_i(1,\cdot) =: J_1^1[u] \quad \text{strongly in } L^2(0,T).$$

To establish that Λ_n satisfies (5.17) it is sufficient to show that $\sigma_\tau(u_0^{(\tau)}u_i^{(\tau)})(x,\cdot) \rightharpoonup (u_0u_1)(x,\cdot)$, $\sigma_\tau u_0^{(\tau)}(x,\cdot) \rightharpoonup u_0(x,\cdot)$ weakly in $L^2(0,T)$ for $x=0,1$. In fact, this result can be proved by straightforward arguments. Then the convergence of $u_i^{(\tau)}(1,\cdot)$ in $L^2(0,T)$ implies that Λ_n solves (5.17). In a similar way, we prove that $\Lambda_s^{(\tau)} \to \Lambda_s$ uniformly in $[0,T]$, and Λ_s solves (5.18).

The initial condition (5.11), understood in the sense of $H^1(\mathcal{D})'$, follows from arguments similar as at the end of the proof of Theorem 2 in [58]. This finishes the proof.

7.3. Stationary states

In this section, we derive some properties of stationary solutions, i.e., solutions $(u_1, u_2, \Lambda_n, \Lambda_s)$ to (5.9)–(5.18), where $\partial_t u_1 = \partial_t u_2 = 0$ and $\partial_t \Lambda_n = \partial_t \Lambda_s = 0$. The former condition implies that the fluxes J_1 and J_2 are constant, and we deduce from the latter condition that the total flux vanishes, $J_1 + J_2 = 0$. Consequently, $J := J_1 = -J_2$. Moreover, if $u_0(1) > 0$ and $u_0(0) > 0$, the stationary solution to (5.17)–(5.18) is given by

$$\Lambda_n = \frac{\beta_1 u_1(1)}{\beta_1 u_1(1) + \alpha_2}, \quad \Lambda_s = \frac{\beta_2 u_2(0)}{\beta_2 u_2(0) + \alpha_1}, \tag{7.16}$$

We assume that a stationary solution exists and that $u_1, u_2 \in W^{1,\infty}(\mathcal{D})$. Then

$$J = -D_1\big(u_0\partial_x u_1 - u_1\partial_x u_0 - u_0 u_1 \partial_x V_1\big) = D_2\big(u_0\partial_x u_2 - u_2\partial_x u_0 - u_0 u_2 \partial_x V_2\big). \tag{7.17}$$

The following situation is approximately satisfied in numerical experiment 1 for large times.

Lemma 34. *Let $u_0(1) > 0$ and $u_0(0) > 0$. Then $\Lambda_n = 0$ if and only $\Lambda_s = 0$, and $u_1(1) = 0$ if and only of $u_2(0) = 0$. In this situation, the flux vanishes, $J = 0$.*

Proof. Let $\Lambda_n = 0$. Then, by (7.16), $u_1(1) = 0$. We insert expressions (7.16) into the boundary conditions (5.13)–(5.14):

$$J = J_1(0) = \frac{\alpha_1\beta_2 u_2(0)}{\beta_2 u_2(0) + \alpha_1} u_0(0) = J_1(1) = \frac{\alpha_2\beta_1 u_1(1)}{\beta_1 u_1(1) + \alpha_2} u_0(1) = 0. \tag{7.18}$$

This shows that $u_2(0) = 0$ and consequently, again by (7.16), $\Lambda_s = 0$. Moreover, we infer from (7.18) that $J = 0$. □

If the parameters are the same for both species, the solution is symmetric around $x = 1/2$, as proved in the following lemma.

Lemma 35. *Let $\alpha_1 = \alpha_2$, $\beta_1 = \beta_2$, $\Lambda_n^{\max} = \Lambda_s^{\max}$, $D_1 = D_2$, and $V_2(x) = V_1(1-x) + const.$ for $x \in \mathcal{D}$. Then $(u_1, u_2, \Lambda_n, \Lambda_s)$ with $u_2(x) = u_1(1-x)$ for $x \in \mathcal{D}$ and $\Lambda_n = \Lambda_s$ is a stationary solution to* (5.9)–(5.16).

Proof. Let u_1 be a solution to (7.17) with $u_0 := 1 - u_1(x) - u_1(1-x)$ and $u_2(x) := u_1(1-x)$ for $x \in \mathcal{D}$. Taking into account that $\partial_x u_2(x) = -\partial_x u_1(1-x)$ and $\partial_x V_2(x) = -\partial_x V_1(1-x)$, we deduce from $u_0(x) = u_0(1-x)$ that

$$\begin{aligned} -J/D_1 &= u_0(x)\partial_x u_1(x) - u_1(x)\partial_x u_0(x) - u_0(x)u_1(x)\partial_x V_1(x) \\ &= -u_0(1-x)\partial_x u_2(1-x) + u_2(1-x)\partial_x u_0(1-x) \\ &\quad + u_0(1-x)u_2(1-x)\partial_x V_2(1-x). \end{aligned}$$

Thus, (u_1, u_2) solves (7.17). We infer from $u_1(1) = u_2(0)$ and (7.16) that $\Lambda_n = \Lambda_s$. Furthermore, since $u_0(0) = u_0(1)$, the boundary conditions (5.13)–(5.16) are satisfied. □

This situation is illustrated in Figure 8.8, section 8.2.

8. Numerical Experiments

In this chapter, we present numerical experiments based on the model (5.4)–(5.7), (5.1) for angiogenesis and the model (5.9)–(5.18) for the transport of vesicles inside neurites.

8.1. Angiogenesis

We illustrate the dynamics of the tip and stalk cells in the two-dimensional ball $\mathcal{D} = B_R(0)$ around the origin with radius $R = 500$ (in units of μm) for one path $t \mapsto X(\omega, t)$. Let $h = 10$ be the space step size and introduce the grid points $x_{ij} = ((k-i)h, (k-j)h) \in \mathbb{R}^2$, where $i, j = 0, \ldots, 2k$ and $k = R/h$. The time step size equals $\tau = 1$ (in units of seconds).

The stochastic differential equations (5.1) are discretised by using the Euler–Maruyama scheme

$$(\widetilde{X}_i^k)^{(n+1)} = (\widetilde{X}_i^k)^{(n)} + g_i[c^n, f^n]\big((\widetilde{X}_i^k)^{(n)}, t\big)\tau + \sigma_i\big((\widetilde{X}_i^k)^{(n)}\big)\sqrt{\tau}\mathcal{N},$$

with initial datum $(\widetilde{X}_i^k)^{(0)} = (X_0)_i^k$, where $\mathcal{N}$ is standard normally distributed and c^n, f^n are approximations of c, f obtained by linear interpolation of the values c_{ij}^n (see below). The non-linearity g_i is chosen as in (5.2) with M, γ, and λ given below in subsection 8.1.1. Furthermore, α_0 and z are taken as in [92, formulas (10) and (14)]. Compared to [8], we neglect the contribution of the Hertz contact mechanics regarding z to guarantee the boundary condition $g_i[c, f](\cdot, t) = 0$ on $\partial\mathcal{D}$. We choose the continuous radially symmetric stochastic diffusion

$$\sigma(x) = \begin{cases} 0 & \text{for } |x| \geq R, \\ (1/R)\sqrt{(R/10)^2 - [R/10 - (R - |x|)^2]} & \text{for } 9R/10 < |x| < R, \\ 1/10 & \text{for } |x| \leq 9R/10. \end{cases}$$

The solutions (5.4) to the ordinary differential equations (5.3) are written iteratively as

$$f_B(x, (n+1)\tau) = f_B(x, n\tau) \exp\bigg(- s_B \int_0^\tau c_M(x, s + n\tau)\mathrm{d}s\bigg), \quad n \in \mathbb{N},$$

and similarly for f_F. The integral is approximated by the trapezoid rule

$$\int_0^\tau c_M(x, s + n\tau)\mathrm{d}s \approx \frac{\tau}{2}(c_{M,ij}^n + c_{M,ij}^{n+1}),$$

where $c_{M,ij}^n$ approximates $c_M(x_{ij}, n\tau)$. We set $f_{ij}^n := (f_B, f_E, f_F)(x_{ij}, n\tau)$.

Finally, we discretise the reaction-diffusion equations (5.5) using the forward Euler method and the central finite-difference scheme

$$\operatorname{div}(D_V(f)\nabla c_V) \approx \frac{1}{h}\big(J_{i+1/2,j} - J_{i-1/2,j} + J_{i,j+1/2} - J_{i,j-1/2}\big),$$

where

$$J_{i+1/2,j} = \frac{1}{2h}(D_V(f^n_{i+1,j}) + D_V(f^n_{ij}))(c^{n+1}_{i+1,j} - c^{n+1}_{ij}),$$
$$J_{i,j+1/2} = \frac{1}{2h}(D_V(f^n_{i,j+1}) + D_V(f^n_{ij}))(c^{n+1}_{i,j+1} - c^{n+1}_{ij}).$$

Notice that we obtain a semi-implicit scheme. The resulting linear system of equations is implemented in the Python-based software environment *SciPy* using sparse matrices and solved by using the `spsolve` function from the `scipy.sparse.linalg` package.

The potentials V^k_j, used in (5.5), are given by

$$V^k_j(x) = \frac{1}{IR^2_m}\exp\left(-\frac{R^2_m}{R^2_m - |x|^2}\right), \quad x \in \mathcal{D},\ j = D, M, U, V,$$

where $R_m = 12.5$, and $I > 0$ is a normalization constant to ensure that $\int_{\mathbb{R}^2} V^k_j(x)\mathrm{d}x = 1$.

It remains to define the initial conditions. The initial positions of the endothelial cells $X^{0,k}_i$ ($i = 1, 2,\ k = 1, \dots, N_i$) are given by

$$X^{0,k}_i = \begin{pmatrix} r\sin\phi \\ r\cos\phi \end{pmatrix},$$

where (r, ϕ) is uniformly drawn from the set $[0.65R, 0.75R] \times [0, \pi/2] = [325, 375] \times [0, \pi/2]$. The initial volume fractions are

$$f^0_F(x) = \begin{cases} 0 & \text{for } |x| \geq R_f, \\ 0.4(1 - \cos(\frac{\pi}{0.3R_f}(R_f - |x|)) & \text{for } 0.7R_f < |x| < R_f, \\ 0.8 & \text{for } |x| \leq 0.7R_f, \end{cases}$$

where $R_f = 0.95R = 475$, as well as $f^0_B = 0.2f^0_F$ and $f^0_E = 1 - f^0_B - f^0_F$. We choose the initial VEGF concentration

$$c^0_V(x) = 0.1\exp\left(-\frac{R_c}{\sqrt{R^2_c - |x|^2}}\right)1_{B_{R_c}}(x),$$

which is concentrated at the origin, and assume that the concentrations of the remaining proteins vanish, $c^0_D = c^0_M = c^0_U = 0$ in $\mathcal{D}$, as they are segregated by the tip cells.

8.1.1. Model parameters and constants

The model parameters and constants are taken from [8]. For the convenience of the reader, we collect here the expressions:

$$\alpha_0 = \frac{b_i R^3_c}{F_i\mu},$$
$$\gamma(x,t) = \frac{0.1 b_i F_i(1 - f_E(x,t))}{\rho_B f_B(x,t) + \rho_F f_F(x,t) + \rho_E f_E(x,t)},$$
$$\lambda(x,t) = \frac{4^3 b_i F_i \widetilde{\lambda}}{30}(1 - f_E(x,t))\left(\frac{1}{2} - f_E(x,t)\right)f_E(x,t),$$

$$
\begin{aligned}
M_i^k(x,t) &= \sum_{j=1}^{2}\sum_{\ell=1}^{N_j} \frac{F_i^2}{20\pi^2 R_c^4}(1-f_E(x,t))\exp\left(\frac{-|X_i^k - X_j^\ell|}{R_c}\right) \\
&\quad - \frac{2\sqrt{2}}{\pi}\left(\frac{\max\{0, R_c - 0.5|X_i^k - X_j^\ell|\}}{R_c}\right)^{5/2}, \\
v_i^k &= \sum_{j=1}^{2}\sum_{\ell=1}^{N_j} \frac{F_i^2}{20\pi^2 R_c^4}(1-f_E(x,t))\exp\left(\frac{-|X_i^k - X_j^\ell|}{R_c}\right), \\
z_i^k &= \frac{v_i^k}{|v_i^k|}.
\end{aligned}
$$

The parameters are chosen as in the following table; see [8, Appendix].

	Value	Unit		Value	Unit		Value	Unit
b_i	0.02	s^{-1}	D_V^E	10	$\mu\mathrm{m}^2\mathrm{s}^{-1}$	r_D	10	$\mu\mathrm{m}^3\mathrm{s}^{-1}$
F_i	1000	nN	D_D^B	0.51	$\mu\mathrm{m}^2\mathrm{s}^{-1}$	r_M	10	$\mu\mathrm{m}^3\mathrm{s}^{-1}$
μ	0.2	–	D_D^F	1.02	$\mu\mathrm{m}^2\mathrm{s}^{-1}$	r_U	10	$\mu\mathrm{m}^3\mathrm{s}^{-1}$
$\widetilde{\lambda}$	15	–	D_D^E	0.051	$\mu\mathrm{m}^2\mathrm{s}^{-1}$	s_V	0.024	$\mu\mathrm{m}^3\mathrm{s}^{-1}$
R_c	11.25	μm	D_M^B	1.23	$\mu\mathrm{m}^2\mathrm{s}^{-1}$	s_D	0.024	$\mu\mathrm{m}^3\mathrm{s}^{-1}$
ρ_B	$1.06 \cdot 10^{-3}$	$\mathrm{ng}\mu\mathrm{m}^{-3}$	D_M^F	2.46	$\mu\mathrm{m}^2\mathrm{s}^{-1}$	s_M	0.024	s^{-1}
ρ_F	$1.06 \cdot 10^{-3}$	$\mathrm{ng}\mu\mathrm{m}^{-3}$	D_M^E	0.123	$\mu\mathrm{m}^2\mathrm{s}^{-1}$	s_U	0.024	s^{-1}
ρ_E	$0.9933 \cdot 10^{-3}$	$\mathrm{ng}\mu\mathrm{m}^{-3}$	D_U^B	0.53	$\mu\mathrm{m}^2\mathrm{s}^{-1}$	s_B	1.21	$\mu\mathrm{m}^3\mathrm{ng}^{-1}\mathrm{s}^{-1}$
D_V^B	100	$\mu\mathrm{m}^2\mathrm{s}^{-1}$	D_U^F	1.06	$\mu\mathrm{m}^2\mathrm{s}^{-1}$	s_F	1.21	$\mu\mathrm{m}^3\mathrm{ng}^{-1}\mathrm{s}^{-1}$
D_V^F	200	$\mu\mathrm{m}^2\mathrm{s}^{-1}$	D_U^E	0.053	$\mu\mathrm{m}^2\mathrm{s}^{-1}$			

8.1.2. Experiment

We choose $N_1 = 2$ tip cells and $N_2 = 200$ stalk cells. Figure 8.1 shows the positions of the tip and stalk cells at different times for one trajectory. The tip cells segregate the DLL4 protein, and the stalk cells detect the local increase of the DLL4 concentration, such that they follow the corresponding tip cell. This effect is slightly more pronounced for the tip cell that starts in an environment with a dense stalk cell population. The position of this tip cell is closer to the origin than the other tip cell with a higher VEGF concentration, leading to a relatively high production of DLL4 proteins. The stalk cells, which do not follow a tip cell, are primarily influenced by the stiffness gradient $\nabla(f_B + f_F)$ and the strain energy density M, which incorporates contact mechanics, resulting to a spreading of these cells.

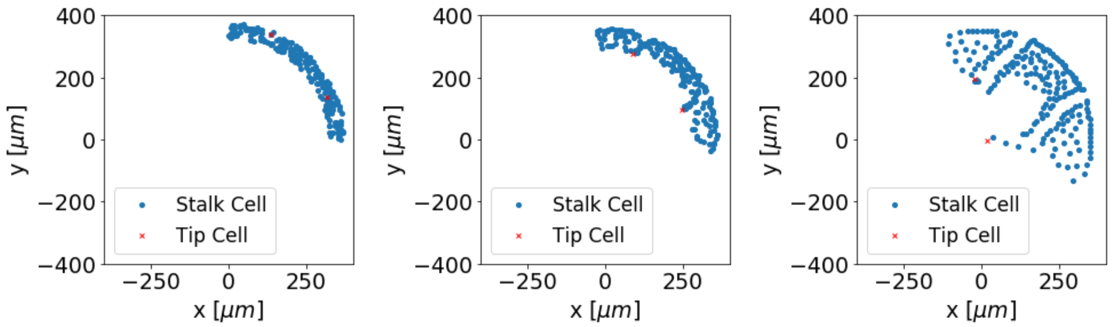

Figure 8.1.: Positions of two tip cells (red crosses) and 200 stalk cells (blue dots) at times $T = 0\,\mathrm{s}$, $T = 400\,\mathrm{s}$, and $T = 1600\,\mathrm{s}$.

The protein concentrations are shown in Figure 8.2 and Figure 8.3. As the diffusion coefficient for VEGF is much larger than the reaction rate s_V, the concentration of the VEGF protein becomes uniform in the large-time limit. The DLL4, MMP, and uPA proteins are produced by the tip cells and hence follow their paths. The corresponding concentrations increase with the availability of VEGF and decrease due to consumption by the stalk cells or by getting exhausted from breaking down the fibrin matrix or the boundary membrane. Since the diffusion is slow, the changes in the concentration are local up to time $T = 1600\,\mathrm{s}$.

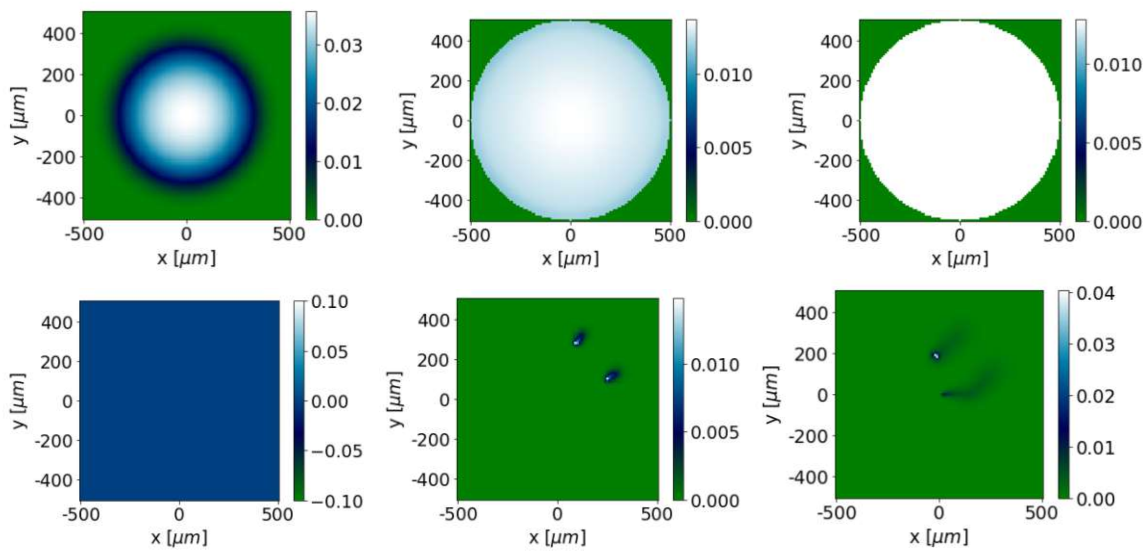

Figure 8.2.: Concentrations of the proteins VEGF (first row), DLL4 (second row) at times $T = 0\,\mathrm{s}$ (left column), $T = 400\,\mathrm{s}$ (middle column), and $T = 1600\,\mathrm{s}$ (right column).

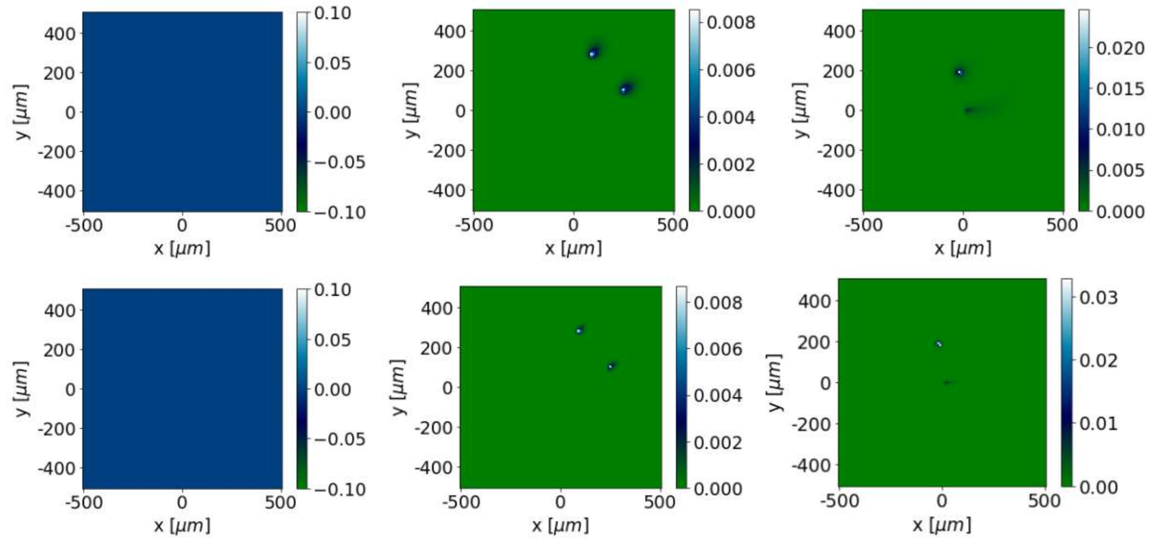

Figure 8.3.: Concentrations of the proteins MMP (first row), and uPA (second row) at times $T = 0\,\mathrm{s}$ (left column), $T = 400\,\mathrm{s}$ (middle column), and $T = 1600\,\mathrm{s}$ (right column).

We present the volume fractions of the basement membrane, fibrin matrix, and extracellular fluid in Figure 8.4 and Figure 8.5. The membrane and fibrin matrix are degraded by the MMP and uPA proteins, thus increasing the volume fraction of the extracellular fluid. As both proteins are produced by the tip cells, the degradation follows their paths.

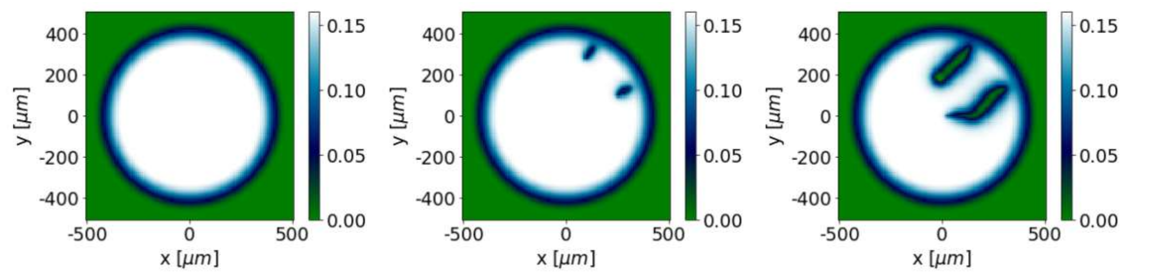

Figure 8.4.: Volume fractions of the basement membrane, at times $T = 0\,\mathrm{s}$ (left column), $T = 400\,\mathrm{s}$ (middle column), and $T = 1600\,\mathrm{s}$ (right column).

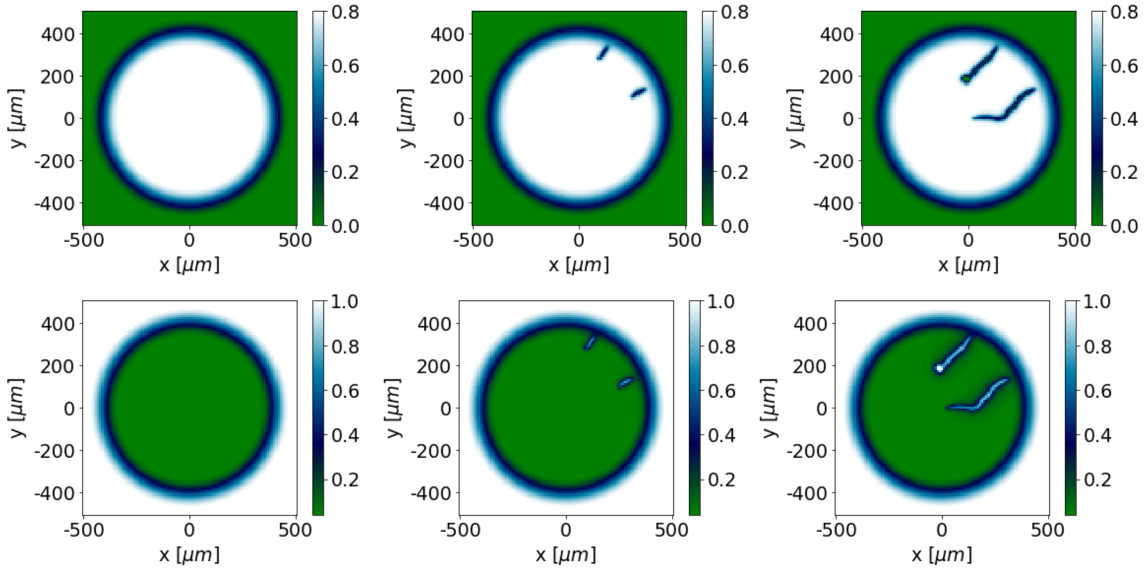

Figure 8.5.: Volume fractions of the fibrin matrix (first row), and extracellular fluid (second row) at times $T = 0\,\mathrm{s}$ (left column), $T = 400\,\mathrm{s}$ (middle column), and $T = 1600\,\mathrm{s}$ (right column).

Summarizing, we see that the model successfully describes the formation of premature sprouts. The experiments from [8] for dermal endothelial cells show that the in vitro angiogenesis sprouting qualitatively well agrees with the numerical tests. Clearly, the proposed system of equations models only a very small number of biological processes, chemical reactions, and signal proteins, and more realistic results can be only expected after taking into account more biological modelling details. Still, the onset of vessel formation is well illustrated by our simple model.

8.2. Vesicle Transport in Neurites

We discretise equations (5.9)–(5.10) by an implicit Euler finite-volume scheme. Let $n, m \in \mathbb{N}$ and set $\tau = T/n$, $h = 1/m$. We divide $\mathcal{D} = (0,1)$ into m cells (x_j, x_{j+1}) for $j = 0, \dots, m-1$, where $x_j = jh$. (Note that the notation is different from section 5.3.2.) We approximate $h^{-1}\int_{x_j}^{x_{j+1}} u_i(x, k\tau)\mathrm{d}x$ by $u_{i,j}^k$, which solves for $k = 1, \dots, n$,

$$\begin{aligned} u_{i,j}^k &= u_{i,j}^{k-1} + \frac{\tau}{h}(J_{i,j+1/2}^k - J_{i,j-1/2}^k), \quad i = 1,2,\ j = 1,\dots,m-1, \\ J_{i,j+1/2}^k &= -\frac{D_i}{h}\big(\bar{u}_{0,j+1/2}^k(u_{i,j+1}^k - u_{i,j}^k) + \bar{u}_{i,j+1/2}(u_{0,j+1}^k - u_{0,j}^k)\big) \\ &\quad - D_i \bar{u}_{0,j+1/2}^k \bar{u}_{i,j+1/2}^k \partial_x V_i(x_{j+1/2}), \end{aligned}$$

where $\bar{u}_{i,j+1/2}^k := (u_{i,j+1}^k + u_{i,j}^k)/2$ for $i = 0,1,2$. At the boundary points $x = 0$ and $x = 1$, we replace $J_{i,1/2}^k$ and $J_{i,m-1/2}^k$ respectively, by the corresponding boundary condition, evaluated at $x_0 = 0$ or $x_m = 1$ and at time $k\tau$. For instance, $J_{1,0}^k = \alpha_1 \Lambda_s(k\tau)u_{0,0}^k$. The differential equations (5.17)–(5.18) are discretised by the implicit Euler scheme, for instance,

$$\Lambda_s^k = \Lambda_s^{k-1} - \tau\alpha_1 \frac{\Lambda_s^k}{\Lambda_s^{\max}} u_{0,0}^k + \tau\beta_2\left(1 - \frac{\Lambda_s^k}{\Lambda_s^{\max}}\right) u_{0,0}^k u_{2,0}^k.$$

The non-linear discrete system is solved by using a damped Newton method. More precisely, let $F : \mathbb{R}^{3m+2} \to \mathbb{R}^{3m+2}$ be given by

$$\begin{aligned} F_{j+m(i-1)}(y) &= u_{i,j}^{k-1} + \frac{\tau}{h}(J_{i,j+1/2}^k - J_{i,j-1/2}^k) - y_{j+m(i-1)}, \quad i = 1, 2, \\ F_{j+2m}(y) &= y_{j+2m} - y_{j+m} - y_j, \\ F_{j+2m+2}(y) &= \Lambda_s^{k-1} - \tau\alpha_1 \frac{y_{3m+2}}{\Lambda_s^{\max}}(1 - y_{2m+1}) \\ &\quad + \tau\beta_2\left(1 - \frac{y_{3m+2}}{\Lambda_s^{\max}}\right)(1 - y_{2m+1})y_{m+1} - y_{3m+2}, \end{aligned}$$

where $y = (y_1, \ldots, y_{3m+2}) \in \mathbb{R}^{3m+2}$ and $F_{3m+1}(y)$ is defined similarly from the implicit Euler scheme for Λ_n^k. The damped Newton method reads as

$$y^{(r+1)} = y^{(r)} + \frac{1}{(r+1)^{3/4}} \frac{\widehat{y}^{(r+1)}}{\|\widehat{y}^{(r+1)}\|_\infty}, \quad r \in \mathbb{N},$$

where $\widehat{y}^{(r+1)}$ solves $F'(y^{(r)})(\widehat{y}^{(r+1)} - y^{(r)}) = -F(y^{(r)})$. The exponent $3/4$ was determined from numerical experiments. We stopped the Newton iterations when $\|F(y^{(r)})\|_\infty < \varepsilon$ with $\varepsilon = 10^{-3}$ is reached. The numerical scheme is implemented in Python version 3.7.1. We collect the values of the parameters, inspired from [48], in Table 8.1. If not otherwise stated, we set $h = 0.0025$ and $\tau = 10^{-4}$.

α_1	0.2666	$\Lambda_n^{\max}$	0.0029	D_1	0.0004
α_2	0.2666	Λ_n^0	0.0015	D_2	0.004
β_1	3	$\Lambda_s^{\max}$	0.175	$V_1(x)$	$1.75x$
β_2	3	Λ_s^0	0.12	$V_2(x)$	$-1.5x$

Table 8.1.: Numerical parameters.

8.2.1. Numerical experiment 1

We choose the initial data $u_1^0 = u_2^0 = 0.1$. Figure 8.6 presents the vesicle concentrations at times $t = 0, 1, 10$ and the evolution of the number $\Lambda_n(t)$ of vesicles in the growth cone. The anterograde vesicles (species 1) are leaving the soma, leading to an increase of the concentration near $x = 0$, while it is decreasing near the tip of the neurite at $x = 1$ because of the small value of Λ_s. The retrograde vesicles (species 2) are leaving the growth cone at $x = 1$, leading to an increase of the concentration, while it is decreasing near the soma. The number Λ_s is decreasing over time, which can be explained by the difference of magnitude of the parameters α_1 and β_2 governing the outflow rate.

The behaviour of the vesicles at $t = 10$ in our model and the model of [48] is similar; see the middle row of Figure 8.6. The difference is largest near the growth cone at $x = 1$ (see the bottom left panel), which comes from the different boundary conditions at this point. Since the boundary value $J_1^1[u]$ contains the factor $u_0 < 1$ in our model, the number Λ_n is decreasing at a faster rate compared to the model of [48] (see the bottom right panel).

8.2.2. Numerical experiment 2

In this example, we choose piecewise constant initial data:

$$u_1^0(x) = \begin{cases} 0.9 & \text{for } 0.1 < x < 0.4, \\ 0 & \text{else,} \end{cases} \qquad u_2^0(x) = \begin{cases} 0.9 & \text{for } 0.6 < x < 0.9, \\ 0 & \text{else,} \end{cases}$$

The numerical results at times $t = 0, 1, 10, 100$ are shown in Figure 8.7. We observe a smoothing effect (due to diffusion) and a drift of the vesicles profiles towards the middle. The drift of the anterograde vesicles is stronger compared to the retrograde vesicles because of $|\partial_x V_1| > |\partial_x V_2|$. Since the boundary values of the vesicles are very small, the results of our model are almost identical to those from the model of [48]; see Figure 8.7 bottom for Λ_n and Λ_s up to $t = 10$.

8.2.3. Numerical experiment 3

We have chosen $\Lambda_n^{\max} = \Lambda_s^{\max} = 0.175$, $\Lambda_n^0 = \Lambda_s^0 = 0.12$, with potentials $V_1(x) = 1.5x$, $V_2(x) = -1.5x$, and initial data $u_1^0 = u_2^0 = 0.1$. The left panel shows the concentrations at $T = 1000$ using the parameters α_i, β_i, and D_i as in Experiment 1. The solution is approximately stationary (the modulus of the flux is less than 0.01). Since $u_2(0) = 0$, Lemma 34 shows that the stationary flux vanishes. In the right panel, we present a case where the stationary flux does not vanish. Here, the solution is computed up to $T = 100$, the parameters are $\alpha_i = \beta_i = D_i = 1$ for $i = 1, 2$, and the flux equals $J = 0.118$.

8.2.4. Convergence rates

We test our numerical scheme by computing the spatial and temporal convergence rates. We choose the initial data $u_1^0 = u_2^0 = 0.1$ and the parameters from Table 8.1. Furthermore, we set $T = 1$. We define the mean error as the discrete L^2 norm $\|u - u^{\mathrm{ref}}\|_2/\sqrt{2(m+1)}$, where $u = (u_1, u_2, \Lambda_n, \Lambda_s)$ and $u^{\mathrm{ref}} = (u_1^{\mathrm{ref}}, u_2^{\mathrm{ref}}, \Lambda_n^{\mathrm{ref}}, \Lambda_s^{\mathrm{ref}})$ is the reference solution.

Figure 8.9 (left) shows the discrete L^2 error for time step sizes $\tau = 10^{-2} \cdot 2^{-k}$ for $k = 1, \ldots, 7$ with fixed $h = 10^{-3}$. The reference solution is computed with $h = 10^{-3}$ and $\tau = 10^{-5}$. The convergence is of first order for rather large values of τ, while it is between first and second order when the time step size is closer to the step size of the reference solution. The spatial convergence is illustrated in Figure 8.9 (right) for grid sizes $h = 10^{-2} \cdot 2^{-k}$ for $k = 1, \ldots, 7$ with fixed $\tau = 10^{-3}$. The reference solution is calculated by using the parameters $h = 10^{-5}$ and $\tau = 10^{-3}$. The convergence is of first order (if τ is not too large), which is expected for the two-point approximation finite-volume scheme.

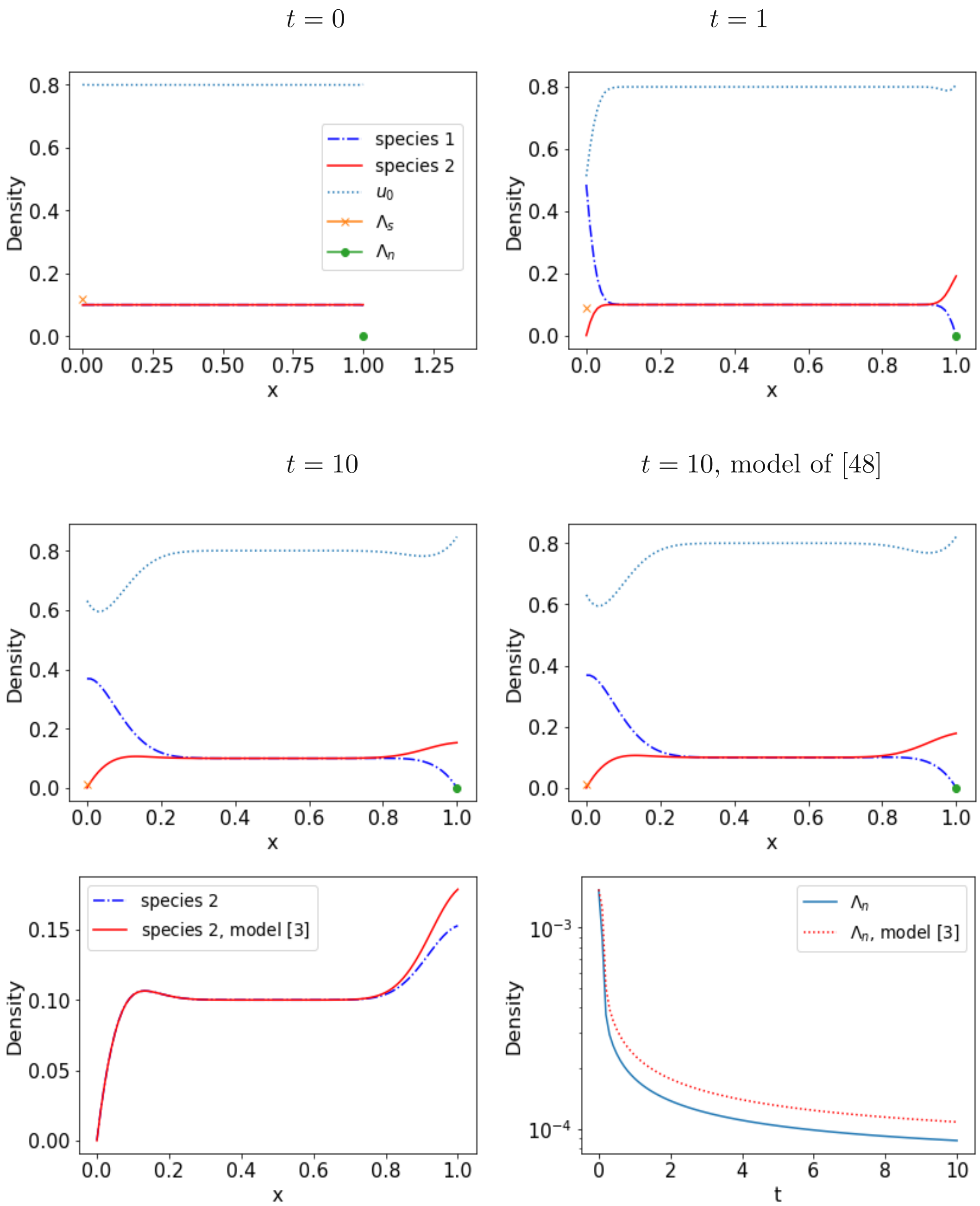

Figure 8.6.: Experiment 1: Concentrations of anterograde vesicles (species 1) and retrograde vesicles (species 2). Top row: $t = 0, 1$. Middle row: $t = 10$. Bottom left: $t = 10$, only species 2. Bottom right: Evolution of $\Lambda_n(t)$.

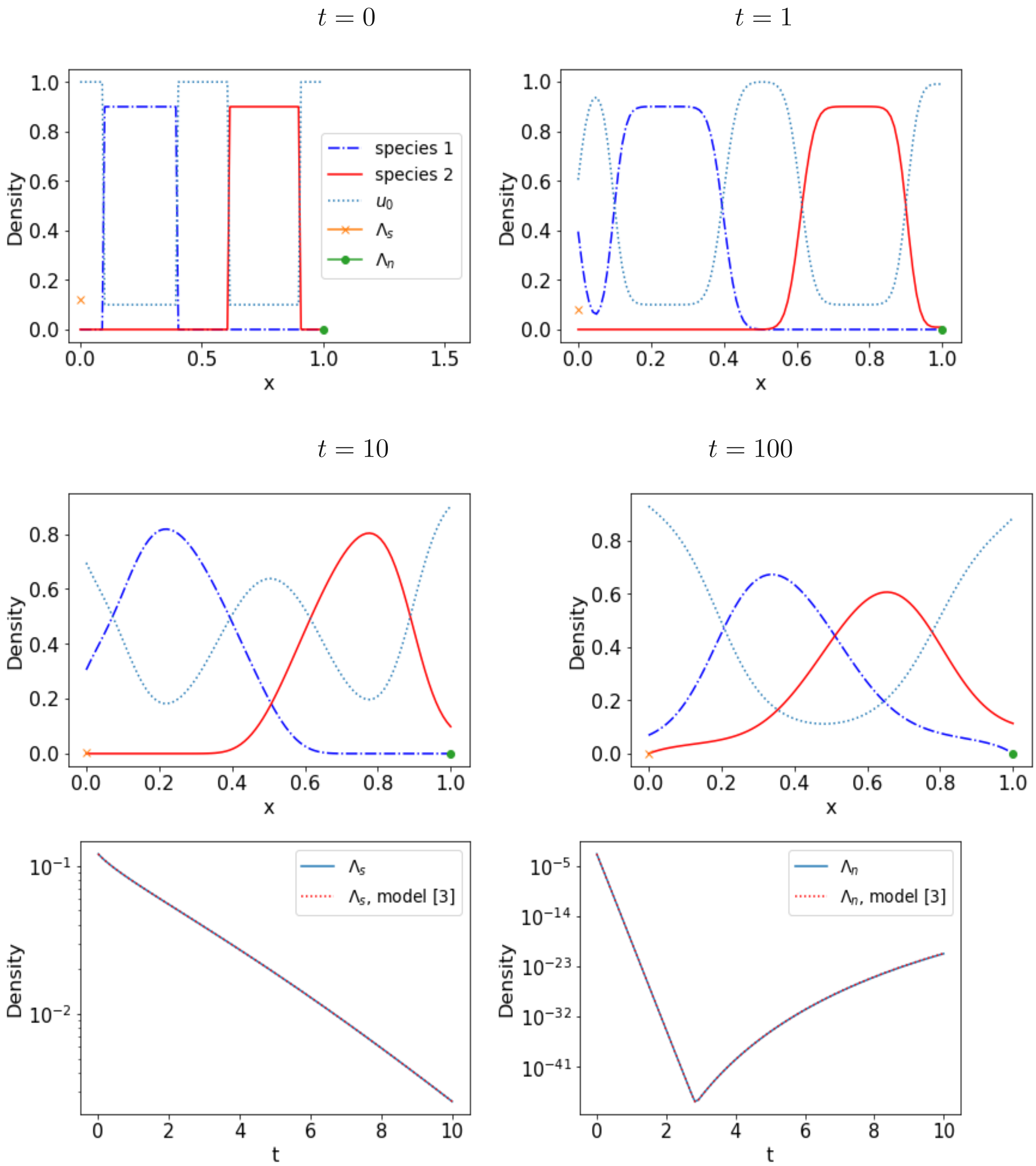

Figure 8.7.: Experiment 2: Concentrations of anterograde vesicles (species 1) and retrograde vesicles (species 2). Top and middle rows: $t = 0, 1, 10, 100$. Bottom row: evolution of Λ_s (left) and Λ_n (right).

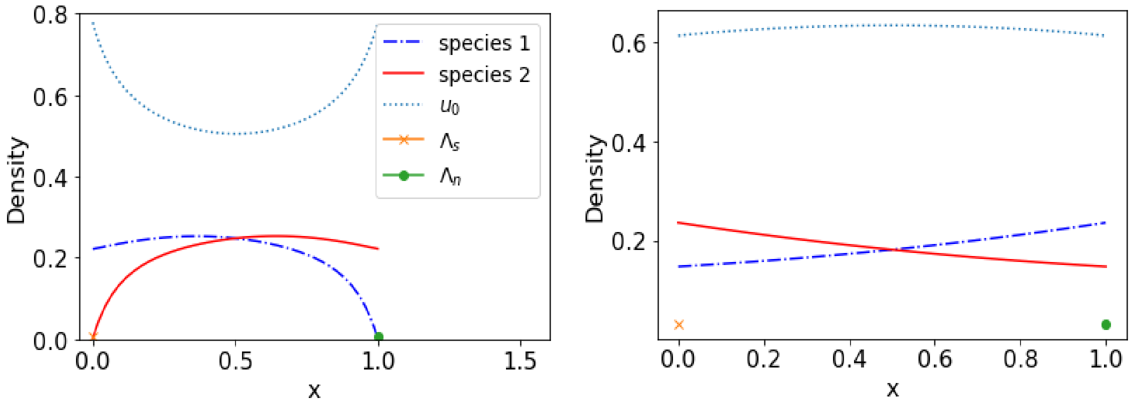

Figure 8.8.: Concentrations of anterograde and retrograde vesicles. Left: $J = 0$. Right: $J \neq 0$.

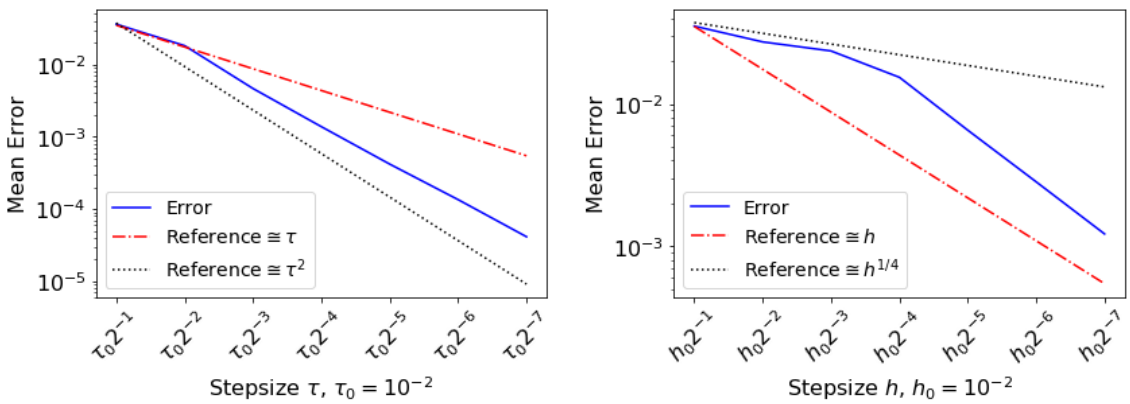

Figure 8.9.: Left: Discrete L^2 error versus time step size τ for fixed $h = 10^{-3}$. Right: Discrete L^2 error versus space step size h for fixed $\tau = 10^{-3}$.

A. Auxiliary Results

For the convenience of the reader, we collect some auxiliary results used in Part I and Part II of this work in this chapter. Its content is partly taken from [29, Appendix] and [35, Appendix].

A.1. Fundamentals of Probability Theory

Let $(\Omega, \mathcal{F}, \mathbb{P})$ be a probability space and $(\mathcal{F}_t)_{t\geq 0}$ with $\mathcal{F}_t \subseteq \mathcal{F}$ be a filtration. For a topological space G we denote the corresponding Borel-σ algebra with $\mathcal{B}(G)$.

A.1.1. Stochastic Differential Equations

We recall some results and definitions from the literature regarding stochastic processes and stochastic differential equations; see [73, Chapter 2-3].

Definition 36. *We call $(\Omega, \mathcal{F}, \mathbb{P})$ complete if $\mathcal{F}$ contains all sets $A \subseteq \Omega$ for which there exists $B \in \mathcal{F}$ such that $A \subseteq B$ and $\mathbb{P}(B) = 0$.*

Definition 37. *We call $(\Omega, \mathcal{F}, (\mathcal{F}_t)_{t\geq 0}, \mathbb{P})$ a stochastic basis.*

Definition 38. *We call a filtration $(\mathcal{F}_t)_{t\geq 0}$ right continuous if $\mathcal{F}_t = \cap_{\epsilon>0}\mathcal{F}_{t+\epsilon}$.*

Definition 39. *We call a filtration $(\mathcal{F}_t)_{t\geq 0}$ complete if $\mathcal{F}_0$ contains all sets $A \subseteq \Omega$ for which there exists $B \in \mathcal{F}$ such that $A \subseteq B$ and $\mathbb{P}(B) = 0$.*

Definition 40. *A filtration $(\mathcal{F}_t)_{t\geq 0}$ which is right continuous and complete is called normal.*

Definition 41. *Let $(\Omega, \mathcal{F}, (\mathcal{F}_t)_{t\geq 0}, \mathbb{P})$ be a stochastic basis, $T > 0$ and $\mathcal{D} \subseteq \mathbb{R}^d$, $d \in \mathbb{N}$ a Borel set. We call a function $Y : \Omega \times \mathcal{D} \times [0,T] \to \mathbb{R}^d$* progressively measurable *with respect to $(\mathcal{F}_t)_{t\geq 0}$, if Y is an $\mathcal{F}_t \times \mathcal{B}(\mathcal{D}) \times \mathcal{B}([0,t])$-measurable function for all $t \in [0,T]$.*

Let $(\Omega, \mathcal{F}, \mathbb{P})$ be a complete probability space, $(\mathcal{F}_t)_{t\geq 0}$ be a normal filtration and $B(t)$ a Brownian motion on $\mathbb{R}^{d'}$, $d' \in \mathbb{N}$ with respect to $(\mathcal{F}_t)_{t\geq 0}$. Additionally let $b(\omega, x, t) : \Omega \times \mathbb{R}^d \times [0,T] \to \mathbb{R}^d$ and $\sigma(\omega, x, t) : \Omega \times \mathbb{R}^d \times [0,T] \to \mathbb{R}^{d\times d'}$ be progressive measurable maps with respect to $(\Omega, \mathcal{F}, (\mathcal{F}_t)_{t\geq 0}, \mathbb{P})$, which are continuous in x for each $(\omega, t) \in \Omega \times [0,\infty)$. Let them satisfy

$$\int_0^T \sup_{|x|\leq R} \left(\|\sigma(\omega, x, t)\|^2 + |b(\omega, x, t)| \right) \mathrm{d}t < \infty, \tag{A.1}$$

for all $0 \leq T, R \leq \infty$ and $\omega \in \Omega$, where

$$\|\sigma\| = \left(\sum_{i=1}^{d} \sum_{j=1}^{d'} |\sigma_{ij}|^2 \right)^{1/2}.$$

Let $T > 0$. We are interested in solutions of the stochastic differential equation

$$dX(t) = b(\omega, X(t), t)\mathrm{d}t + \sigma(\omega, X(t), t)\mathrm{d}B(t), \quad X(0) = X^0, \quad t \in [0, T]. \tag{A.2}$$

Definition 42 (Strong Solution). *Let $X^0 : \Omega \to \mathbb{R}^d$ be $\mathcal{F}_0$ measurable and $T > 0$. Furthermore let σ, b and $B(t)$ be as above, especially satisfying (A.1). We call an almost surely continuous $(\mathcal{F}_t)$-adapted stochastic process $(X(t))_{t\geq 0}$ a strong solution of the stochastic differential equation (A.2), if the following identity holds almost surely for all $t \in [0, T]$:*

$$X(t) = X^0 + \int_0^t b(\omega, X(s), s)\mathrm{d}s + \int_0^t \sigma(\omega, X(s), s)\mathrm{d}B(s). \tag{A.3}$$

Theorem 43 ([73], Theorem 3.1.1). *Let $X^0 : \Omega \to \mathbb{R}^d$ be $\mathcal{F}_0$ measurable, σ and b as in definition 42 above. Furthermore let the following conditions hold for all for all $(\omega, t) \in \Omega \times [0, \infty)$, $x, y \in \mathbb{R}^d$ with $|x|, |y| \leq R$ and $R \in [0, \infty)$:*

$$\begin{aligned} 2\langle x - y, b(\omega, x, t) - b(\omega, y, t)\rangle + \|\sigma(\omega, x, t) - \sigma(\omega, y, t)\|^2 &\leq K(\omega, R, t)|x - y|^2, \\ 2\langle x, b(\omega, x, t)\rangle + \|\sigma(\omega, x, t)\|^2 &\leq K(\omega, 1, t)(1 + |x|^2), \end{aligned}$$

where $K(\omega, R, t) : \Omega \times [0, \infty)^2 \to [0, \infty)$ is an $(\mathcal{F}_t)_{t\geq 0}$ adapted process for arbitrary fixed R. Additionally we assume

$$\int_0^T K(\omega, R, t)\mathrm{d}t < \infty,$$

for all $(\omega, R) \in \Omega \times [0, \infty)$ and $T \geq 0$. Then there exists a solution to (A.2) in the sense of definition 42, which is unique up to $\mathbb{P}$- indistinguishability and where (A.3) holds for all $t \geq 0$.

A.1.2. Conditional Expectation

We recall some results involving the conditional expectation; see [34, Chapter 5].

Lemma 44. *Let $\mathcal{H}$ be a sub-σ-algebra of $\mathcal{F}$ and let X, $Y : \Omega \to \mathbb{R}^d$ be random variables such that X is $\mathcal{H}$-measurable. Then*

$$\mathbb{E}(X|\mathcal{H}) = X, \quad \mathbb{E}(XY|\mathcal{H}) = X\mathbb{E}(Y|\mathcal{H}).$$

In particular, the law of total expectation holds: $\mathbb{E}[\mathbb{E}(X|\mathcal{H})] = \mathbb{E}(X)$.

Lemma 45. *Let $\mathcal{G} \subset \mathcal{F}$ be a σ-algebra, and $(X(t))_{t\geq 0}$ be an integrable stochastic process. Then, for any $t > 0$,*

$$\mathbb{E}\left(\int_0^t X(s)\mathrm{d}s \middle| \mathcal{G} \right) = \int_0^t \mathbb{E}(X(s)|\mathcal{G})\mathrm{d}s.$$

The lemma is a consequence of Fubini's theorem [14, Lemma 2.3].

Lemma 46. *Let $T > 0$, $(B(t))_{t\geq 0}$ be a d-dimensional Brownian motion, and $\mathcal{F}_t = \sigma(B(s), s \leq t)$ for $t \leq T$. Furthermore, let $X(t) \in \mathbb{R}^d$ be a square integrable, progressively measurable process with respect to $\mathcal{F}_t$. Then, for any $0 \leq s_1 \leq s_2 \leq T$,*

$$\mathbb{E}\left(\int_{s_1}^{s_2} X(t) \mathrm{d}B(t) \middle| \mathcal{F}_{s_1} \right) = 0.$$

This lemma follows from the fact that $S(t) := \int_0^t X(s)\mathrm{d}B(s)$ is a martingale and consequently, $\mathbb{E}(S(s_1) - S(s_2)) = 0$ a.s. for $0 \leq s_1 \leq s_2 \leq T$.

A.2. Existence and Regularity Results for Elliptic and Parabolic Equations

We present some known regularity and existence results for the solutions of elliptic and parabolic partial differential equations from the literature.
We assume $\mathcal{D} \subset \mathbb{R}^d$ with $d \in \mathbb{N}$, $d \geq 1$, is a bounded domain and ν the outwards pointing unit-normal on $\partial\mathcal{D}$. Let α, $\beta \in (0, 1]$. The space $C^{\alpha,\beta}(\overline{\mathcal{D}} \times [0, T])$ consists of all functions $u : \overline{\mathcal{D}} \times [0, T] \to \mathbb{R}$ such that there exists $C > 0$ such that for all (x, t), $y, s) \in \overline{\mathcal{D}} \times [0, T]$,

$$|u(x, t) - u(y, s)| \leq C(|x - y|^\alpha + |s - t|^\beta) \quad \text{for all } (x, t),\ (y, s) \in \overline{\mathcal{D}} \times [0, T].$$

The space $C^{k+\beta}(\overline{\mathcal{D}})$ is the space of all functions $u \in C^k(\overline{\mathcal{D}})$ such that $\mathrm{D}^k u$ is Hölder continuous with index $\beta > 0$. For $k = 0$ we also write $C^\beta(\overline{\mathcal{D}})$.

A.2.1. Elliptic Equations

Let γ, a_{ij}, b_j, c_j and c_0 be measurable and bounded functions on $\mathcal{D}$ for $1 \leq i, j \leq d$. We consider the problem

$$Lu = f_0(x) - \sum_{j=1}^d \partial_j f_j(x), \quad x \in \mathcal{D}, \tag{A.4}$$

where

$$Lu = -\sum_{j=1}^d \partial_j \left(\sum_{i=1}^d a_{ij}(x)\partial_i u + b_j(x)u \right) + \sum_{j=1}^n c_j(x)\partial_j u + c_0(x)u, \quad x \in \mathcal{D}, \tag{A.5}$$

supplemented with the boundary condition

$$\sum_{j=1}^d \left(\sum_{i=1}^d a_{ij}(x)\partial_i u + b_j(x)u \right) \nu_j + \gamma(x)u = g(x) + \sum_{j=1}^d f_j(x)\nu_j, \quad x \in \partial\mathcal{D}. \tag{A.6}$$

The operator L can also be written in divergence- form,

$$Lu = -\operatorname{div}(a(x)\nabla u + b(x)u) + c(x) \cdot \nabla u + c_0(x)u.$$

Problem (A.4)-(A.6) has the following weak formulation for all $\phi \in C^1(\bar{\mathcal{D}})$:

$$\int_{\mathcal{D}} \nabla\phi(x)\cdot(a(x)\nabla u) + b(x)\cdot\nabla\phi(x)u dx + \int_{\mathcal{D}} c_j(x)\phi(x)\partial_j u + c_0(x)\phi(x)u dx$$
$$+ \int_{\partial\mathcal{D}} \gamma(x)\phi(x)u d\sigma = \int_{\partial\mathcal{D}} g(x)\phi(x)d\sigma + \int_{\mathcal{D}} f_0(x)\phi(x)\mathrm{d}x + \int_{\mathcal{D}} f(x)\cdot\nabla\phi(x)dx. \quad \text{(A.7)}$$

From the literature we have the following regularity result referring to solutions u of (A.7):

Proposition 47 ([79], Proposition 3.6)**.** *Let $\mathcal{D} \subseteq \mathbb{R}^d$ be a bounded domain with Lipschitz boundary and $p > d$. Furthermore let there exist $\kappa > 0$ such that $\sum_{i,j=1}^d a_{ij}(x)y_iy_j \geq \kappa|y|^2$ holds for all $y \in \mathbb{R}^d$ and almost all $x \in \mathcal{D}$. Then there exist constants $C, \beta > 0$ such that, if $f_0 \in L^{p/2}(\mathcal{D})$, $f_j \in L^p(\mathcal{D})$ for $1 \leq j \leq d$ and $g \in L^{p-1}(\partial\mathcal{D})$, every solution of (A.7) is an element of the Hölder space $C^{0+\beta}(\overline{\mathcal{D}})$ and the following estimate holds:*

$$\|u\|_{C^{0+\beta}(\overline{\mathcal{D}})} \leq C\left(\|u\|_{L^2(\mathcal{D})} + \|f_0\|_{L^{p/2}(\mathcal{D})} + \sum_{j=1}^d \|f_j\|_{L^p(\mathcal{D})} + \|g\|_{L^{p-1}(\partial\mathcal{D})}\right).$$

A.2.2. Parabolic Equations

The following regularity results hold for the parabolic problem

$$\begin{aligned} &\partial_t u - \operatorname{div}(a(x,t)\nabla u) = f \text{ in } \mathcal{D},\ t > 0, \\ &a(x,t)\nabla u\cdot\nu = 0 \text{ on } \partial\mathcal{D}, \quad u(0) = u^0 \text{ in } \mathcal{D}. \end{aligned} \quad \text{(A.8)}$$

Theorem 48 ([90], Section II.3, Theorem 3.3)**.** *Let $a \in L^\infty(Q_T)$ be such that $a(x,t) \geq a_0 > 0$ for all $(x,t) \in \overline{\mathcal{D}}\times[0,T]$, $f \in L^2(Q_T)$, and $u^0 \in H^1(\mathcal{D})$. Then there exists a unique weak solution to* (A.8) *such that $u \in C^0([0,T]; H^1(\mathcal{D}))$, $\partial_t u \in L^2(Q_T)$, and there exists a constant $C > 0$, not depending on a, u, u^0, or f, such that*

$$\|u\|_{L^\infty(0,T;H^1(\mathcal{D}))} + \|\partial_t u\|_{L^2(Q_T)} \leq C\big(\|f\|_{L^2(Q_T)} + \|u^0\|_{H^1(\mathcal{D})}\big).$$

Proof. The a priori estimate is a consequence of the proof of [90, Theorem 3.3]. □

Theorem 49 ([72], Theorem 1.2)**.** *Let $\beta \in (0,1)$, $\partial\mathcal{D} \in C^{1+\beta}$, $a \in C^{\beta,\beta/2}(\overline{\mathcal{D}}\times[0,T])$ be such that $a(x,t) \geq a_0 > 0$ for all $(x,t) \in \overline{\mathcal{D}}\times[0,T]$, $f \in L^\infty(0,T; L^\infty(\mathcal{D}))$, and $u^0 \in C^{1+\beta}(\overline{\mathcal{D}})$ be such that $a(x,t)\nabla u_0\cdot\nu = 0$ on $\partial\mathcal{D}$. Furthermore, let $u \in C^0([0,T]; L^2(\mathcal{D}))\cap L^2(0,T; H^1(\mathcal{D}))$ be a weak solution to* (A.8)*. Then there exists a constant $C_\beta > 0$, only depending on the data, such that*

$$\|u\|_{C^{1+\beta,(1+\beta)/2}(\overline{\mathcal{D}}\times[0,T])} \leq C_\beta.$$

Theorem 50 ([67], Section IV.9, Theorem 9.1)**.** *Let $\partial\mathcal{D} \in C^2$, $q > 3$, $T > 0$, $a \in C^0(\overline{\mathcal{D}}\times[0,T])$ be such that $a(x,t) \geq a_0 > 0$ for all $(x,t) \in \overline{\mathcal{D}}\times[0,T]$, $f \in L^q(0,T; L^q(\mathcal{D}))$, $u^0 \in W^{2,q}(\mathcal{D})$ be such that $a(x,t)\nabla u^0\cdot\nu = 0$ on $\partial\mathcal{D}$. Then there exists a unique strong solution $u \in L^q(0,T; W^{2,q}(\mathcal{D}))$ to* (A.8) *satisfying $\partial_t u \in L^q(0,T; L^q(\mathcal{D}))$, and there exists a constant $C > 0$, not depending on u, f, or u_0, such that*

$$\|u\|_{L^q(0,T;W^{2,q}(\mathcal{D}))} + \|\partial_t u\|_{L^q(0,T;L^q(\mathcal{D}))} \leq C\big(\|f\|_{L^q(0,T;L^q(\mathcal{D}))} + \|u_0\|_{W^{2,q}(\mathcal{D})}\big).$$

Theorem 51 ([67], Section V.5, Theorem 5.4)**.** *Let $\beta \in (0,1)$, $\partial\mathcal{D} \in C^{2+\beta}$, $T > 0$, a_{ij}, b_i, $c \in C^{\beta,\beta/2}(\overline{\mathcal{D}} \times [0,T])$ be such that $a_{ij}(x,t) \geq a_0 > 0$ for all $(x,t) \in \overline{\mathcal{D}} \times [0,T]$ for $i,j = 1,\ldots,m$, $f \in C^{\beta,\beta/2}(\overline{\mathcal{D}} \times [0,T])$, and $u^0 \in C^{2+\beta}(\overline{\mathcal{D}})$ be such that $\nabla u_0 \cdot \nu = 0$ on $\partial\mathcal{D}$. Then there exists a unique classical solution $u \in C^{2+\beta,1+\beta}(\overline{\mathcal{D}} \times [0,T])$ to*

$$\partial_t u - \sum_{i,j=1}^{m} a_{ij}(x,t)\frac{\partial^2 u}{\partial x_i \partial x_j} + b(x,t)\cdot\nabla u + c(x,t)u = f \quad \text{in } \mathcal{D},\ t > 0,$$
$$\nabla u \cdot \nu = 0 \quad \text{on } \partial\mathcal{D},\ t > 0, \quad u(0) = u^0 \quad \text{in } \mathcal{D},$$

and there exists a constant $C > 0$, not depending on u, f, or u_0, such that

$$\|u\|_{C^{2+\beta,1+\beta}(\overline{\mathcal{D}}\times[0,T])} \leq C\big(\|f\|_{C^{\beta;\beta/2}(\overline{\mathcal{D}}\times[0,T])} + \|u_0\|_{C^{2+\beta}(\overline{\mathcal{D}})}\big).$$

Bibliography

[1] G. Albi and L. Pareschi. Binary interaction algorithms for the simulation of flocking and swarming dynamics. *Multiscale Model. Simul.* 11 (2013), 1–29.

[2] D. Aldous. Interacting particle systems as stochastic social dynamics. *Bernoulli* 19 (2013), 1122–1149.

[3] S. Alt, P. Ganguly and G. Salbreux. Vertex models: from cell mechanics to tissue morphogenesis. *Philos. Trans. R. Soc. B* 372 (2015), 20150520.

[4] A. Bakhta and V. Ehrlacher. Cross-diffusion systems with non-zero flux and moving boundary conditions. *ESAIM Math. Model. Numer. Anal.* 52 (2018), 1385–1415.

[5] Y. D. Bansod and J. Bursa. Continuum-based modelling approaches for cell mechanics. *Int. J. Eng. Technol.* 9 (2015), 9.

[6] G. Beylkin, R. Coifman, and V. Rokhlin. Fast wavelet transforms and numerical algorithms. I. *Commun. Pure Appl. Math.* 44 (1991), 141–183.

[7] R. Blanco and H. Gerhardt. VEGF and notch in tip and stalk cell selection. *Cold Spring Harb. Perspect. Med.* 3 (2013), a006569.

[8] F. Bookholt, H. Monsuur, S. Gibbs, and F. Vermolen. Mathematical modelling of angiogenesis using continuous cell-based models. *Biomech. Model. Mechanobiol.* 15 (2016), 1577–1600.

[9] P. Bressloff. Stochastic model of protein receptor trafficking prior to synaptogenesis. *Phys. Rev. E* 74 (2006), 031910, 6 pages.

[10] P. Bressloff. Aggregation–fragmentation model of vesicular transport in neurons. *J. Phys. A* 49 (2016), 145601, 16 pages.

[11] P. Bressloff and B. Karamched. Model of reversible vesicular transport with exclusion. *J. Phys. A* 49 (2016), 345602, 26 pages.

[12] P. Bressloff and E. Levien. Synaptic democracy and active intracellular transport in axons. *Phys. Rev. Lett.* 114 (2015), 168101, 5 pages.

[13] N. Britton and M. Chaplain. A qualitative analysis of some models of tissue growth. *Math. Biosci.* 113 (1993), 77–89.

[14] R. A. Brooks. Conditional expectations associated with stochastic processes. *Pacific J. Math.* 41 (1972), 33–42.

[15] M. Burger, M. Di Francesco, J.-F. Pietschmann, and B. Schlake. Nonlinear cross-diffusion with size exclusion. *SIAM J. Math. Anal.* 42 (2010), 2842–2871.

[16] M. Burger, I. Humpert, and J.-F. Pietschmann. On Fokker–Planck equations with in- and outflow of mass. *Kinet. Relat. Models* 13 (2020), 249–277.

[17] M. Burger and J.-F. Pietschmann. Flow characteristics in a crowded transport model. *Nonlinearity* 29 (2016), 3528–3550.

[18] H. Byrne and D. Drasdo. Individual-based and continuum models of growthing cell populations: a comparison. *J. Math. Biol.* 58 (2009), 657–687.

[19] R. E. Caflisch. Monte Carlo and quasi-Monte Carlo methods. *Acta Numer.* 1998 (1998), 1–49.

[20] V. Capasso and F. Flandoli. On the mean field approximation of a stochastic model of tumour-induced angiogenesis. *Europ. J. Appl. Math.* 30 (2019), 619–658.

[21] V. Capasso and D. Morale. Stochastic modelling of tumour-induced angiogenesis. *J. Math. Biol.* 58 (2009), 219–233.

[22] A. Carlier, L. Geris, K. Bentley, G. Carmeliet, P. Carmeliet, and H. van Oosterwyck. MOSAIC: a multiscale model of osteogenesis and sprouting angiogenesis with lateral inhibition of endothelial cells. *PLOS Comput. Biol.* 8 (2012), e1002724.

[23] J. A. Carrillo, S. Jin and Y. Tang. Random batch particle methods for the homogeneous Landau equation. *Commun. Comput. Phys.* 31 (2022), no. 4, 997–1019.

[24] M. Chaplain, S. McDougall, and A. Anderson. Mathematical modeling of tumor-induced angiogenesis. *Ann. Rev. Biomed. Engin.* 8 (2006), 233–257.

[25] L. Chen, E. S. Daus, and A. Jüngel. Rigorous mean-field limits and cross diffusion. *Z. Angew. Math. Phys.* 70 (2019), 122, 21 pages.

[26] L. Chen, E. S. Daus, A. Holzinger, and A. Jüngel. Rigorous derivation of population cross-diffusion systems from moderately interacting particle systems. *J. Nonlin. Sci.* 31 (2021), no. 94, 38 pages.

[27] L. Corrias, B. Perthame, and H. Zaag. Global solutions of some chemotaxis and angiogenesis systems in high space dimensions. *Milan J. Math.* 72 (2004), 1–28.

[28] E. S. Daus, L. Desvillettes, A. Jüngel. Cross-diffusion systems and fast-reaction limits. *Bull. Sci. Math.* 159 (2020), 102824.

[29] E. S. Daus, M. Fellner and A. Jüngel. Random-batch method for multi-species stochastic interacting particle systems. *J. Comput. Phys.* Volume 463 (2022), 111220.

[30] M. Dreher and A. Jüngel. Compact families of piecewise constant functions in $L^p(0,T;B)$. *Nonlin. Anal.* 75 (2012), 3072–3077.

[31] R. M. Dudley. *Real Analysis and Probability.* 2nd edition. Cambridge, Cambridge University Press, 2002.

[32] L. Evans. *Partial Differential Equations.* 2nd ed. Amer. Math. Soc., Providence, 2010.

[33] S. Fagioli and E. Radici. Opinion formation systems via deterministic particles approximation. *Kinetic Related Models* 14 (2021), 45–76.

[34] W. Feller. *An Introduction to Probability Theory and Its Applications.* John Wiley & Sons, New York, 1970.

[35] M. Fellner and A. Jüngel. A coupled stochastic differential reaction-diffusion system for angiogenesis. Submitted for publication, 2022. arXiv:2206.11510.

[36] M. Fellner and A. Jüngel. Existence analysis of a cross-diffusion system with nonlinear Robin boundary conditions for vesicle transport in neurites. Submitted for publication, 2023. arXiv:2305.15281.

[37] E. Gaffney, K. Pugh, and P. Maini. Investigating a simple model for cutaneous wound healing angiogenesis. *J. Math. Biol.* 45 (2002), 337–374.

[38] A. Gerstenmayer and A. Jüngel. Analysis of a degenerate parabolic cross-diffusion system for ion transport. *J. Math. Anal. Appl.* 461 (2018), 523–543.

[39] D. Gilbarg and N. Trudinger. *Elliptic Partial Differential Equations of Second Order.* Springer, Berlin, 1998.

[40] H. Eberl, D. Parker, and M. van Loosdrecht. A new deterministic spatio-temporal continuum model for biofilm development. *Comput. Math. Meth. Medicine* 3 (2001), no. 429794, 15 pages.

[41] M. Efendiev, S. Zelik, and H. Eberl. Existence and longtime behaviour of a biofilm model. *Commun. Pure Appl. Anal.* 8 (2009), 509-531.

[42] F. Golse, S. Jin, and T. Paul. The random batch method for N-body quantum dynamics. *J. Comput. Math.* 39 (2021), 897–922.

[43] F. Graner and J. Glazier. Simulation of biological cell sorting using a two-dimensional extended Potts model. *Phys. Rev. Lett.* 69 (1992), 2013–2016.

[44] L. Greengard and V. Rokhlin. A fast algorithm for particle simulations. *J. Comput. Phys.* 73 (1987), 325–348.

[45] A.-L. Haji-Ali and R. Tempone. Multilevel and multi-index Monte Carlo methods for the McKean–Vlasov equation. *Stat. Comput.* 28 (2018), 923–935.

[46] T. Hayashi, F. Yura, J. Mada, H. Kurihara, T. Tokihiro. Pattern formation of elliptic particles by two-body interactions: A model for dynamics of endothelial cells in angiogenesis. *J. Theor. Biol.* 555 (2022), 111300, 11 pages.

[47] S. Hiremath, C. Surulescu, A. Zhigun, and S. Sonner. On a coupled SDE-PDE system modeling acid-mediated tumor invasion. *Discrete Contin. Dyn. Sys. B* 23 (2018), 2339–2369.

[48] I. Humpert, D. Di Meo, A. Püschel, and J.-F. Pietschmann. On the role of vesicle transport in neurite growth: Modeling and experiments. *Math. Biosci.* 338 (2021), 108632, 15 pages.

[49] P.-E. Jabin and Z. Wang. Mean field limit for stochastic particle systems. In: *Active Particles*, Vol. 1, 379–402. Springer, Boston, 2017.

[50] S. Jin and L. Li. On the mean field limit of the Random Batch Method for interacting particle systems. *Sci. China Math.* 6 (2022), 169–202.

[51] S. Jin and L. Li. Random Batch Methods for classical and quantum interacting particle systems and statistical samplings. To appear as a chapter in: N. Bellomo, J. A. Carrillo, and E. Tadmor (eds.), *Active Particles II*, 2022. arXiv:2104.04337.

[52] S. Jin, L. Li, and J.-G. Liu. Random batch methods (RBM) for interacting particle systems. *J. Comput. Phys.* 400 (2020), 108877, 30 pp.

[53] S. Jin, L. Li, and J.-G. Liu. Convergence of Random Batch Method for interacting particles with disparate species and weights. *SIAM J. Numer. Anal.* 59 (2021), 746–768.

[54] S. Jin, L. Li, and Y. Sun. On the Random Batch Method for second order interacting particle systems. Submitted for publication, 2020. arXiv:2011.10778.

[55] S. Jin, L. Li, X. Ye and Z. Zhou. Ergodicity and long-time behaviour of the random batch method for interacting particle systems. *Math. Models Methods Appl. Sci.* 33 (2023), 67–102.

[56] K. Jisheng, S. Shuyu and W. Yuanqing. Mixed finite element-based fully conservative methods for simulating wormhole propagation. *Comput. Methods Appl. Mech. Eng.* 298 (2016), 279–302.

[57] B. Jourdain, C. Le Bris and T. Lelièvre. Coupling PDEs and SDEs: the illustrative example of the multiscale simulation of viscoelastic flows. In: B. Engquist, O. Runborg, and P. Lötstedt (ed.s), *Multiscale Methods in Science and Engineering*, Lect. Notes Comput. Sci. Eng. 44, 149–168. Springer, Berlin, 2005.

[58] A. Jüngel. The boundedness-by-entropy method for cross-diffusion systems. *Nonlinearity* 28 (2015), 1963–2001.

[59] A. Jüngel. *Entropy Methods for Diffusive Partial Differential Equations*. Springer Briefs Math., Springer, 2016.

[60] A. Jüngel and A. Zurek. A discrete boundedness-by-entropy method for finite-volume approximations of cross-diffusion systems. *IMA J. Numer. Anal.* 43 (2023), 560-589.

[61] O. Kallenberg. *Foundations of Modern Probability.* 3rd edition. Springer, Cham, 2021.

[62] J. Karatzas and S. Shreve. *Brownian Motion and Stochastic Calculus.* 2nd edition. Springer, New York, 1991.

[63] P. Kloeden and E. Platen. *Numerical Solution of Stochastic Differential Equations.* Springer, Berlin, 1992.

[64] P. Kloeden, S. Sonner, and C. Surulescu. A nonlocal sample dependence SDE-PDE system modeling proton dynamics in a tumor. *Discrete Contin. Dyn. Sys. B* 21 (2016), 2233–2254.

[65] D. Ko, S.-Y. Ha, S. Jin, and D. Kim. Uniform error estimates for the random batch method to the first-order consensus models with antisymmetric interaction kernels. *Stud. Appl. Math.* 146 (2021), 983–1022.

[66] D. Ko and E. Zuazua. Model predictive control with random batch methods for a guiding problem. Submitted for publication, 2020. arXiv:2004.14834.

[67] O. A. Ladyženskaja, V. A. Solonnikov, and N. N. Ural'ceva. *Linear and Quasi-linear Equations of Parabolic Type.* Amer. Math. Soc., Providence, 1968.

[68] A. Latif. Banach contraction principle and its generalizations. In: S. Almezel, Q. H. Ansari, and M. A. Khamsi (eds.), *Topics in Fixed Point Theory*, Springer, Cham (2014), 33–64..

[69] L. Li, Y. Li, J.-G. Liu, Z. Liu, and J. Lu. A stochastic version of Stein variational gradient descent for efficient sampling. *Commun. Appl. Math. Comput. Sci.* 15 (2020), 37–63.

[70] L. Li, J.-G. Liu, and Y. Tang. A direct simulation approach for the Poisson–Boltzmann equation using the Random Batch Method. Submitted for publication, 2020. arXiv:2004.05614.

[71] M. Li, T. Zhang, Y. Chen, and A. Smola. Efficient mini-batch training for stochastic optimization. In: *Proceedings of the 20th ACM SIGKDD International Conference on Knowledge Discovery and Data Mining*, New York, pp. 661–670.

[72] G. Lieberman. Hölder continuity of the gradient of solutions of uniformly parabolic equations with conormal boundary conditions. *Ann. Mat. Pura Appl.* 148 (1987), 77–99.

[73] W. Liu and M. Röckner. *Stochastic Partial Differential Equations: an Introduction.* Springer, Cham, 2015.

[74] P. Lötstedt. Derivation of continuum models from discrete models of mechanical forces in cell populations. *J. Math. Biol.* 83 (2021), 75.

[75] G. Marino, J.-F. Pietschmann, and M. Winkler. A free boundary model for transport induced neurite growth. Submitted for publication, 2023. arXiv:2302.00527.

[76] J. Metzcar, Y. Wang, R. Heiland and P. Macklin. A review of cell-based computational modeling in cancer biology. *JCO Clin. Cancer Inform.* 3 (2019), 1–13.

[77] S. Motsch and E. Tadmor. Heterophilious dynamics enhances consensus. *SIAM Rev.* 56 (2014), 577–621.

[78] J. M. Nava-Sedeño, A. Voß-Böhme, H. Hatzikirou, A. Deutsch and F. Peruani. Modelling collective cell motion: are on- and off lattice models äquivalent? *Philos. Trans. R. Soc. B* 375 (2019), 20190378.

[79] R. Nittka. Regularity of solutions of linear second order elliptic and parabolic boundary value problems on Lipschitz domains. *J. Diff. Eqs.* 251 (2011), 860–880.

[80] H. Oliveri and A. Goriely. Mathematical models of neuronal growth. *Biomech. Model. Mechanobiol.* 21 (2022), 89–118.

[81] S. Pierce. Computational and mathematical modeling of angiogenesis. *Microcirculation* 15 (2008), 739–751.

[82] N. Rahman and D. Oelz. A mathematical model for axonal transport of large cargo vesicles. Submitted for publication, 2023. bioRxiv preprint, https://doi.org/10.1101/2023.01.18.524542.

[83] A. M. Reynolds1, G. E. McIvor, A. Thornton, P. Yang and N. T. Ouellette. Stochastic modelling of bird flocks:accounting for the cohesiveness ofcollective motion. *R. Soc. Interface* 19: 20210745.

[84] G. Rotskoff and E. Vanden-Eijnden. Trainability and accuracy of neural networks: An interacting particle system approach. Preprint, 2018. arXiv:1805.00915.

[85] F. Spill, P. Guerrero, T. Alarcon, P. Maini, and H. Byrne. Mesoscopic and continuum modelling of angiogenesis. *J. Math. Biol.* 70 (2015), 485–532.

[86] N. Shigesada, K. Kawasaki, E. Teramoto. Spatial segregation of interacting species. *J. Theoret. Biol.* 79 (1) (1979), 83—99.

[87] C. Stokes and D. Lauffenburger. Analysis of the roles of microvessel endothelial cell random motility and chemotaxis in angiogenesis. *J. Theor. Biol.* 152 (1991), 377–403.

[88] D. Strömbom, R. Mann, A. Wilson, S. Hailes, A. Morton, D. J. T. Sumpter, and A. King. Solving the shepherding problem: heuristics for herding autonomous, interacting agents. *J. Roy. Soc. Interface* 11 (2014), 20140719, 9 pages.

[89] T. V. Ta and L. T. H. Nguyen. A stochastic differential equation model for the foraging behaviour of fish schools. *Phys. Biol.* 15 (2018), 036007.

[90] R. Temam. *Infinite-Dimensional Dynamical Systems in Mechanics and Physics.* 2nd edition. Springer, New York, 1997.

[91] A. Ucuzian, A. Gassman, A. East, and H. Greisler. Molecular mediators of angiogenesis. *J. Burn Care Res.* 31 (2010), no. 158.

[92] F. Vermolen and A. Gefen. A semi-stochastic cell-based formalism to model the dynamics of migration of cells in colonies. *Biomech. Model. Mechanobiol.* 11 (2012), 183–195.

[93] X. Yang and X. Liu. Numerical analysis of two new finite difference methods for time-fractional telegraph equation. *Discrete and Continuous Dynamical Systems - B* 26 (7) (2021), 3921–3942.

[94] X. Ye and Z. Zhou. Efficient sampling of thermal averages of interacting quantum particle systems with random batches. *J. Chem. Phys.* 154 (2021), 204106, 24 pages.

[95] X. Ye and Z. Zhou. Error analysis of time-discrete random batch method for interacting particle systems and associated mean-field limits. *IMA J. Numer. Anal.* 00 (2023), 1–39.

[96] N. Zamponi and A. Jüngel. Analysis of degenerate cross-diffusion population models withvolume filling. *Ann. Inst. H. Poincaré – Anal. Non Lin.* 34 (2017), 1–29.

Curriculum Vitae

Persönliche Daten

Name	**Markus Fellner**
Geburtsdatum	[redacted]
Geburtsort	[redacted]
Nationalität	[redacted]
Email	[redacted]

Anstellung

seit 03/2020	Projektassistent am Institut für Analysis and Scientific Computing, TU Wien, Österreich.
03/2016 – 09/2016	Karenzvertretung, Studienassistent am Institut für Diskrete Mathematik und Geometrie, TU Wien, Österreich.

Ausbildung

seit 03/2020	Doktoratsstudent unter der Betreuung von Prof. Dr. Ansgar Jüngel, TU Wien, Österreich.
2012–2020	Bachelor und Master in Technische Mathematik mit Auszeichnung, TU Wien, Österreich.
06/2012	Matura mit Auszeichnung, HTL Steyr, Österreich.

Lehrtätigkeit

2021	Tutor für Analysis 1 und 3, TU Wien, Österreich.
2016-2017	Tutor für Mathematik 1 für Maschinenbau, Wirtschaftsingenieurwesen - Maschinenbau und Verfahrenstechnik, TU Wien, Österreich.

Wissenschaftliche Publikationen

1. M. Fellner, A. Jüngel: *Existence analysis of a cross-diffusion system with nonlinear Robin boundary conditions for vesicle transport in neurites.* Eingereicht zur Publikation, arXiv:2305.15281 (2023).

2. M. Fellner, A. Jüngel: *A coupled stochastic differential reaction-diffusion system for angiogenesis.* Eingereicht zur Publikation, arXiv:2206.11510 (2022).

3. E. S. Daus, M. Fellner, A. Jüngel: *Random-batch method for multi-species stochastic interacting particle systems. J. Comput. Phys.* Volume 463 (2022), 111220.

Zusätzliche Informationen

- Sprachen: Deutsch, Englisch.
- Programmiersprachen: R, C, C++, Matlab, Python.
- Forschungsinteressen: Maschinelles Lernen, Partielle Differentialgleichungen, Stochastische Differentialgleichungen, Lebenswissenschaften.

Wien, am 17. Juli 2023

Markus Fellner